AFFDL-TR-65-218

ESTIMATION OF FLYING QUALITIES OF PILOTED AIRPLANES

ROBERT J. WOODCOCK, AFFDL

DOUGLAS E. DRAKE, DOUGLAS AIRCRAFT CO.

FOREWORD

This material is an extensive revision of work at Douglas Aircraft Company, Long Beach, California, Contract AF33(616)-6460, intended originally to be published as part of the USAF Stability and Control DATCOM. That volume, however, has grown so full of aerodynamic data that it seems more appropriate to issue the flying-qualities estimation methods as a separate report. The work, spanning the last several years as time has been available, has been conducted under Project 8219, Stability and Control Investigations, by the authors. The manuscript was released by the authors in December 1965 for publication as an RTD technical report.

This technical report has been reviewed and is approved.

C. B. Westbrook

C. B. WESTBROOK
Chief, Control Criteria Branch
Flight Control Division
Air Force Flight Dynamics Laboratory

ABSTRACT

Methods, ranging from rigorous and complicated to simple and approximate, are presented for estimating flying qualities in accordance with such specifications as MIL-F-8785 (ASG). Aerodynamic and inertial data are assumed to be known. Intended mainly for design use, the report gives enough detail to indicate derivations and conditions for validity. Topics include the static and dynamic, controls-fixed and controls-free aspects of aircraft stability, control, and trim. Although emphasis is on linear analysis, methods are given or indicated for such nonlinear problems as drag, pitch-up, inertial coupling, and spinning. Appendixes give an introduction to aeroelastic effects, ways to analyze control tabs, a derivation of the controls-free equations of motion, and an introduction to root locus analysis.

TABLE OF CONTENTS

TABLE OF CONTENTS (Continued)

TABLE OF CONTENTS (Continued)

ILLUSTRATIONS

ILLUSTRATIONS (Continued)

TABLES

SYMBOLS

(Ft-lb-sec units; one can hardly go wrong in using radians for all angular measure. Directions are generally from the pilot's viewpoint. See Figure 1.)

a	Acceleration, ft/sec^2
b	Wing span, ft
B	Boost ratio = $\frac{\text{control-surface hinge moment (total)}}{\text{control-surface hinge moment (pilot effort)}}$
c	Reference chord, ft
$\bar{c}$	Mean aerodynamic chord (of wing, unless subscript), ft
cg	Center of gravity, percent m.a.c.
D	Drag, lb
e	Exponential base $\doteq$ 2.718
EAS	Equivalent airspeed, $V\sqrt{\rho/\rho_{SL}}$
F	Stick or pedal force, lb (positive when tending to move the stick aft or right, or right pedal forward)
g	Acceleration due to gravity, 32.2 ft/sec^2 at aircraft altitudes
G	Surface-to-stick (or pedal) gearing, $-\frac{\partial \delta_{surface}}{\partial \Delta_{stick}}$, rad/ft (See Figures 4 and 7). $G_a = \frac{-\partial \delta_a}{\partial \Delta'_s}$, $G_r = -\frac{\partial \delta_r}{\partial \Delta_p}$
h	Altitude above sea level, ft
H	Hinge moment, lb-ft; generally aerodynamic hinge moment (same sense as δ).
i_H	Incidence of horizontal stabilizer to α = 0 reference line, rad (positive trailing edge down)
Δi_H	Horizontal stabilizer deflection from incidence for trim, rad
i_T	Thrust-line inclination to α = 0 reference line, rad (positive in direction of positive α).
I_x	Moment of inertia in roll, slug ft^2 [$I_x = I_{x_p}\cos^2\eta + I_{z_p}\sin^2\eta$ where subscript p denotes principal axes and η is the principal-axes inclination in the sense of α. See Reference 6.]
I_{xz}	Product of inertia, slug ft^2 [$I_{xz} = \frac{1}{2}(I_{x_p} - I_{z_p})\sin 2\eta$. See I_x above.]
I_y	Moment of inertia in pitch, slug ft^2
I_z	Moment of inertia in yaw, slug ft^2 [$I_z = I_{z_p}\cos^2\eta + I_{x_p}\sin^2\eta$. See I_x above.]

SYMBOLS (Continued)

K_x^2	I_x/mb^2, nondimensional radius of gyration squared in roll
K_y^2	$I_y/m\bar{c}^2$, nondimensional radius of gyration squared in pitch
K_z^2	I_z/mb^2, nondimensional radius of gyration squared in yaw
L	Lift, lb; rolling moment, lb-ft (positive "up" or right-wing down, resp.)
m	Mass; without subscript, mass of entire vehicle; slugs
M	Mach number; pitching moment, lb-ft: unless designated otherwise, aerodynamic pitching moment. (positive nose up)
m.a.c.	Mean aerodynamic chord, ft
n	Load factor, $\frac{1}{W}\sum$(force normal to flight path) (positive up)
N	Normal force, lb; yawing moment, lb-ft (positive up or nose right, resp.); numerator (of a transfer function); neutral point, $\%\bar{c}/100$.
p	Roll rate, rad/sec (positive right-wing down)
q	Pitch rate, rad/sec (positive nose-up)
q*	Dynamic pressure, $\frac{1}{2}\rho V^2$, lb/ft^2
r	Yaw rate, rad/sec (positive nose right); normal distance from hinge line (See $\bar{r}$)
$\bar{r}$	Normal distance from hinge line to control-surface cg (positive forward), ft
R	Reynolds number
S	Area (of wing, unless subscript), ft^2
t	Time, sec
T	Thrust, lb; response time, sec
u	Incremental speed in x-direction, ft/sec
v	Incremental speed in y-direction, ft/sec
V	True airspeed, ft/sec except as noted; In Section IIIC, V is ground speed.
w	Incremental z-velocity, ft/sec
W	Weight; without subscript, weight of entire vehicle; lb
x,y,z	(a) Axes: generally "wind-tunnel stability axes" for static analysis. For analyzing dynamics, x,y, and z are fixed in the vehicle; they coincide with the static x,y, and z at the operating point (stability axes) or with the principal axes (for which $I_{xz} = 0$) (See Figure 1).

SYMBOLS (Continued)

(b) Distances along appropriate axes from the center of gravity, ft

z_T Perpendicular distance from cg to thrust line (positive for thrust line below cg).

X, Y, Z Forces along x,y,z axes; without subscript, aerodynamic forces; lb

$Y(s)$ Transfer function

C_D Drag coefficient = $\frac{\text{Drag}}{q^*S}$

C_{D_o} Untrimmed drag coefficient at zero lift

$C_{D_{C_L^2}}$ Untrimmed coefficient of drag proportional to $C_L^2 (\partial C_D / \partial C_L^2)_{\delta e, etc}$.

$C_{D_\alpha}, C_{D_\delta}$ Drag-coefficient derivative with respect to angle of attack and pitch-control deflection

C_h Hinge-moment coefficient based on free-stream dynamic pressure and control-surface area and chord;[1] without subscript, longitudinal-control-surface hinge moment (positive in the sense of positive surface deflection).

$C_{h_\alpha}, C_{h_\delta}, C_{h_{\delta t}}, C_{h_{i_H}}, C_{h_q}$ Pitch-control hinge-moment coefficient derivatives with respect to vehicle angle of attack $\left[\text{not local } \alpha; C_{h_\alpha} = \eta_H C_{h_{\alpha_H}} \left(1 - \frac{\partial \epsilon}{\partial \alpha}\right)\right]$, control deflection, tab deflection, horizontal-tail deflection, and pitch rate $(q\bar{c}/2V)$, respectively, per radian

$C_{h_{\alpha H}}$ Elevator hinge-moment-coefficient derivative with respect to horizontal-tail angle of attack, based on local dynamic pressure, per radian

C_{h_t} Tab hinge-moment coefficient, based on free-stream dynamic pressure and tab area and chord (positive in the sense of positive tab deflection).

$C_{\ell_p}, C_{\ell_r}, C_{\ell_\beta}, C_{\ell_{\delta_a}}, C_{\ell_{\delta_r}}, C_{\ell_{\dot\beta}}$ Rolling-moment derivative with respect to roll rate $(pb/2V)$, yaw rate $(rb/2V)$, sideslip angle, aileron deflection, rudder deflection, and sideslip rate $(\dot\beta b/2V)$, respectively, per radian

C_L Lift coefficient, L/q*S (positive up)

$C_{L_{i_H}}, C_{L_q}, C_{L_{\dot\alpha}}, C_{L_\alpha}, C_{L_\delta}$ Lift-coefficient derivative with respect to horizontal-stabilizer incidence, pitch rate $(q\bar{c}/2V)$, angle-of-attack rate $(\dot\alpha\bar{c}/2V)$, angle of attack, and elevator deflection, respectively, per radian

C_{L_1} W/q*S

[1] With ailerons, for example, carefully determine whether reference area of data is that of one or both ailerons; likewise for aileron deflection.

SYMBOLS (Continued)

C_m Pitching-moment coefficient, M/q*S$\bar{c}$ (positive nose up)

$C_{m_{i_H}}, C_{m_q}, C_{m_{\dot{\alpha}}}, C_{m_\alpha}, C_{m_\delta}, C_{m_{\delta t}}$ Pitching-moment-coefficient derivative with respect to horizontal-stabilizer incidence, pitch rate ($q\bar{c}/2V$), angle-of-attack rate ($\dot{\alpha}\bar{c}/2V$), angle of attack, elevator deflection, and tab deflection, respectively, per radian

C_{m_o} Pitching-moment coefficient at zero lift, zero elevator deflection, etc.

C_n Yawing-moment coefficient, N/q*Sb (positive nose right)

$C_{n_\beta}, C_{n_{\delta a}}, C_{n_{\delta r}}, C_{n_p}, C_{n_r}, C_{n_{\dot{\beta}}}$ Yawing-moment-coefficient derivative with respect to sideslip angle, aileron deflection, rudder deflection, roll rate ($pb/2V$), yaw rate ($rb/2V$), and sideslip rate ($\dot{\beta}b/2V$), respectively, per radian

C_N Normal-force coefficient, N/q*S (positive up)

C_{N_α} Normal-force-coefficient derivative with respect to angle of attack, per radian ($C_{N_\alpha} = C_{L_\alpha} + C_D$)

C_y Side-force coefficient, Y/q*S (positive to the right)

$C_{y_p}, C_{y_r}, C_{y_\beta}, C_{y_{\delta a}}, C_{y_{\delta r}}, C_{y_{\dot{\beta}}}$ Side-force-coefficient derivative with respect to roll rate ($pb/2V$), yaw rate ($rb/2V$), sideslip angle, aileron deflection, rudder deflection, and sideslip rate ($\dot{\beta}b/2V$), respectively, per radian

α Angle of attack, radians (positive for nose above the flight path)

$\Delta\alpha$ w/V

β Sideslip angle, rad (positive for right slip)

γ Flight-path angle, rad (positive nose up)

δ Control deflection, rad

δ_t Tab deflection, rad (positive in same sense as control-surface deflection).

Δ_p Linear deflection of rudder pedals (See Figure 1 or 7), inches

Δ_s Linear deflection of control stick grip or wheel (positive aft), inches

Δ'_s Linear deflection of control stick grip or wheel (positive right), inches

ϵ Downwash angle, rad

ζ Damping ratio

η Efficiency factor, local q*/free-stream q*

SYMBOLS (Continued)

θ	Pitch angle, rad (positive nose up)
Λ	Sweep angle (of control-surface hinge line)
μ_1	Relative density $m/\rho S\bar{c}$
μ_2	Relative density $m/\rho Sb$
ξ	$i_T + \alpha$trim
ρ	Air density, slugs/ft^3
τ	Aerodynamic time, $m/\rho SV$ sec
ϕ	Bank angle, rad (positive right wing down)
ψ	Yaw angle, rad (positive nose right); phase angle
ω_n	Undamped natural frequency, rad/sec

Subscripts

a	Aileron (positive deflection right aileron trailing edge up, left down)
ac	Aerodynamic center; distance from cg to ac
B	Bobweight; at bobweight location
c	Canard surface; pilot command; crosswind
cg	center of gravity
d	Dutch roll
e	Elevator (positive deflection trailing edge down); equivalent (See EAS)
F	Flap
FE	With all landing gear fully extended
g	Gust
H	Horizontal tail
L	Left; landing configuration
o	At zero time or zero lift
p	Rudder pedal; phugoid mode
P	At pilot's location

SYMBOLS (Continued)

r	Rudder (positive deflection trailing edge left)
R	Roll mode; right
s	Stick; stall; spiral mode
sp	Short-period mode
t	Tab; trim
T	Throttle; thrust
W	Wind

Mathematical Symbols

$\doteq$	approximately equals
$\triangleq$	is defined as
$\|Q\|$	absolute value (magnitude) of Q; determinant of Q
$Q\|_X$	Q evaluated at condition X
Δ	characteristic determinant; change in quantity following.
$\propto$	is proportional to
$\frac{d}{dx}$	total derivative with respect to x
$\dot{Q}$	total derivative of Q with respect to time
$\frac{\partial}{\partial x}$	partial derivative with respect to x
F(Q)	F as a function of Q, with other variables zero
s	Laplace operator

SECTION I

INTRODUCTION

This report provides a compendium of methods for estimating vehicle characteristics, static and dynamic, relevant to flying qualities. Related subjects include closed-loop, pilot-vehicle analysis, determination of vehicle sensitivity to aerodynamic or configuration changes, synthesis of artificial stabilization, manual and automatic control systems, simulation, and flight testing. These additional subjects are given no more than cursory notice here, but have received considerable attention in the recent literature.

The methods presented are not unique, and this publication is not intended as an endorsement of complete applicability and validity. Variants will suggest themselves to take the best advantage of available data and the nature of the specific problem. Although the methods are stated primarily for conventional aircraft, the most general forms are complete enough to be used with a minimum of caution for any vehicle. The effect of earth curvature, important at hypersonic speeds, is considered in Reference 1. References and approximations for hovering and VTOL transition are given in Reference 2.

The reader's general knowledge of stability and control phenomena is assumed. The intent here is to complement texts such as References 3 and 4 by presenting rigorous and simplified solutions for handling-quality parameters, indicating derivations and assumptions so that one can readily determine validity or modify the methods to suit peculiar needs. The aerodynamic characteristics are assumed to be known. The derivatives can be estimated from wind-tunnel test results, Reference 5, NASA reports, and other available sources, corrected as necessary for aeroelastic effects (Appendix I gives a brief introduction to the effects of aeroelasticity on stability derivatives). Effects of compressibility, aeroelasticity, thrust, etc. on the aerodynamic data are assumed here to have been accounted for; for example, we generally write $C_L(\alpha)$, not $C_L(\alpha, M, q^*, T, \text{etc.})$.

The nondimensional stability derivatives used herein are referred to the "wind-tunnel stability axes" system of Figure 1. For a detailed treatment of axes systems, transformations, and equations of motion, see References 6 and 7. The notation here is generally[2] consistent with that of References 5 and 6, but may differ occasionally from the notation in other references.

Artistic parts of stability and control analysis do remain: estimation of the coefficients and a priori simplification of the analysis method. In the interests of rigor the relations presented tend to be overly inclusive. With the multitude of configurations possible it has been impractical to state where each factor is significant or unimportant. The items given such attention should be considered typical rather than inclusive. Nevertheless, a general feeling for the aerodynamic and inertia characteristics of the design vehicle, together with the assumptions listed herein, should allow confident analysis with a minimum of work.

---

[2] Note the definitions herein of hinge-moment derivatives, and, in Section IV, of real-time acceleration derivatives in terms of F/mV rad/sec or M/I rad/sec^2.

Trim and maneuver capabilities not covered explicitly here can be checked by using the appropriate control deflection and force equations, remembering that pilot force restrictions and hinge-moment limitations, cable stretch, etc. cause available control and trim deflections to vary with speed and altitude.

Stability augmentation is discussed at appropriate points throughout the report. Examples of generally applicable analysis methods are: equivalent derivatives (Sections IIC, IIIA), and root locus (Appendix IV). More information about methods of analysis and synthesis can be found in References 8 through 14.

In addition to the detailed presentation, the following summary presents simplified methods and critical conditions for showing compliance with military flying qualities specifications such as Reference 15. Table I furnishes a convenient starting point for flying qualities analysis. Critical flight conditions can be determined, at least in a general way. The rough formulas tabulated there can give quick answers, and sections of this report and other references giving detailed treatments afford additional help.

α is measured in the plane of symmetry, β normal to it.

$V_{X_s} = V \cos \beta$

$V_{Y_s} = V \sin \beta$

$V_{Z_s} = 0$

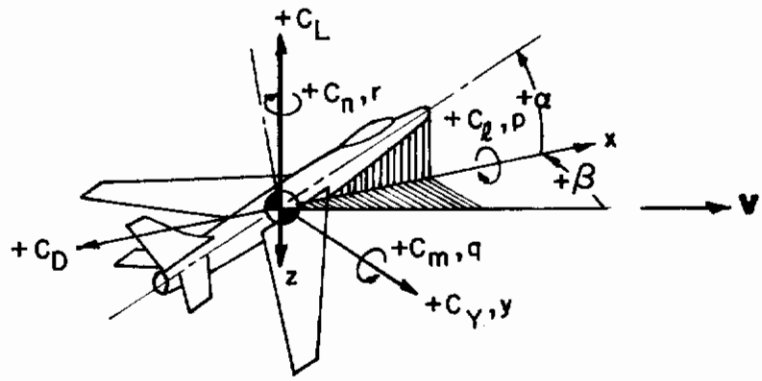

a. Wind - Tunnel Stability Axes

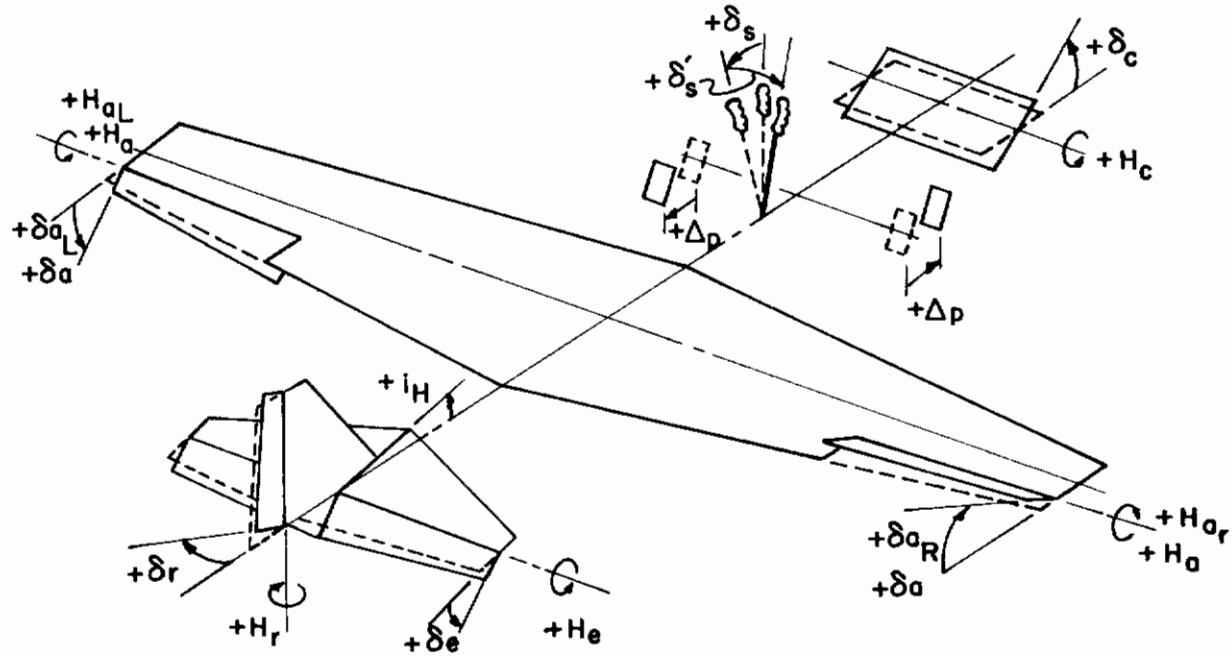

b. Sense of Positive Deflections and Hinge Moments

Figure 1. Axes System and Sign Conventions

TABLE I FLYING QUALITIES

SPEC. MIL-F-8785 PARA.	SUBJECT	SEE PARA. (This Report)	SEE REF
3.1	GENERAL		
3.1.1	Airplane Loadings	—	—
3.1.2	Altitudes	—	—
3.1.3	Operational Flight Envelopes	—	—
3.1.4	Maximum Permissible Speed Envelope	—	NACA TN 829; 6,7
3.1.5	External Stores	III D	—
3.1.6	Effects of Armament Provisions	II A4	—
3.1.7	Release of Stores	II A4	18
3.1.8	Deceleration Devices	II A4	—
3.1.9	Configurations	—	—
3.1.10	Effects of Asymmetry	III D	—
3.2	MECHANICAL CHARACTERISTICS OF CONTROL SYSTEMS		
3.2.1	Control Friction and Breakout Force	IV C,E	16, 39
3.2.2	Adjustable Controls	—	—
3.2.3	Rate of Control Displacement	IV E	39
3.2.4	Cockpit Control Free Play	IV E	—
3.2.5	Artificial Stability Devices	II C, III A, App. IV	8,9,13,14,22,23,61
3.3	LONGITUDINAL STABILITY AND CONTROL		
3.3.1	Elevator-Fixed Static Stability	II B 1	20
3.3.2	Elevator-Free Static Stability	II B 2	3
3.3.3	Exception in Transonic Flight	II B 1, 2	58
3.3.4	Stability in Accelerated Flight	II C 1, V A	21,55,56,57,58
3.3.5	Short-Period Oscillations	IV B 1, IV C 1	6,8,13,31,33,34,66
3.3.6	Long-Period Oscillations	IV B 1, IV C 1	6,8,33,37
3.3.7	Control Effectiveness in Unaccelerated Flight	II A 1,2,3	—
3.3.8	Control Effectiveness in Accelerated Flight	II A 1, 2,3; II C 1	—
3.3.9	Control Forces in Steady Accelerated Flight	II C 2	—
3.3.10	Control Forces in Sudden Pullups	IV E	38,39,40
3.3.11	Control Effectiveness in Takeoff	II D	—
3.3.12	Control in Catapult Takeoff	—	—
3.3.13	Control Forces in Takeoff	II D; II B 2	—
3.3.14	Control Effectiveness in Landing	II A 1, 2, 3	—
3.3.15	Control Forces in Landing	II A 1,2,3; II B 2	—
3.3.16	Control Forces in Dives	II B 2; II C 2	—
3.3.17	Auxiliary Dive Recovery Devices	II A 4	—
3.3.18	Effects of Drag Devices	II A 4	—
3.3.19	Longitudinal Trim Changes	II A 4	—
3.3.20	Longitudinal Trim Change Caused by Sideslip	II A 4	—
3.4	LATERAL-DIRECTIONAL STABILITY AND CONTROL		
3.4.1	Damping of Lateral-Directional Oscillations	IV B 2, IV C 2	3,4,8,9,26,66
3.4.2	Spiral Stability	IV B 2, IV C 2	3,26
3.4.3	Steady Sideslip	III A 1, 2	3,21
3.4.4	Static Directional Stability (Rudder Position)	III A 1	—

ESTIMATION SUMMARY

CRITICAL ITEMS AND ROUGH FORMULAS (SEE SECTION INDICATED TO FIND ASSUMPTIONS)

Aft cg, light weight critical for static stability & low ω_n ; fwd cg, heavy wt for control & high ω_n.
Maneuvering & damping deteriorate at high altitude; aeroelastic effects greatest (for the same speed) at low alt.
Limited by stall, thrust, control power.
Altitude lost in dive recovery: $\Delta h = \frac{V^2}{g} \ell n \left(\frac{n - \cos \gamma_o}{n-1} \right) + V \left| \sin \gamma_o \right|$, fps units; A 25% safety margin may be added.

Asymmetric stores: find lateral trim from asymmetric-thrust formulas.
Buffet, trim change (3.3.19)

$$\dot{V} = \frac{\Delta C_D q^* S}{m} \text{ ft/sec}^2$$

See asymmetric-thrust formulas.

Worst effect is with low stability, low force gradients, augmentation off.

Low q^*, gross maneuvering, augmentation operation, forward cg, heavy weight, landing flare influence needed rate.

Undesirable: cockpit-control movement, residual oscillations, insufficient authority, lack of turn coordination, etc.
Failure modes: transients, lack or delay of pilot adaptation, handling qualities after partial or complete failure.

$\left(\frac{-T z_T}{q^* S \bar{c}} + \frac{V}{2} \frac{\partial C_m}{\partial u} \right) (C_{L_\alpha} + C_D) - C_{m_\alpha} \left(C_L + \frac{V}{2} \frac{\partial C_L}{\partial u} \right) > 0$; $C_{m_\alpha} < 0$. Derivatives vary with M, α, q^*, T; aft cg critical. Light weight gives higher thrust coeff. at spec. speed.

Reversible Controls: $\left[\left(\frac{-T z_T}{q^* S \bar{c}} - \frac{C_{m_\delta}}{C_{h_\delta}} C_h \right) + \frac{V}{2} \left(\frac{\partial C_m}{\partial u} - \frac{C_{m_\delta}}{C_{h_\delta}} \frac{\partial C_h}{\partial u} \right) \right] \left(C_{N_\alpha} - \frac{C_{h_\alpha}}{C_{h_\delta}} C_{L_\delta} \right) - \left(C_{m_\alpha} - \frac{C_{h_\alpha}}{C_{h_\delta}} C_{m_\delta} \right) \left[\left(C_L - \frac{C_{L_\delta}}{C_{h_\delta}} C_h \right) + \frac{V}{2} \left(\frac{\partial C_L}{\partial u} - \frac{C_{L_\delta}}{C_{h_\delta}} \frac{\partial C_h}{\partial u} \right) \right] > 0$

$$\text{where } C_h = \frac{1}{q^* S_e \bar{c}_e} \left[W_e \bar{z}_e - H_D - \frac{B}{G} \left(\frac{\partial F_e}{\partial n} \right)_B \right]$$

Affected by wing & tail airfoil, sweep, aspect ratio, control-surface form, etc.

$N_m - cg\,(\%\bar{c}/100) \doteq -\left(\frac{C_{m_\alpha}}{C_{N_\alpha}} + \frac{\rho g \bar{c}}{4W/S} C_{m_q} \right) > 0$ Function of cg, M, h, q^*, T; possible effects of α. Aft cg critical.

$\omega_{n_{sp}} \doteq \sqrt{\frac{q C_{N_\alpha}}{C_{L_1} K_Y^2 \bar{c}} (N_m - cg)}$; $\zeta_{sp} \doteq \frac{1}{4\tau \omega_{n_{sp}}} \left[C_{N_\alpha} - \frac{1}{2K_Y^2} (C_{m_q} + C_{m_{\dot{\alpha}}}) \right]$; $\frac{1}{T_\theta} = \frac{1}{2\tau} C_{N_\alpha}$

$\omega_{n_p}^2$ (or $\frac{1}{T_{p_1}} \cdot \frac{1}{T_{p_2}}$) $\doteq \frac{\rho S g}{m} \frac{1}{(N_m - cg)} \left[\frac{-T z_T}{q^* S \bar{c}} + \frac{V_o}{2} \frac{\partial C_m}{\partial u} - \frac{C_{m_\alpha}}{C_{N_\alpha}} \left(C_L + \frac{V_o}{2} \frac{\partial C_L}{\partial u} \right) \right] \doteq 2 \left(\frac{g}{V_o} \right)^2 \left(\frac{-C_{m_\alpha}/C_{N_\alpha}}{N_m - cg} \right)$;

$(2\zeta\omega_n)_p$ or $\left(\frac{1}{T_{p_1}} + \frac{1}{T_{p_2}} \right) \doteq \frac{1}{\tau} \left[C_D + \frac{V_o}{2} \frac{\partial C_D}{\partial u} - \frac{C_{D_\alpha}}{C_{m_\alpha}} \left(\frac{-T z_T}{q^* S \bar{c}} + \frac{V}{2} \frac{\partial C_m}{\partial u} \right) \right] \doteq \frac{C_D}{\tau}$

$\delta e_{trim} \doteq -\frac{1}{C_{m_\delta} C_{N_\alpha}} \left[(C_L + C_{L_\alpha} a_o) C_{m_\alpha} + \left(C_{m_o} - \frac{T z_T}{q^* S \bar{c}} - C_{m_\alpha} a_o \right) C_{N_\alpha} \right] \doteq -\frac{C_{m_\alpha}}{C_{m_\delta} C_{N_\alpha}} C_L$ Forward cg, low and high C_L; H limitation.

$\delta e = \delta e_{trim} + \frac{\partial \delta e}{\partial n} \Delta n$; $\frac{\partial \delta e}{\partial n} \doteq \frac{W}{q^* S} \frac{(N_m - cg)}{C_{m_{\delta_e}}}$ Forward cg critical. M and q^* effects on $C_{m_{\delta e}}$, H, N_m, δe_{trim}

$\frac{dF_e}{dn} \doteq \left(\frac{\partial F_e}{\partial n} \right)_B + \frac{G}{B} \frac{W}{S} S_e \bar{z}_e \left[\frac{C_{h_\delta}}{C_{m_\delta}} (N_m - cg) + \frac{C_{h_\alpha}}{C_{N_\alpha}} \right]$ (Reversible controls). Control forces max. at fwd cg, heavy; min. at aft cg, light. M, q^* effects, pitch-up.

F_e must lead normal acceleration. Bobweight, lag

Nose-wheel lift-off at $V_{e_{LO}} \doteq 15.8 \sqrt{\frac{W - T \left[(z_T/\ell_{cg}) + (\alpha + i_t, \text{rad}) \right]}{S \left[C_L + (C_m \bar{c}/\ell_{cg}) \right]}}$ kt. (Main gear at static defl; nose gear fully extended). See Fig. 5.

Consider ground effect for 3.3.11. Forward cg, heavy weight critical for 3.3.11 and 3.3.12.

F_e at nose-wheel lift-off: $F_e = \frac{G}{B} \frac{.00238}{2} V_{e_{LO}}^2 S_e E_e \left[C_{h_\alpha} (\alpha - \alpha_{trim}) + C_{h_\delta} \delta_{LO} \right] + (\Delta F_e)_{feel}$ (Reversible controls). Forward cg, high weight. Ground effect.

See 3.3.7; consider ground effect on all factors. Forward cg critical; high I_y may also be critical for flare.

$F_e \doteq \frac{G}{B} \cdot \frac{.00238}{2} V_{S_L}^2 S_e \bar{z}_e \left[C_{h_\alpha} (\alpha_{S_L} - \alpha_{1.2 V_{S_L}}) + C_{h_\delta} (\delta_{S_L} - \delta_{1.2 V_{S_L}}) \right] + (\Delta F_e)_{feel}$ (Reversible controls) Forward cg, heavy weight critical; ground effect.

See 3.3.2, 3.3.9

Trim change (3.3.19), buffet

$\Delta F_e \doteq \frac{G}{B} q^* S_e \bar{z}_e (C_{h_\alpha} \Delta\alpha + C_{h_\delta} \Delta\delta) + \left(\frac{\partial F_e}{\partial \delta} \right)_{feel} \Delta\delta$; $\Delta\alpha \doteq \frac{C_{L_\delta} \Delta C_m - C_{m_\delta} \Delta C_L}{C_{L_\alpha} C_{m_\delta} - C_{m_\alpha} C_{L_\delta}} \doteq \frac{-\Delta C_L}{C_{L_\alpha}}$; $\Delta\delta \doteq \frac{C_{m_\alpha} \Delta C_L - C_{L_\alpha} \Delta C_m}{C_{L_\alpha} C_{m_\delta} - C_{m_\alpha} C_{L_\delta}}$ (Applies when ΔF_e occurs before a significant speed change has occurred; reversible controls).

Find ΔF_e for $\Delta\delta_e$ to produce $-\Delta C_m (\beta)$

$\omega_{n_d} \doteq \sqrt{\frac{q C_{n'_\beta}}{C_{L_1} K_z^2 b}}$; $\zeta_d \doteq \frac{-1}{2\tau\omega_{n_d}} \left[C_{Y_\beta} + \frac{1}{2K_z^2} C'_{n_r} - \frac{K_x^2}{K_z^2} \frac{C'_{\ell_\beta}}{C'_{n_\beta}} \left(C_{L_1} - \frac{1}{2K_z^2} C'_{n_p} \right) \right]$; $\left| \frac{\phi}{V_e} \right| \doteq \frac{34}{V_e, \text{kt}} \frac{K_z^2 C'_{\ell_\beta}}{K_x^2 C'_{n_\beta}} \left(1 + \frac{1}{T_R^2 \omega_{n_d}^2} \right)^{-1/2} \frac{\text{deg}}{\text{ft/sec}}$;

$\left(\frac{\omega_{n_\phi}}{\omega_{n_d}} \right)^2 \doteq 1 - \frac{C'_{n_\delta}}{C'_{\ell_\delta}} \frac{C'_{\ell_\beta}}{C'_{n_\beta}}$ Small cg effect on ω_{n_d}; aft cg critical.

$\frac{1}{T_S} \doteq \frac{T_r q}{4 V_o \tau K_x^2} \left(\frac{C'_{\ell_\beta}}{C'_{n_\beta}} C'_{n_r} - C'_{\ell_r} \right) + C_{\ell_\beta}$ critical.

Light weight gives lower spec. speed, thus higher thrust coefficient. Small cg effect: aft cg critical. Derivatives can vary with α, M, q^*, β, T.

$\frac{d\delta_r}{d\beta} \doteq -\frac{C_{n_\beta}}{C_{n_{\delta_r}}} \left(1 - \frac{C_{n_{\delta_a}}}{C_{\ell_{\delta_a}}} \frac{C_{\ell_\beta}}{C_{n_\beta}} \right) > 0$ for aft rudder: left rudder to hold right sideslip

TABLE I (Concluded) - FLYING QUALITIES

SPEC. MIL-F-8785 PARA.	SPEC. MIL-F-8785 SUBJECT	SEE PARA. (This Report)	SEE REF
3.4.5	Static Directional Stability (Rudder Force)	III A 2	—
3.4.6	Dihedral Effect (Aileron Position)	III A 1	—
3.4.7	Dihedral Effect (Aileron Force)	III A 2	—
3.4.8	Side Force in Sideslips	III A 1	—
3.4.9	Adverse Yaw	IV D, F	13, 26
3.4.10	Asymmetric Power (Rudder Free)	III D	—
3.4.11	Directional Control (Symmetric Power)	III A	—
3.4.12	Directional Control (Asymmetric Power)	III D	—
3.4.13	Directional Control during Takeoff and Landing	III C	—
3.4.14	Directional Control to Counteract Adverse Yaw	IV D	—
3.4.15	Directional Control in Dives	III A	—
3.4.16	Lateral Control	III B 1, 2, 3	See 3.4.1 refs 30
3.5	GENERAL CONTROL AND TRIMMABILITY REQUIREMENTS		
3.5.1	Control for Spin Recovery	IV G	41,42,43,44,45,46
3.5.2	Control for Taxiing	II D, III C	—
3.5.3	Control Surface Oscillations	IV C	16,37,61,66
3.5.4	Primary Flight Control Trimmability	II A 1,3; IV A 2	61
3.5.5	Irreversibility of Trim Controls		61
3.5.6	Trim System Failure	II A 4	61
3.5.7	Roll-Pitch-Yaw Coupling	IV F	42
3.6	STALL CHARACTERISTICS		
3.6.1	Required Flight Conditions	—	—
3.6.2	Definition of Stalling Speed, V_s	—	—
3.6.3	Stall-Warning Requirements	V A	53
3.6.4	Stalling Characteristics	V A	50,51,52,54
3.7	REQUIREMENTS FOR POWER- AND BOOST-CONTROL SYSTEMS		
3.7.1	Normal Control System Operation	V D	61
3.7.2	Power or Boost Failure	V D	14,66
3.7.3	Transfer to Alternate Control System	IIA3;IIB2;IIIA2;IVB,C	—
3.7.4	Longitudinal Control on Alternate System	II C 1,2	—
3.7.5	Lateral Control on Alternate System	III B 1,2	—
3.7.6	Directional Control on Alternate System	III C	—
3.7.7	Ability to Trim on Alternate System	II A 1,3; III A 2	—
3.7.8	Feel System Failure	—	—
4	QUALITY ASSURANCE PROVISIONS		
6	NOTES		
6.1	Intended Use	—	—
6.2	Definitions	—	—
6.3	Interpretation of Qualitative Requirements	—	—
6.4	Rates of Operation of Auxiliary Devices	II A 4	—
6.5	Control Force Coordination	II C 2, III B 2, IV D	—
6.6	Artificial Stability Devices	V D	8,13,14,30,33,61
6.7	Aeroelastic, Control Equipment, etc. Effects	V D, App. I, II	61,62,63,64
6.8	Lateral Oscillations	—	—
6.9	Control Position Measurement	—	—
6.10	Engine Considerations	—	31,32
6.11	Control System Characteristics	V D	39,61

ESTIMATION SUMMARY

CRITICAL ITEMS AND ROUGH FORMULAS (SEE SECTION INDICATED TO FIND ASSUMPTIONS)

$F_r \doteq \frac{G_r}{B_r} q^* S_r \bar{z}_r \left(C_{h_{r_\beta}} \beta + C_{h_{r_{\delta r}}} \delta r \right) > 0$

$\frac{d\delta a}{d\beta} \doteq -\frac{1}{C_{\ell_{\delta a}}} \left(C_{\ell_\beta} - \frac{C_{\ell_{\delta r}}}{C_{n_{\delta r}}} C_{n_\beta} \right) > 0$ Right aileron to hold right sideslip

$F_a \doteq \frac{1}{2} \frac{G_a}{B_a} q^* S_o \bar{z}_a C_{h_{a_{\delta a}}} \delta a > 0$

$\frac{d\phi}{d\beta} \doteq -\frac{1}{C_{L_1}} \left(C_{y_\beta} - \frac{C_{y_{\delta r}}}{C_{n_{\delta r}}} C_{n_\beta} \right) > 0$ Right bank to hold right sideslip

Amount of Dutch roll in aileron rolls varies directly with $\left[1 - \left(\frac{\omega n_\phi}{\omega n_d} \right)^2 \right] \doteq \left(C_{n_{\delta a}} + \frac{I_{xz}}{I_x} C_{\ell_{\delta a}} \right) \left(C_{\ell_\beta} + \frac{I_{xz}}{I_z} C_{n_\beta} \right) / \left(C_{\ell_{\delta a}} + \frac{I_{xz}}{I_z} C_{n_{\delta a}} \right) \left(C_{n_\beta} + \frac{I_{xz}}{I_x} C_{\ell_\beta} \right)$,
inversely with ζ_d, ω_{n_d}.

Static, $C_\ell(\Delta T) \doteq 0$; Reversible controls:
$V_{MC} \doteq 17.2 \sqrt{\frac{\gamma_T \Delta T C_{\ell_\beta}^*}{b S C_{n_\beta}^T C_{\ell_{\delta a}} \delta a_{max}}}$ kt EAS; $C_{n_\beta}^T = C_{n_\beta}^* \left(1 - \frac{C_{n_{\delta a}}}{C_{\ell_{\delta a}}} \frac{C_{\ell_\beta}^*}{C_{n_\beta}^*} \right)$, $C_{n_\beta}^* = C_{n_\beta} \left(1 - \frac{C_{h_{r_\beta}}}{C_{h_{r_{\delta r}}}} \frac{C_{n_{\delta r}}}{C_{n_\beta}} \right)$, $C_{\ell_\beta}^* = C_{\ell_\beta} - \frac{C_{h_{r_\beta}}}{C_{h_{r_{\delta r}}}} C_{\ell_{\delta r}}$

$\beta_{max} \doteq \frac{-C_{n_{\delta r}} \delta r_{max}}{C_{n_\beta} \left(1 - \frac{C_{n_{\delta a}}}{C_{\ell_{\delta a}}} \frac{C_{\ell_\beta}}{C_{n_\beta}} \right)}$; Asymmetric stores: see 3.4.12

$\phi = 5°$, $C_\ell(\Delta T) \doteq 0$: $V_{MC} \doteq 17.2 \sqrt{\frac{\left| 0.0873 (W/S) \frac{\gamma_T \Delta T}{b S} \frac{C_{y_\beta}}{C_{n_\beta}^T} \right|}{\left| C_{y_{\delta r}} - \frac{C_{y_\beta}}{C_{n_\beta}^T} C_{n_{\delta r}} \right| \delta r_{max}}}$ kt EAS; $C_{n_\beta}^T = C_{n_\beta} \left(1 - \frac{C_{n_{\delta a}}}{C_{\ell_{\delta a}}} \frac{C_{\ell_\beta}}{C_{n_\beta}} \right)$

Snow or ice on runway; drag chute

Rudder to coordinate aileron rolls: $\delta r \doteq -\frac{C_{n_{\delta a}} + (I_{xz}/I_x) C_{\ell_{\delta a}}}{C_{n_{\delta r}} + (I_{xz}/I_x) C_{\ell_{\delta r}}} \delta a$, neglecting nonlinear inertial coupling and steady sideslip.

M, α effects

$\left(\frac{pb}{2V} \right)_\infty = -\frac{C'_{\ell_{\delta a}}}{C'_{\ell_p}} \left[\frac{1 - \frac{C'_{n_{\delta a}}}{C'_{\ell_{\delta a}}} \frac{C'_{\ell_\beta}}{C'_{n_\beta}}}{1 - \frac{C'_{n_p}}{C'_{\ell_p}} \frac{C'_{\ell_\beta}}{C'_{n_\beta}}} \right]$; $\dot{p}_{max} = \frac{q}{C_{L_1} K_x^2 b} C_{\ell_{\delta a}} \delta a_{max}$; $\frac{1}{T_R} \doteq \frac{-1}{4\tau K_x^2} \left[C'_{\ell_p} - \frac{C'_{\ell_\beta}}{C'_{n_\beta}} (C'_{n_p} - 2K_z^2 C_{L_1}) \right]$; See Fig. 8 for time to bank.

Crosswind
Mass balance, control system natural frequency, friction and other nonlinearities. Babweights.

Elevator tab: $\delta t \doteq \left[\frac{(C_L + C_{L_\alpha} \alpha_o) C_{m_\alpha} + (C_{m_o} + \frac{T}{q^* S} \frac{z_T}{\bar{c}} - C_{m_\alpha} \alpha_a) C_{N_\alpha}}{C_{m_\delta} C_{N_\alpha} - C_{L_\delta} C_{m_\alpha}} \right] \frac{C_{h_\delta}}{C_{h_{\delta t}}} - \frac{C_{h_o} + \frac{H_{test}}{q^* S \bar{c}}}{C_{h_{\delta t}}}$

High H, q^*
Sensitive regions; i.e., low stability. Runaway: pilot's ability to stop, and remaining controllability (force, deflection).

$(\omega_{n_{sp}}^2 - I_1 \beta^2 K \omega_{n_d}^2 - I_3 p^2) \gg (I_1 C_{y_\beta} + \frac{C_{m_q}}{2K_y^2})(I_3 C_{N_\alpha} - \frac{C_{n_r}}{2K_z^2}) \frac{p^2}{4\tau^2}$ $\left(I_1 = \frac{I_z - I_x}{I_y}, I_3 = \frac{I_y - I_x}{I_z} \right)$ for freedom from inertial coupling.

Stalls out of turns can be more severe than level-flight stalls.
Stall approach technique, thrust coefficient, cg, normal acceleration, as well as weight and $C_L(\alpha)$ can have appreciable effects.
Low speed (light weight, usually high-lift devices) critical.
Aft cg, stalls from accelerated flight usually critical.

Hinge moment limiting at high q^*.
Hinge moment limiting at high q^*.
Possibility of transients, remaining maneuverability, control forces for return, descent and landing.
Dive recovery
Control force for rolling.
Control force in crosswind landing.

Effects of failures that are not extremely remote; for example, "q^*" bellows, trim.

Compare $\frac{2}{3}(n_L - 1) \frac{dF_s}{dn}$, $\frac{2}{3} F_{a_{max}}(\delta, \rho)$, F_r

---

Aeroelastic modes can alter the response at pilot or sensor location, also can couple with flight control system.

Cockpit control deflection is a function of surface position, linkage (passible nonlinearities, stretch, dynamics), structure deformation, series trim or stability augmentation.
Fuel control effect on cg, inlet control, automatic feathering, etc: normal operation and failure modes.

$C'_{n_i} \doteq \frac{C_{n_i} + (I_{xz}/I_x) C_{\ell_i}}{1 - (I_{xz}^2/I_x I_z)}$; $C'_{\ell_i} \doteq \frac{C_{\ell_i} + (I_{xz}/I_z) C_{n_i}}{1 - (I_{xz}^2/I_x I_z)}$; $i = \beta, p(b/2V), r(b/2V), \delta a, \delta r$.

$\tau = \frac{(W/S)}{\rho g V}$; $C_{L_1} \doteq \frac{W}{q^* S}$

SECTION II

STATIC LONGITUDINAL STABILITY AND CONTROL

A. LONGITUDINAL TRIM

1. General Remarks

Stability is the tendency to return to the operating point, or trim condition, after a disturbance. This section outlines methods for calculating these operating points. In general, requirements specify stability in terms of departure from steady, straight, wings-level flight. Since the static stability concept implies constant throttle setting, and throttle setting for steady flight varies with speed, data obtained from the trim equations are not necessarily indicative of stability or lack of it (Section II B).

Starting with general nonlinear equations, successive simplifications are introduced to reduce computational effort. Choice of a method depends upon accuracy of input data, desired accuracy of the result, and any peculiarities of mission or vehicle. Usually it will be possible to simplify the more complicated relations a priori by omitting negligible terms, assuming piecewise linearity, etc.

Steady flight here infers constant speed. For straight, steady flight, additionally, all angular rates are zero but flight-path orientation (γ, ψ) remains arbitrary unless further specified. Trim may have two meanings, representing nulls of either airframe or control system. In general, the former interpretation applies here; zero pilot force is indicated by "force trim." With artificial feel, force trim does not generally imply hinge-moment trim. The distinctions are obvious but should be kept in mind.

The lift, drag, and moment equations are basic in establishing longitudinal trim conditions. For force trim an additional equation is added. In a fairly general form the four equations for a reversible control system and steady, straight, symmetric flight[3] are:

$$L = \left[C_L(\alpha, \delta, i_H, \delta t) \right] \frac{1}{2} \rho V^2 S = W \cos\gamma - T \sin(i_T + \alpha) \quad (1)$$

$$D = \left[C_D(\alpha, \delta, i_H, \delta t) \right] \frac{1}{2} \rho V^2 S = T \cos(i_T + \alpha) - W \sin\gamma \quad (2)$$

$$M = \left[C_m(\alpha, \delta, i_H, \delta t) \right] \frac{1}{2} \rho V^2 S \bar{c} = -T z_T \quad (3)$$

$$H = \left[C_h(\alpha, \delta, i_H, \delta t) \right] \frac{1}{2} \rho V^2 S_e \bar{c}_e = -H_{\text{feel + unbalance + breakout, etc}} . \quad (4)$$

[3] Equations for other cases can be derived simply from the general dynamic equations of motion such as given in References 3 and 4. For example, consider "steady" wings-level pitching, with constant angle of attack and constant pitch rate. Besides the obvious addition of pitch-rate derivatives to all of the equations, Equations 1 and 2 become:

$$L + T \sin(i_T + \alpha) - W \cos\gamma = mV\dot{\gamma}$$

$$D - T \cos(i_T + \alpha) + W \sin\gamma = \dot{V}$$

(Note that $\dot{\theta} = \dot{\gamma} + \dot{\alpha} = \dot{\gamma}$, and that in our flight-path axis system $w = 0$. Reference 16 discusses the principal effects of "steady" longitudinal acceleration and some other cases of possible interest.)

Some quantities may not be present (for example, i_H or δt), and others may be negligible. Control through a tab requires an additional equation to account for tab hinge moments (See Appendix II). The functional terms are, in general, dependent also upon Mach number, dynamic pressure, and thrust (and, in ground effect, upon height above the ground); thrust at constant throttle varies with ρ and V, and sometimes with α.

Often a simpler method will work, but the nonlinear equations can be solved graphically or by machine. To illustrate, a graphical procedure is presented to give δe (V) in straight, steady flight, with no horizontal stabilizer adjustment but hinge moments balanced by a trim tab. Equations 1 through 4 become, in our example,

$$\left[C_L(\alpha) + C_L(\delta) + C_L(\delta t) \right] q^* S = W \cos\gamma - T \sin(i_T + \alpha) \tag{5}$$

$$\left[C_D(\alpha) + C_D(\delta) + C_D(\delta t) \right] q^* S = T \cos(i_T + \alpha) - W \sin\gamma \tag{6}$$

$$\left[C_m(\alpha) + C_m(\delta) + C_m(\delta t) \right] q^* S\bar{c} = -Tz_T \tag{7}$$

$$\left[C_h(\alpha) + C_h(\delta) + C_h(\delta t) \right] q^* S_e \bar{c}_e = -H_{feel} \tag{8}$$

Choice of altitude (ρ), and V determines dynamic pressure q^* and Mach number M in a standard atmosphere. The functional relationships normally are defined in terms of these quantities (aeroelastic and compressibility effects), leaving $\gamma, \alpha, \delta, T$, and δt unknown. (A quantity depending on thrust can be plotted as a family of curves with thrust as a parameter.) Vehicle weight and center of gravity must also, of course, be specified; and the pitching-moment reference center must coincide with the center of gravity. H_{feel} is described in Section IIB2. To make the problem determinate, choose γ (for example, level flight) or T (for example, maximum thrust). Here we will choose γ, although the choice of T often results in a simpler problem. The procedure is then: (1) From Equation 7, plot $\delta (T = 0)$ versus α with δt as a parameter. Do the same with Equation 8. Then by superimposing the two families of curves, points where curves for the same δt cross define the locus of δ versus α for $T = 0$ (the dashed line of Figure 2). Repeat for other values of thrust. The

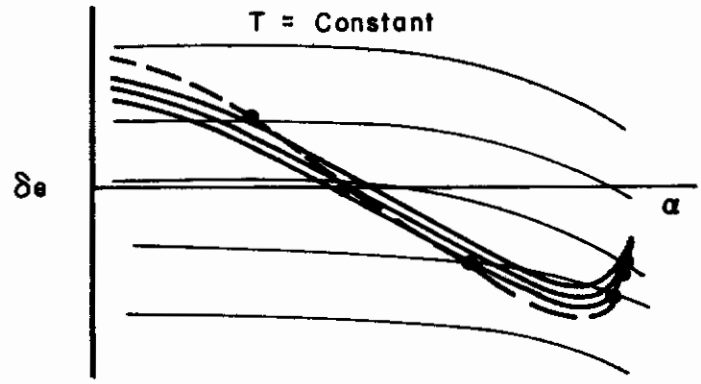

Figure 2. Determination of δe Versus α at Constant Thrust

result is a set of curves of δ versus α with thrust as a parameter and δt indexed along the curves; (2) Find $C_L(\delta)$, $C_L(\delta t)$, $C_D(\delta)$, and $C_D(\delta t)$ as functions of α and T, if necessary. Then, knowing $\delta e(\alpha,T)$ and $\delta t(\alpha,T)$ from the last step, solve Equations 5 and 6 separately for $\alpha(T)$ and plot as in Figure 3. The intersection of the two curves defines the operating point for the given q*.

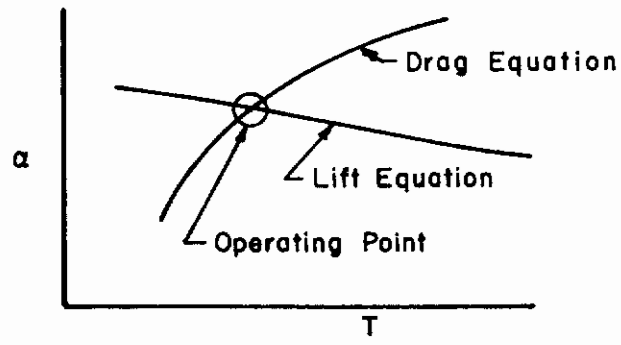

Figure 3. Determination of Operating Point

The accuracy of input data normally does not warrant such complexity except for gross nonlinearities in addition to $C_D(\alpha^2)$.

2. Trim Drag

The first simplification is to assume at least piecewise linearity of all functional relationships except $C_D(\alpha)$ and to consider only the change in trim angle of attack in calculating trim drag. In the absence of a handy performance specialist the method below can be used to estimate the trimmed drag coefficient. Considering γ, α, δ, and T in Equations 1 through 3, after linearizing,

$$C_D = C_{D_o}(\delta = 0) + \sigma C_{D_{C_L^2}} C_L^2 + C_D(\delta)$$

$$\doteq C_{D_o}(\delta = 0) + \sigma C_{D_{C_L^2}} C_L^2$$

where

$$C_L = \frac{1}{q^* S}\left[W\cos\gamma - T\sin(i_T + \alpha)\right]$$

$$\sigma = \left[\frac{1 + \dfrac{C_{L_\delta}}{C_{m_\delta} C_L}\left(C_{m_o} + \dfrac{T}{q^* S}\dfrac{z_T}{\bar{c}}\right)}{1 - \dfrac{C_{L_\delta}}{C_{m_\delta}}\dfrac{C_{m_\alpha}}{C_{L_\alpha}}}\right]^2 > 1$$

T and α both appear explicitly above, but since the correction factor σ is not normally too much greater than 1, untrimmed drag and lift equations can be used to find σ :

$$\alpha \doteq \frac{C_L}{C_{L_\alpha}} + \alpha_o$$

$$T \doteq \left[q^*S\left(C_{D_o} + C_{D_{C_L{}^2}} C_L{}^2\right) + W \sin\gamma \right] \frac{1}{\cos(i_T + \alpha)}$$

The correction factor σ is a function of center-of-gravity position (C_{m_α}). As shown in the following, δ can be approximated similarly if desired; $C_D(\delta)$ is most negligible for long tail length. Additional simplification is often possible. The expression $\sigma < 1$ represents an upload on an aft tail or elevon; the resulting decrease in drag is usually about compensated by tail or elevon drag and so is normally neglected in performance analyses. The extension to stabilizer trim, etc. is obvious. Having thus disposed of the only universal nonlinearity and the drag equation, we proceed to write analytical expressions for the solutions.

3. Linear Trim Equations

With linear derivatives, γ such that $\sin\gamma \doteq \gamma$ and $\cos\gamma \doteq 1$, and $i_T + \alpha$ such that $\sin(i_T+\alpha) \doteq i_T + \alpha$ and $\cos(i_T+\alpha) \doteq 1$, Equations 1, 3, and 4 become completely linear. The equations for zero pilot force in straight, steady flight with fixed i_H are, in matrix form:

$$\begin{bmatrix} C_{L_\alpha} + \frac{T}{q^*S} & C_{L_\delta} & 0 \\ C_{m_\alpha} & C_{m_\delta} & C_{m_{\delta t}} \\ C_{h_\alpha} & C_{h_\delta} & C_{h_{\delta t}} \end{bmatrix} \begin{pmatrix} \alpha_{trim} \\ \delta_{trim} \\ \delta t_{trim} \end{pmatrix} = \begin{pmatrix} \frac{W\cos\gamma - Ti_T}{q^*S} + C_{L_\alpha}\alpha_o \\ -C_{m_o} - \frac{T}{q^*S}\frac{z_T}{\bar{c}} + C_{m_\alpha}\alpha_o \\ -C_{h_o} - \frac{H_{feel,etc}}{q^*S_e\bar{c}_e} \end{pmatrix} \triangleq \begin{pmatrix} C_L^* \\ -C_m^* \\ -C_h^* \end{pmatrix}$$

where $C_{L_{\delta t}}$ is neglected and where all quantities are evaluated at the trim conditions (W, cg, V, ρ, T, etc.). C_{h_o} is explained in Footnote 4. H_{feel} is described in Section IIB2. Solutions are presented in terms of the trim characteristic determinant, Δ_t:

$$\Delta_t \triangleq \begin{vmatrix} C_{L_\alpha} + \frac{T}{q^*S} & C_{L_\delta} & 0 \\ C_{m_\alpha} & C_{m_\delta} & C_{m_{\delta t}} \\ C_{h_\alpha} & C_{h_\delta} & C_{h_{\delta t}} \end{vmatrix}$$

$$= \underbrace{C_{h_{\delta t}}\left[\left(C_{L_\alpha} + \frac{T}{q^*S}\right)C_{m_\delta} - C_{m_\alpha}C_{L_\delta}\right]}_{\text{major term}} - C_{m_{\delta t}}\left[\left(C_{L_\alpha} + \frac{T}{q^*S}\right)C_{h_\delta} - C_{L_\delta}C_{h_\alpha}\right]$$

[4] Take, for a rigid, tailed airplane, the following equalities:

$$\alpha_H = i_H + \alpha - \epsilon$$

$$C_{h_o} = C_h(\alpha_H = 0) + C_{h_{i_H}} i_H + \frac{1}{\eta} C_{h_{\alpha_H}}(\alpha_o - \epsilon_o)$$

For a flexible airplane the last two terms can be altered to account for static aeroelasticity.

Using Cramer's rule,

$$\alpha_{trim} = \frac{1}{\Delta_t}\left[\underbrace{C_{h_{\delta_t}}(C_L^* C_{m_\delta} + C_m^* C_{L_\delta})}_{\text{major term}} - C_{m_{\delta_t}}(C_L^* C_{h_\delta} + C_h^* C_{L_\delta})\right] \doteq \frac{C_L^* C_{m_\delta} + C_m^* C_{L_\delta}}{C_{N_\alpha} C_{m_\delta} - C_{m_\alpha} C_{L_\delta}} \doteq \frac{C_L^*}{C_{N_\alpha}}$$

$$\delta_{trim} = \frac{1}{\Delta_t}\left\{C_{m_{\delta_t}}\left[C_h^*\left(C_{L_\alpha} + \frac{T}{q^* S}\right) + C_L^* C_{h_\alpha}\right] - \underbrace{C_{h_{\delta_t}}\left[C_m^*\left(C_{L_\alpha} + \frac{T}{q^* S}\right) + C_L^* C_{m_\alpha}\right]}_{\text{major term}}\right\} \doteq -\frac{C_L^* C_{m_\alpha} + C_m^* C_{N_\alpha}}{C_{m_\delta} C_{N_\alpha} - C_{L_\delta} C_{m_\alpha}}$$

$$\delta t_{trim} = \frac{1}{\Delta_t}\left\{\underbrace{C_L^*\left[C_{m_\alpha} C_{h_\delta} - C_{h_\alpha} C_{m_\delta}\right]}_{\text{always important}} - C_m^*\left[C_{h_\alpha} C_{L_\delta} - \left(C_{L_\alpha} + \frac{T}{q^* S}\right) C_{h_\delta}\right] -\right.$$

$$\left.\underbrace{- C_h^*\left[\left(C_{L_\alpha} + \frac{T}{q^* S}\right) C_{m_\delta} - C_{m_\alpha} C_{L_\delta}\right]}_{\text{involves artificial feel., flaps}}\right\} \doteq \frac{(C_L^* C_{m_\alpha} + C_m^* C_{N_\alpha}) C_{h_\delta}}{(C_{m_\delta} C_{N_\alpha} - C_{L_\delta} C_{m_\alpha}) C_{h_{\delta_t}}} - \frac{C_h^*}{C_{h_{\delta_t}}}$$

Aside from the more obvious assumptions, the approximations assume that $T \doteq D$, so that

$$C_{L_\alpha} + \frac{T}{q^* S} = C_{L_\alpha} + C_D = C_{N_\alpha}$$

For trim through an adjustable stabilizer, $C_{L_{i_H}} \Delta i_H$ can have an important secondary contribution. In that case Δi_H replaces δt throughout and the following terms are added to the most rigorous trim solutions only, as follows:

$$\Delta\Delta_t = C_{L_{i_H}}\left[C_{m_\alpha} C_{h_\delta} - C_{h_\alpha} C_{m_\delta}\right]$$

$$\Delta(\alpha\Delta_t) = C_{L_{i_H}}\left[C_h^* C_{m_\delta} - C_m^* C_{h_\delta}\right]$$

$$\Delta(\delta\Delta_t) = C_{L_{i_H}}\left[C_m^* C_{h_\alpha} - C_h^* C_{m_\alpha}\right]$$

$$\Delta(\Delta i_H \Delta_t) = 0$$

(a.) Nonzero Pilot or Actuator Force

For a given trim setting (Δi_H and δt) or for an irreversible control system, we will still have, in general:

$$\begin{bmatrix} C_{L_\alpha} + \frac{T}{q^*S} & C_{L_\delta} \\ C_{m_\alpha} & C_{m_\delta} \end{bmatrix} \begin{pmatrix} \alpha \\ \delta \end{pmatrix} = \begin{pmatrix} \frac{W\cos\gamma - Ti_T}{q^*S} + C_{L_\alpha}\alpha_o - C_{L_{i_H}}\Delta i_H \\ -C_{m_o} - \frac{T}{q^*S}\frac{z_T}{\bar{c}} + C_{m_\alpha}\alpha_o - C_{m_{i_H}}\Delta i_H - C_{m_{\delta t}}\delta t \end{pmatrix} \triangleq \begin{pmatrix} C_L^+ \\ -C_m^+ \end{pmatrix}$$

$$\Delta^+ \triangleq (C_{L_\alpha} + \frac{T}{q^*S})C_{m_\delta} - C_{m_\alpha} C_{L_\delta} \doteq C_{N_\alpha} C_{m_\delta}$$

$$\alpha = \frac{1}{\Delta^+}\left[C_L^+ C_{m_\delta} + C_m^+ C_{L_\delta}\right] \doteq \frac{C_L^+}{C_{N_\alpha}}$$

$$\delta = \frac{-1}{\Delta^+}\left[(C_{L_\alpha} + \frac{T}{q^*S})C_m^+ + C_{m_\alpha} C_L^+\right] \doteq -\frac{C_L^+ C_{m_\alpha} + C_m^+ C_{N\alpha}}{C_{m_\delta} C_{N_\alpha}} \doteq -\frac{C_L^+ C_{m_\alpha}}{C_{m_\delta} C_{N_\alpha}}$$

To find the elevator stick force F_e for a reversible control system, solve the hinge-moment equation for C_h and convert; for an irreversible system, the artificial feel characteristics plus friction, preload, etc. determine F_e (See Section IIB2).

For an all-moving tail, substitute δH for δ and retain i_H if needed as a reference setting for δH. For a canard controller, δ becomes δc and it may be necessary to consider the effect of canard-induced downwash on the wing C_L (α). For elevons the equations hold as written, but C_{L_δ} becomes more important and C_{D_δ} may have to be considered.

The mechanization of stability augmentation may conceivably affect the relative settings of elevator and tab for hinge-moment trim, but, still, the pitching- and hinge-moment equations have to balance. If necessary, stability augmentation effects can be treated as equivalent derivatives (See, for example, Section IIC1) in any of the equations above. For the effects of control tabs, see Appendix II.

4. Trim Changes; Release of Stores

Most thrust, secondary control, or configuration changes are fairly rapid, being essentially completed within a very few seconds of initiation. In those cases the trim change can be calculated from the force-trim equations at constant speed (See Table I). Throttle, speed brakes, and landing gear normally fall in this category.

Flap retraction, however, on some aircraft is a slow process during which significant speed changes occur. In such cases a step-by-step calculation procedure is suggested. For example, consider flap retraction in a climbout at constant throttle, constant rate of climb or constant attitude; in any case a flight procedure must be specified as well as a trim setting; see the applicable specification.

The trim equations, modified to include acceleration along the flight path, yield the initial longitudinal acceleration and the control force. Take the new flight conditions one increment of time later: $V_1 = V_0 + a_x \Delta t, \rho(h_1) = \rho(h_0 + \dot{h}\Delta t)$, $\delta_{F_1} = \delta_{F_0} + \dot{\delta}_F \Delta t$. Again the trim equations (with new derivatives, thrust, angle of zero lift, etc.) yield the longitudinal acceleration and the control force. Continue the process until equilibrium is reached or the control force peaks. Such a method should give good results if changes during the time increment are not excessive, although it may not reproduce the effects of short-period or phugoid oscillations excited in the actual case.

Large thrust changes, full deflection of large speed brakes, etc. obviously can involve rapid speed changes. A quick estimate of acceleration effects can be made by taking one step of five seconds (the time limit of Reference 15). If a force appreciably higher than allowable is calculated or thought possible, the analysis can be repeated with smaller steps.

Drag chutes tend to trail at the local flow angle. Thus, a stable drag chute imparts a force at its attachment, proportional to dynamic pressure at the chute location in the wake, at roughly the angle ϵ below the flight path (where the downwash angle ϵ is also taken at the chute location). Thrust reversers can disturb the flow over the vehicle severely, thus changing stability and control derivatives, local flow angles, and dynamic pressures.

Release of stores involves weight changes as well. (Finding the forces and moments caused by opening armament bay doors, etc. is another subject but, once found, these effects are amenable to analysis.) The trim changes could be found by step-by-step calculation, but for large trim changes it is better to get a time history from the dynamic equations of motion. In most situations the linear equations of Section IV[5] will do. The operating point could be the final trim condition, and initial conditions those at release. Initial conditions are Laplace transformed as follows (See Reference 17):

$$\mathcal{L}\left[y(t)\right] = Y(s)$$

$$\mathcal{L}\left[\dot{y}(t)\right] = sY(s) - y(0+)$$

$$\mathcal{L}\left[\ddot{y}(t)\right] = s^2 Y(s) - y(0+)s - \dot{y}(0+)$$

where, as stated above, Y(s) is the Laplace transform of y(t); t = 0+ is the instant after store release. These terms are incorporated into the equations of motion developed later (Section IV). Extraction or pickup of heavy cargo is a more complicated problem, but even here it is usually sufficient to consider the extracted load as a forcing function on the vehicle. Equations can be formulated analogous to the two-mass problem found in any text on dynamics (for example, the work cited above), or the equations of Reference 18 might be used, for a more comprehensive analysis.

[5] Note that in the trim equations x stays with the relative wind, but in the dynamic equations x is fixed in the body once the rotation starts.

B. SPEED STABILITY

Static longitudinal stability has been variously defined. Here we take the definition used in the military flying qualities requirements (References 15 and 19): In a stable vehicle the cockpit-longitudinal-control force and deflection required to maintain straight, steady flight at a speed different from the trim speed are in the same sense required to initiate the speed change, that is, airplane-nose-down control to fly faster, nose-up to fly slower.

"Stick-fixed" stability refers to the variation in control deflection, "stick-free" to control force. Usually control-surface deflection is equivalent to cockpit-control deflection in determining static stability. As noted earlier, longitudinal stability is customarily defined with throttle and trim control deflections fixed at their steady-flight operating-point settings.

This definition reduces exactly[6] (for linear equations) to the concept of static stability as a limiting case of dynamic stability (for example, Reference 20). Except in simple cases, however, it differs from the angle-of-attack stability of Reference 3 and the lift-coefficient stability of Reference 21. Besides its use in in requirements, the definition adopted appears the most natural one and the most generally applicable.

Static longitudinal stability is generally a strong function of center of gravity location. The center of gravity at which neutral stability is evidenced is called the "neutral point;" the distance (in percent mean aerodynamic chord) that this neutral point lies behind the actual center of gravity is the "static margin."

Most practical airplane configurations are deficient in the transonic range. Current military flying-quality specifications do not always require static stability transonically, but place limitations principally on ΔF_e and $d F_e/dV$. Thus it is often useless to calculate neutral points in an unstable transonic range.

Normally the neutral point is evaluated only for excursions from level-flight trim and from trim at maximum rate of climb.

Note that all of these calculations must include any effects of compressibility, aeroelasticity, and engine thrust or power, and that the reference center for the moment derivatives must coincide with the center of gravity being considered.

1. Stick Fixed

There are several methods by which the stick-fixed neutral point and static stability or static margin can be found. The most graphic of these methods uses plots of control-surface position required for straight, steady flight versus airspeed. First, find operating-point trim and throttle settings from the trim equations of Section IIA. Then at other speeds the elevator deflection is found from the trim lift and pitching-moment equations at constant trim setting, with allowance for thrust variation with speed, etc. at constant throttle. Any coefficient or derivative changes with speed must be incorporated. Normally, changes in γ can be neglected. If the drag equation is to be considered, σ can be recalculated at off-operating-point conditions or a linear drag variation taken over

[6] By ignoring the effect of density gradient; see Section IVB1.

a limited range of angle of attack. The control-surface deflection is obtained for two or more center-of-gravity positions over the speed range of interest. Ths stick-fixed neutral point is then found by plotting the slope $d\delta/dV$ against center of gravity location. The neutral point is that center of gravity at which the slope is zero.

An exact solution for the stick-fixed neutral point can also be determined by means of the longitudinal characteristic equation.[6] The characteristic equation is generally of fourth degree with two pairs of complex roots--one pair indicating the stability of short-period motions and the other, long-period motions. The stick-fixed static stability is representative of the stability of the long-period motions: when the center of gravity is moved aft to the stick-fixed neutral point, the long-period motion degenerates into two real roots, one of them zero. This occurs when the zero-degree term of the characteristic equation becomes zero. Thus, the stick-fixed neutral point can be found by determining the center of gravity for which (in fairly complete linear form)

$$E\alpha\cos\gamma_o\left[(C_{L_\alpha}+C_D)\left(\frac{V_o}{2}\frac{\partial C_m}{\partial u}-\frac{T}{q^*S}\frac{z_T}{z}+\frac{z_T}{\rho V_o S\bar{c}}\frac{\partial T}{\partial u}\right)-C_{m_\alpha}\left(C_L+\frac{V_o}{2}\frac{\partial C_L}{\partial u}+\frac{\sin\xi}{\rho V_o S}\frac{\partial T}{\partial u}\right)\right]$$

$$+\sin\gamma_o\left[\left(\frac{V_o}{2}\frac{\partial C_m}{\partial u}-\frac{T}{q^*S}\frac{z_T}{\bar{c}}+\frac{z_T}{\rho V_o S\bar{c}}\frac{\partial T}{\partial u}\right)\left(C_L-C_{D_\alpha}\right)+C_{m_\alpha}\left(C_D+\frac{V_o}{2}\frac{\partial C_D}{\partial u}-\frac{\cos\xi}{\rho V_o S}\frac{\partial T}{\partial u}\right)\right]=0$$

where the subscript o refers to the operating point, the trim condition, and $\xi = i_T + \alpha_{trim}$. The expression above can be evaluated and plotted as a function of center of gravity to find the center of gravity at which the function is zero. Simplifications for level flight, constant thrust, incompressible flow, etc. are obvious.

As indicated, in many situations a number of other simplifications are possible. Negligibly small and nonexistent terms may be dropped to make the expressions more tractable. For the simplest forms, at least, the stick-fixed neutral point can then be found readily by setting the total derivative $d\delta/dC_L$, evaluated in straight steady, level flight ($C_L = \left[W - T\sin(i_T + \alpha)\right]/q^*S$) at constant throttle equal to zero and finding the center of gravity necessary for the differential equation to hold (for example, References 3 and 21). Normally C_{m_α} is the only term grossly affected by small shifts in center of gravity, and it varies linearly with fore-and-aft center of gravity position. The very simplest neutral-point approximation is

$$\frac{-x_{ac}}{\bar{c}} \doteq -\frac{C_{m_\alpha}}{C_{L_\alpha}}$$

or

$$N_o\,(\%\,\bar{c}/100) \doteq \frac{(-x'_{ref})}{\bar{c}} - \frac{C_{m_\alpha}}{C_{L_\alpha}}$$

where $(-x'_{ref})$ is the moment-reference-center distance aft of the mean aerodynamic chord leading edge. However, this method is often a gross oversimplification.

2. Stick Free

Stick-free static longitudinal stability refers to the variation with airspeed of control force (discounting breakout force) required to maintain straight, steady flight. In configurations that have irreversible control systems, stick-free static stability is generally identical to the stick-fixed static stability treated in Section IIB1 (Flight control system nonlinearities and certain types of feel and augmentation, however, can make a difference.) The treatment that follows deals with both reversible and irreversible control systems. A convenient method of determining stick-free static stability, static margin, or neutral point uses the variations of control-surface position required for steady flight, Section IIB1; the corresponding stick force is given by the equations under "Reversible Longitudinal Control". Figure 4 shows the sign conventions, which agree with those of Reference 3 but not Reference 21. Negative dF_e/dV is stable. Stick-free stability is also indicated by variation with speed of tab deflection required for stick-force trim.

Stick-free static stability is often most critical at very low speeds, where the angle of attack is high and power effects are strong. Care should be taken in this case to account for nonlinear hinge-moment characteristics, which are quite prevalent. Test data should be used wherever possible. The stick-free neutral point can be found by plotting the calculated stick force versus speed, with center of gravity as the parameter, over the speed range of interest, and cross-plotting the slopes against center of gravity position. The center of gravity at which the slope is zero is the stick-free neutral point.

Although static stick-free stability in the transonic regime is not generally required by current military flying-quality specifications the force reversal must be mild, gradual, and not seriously objectionable to the pilot. The permissible reversal is defined by specification. Static stick-free stability in the transonic range is required by the military services only of airplanes with cruising speeds or mission requirements necessitating prolonged transonic operation. Such stability may be obtained aerodynamically or, for example, by an incremental $C_m(M)$ transonically through the longitudinal control surface.

(a) Reversible Longitudinal Control

The control force, including the effect of boost, is given by

$$F_e = \frac{G}{B}\left\{\frac{1}{2}\rho V^2 S_e \bar{c}_e \left[C_{h_e}(\alpha,\delta,\delta_t,\ldots)\right]\right\} + (\Delta F_e)_{feel}$$

~~$C_h(\alpha) - C_h(\alpha_{trim}) + C_h(\delta) - C_h(\delta_{trim})$~~

~~where the subscript "trim" refers to the flight condition in which force is trimmed to zero;~~ $(\Delta F_e)_{feel}$ includes friction and preload as well as incremental forces from mass unbalance, springs, bobweights, etc. (See, for example, References 3, 21, 22, and 23). A bobweight not statically balanced or a downspring adds a constant incremental F_e that, as shown in Section IVC1 increases the static stick-free speed stability. The quantities α, δ and their trim values are determined in Section IIA. ~~Often C_{h_α} is designed to be small, and for linear hinge moments $C_h(\alpha) - C_h(\alpha_{trim}) = C_{h_\alpha}(\alpha - \alpha_{trim})$, etc. Where compressibility or aeroelastic effects are important, $C_h(\delta - \delta_{trim})$ etc. must be evaluated at the applicable Mach number, not the trim Mach number;~~ G can change with q* because of cable stretch, etc.

as is true for C_{h_α}. For linear hinge moments, $C_{h_e}(\alpha,\delta,\delta_t,\ldots) = C_{h_0} + C_{h_\alpha}\alpha + C_{h_\delta}\delta + C_{h_{\delta_t}}\delta_t + \ldots$

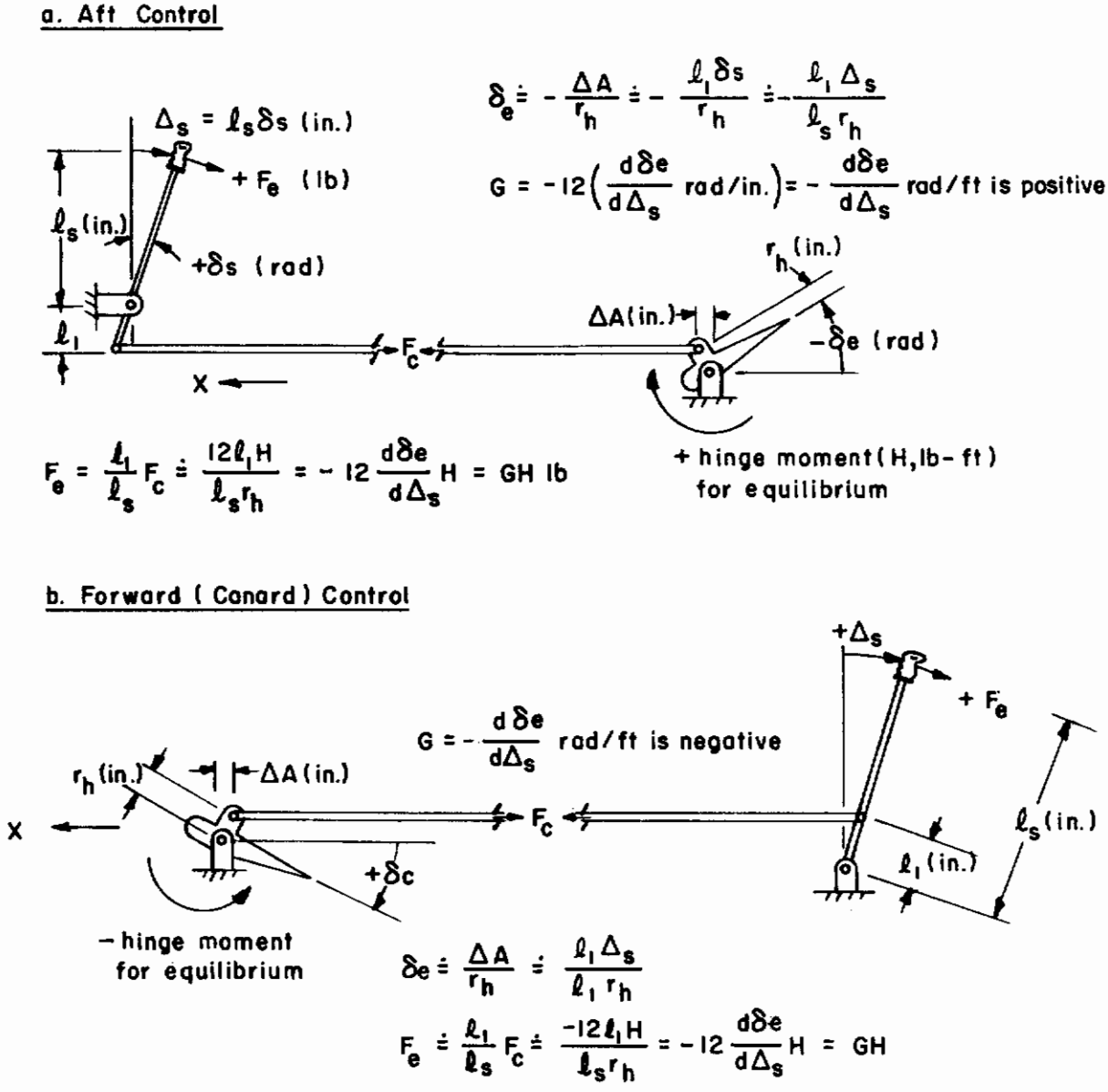

Figure 4. Longitudinal Control Force Related to Surface Deflection

The control-surface mass-unbalance effect in 1-g flight, for either forward or aft control, is

$$\Delta F_e = -\frac{G}{B} W_e \bar{r}_e$$

where $\bar{r}_e$ is the distance, normal to the hinge line, of the elevator center of gravity forward of the hinge line. A downspring contributes a constant $\Delta F_e = (G/B) H_D$ where H_D is the downspring hinge moment. A nonstatic-balanced bobweight contributes $\Delta F_e = (\partial F_e / \partial n)_B$. For the effects of control tabs see Appendix II, which gives examples of tabs and their treatment.

(b.) Irreversible Longitudinal Control

Mechanization may vary, but normally, in the absence of any special feel such as $\partial F_e / \partial M$, a spring provides $F_e(\delta s)$; add trim, friction, and preload forces. Feel bobweights can alter stick-free speed stability. A "q-spring" ($F_e = Kq * \delta$) can eliminate the large change in force sensitivity with dynamic pressure inherent in a constant-rate spring at the expense of some added complexity. Nonlinear springs are also used for this purpose, but some of the nonlinear effects are undesirable; for example, lightening of stick force per g at high load factor, and unequal response to up and down control. Similarly, G may be nonlinear.

The comments on reversible control apply here, too. Maximum deflection is limited, of course, by maximum actuator output or control stops.

C. MANEUVERING FLIGHT

Although "maneuvering stability" concerns the control force and surface deflection required to effect a change of steady normal acceleration, the term also indicates the stability of the vehicle's short-term response to any longitudinal disturbance and the frequency of the short-period longitudinal oscillation; it can be visualized as a pitching spring rate. Maneuvering stability is easy to measure at large departures from 1-g flight, and it more or less generally guarantees against short-period dynamic instability in large-perturbation maneuvers. Maneuvering stability is usually investigated in level flight.

To agree with this rationale, $d\delta/dn$ and dFe/dn are normally taken in wings-level flight as the vehicle passes through a horizontal attitude at the trim speed with steady normal acceleration. This practice is followed herein. Trim and throttle settings are those for level, 1-g flight at the same speed, altitude, weight, and center of gravity.

Define nW as the force applied normal to the flight path (positive "up"). (Note that an on-board accelerometer gives a slightly different n, in terms of body axes.) With $\dot{\alpha} = 0$ in a steady wings-level pullup, the normal acceleration is

$$\begin{aligned} a_z &= -(n - \cos\gamma \cos\phi)g \\ &= -(n - \cos\gamma)g \\ &= Vq \end{aligned}$$

Passing through level flight, $\cos\gamma = 1$. Then the pitch rate q is $(g/V)(n - 1)$; while in a coordinated level turn it is $[g/V]\left[n - (1/n)\right]$ since then $n = 1/\cos\phi$. To find $d\delta/dn$ in a level turn, then use

$$\left(\frac{d\delta}{dn}\right)_{\text{level turn}} = \frac{d\delta_e}{dq}\left(\frac{dq}{dn}\right)_{\text{level turn}} = \left(1 + \frac{1}{n^2}\right)\left(\frac{d\delta}{dn}\right)_{\text{pullup}}$$

The stick-fixed maneuver margin is the distance (in percent $\bar{c}$) of the center of gravity forward of the stick-fixed "maneuver point." Although stick-fixed maneuvering stability is required by current military handling-quality specifications, the degree required is not specified. A minimum maneuvering margin of 5 percent mean aerodynamic chord is generally desirable.

1. Stick Fixed

Stick-fixed maneuvering stability in symmetrical pullups can be found by solving the normal-acceleration equation of Section II together with the linear incremental lift and moment equations.

Assuming T invariant with α,

$$mg(n-1) = (C_{L_\alpha}\Delta\alpha + C_{L_q}\frac{q\bar{c}}{2V} + C_{L_\delta}\Delta\delta)q^*S + T\left[\sin(i_T + \alpha_{trim} + \Delta\alpha) - \sin(i_T + \alpha_{trim})\right]$$

$$\doteq \left[(C_{L_\alpha} + \frac{T}{q^*S})\Delta\alpha + C_{L_q}\frac{q\bar{c}}{2V} + C_{L_\delta}\Delta\delta\right]q^*S$$

$$\Delta M = (C_{m_\alpha}\Delta\alpha + C_{m_q}\frac{q\bar{c}}{2V} + C_{m_\delta}\Delta\delta)\,q^*S\bar{c} = 0$$

(in the approximate form with $T \doteq D$ and small $i_T + \alpha$). The result is

$$\frac{d\delta}{dn} = \left(\frac{n-1}{\Delta\delta}\right)^{-1} = \frac{-W}{q^*S}\left[\frac{\dfrac{C_{m_\alpha}}{C_{L_\alpha} + \frac{T}{q^*S}}\left(1 - \dfrac{\rho g S\bar{c}}{4W}C_{L_q}\right) + \dfrac{\rho g S\bar{c}}{4W}C_{m_q}}{C_{m_\delta} - \dfrac{C_{m_\alpha}}{C_{L_\alpha} + \frac{T}{q^*S}}C_{L_\delta}}\right]$$

$$\doteq \frac{-W}{q^*SC_{m_\delta}}\left(\frac{C_{m_\alpha}}{C_{N_\alpha}} + \frac{1}{4\mu_1}C_{m_q}\right)$$

the further approximation holding when C_{L_q} and C_{L_δ} are negligible. It may be recognized that $d\delta/dn$ is proportional to the short-period natural frequency squared. A negative gradient is stable. Again, for all-moving-tail, elevon, or canard control the substitutions are obvious. Note that effects of compressibility, aeroelasticity and thrust on the derivatives can be important. For the effects of tabs, see Appendix II.

Replacement for last paragraph of Section IIC, pp. 19 and 20

Define $n_z W$ as the force applied normal to the flight path (positive "up"). (Note that an accelerometer fixed to the aircraft gives a slightly different n_z because in general it is not aligned exactly normal to the flight path).

Take stability axes, which are also fixed in the body during dynamic motion but chosen so that in steady flight the x axis parallels the projection of the velocity vector onto the plane of symmetry, the x-z plane. The aircraft attitude with respect to a fixed horizontal reference is described by the Euler angles Ψ,Θ,Φ: yaw through Ψ, pitch through Θ and roll through Φ in turn to reach the aircraft attitude. The flight path is described by its azimuth (generally different from Ψ) and its inclination to the horizontal, γ. If $\beta = 0$, stability-axis Θ equals γ in the steady state; but in the general case the x axis is inclined differently than the velocity vector. For stability axes it can be shown that

$$\Theta = \tan^{-1}(\tan\beta \sin\Phi) + \sin^{-1}\left(\frac{\sin\gamma}{\sqrt{1 + \tan^2\beta \sin^2\phi} \cdot \cos\beta}\right)$$

Other quantities we will need to describe the motion are P, Q, R, the angular rates about the aircraft x, y, z axes respectively; U,V,W, the linear velocity components along x, y, z respectively; n_x, n_y, n_z, the sensed linear accelerations in g's at the center of gravity, i.e. the sum of inertial and gravitational accelerations (equal, in Newtonian mechanics, to the applied forces divided by the vehicle weight). The equations of motion are developed, for example, in Refs. 3 and 4. For steady maneuvers $\dot{U}=\dot{V}=\dot{W}=\dot{P}=\dot{Q}=\dot{R}=0$ and in stability axes W=0 also, leaving $V=V_R\sin\beta$ and $U=V_R\cos\beta$. The force equations then yield

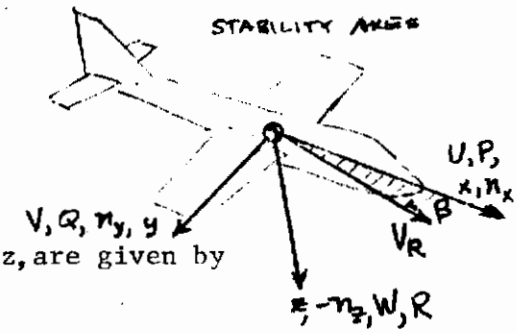

$$n_x = X/(mg) = -\frac{1}{g}\dot{V}_R + \sin\Theta$$

$$n_y = Y/(mg) = \frac{1}{g}UR - \cos\Theta \sin\Phi$$

$$n_z = -Z/(mg) = \frac{1}{g}UQ - \frac{1}{g}\dot{V}P + \cos\Theta \cos\Phi$$

L, M, N, the ~~steady~~ applied moments about x, y, z, are given by

$$L = (I_z - I_y)\, QR - I_{xz}PQ$$

$$M = -(I_z - I_x)PR + I_{xz}(P^2 - R^2)$$

$$N = (I_y - I_x)PQ + I_{xz}QR$$

where I_x, I_y, I_z are the moments of inertia about x, y, z and I_{xz} is the product of inertia, $\int xz\,dm$.

In a vertical-plane pullup with $\gamma=\Theta$ and $\dot{V}_R=0$, the force equations in flight-path axes become

$$n_x = \sin\gamma$$
$$n_y = 0$$
$$n_z = \frac{UQ}{g} + \cos\gamma$$

With V=W=0, $U=V_R$ and $\Theta=\gamma$, so that

$$Q = \frac{g}{V_R}(n_z - \cos\gamma)$$

This is not really a steady flight condition because $\Theta = Qt$ varies with time; but instantaneous, or quasi-steady, solutions are of interest. Passing through level flight, $\dot{Q}=0$ if $\dot{n}_z = 0$; also

$$Q = \frac{g}{V_R}(n_z - 1)$$

Simple balance of forces gives the same results.

In flight tests, maneuvering stability can be evaluated more quickly in turns than in pullups. Normally, corresponding to operational practice, coordinated turns are investigated. (To coordinate a turn a pilot zeros the side acceleration he feels; in a steady turn this is the same as zeroing n_y at the center of gravity.) The test technique is either to bank slowly into a turn, descending to maintain airspeed as the turn tightens, or to perform a series of slowly decelerating turns at constant altitude with varying constant values of n_z. As with pullups, here we consider the steady or quasi-steady state. Some simple approximate solutions have generally good accuracy. According to the references cited, in turning flight about a vertical axis ($\Theta=\Phi=0$) the body-axis components of turn rate are exactly

$$P = -\dot{\Psi}\sin\Theta$$
$$Q = \dot{\Psi}\cos\Theta\,\sin\Phi$$
$$R = \dot{\Psi}\cos\Theta\,\cos\Phi$$

Even for a coordinated turn the equations are all coupled and quite nonlinear. Substituting for P, Q and R in the n_y equation, in the general case of steady flight

$$n_y = (1/g)(V_R\cos\beta)(\dot{\Psi}\cos\Theta\,\cos\Phi) - \cos\Theta\,\sin\Phi$$

in a stability axis system. Then the turn rate is

$$\dot{\Psi} = \frac{g}{V_R\cos\beta}\left(\tan\Phi + \frac{n_y}{\cos\Phi\,\cos\Theta}\right)$$

With β generally small in coordinated turns (this may not hold at very low speed)

$$\dot{\Psi} = (g/V_R)\tan\Phi$$

Similarly, in coordinated turns the kinematic and motion equations yield

$$n_x = \sin\Theta - \tan\beta\,\sin\Phi\,\cos\Theta \approx \sin\Theta \approx \sin\gamma/\cos\beta \approx \sin\gamma$$
$$n_z = (\cos\Theta + \tan\beta\,\sin\Phi\,\sin\Theta)/\cos\Phi \approx \cos\Theta/\cos\Phi \approx \cos\gamma/\cos\Phi$$
$$Q = (gn_z/V_R)\,\sin^2\Phi \approx (g/V_R)(n_z - \cos^2\gamma/n_z)$$
$$P \approx \mp\,(g/V_R)\sqrt{n^2_z - \cos^2\gamma}\,\tan\gamma$$
$$R \approx \pm\,(g/V_R)\sqrt{1 - \cos^2\gamma/n_z^2}\,\cos\gamma$$

where the appearance of γ infers application to flight-path axes.

For turns to starboard R is positive, P is negative for positive γ. For turns to port the signs are reversed; but Q is always positive in a steady erect turn. These angular rates may be transferred to principal axes ($I_{xz}=0$):

$$P_p = P\cos\alpha - R\sin\alpha$$

$$R_p = R\cos\alpha + P\sin\alpha$$

where α is the inclination of the principal x axis to the flight path, the angle of attack of the principal x axis. Q_p of course equals Q.

Returning to the lift and pitching moment equations, the increments from steady coordinated, straight, level flight are given by

$$\Delta L = (n_z-1)\,W$$

$$\Delta C_L = (n_z-1)\,\frac{W}{qs}$$

$$(n_z-1)\,C_{L_1} = C_{L_\alpha}\Delta\alpha + C_{L_q}\,\frac{Qc}{2V} + C_{L_\delta}\,(\delta_p + kQ)$$

(positive k for added damping) including a pitch damper which is not washed out. Then

$$\Delta\alpha = [(n_z-1)\,C_{L_1} - (C_{L_q}\,\frac{c}{2V} + C_{L_\delta}k)\,Q - C_{L_\delta}\,\delta p)]/C_{L_\alpha}$$

In terms of rates about the aircraft principal axes (see, e.g. section IV F),

$$\Delta M = 0 = \bar{q}Sc\,[C_{m_\alpha}\,\Delta\alpha + C_{m_q}\frac{Qc}{2V} + C_{m_\delta}(\delta_p + kQ)] + (I_{z_p}-I_{x_p})P_pR_p - H_e(R_p\cos\varepsilon + P_p\sin\varepsilon)$$

where $H_e=I_e\,\omega_e$, the engine angular momentum, and ε is the inclination of the engine rotor axis to the principal x axis. Substituting, for a steady turn

$$-(C_{m_\delta}-\frac{C_{m_\alpha}C_{L_\delta}}{C_{L_\alpha}})\delta_p = \frac{C_{m_\alpha}}{C_{L_\alpha}}(n_z-1)C_{L_1} + \left[(C_{m_q}-\frac{C_{m_\alpha}C_{L_q}}{C_{L_\alpha}})\frac{c}{2V} + (C_{m_\delta}-\frac{C_{m_\alpha}C_{L_\delta}}{C_{L_\alpha}})k\right]\frac{g}{V}\,(n_z-\frac{\cos^2\gamma}{n_z})$$

$$-\frac{(I_{z_p}-I_{x_p})}{\bar{q}Sc}\,\frac{g^2}{V^2}\,(1-\frac{\cos^2\gamma}{n_z^2})[(\cos^2\gamma-n_z^2\tan^2\gamma)\sin\alpha\cos\alpha + n_z\sin\gamma(\cos^2\alpha-\sin^2\alpha)]$$

$$\mp\frac{H_e}{\bar{q}Sc}\,\frac{g}{V}\sqrt{1-\frac{\cos^2\gamma}{n_z^2}}\,[(\cos\gamma\cos\alpha-n_z\tan\gamma\sin\alpha)\cos\varepsilon - (\cos\gamma\sin\alpha + n_z\tan\gamma\cos\alpha)\sin\varepsilon]$$

To simplify this, take level flight ($\gamma \approx 0$) and implicitly define equivalent derivatives:

$$-C^*_{m_\delta}\,\delta_p = \frac{C_{m_\alpha}}{C_{L_\alpha}}(n_z-1)\,C_{L_1} + \left(C^*_{m_q} + \frac{2Vk}{c}C^*_{m_\delta}\right)\frac{2mg}{\rho V^2 S}\,\rho\frac{Sc}{4m}\left(n_z-\frac{1}{n_z}\right)$$

$$-\frac{(I_{z_p}-I_{x_p})}{mc^2}\,\frac{2mg}{\rho V^2 S}\,\frac{gc}{V^2}\left(1-\frac{1}{n_z^2}\right)\sin\alpha\cos\alpha \mp \frac{H_e}{mVc}\,\frac{2mg}{\rho V^2 S}\sqrt{1-\frac{1}{n_z^2}}\,(\cos\alpha\cos\varepsilon-\sin\alpha\sin\varepsilon)$$

or

$$\delta_p = \frac{-C_{L_1}}{C^*_{m_\delta}}\left\{\frac{C_{m_\alpha}}{C_{L_\alpha}}(n_z-1) + \left[(C^*_{m_q} + \frac{2Vk}{c}C^*_{m_\delta})/(4\mu) - \frac{(I_{z_p}-I_{x_p})}{n_z mc^2}\frac{gc}{V^2}\sin\alpha\cos\alpha\right]\left(n_z-\frac{1}{n_z}\right)\right.$$
$$\left. \mp \frac{H_e}{mVc}(\cos\alpha\cos\varepsilon - \sin\alpha\sin\varepsilon)\sqrt{1-\frac{1}{n_z^2}}\right\}$$

A normal accelerometer inclined at α_A to $-z_s$ will sense a load factor $n_A = n_z\cos\alpha_A - n_x\sin\alpha_A$ (with n_z positive upward and n_x positive forward). In coordinated flight with $\beta \approx 0$, $n_x \approx \sin\gamma$, so that the accelerometer will read

$$n_A \approx n_z\cos\alpha_A$$

where n_z is the load factor normal to the flight path, because n_x, γ and likely α_A too are small.

Except at very low speed, as in STOL operation, the contributions of the inertia and engine momentum terms should be negligible.

The essential difference in pitch control deflection between pullups and turns is the intrusion of roll and yaw rates for the latter. At high speed the terms coupling the longitudinal and lateral-directional perturbed motions from steady coordinated turns are minimal. Then, at least, pitch - heave motions can occur without exciting roll-yaw-lateral motion. Therefore, in steady turns, paradoxically the control gradient in pullups is more indicative of dynamic stability than is the gradient in turns. The expressions developed can be used to account for the difference.

Maneuvering stability requirements generally apply at constant throttle setting (to balance drag in 1g level flight). If either thrust is increased or speed is decreased to maintain a constant-altitude turn,

$$n_z \approx 1/\cos\Phi$$
$$Q \approx (g/V_R)(n_z - 1/n_z)$$

Neglecting trim changes and the effect of any thrust changes on the stability derivatives, Ref. 21 derives expressions for $\Delta\delta_e$, $d\delta_e/dn_z$, ΔF_e and dF_e/dn_z for this simplified but common case.

Hereafter, attention is restricted to symmetrical pullups.

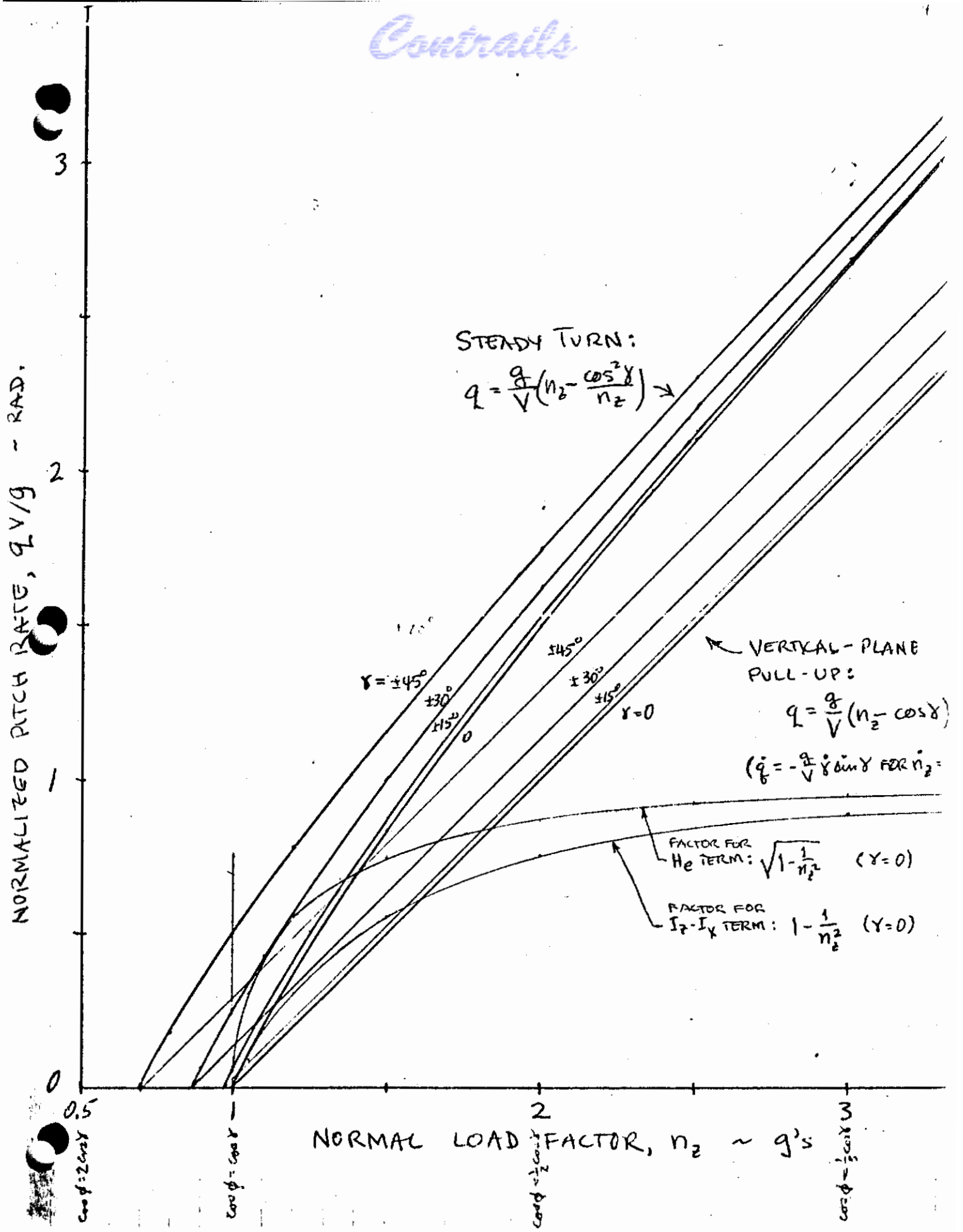

The stick-fixed maneuver point is that center of gravity at which $d\delta/dn$ vanishes. It can be related to the aerodynamic center, the hypothetical neutral point associated with angle-of-attack change only (References 3 and 21). Define the aerodynamic center as the center of gravity at which C_{m_α} would be zero. Then with

$$-\frac{C_{m_\alpha}}{C_{N_\alpha}} \doteq -\frac{x_{ac}}{\bar{c}},$$

(negative x for the aerodynamic center aft of the center of gravity), the stick-fixed maneuvering neutral point is at the center of gravity for which

$$\frac{x_{ac}}{\bar{c}} \doteq -\frac{1}{4\mu_1} C_{m_q}$$

The maneuver point may vary from several percent mean aerodynamic chord aft of the constant-speed aerodynamic center for tailed configurations at low altitude to approximate coincidence at extreme altitude. The control-deflection gradient is

$$\frac{d\delta}{dn} \doteq \frac{+W}{q^*S} \frac{(N_m - cg)}{C_{m_\delta}\left(1 - \frac{C_{L_\delta}}{C_{m_\delta}} \frac{C_{m_\alpha}}{C_{N_\alpha}}\right)} \; ; \; N_m - cg \doteq -\left(\frac{C_{m_\alpha}}{C_{N_\alpha}} + \frac{1}{4\mu_1} C_{m_q}\right)$$

with the maneuvering neutral point N_m and the center of gravity stated in percent mean aerodynamic chord divided by 100. (N_m is measured aft from the mean aerodynamic chord leading edge). N_m-cg is the maneuver margin.

To include the effects of stability augmentation, effective derivatives can be calculated. For example, if $\delta = \delta_c + Kq$, substitute $(C_{m_q} + \frac{2V}{\bar{c}} K C_{m_\delta})$ for C_{m_q} and $(C_{L_q} + \frac{2V}{\bar{c}} K C_{L_\delta})$ for C_{L_q}. The result will be, as desired, $d\delta_c/dn$; normally the major effect will be the augmentation of C_{m_q}. Note that augmentation may introduce new stability derivatives and increase the importance of some in the original set. An alternative to the equivalent-derivative approach is to use servo-analysis techniques (See References 8 and 9 and Appendix IV for some pertinent applications), which give not only $d\delta/dn$ but all the transfer-function coefficients as functions of augmentation gain. Authority-limited augmentation becomes ineffective statically, of course, in sufficiently large amplitude maneuvers.

Where C_m is a nonlinear function of α such as pitch-up, control deflection can still be calculated as a function of load factor using $C_m(\alpha)$, or δ versus n can be calculated directly by using the nonlinear equations or the local slope C_{m_α} at the angle of attack corresponding to a given load factor.

2. Stick Free

Stick-free maneuvering stability refers to the maneuvering control force gradient, dF_e/dn, under flight conditions the same as those for stick-fixed maneuvering stability. The permissible force gradients are specified in current military handling-quality requirements according to airplane class. A pull force to increase normal load factor (positive gradient) is indicative of stability and is required. Stick-free maneuvering stability is a function of the stick-fixed maneuvering stability, the nature of the control system, and the feel system. N_m', the stick-free maneuver point, is the center of gravity (expressed in percent m.a.c./100) for zero stick force per g.

(a.) Reversible Control Systems

Using the linear stick-fixed equations to find $d\delta/dn$, $d\alpha/dn$, and $d(\frac{q\bar{c}}{2V})/dn$, the stick-force equation

$$\frac{dF_e}{dn} = \frac{\partial F_e}{\partial n} + \frac{\partial F_e}{\partial \delta}\frac{d\delta}{dn} + \frac{\partial F_e}{\partial \alpha}\frac{d\alpha}{dn} + \frac{\partial F_e}{\partial\left(\frac{q\bar{c}}{2V}\right)}\frac{d\left(\frac{q\bar{c}}{2V}\right)}{dn}$$

gives

$$\frac{dF_e}{dn} = \frac{\partial F_e}{\partial n} + \frac{G}{B}\frac{W}{S}S_e\bar{c}_e\left[\left(\frac{C_{m_\alpha}\left(1-\frac{1}{4\mu_1}C_{L_q}\right)+\frac{1}{4\mu_1}\left(C_{L_\alpha}+\frac{T}{q^*S}\right)C_{m_q}}{C_{L_\delta}C_{m_\alpha}-C_{m_\delta}\left(C_{L_\alpha}+\frac{T}{q^*S}\right)}\right)C_{h_\delta}\right.$$

$$\left. + \left(\frac{C_{m_\delta}\left(1-\frac{1}{4\mu_1}C_{L_q}\right)+\frac{1}{4\mu_1}C_{L_\delta}C_{m_q}}{C_{m_\delta}\left(C_{L_\alpha}+\frac{T}{q^*S}\right)-C_{L_\delta}C_{m_\alpha}}\right)C_{h_\alpha} + \frac{1}{4\mu_1}C_{h_q}\right]$$

$$\doteq \frac{\partial F_e}{\partial n} + \frac{G}{B}\frac{W}{S}S_e\bar{c}_e\left[\underbrace{-\frac{C_{h_\delta}}{C_{m_\delta}}\left(\frac{C_{m_\alpha}}{C_{N_\alpha}}+\frac{1}{4\mu_1}C_{m_q}\right)}_{\text{usually major term}} + \frac{C_{h_\alpha}}{C_{N_\alpha}} + \frac{1}{4\mu_1}C_{h_q}\right]$$

where $\partial F_e/\partial n$ accounts for bobweight and mass unbalance:

$$\frac{\partial F_e}{\partial n} = \left(\frac{\partial F_e}{\partial n}\right)_B - \frac{G}{B}W_e\bar{r}_e$$

with $\bar{r}_e$ the distance, normal to the hinge line, from the hinge line forward to the elevator center of gravity. The matrix approach of Section IIA3 leads to the same result. As with stick-fixed maneuvering stability, augmentation can be treated by using equivalent derivatives or servo analysis techniques. For the effects of control tabs, see Appendix II.

Note that the force gradient is independent of speed, (except for Mach number and Reynolds number effects) and, except at aft centers of gravity, is only weakly dependent on altitude.

Although feel springs are normally associated with irreversible systems, these devices can be used in reversible systems. Then the feel-spring term below would be added to the reversible-control equation.

(b.) Irreversible Control Systems

$$\frac{dF_e}{dn} = -\frac{1}{G}\frac{dF_e}{d\Delta_s}\frac{d\delta}{dn} + \left(\frac{\partial F_e}{\partial n}\right)_B$$

where $d\delta/dn$ can be determined from Section IIC1. Appropriate substitutions for δ adapt the force expressions to other types of control surfaces.

The stick-free maneuver point is that center of gravity value at which the stick-free maneuvering stability vanishes (the maneuvering control force gradient becomes zero). The stick-free maneuver margin is the distance of the center of gravity in percent $\bar{c}$ forward of the stick-free maneuver point. It should be noted that although feel springs and bobweights can be used to increase the stick-free maneuvering stability, feel springs do not increase the maneuver margin. Bobweights do, however. A nonstatic-balanced bobweight affects the static and maneuvering stick-free neutral points equally when the derivatives are invariant with speed. A simple bobweight does not provide the load-factor anticipation that "spring" feel gives the pilot in maneuvering. Further, it tends to reduce the stability of the elevator-oscillation mode and can even cause, in the extreme, severe detrimental effects on the short-period motion (See Section IVC1 and Appendix IV). The requirement of Reference 15 on control forces in sudden pullups and the discussions of the intricacies of control system design are pertinent here (See Section IVE).

Because of their mechanization, bobweights measure normal acceleration and their weight components in body axes; at extreme angles of attack and attitudes this behavior must be taken into account (Reference 6).

D. TAKEOFF

At nose-wheel lift-off speed, full airplane-nose-up control deflection will just balance the vehicle with the nose wheel fully extended (touching the runway but bearing no weight). This speed must generally be lower than the takeoff speed. It should be noted that careful attention to takeoff trim requirements is essential--say a 10-pound push at $1.3V_{s_{TO}}$. This is an important element of the problem. The calculation of nose-wheel lift-off speed has essentially three steps. First the angle of attack at nose-wheel lift-off is calculated, accounting for landing gear deflection. Then certain dimensions are scaled, using coordinates parallel and perpendicular to the runway. The dynamic pressure at lift-off can then be calculated and converted into airspeed.

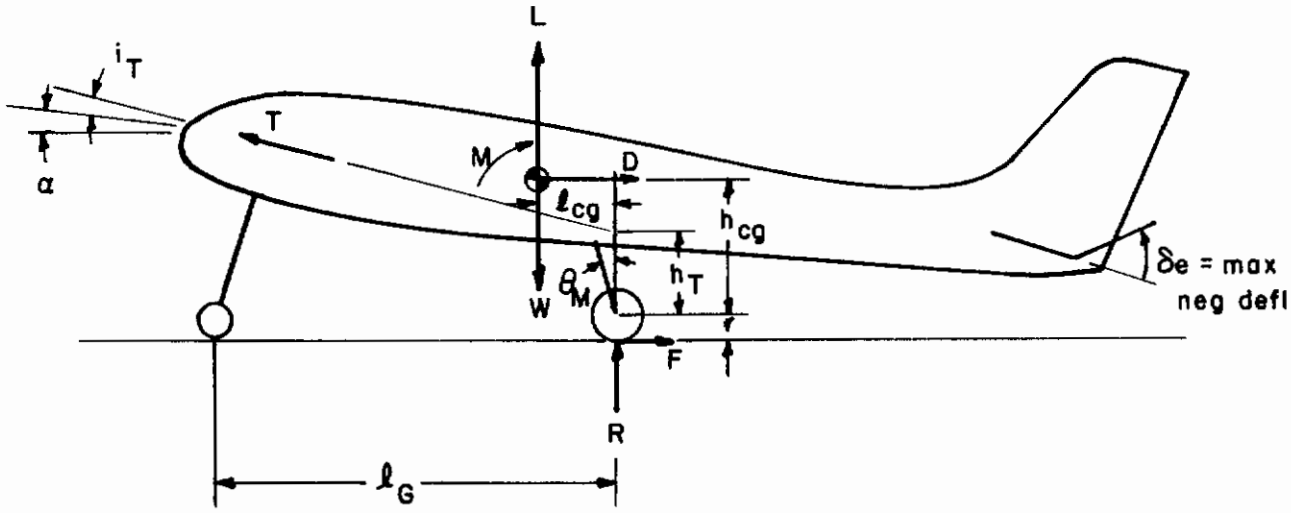

Figure 5. Nose-Wheel Lift-Off Calculation

Since $F = \mu R$ (μ is the coefficient of rolling friction; MIL-C-5011A and MIL-H-7700 specify a value of 0.025 for takeoff performance calculations), the main gear deflection from its fully-extended position is given by

$$\Delta_M = \frac{R(\cos\theta_M - \mu \sin\theta_M)}{K} \doteq \frac{R}{K}$$

because θ_M is generally small. K is then the effective spring constant of both main gear (lb/ft). The deflection can be measured normal to the approximate ground plane. (Use, for instance, static main-gear deflection.) This usage of K may require a correction to the value obtained from the load-stroke curve.

The main-gear reaction is given by $R = W - L - T \sin(i_T + \alpha)$ and, using the small-angle approximation for $\Delta\alpha$ and θ_M,

$$\alpha \doteq \alpha_{FE} + \frac{\Delta_M}{\ell_G}$$

where α_{FE} is measured with all gear fully extended. Strictly speaking, ℓ_G varies with Δ_M. The variation, however, is usually so slight that a fixed value can be introduced, using, again, static main-gear deflection.

It is apparent that this part of the analysis is approximate. Calculating the conditions for validity would seem to be more trouble than performing an iteration to improve the accuracy. On the other hand, good results are usually obtained using an angle of attack based only on static main-gear deflection. The method given, however, uses the calculated approximate α.

Combining these relations and taking

$$L = q^*S\left[C_{L_\alpha}(\alpha - \alpha_o) + C_L(\delta)\right],$$

for small α and i_T there results

$$\alpha \doteq \frac{\alpha_{FE} + \frac{W}{K\ell_G} - \left[C_L(\delta) - C_{L_\alpha}\alpha_o + \frac{T}{q^*S} i_T\right]\frac{q^*S}{K\ell_G}}{1 + \left(C_{L_\alpha} + \frac{T}{q^*S}\right)\frac{q^*S}{K\ell_G}}$$

Accounting for possible variation of T with q*, this relation gives α as a function of q*.

Next consider the moment balance about the main-gear axle:

$$M + L\ell_{cg} + Dh_{cg} - Th_T\cos(i_T + \alpha) - W\ell_{cg} - Fr + ma_x h_{cg} = 0$$

where

$$M = q^*S\bar{c}\,C_m(\alpha,\delta)$$

$$ma_x = T\cos(i_T + \alpha) - D - F.$$

When the relations above are combined, drag drops out and the result is

$$q^* = \frac{W\left[\ell_{cg} + \mu(h_{cg} + r)\right] - T\left[(h_{cg} - h_T)\cos(i_T + \alpha) + \mu(h_{cg} + r)\sin(i_T + \alpha)\right]}{\left\{C_m + \left[\frac{\ell_{cg}}{\bar{c}} + \mu\frac{(h_{cg} + r)}{\bar{c}}\right]C_L\right\}S\bar{c}}$$

To summarize the method, then, in its simple form:

(1) For q* values over the range of interest (say, three points), calculate (considering ground effect)

$$\alpha_i \doteq \frac{\alpha_{FE} + \frac{W}{K\ell_G} - \left[C_L(\delta) - C_{L_\alpha}\alpha_o + \frac{T}{q_i^*S} i_T\right]\frac{q_i^*S}{K\ell_G}}{1 + \left(C_{L_\alpha} + \frac{T}{q_i^*S}\right)\frac{q_i^*S}{K\ell_G}}$$

(2) For each α_i sketch the gear extensions and the ground line on a profile drawing in the manner of Figure 5. Scale the dimensions ℓ_{cg}, $(h_{cg} + r)_i$ and $(h_{cg} - h_T)_i$ normal to the appropriate ground line [$(h_{cg} - h_T)$ is relatively constant, varying only as $\cos\Delta\alpha$]. Calculate C_{L_i} and C_{M_i} for each α_i, in the takeoff configuration, considering ground effect.

(3) For each α_i, calculate

$$q_j^* \doteq \frac{W\left[\frac{\ell_{cg}}{\bar{c}} + \frac{\mu(h_{cg}+r)_i}{\bar{c}}\right] - T\left[\frac{(h_{cg}-h_T)_i}{\bar{c}} + \mu\,\frac{(h_{cg}+r)_i}{\bar{c}}\sin(i_T+\alpha_i)\right]}{\left\{C_{m_i} + \left[\frac{\ell_{cg}}{\bar{c}} + \mu\,\frac{(h_{cg}+r)}{\bar{c}}\right] C_{L_i}\right\} S}$$

(4) On the same graph plot q_i^* versus α_i and q_j^* versus α_i. The point of intersection determines q_{LO}^*, the dynamic pressure at nose-wheel lift-off. Finally,

$$V_{LO} = 17.2\ \sqrt{q_{LO}^*}\ \text{knots EAS}$$

SECTION III

STATIC LATERAL-DIRECTIONAL STABILITY AND CONTROL

A. STEADY SIDESLIPS

Static lateral-directional stability is indicated by the following phenomena (Notice that the term stability is used rather loosely in some of these cases):

(a) Rudder deflection and rudder pedal force variations in steady sideslips: Increasing right rudder deflection and increasing right pedal force in increasing left sideslips indicate directional, or weathercock, stability.

(b) Aileron deflection and lateral stick-force variations in steady sideslips (dihedral effect): Increasing left aileron deflection and increasing left lateral control force in increasing left sideslips are desired as indicators of spiral stability and for uniformity of pilot control. Excessive dihedral effect, however, cannot be tolerated in piloted aircraft because it would preclude control of the roll due to attainable sideslip, and would change the form of the vehicle's response (See Reference 8 and Section IVB2).

(c) Bank-angle variations in steady sideslips: Increasing left bank angles in increasing left sideslips is normal and rational, and thus desirable.

Reference 15 specifies static lateral-directional stability in steady, straight sideslips, but U.S. civil aeronautics regulations, References 24 and 25, specify wings-level skidding turns as well. The development that follows concerns only zero angular rates, but the extension to find rudder and aileron deflections and force variations with β in wings-level skids is straightforward: add appropriate yaw-rate terms and set $\phi = 0$ in the given matrix equations. Differences are generally minor, except possibly at very low speeds as in the STOL operation.

This analysis assumes that the trim conditions are $\beta = \phi = \delta a = \delta r = 0$, although small initial values do not alter the linear solutions for $d\delta r/d\beta$, etc, and so usually have no significance to the stability problem. Extension for trim in the presence of propeller slipstream torque, wing-heaviness, aerodynamic asymmetries, etc. is straightforward. An example of such calculations can be found in Section IIID, in which trim has been considered for asymmetric thrust. To handle unequal right and left aileron gearing, the intermediate equations of Appendix III can be used directly or combined for the specific application to find aileron force.

Both stability and controllability are given by the sideslip equations. It is usual to specify a margin (25 percent in Reference 15) of aileron control over that required to achieve a large sideslip angle (10 degrees in Reference 15) at low speed.

1. Controls Fixed

Steady straight sideslip equilibrium conditions involve zero lateral acceleration, rolling velocity and yawing velocity and occur as a result of zero net side force, rolling moment, and yawing moment. In the general case there are four variables: sideslip angle, bank angle, lateral-control (aileron) deflection, and directional-control (rudder) deflection. Some derivatives are functions of (trim)

angle of attack. Drag due to sideslip will change the trim speed or flight-path angle, but that effect is neglected here.

The following steady-state lateral-directional functional equations apply for straight steady sideslips at small flight-path angle (γ):

$$C_n(\delta a, \delta r, \beta) = 0$$

$$C_\ell(\delta a, \delta r, \beta) = 0$$

$$C_y(\delta a, \delta r, \beta) + \frac{W}{q^* S}\sin\phi = 0$$

Possible variation of derivatives, particularly C_{n_β}, with center of gravity should not be overlooked. In linearized form these equations become:

$$\begin{pmatrix} 0 & C_{n_\beta} & C_{n_{\delta a}} & C_{n_{\delta r}} \\ 0 & C_{\ell_\beta} & C_{\ell_{\delta a}} & C_{\ell_{\delta r}} \\ \frac{W}{q^* S} & C_{y_\beta} & C_{y_{\delta a}} & C_{y_{\delta r}} \end{pmatrix} \begin{pmatrix} \phi \\ \beta \\ \delta a \\ \delta r \end{pmatrix} = \begin{pmatrix} 0 \\ 0 \\ 0 \end{pmatrix}$$

Solutions can be found by moving a column of derivatives to the right-hand side and reversing their signs, then solving by Cramer's rule. For example,

$$\begin{bmatrix} 0 & C_{n_{\delta a}} & C_{n_{\delta r}} \\ 0 & C_{\ell_{\delta a}} & C_{\ell_{\delta r}} \\ \frac{W}{q^* S} & C_{y_{\delta a}} & C_{y_{\delta r}} \end{bmatrix} \begin{pmatrix} \phi \\ \delta a \\ \delta r \end{pmatrix} = \begin{pmatrix} -C_{n_\beta} \\ -C_{\ell_\beta} \\ -C_{y_\beta} \end{pmatrix} \beta$$

can be solved directly to get:

$$\frac{d\delta r}{d\beta} = -\frac{C_{n_\beta}}{C_{n_{\delta r}}} \left(\frac{1 - \frac{C_{n_{\delta a}}}{C_{\ell_{\delta a}}} \frac{C_{\ell_\beta}}{C_{n_\beta}}}{1 - \frac{C_{n_{\delta a}}}{C_{\ell_{\delta a}}} \frac{C_{\ell_{\delta r}}}{C_{n_{\delta r}}}} \right) \doteq -\frac{C_{n_\beta}}{C_{n_{\delta r}}}$$

$$\frac{d\delta a}{d\beta} = -\frac{C_{\ell_\beta} - \frac{C_{\ell_{\delta r}}}{C_{n_{\delta r}}} C_{n_\beta}}{C_{\ell_{\delta a}} \left(1 - \frac{C_{n_{\delta a}}}{C_{\ell_{\delta a}}} \frac{C_{\ell_{\delta r}}}{C_{n_{\delta r}}} \right)} \doteq -\frac{C_{\ell_\beta}}{C_{\ell_{\delta a}}}$$

$$\frac{d\phi}{d\beta} = -\frac{q^*S}{W} C_{y_\beta} \left[1 - \frac{C_{y_{\delta r}}}{C_{n_{\delta r}}} \frac{C_{n_\beta}}{C_{y_\beta}} \left(\frac{1 - \frac{C_{n_{\delta a}}}{C_{\ell_{\delta a}}} \frac{C_{\ell_\beta}}{C_{n_\beta}}}{1 - \frac{C_{n_{\delta a}}}{C_{\ell_{\delta a}}} \frac{C_{\ell_{\delta r}}}{C_{n_{\delta r}}}} \right) - \frac{C_{y_{\delta a}}}{C_{\ell_{\delta a}}} \frac{\left(C_{\ell_\beta} - \frac{C_{\ell_{\delta r}}}{C_{n_{\delta r}}} C_{n_\beta} \right)}{C_{y_\beta} \left(1 - \frac{C_{n_{\delta a}}}{C_{\ell_{\delta a}}} \frac{C_{\ell_{\delta r}}}{C_{n_{\delta r}}} \right)} \right]$$

$$\doteq -\frac{1}{C_{L_1}} \left(C_{y_\beta} - \frac{C_{y_{\delta r}}}{C_{n_{\delta r}}} C_{n_\beta} \right)$$

Other derivatives may be formed in this manner: $d\delta a/d\delta r = (d\delta a/d\beta) \div (d\delta r/d\beta)$, etc.

The approximations apply when $C_{\ell_{\delta a}} \gg C_{n_{\delta a}}$ and $C_{n_{\delta r}} \gg C_{\ell_{\delta r}}$ and, for $d\phi/d\beta$, when $C_{y_{\delta a}}$ is negligible. Intermediate approximations are apparent. Note that the units of all terms in these equations must be consistent. The linearization of sin ϕ to ϕ presumes that radian measure is used throughout. Positive values of $\frac{d\delta r}{d\beta}$ for an aft rudder, $\frac{d\delta a}{d\beta}$, and $\frac{d\phi}{d\beta}$ are required.

With an aileron-rudder linkage or static stability augmentation[7], effective stability derivatives can be formed. For example, in the steady state a lateral accelerometer will measure $a_y = -g \sin \phi = Y/m$. If we have

$$\delta r = \delta r_c + \frac{\partial \delta r}{\partial \beta} \beta + \frac{\partial \delta r}{\partial a_y} a_y + \frac{\partial \delta r}{\partial \delta a} \delta a,$$

primary interest is in δr_c. As long as no rudder-deflection limit is reached, the linear steady-state equations can be written:

$$\begin{bmatrix} \frac{W}{q^*S} - g \frac{\partial \delta r}{\partial a_y} C_{y_{\delta r}} & C_{y_\beta} + \frac{\partial \delta r}{\partial \beta} C_{y_{\delta r}} & C_{y_{\delta a}} + \frac{\partial \delta r}{\partial \delta a} C_{y_{\delta r}} \\ -g \frac{\partial \delta r}{\partial a_y} C_{n_{\delta r}} & C_{n_\beta} + \frac{\partial \delta r}{\partial \beta} C_{n_{\delta r}} & C_{n_{\delta a}} + \frac{\partial \delta r}{\partial \delta a} C_{n_{\delta r}} \\ -g \frac{\partial \delta r}{\partial a_y} C_{\ell_{\delta r}} & C_{\ell_\beta} + \frac{\partial \delta r}{\partial \beta} C_{\ell_{\delta r}} & C_{\ell_{\delta a}} + \frac{\partial \delta r}{\partial \delta a} C_{\ell_{\delta r}} \end{bmatrix} \begin{pmatrix} \phi \\ \beta \\ \delta a \end{pmatrix} = \begin{pmatrix} -C_{y_{\delta r}} \\ -C_{n_{\delta r}} \\ -C_{\ell_{\delta r}} \end{pmatrix} \delta r_c$$

[7] Angular-rate feedback is of no concern here because we take p and r to be zero. Even for the wings-level skids of References 24 and 25 the yaw-rate signal is usually washed out so that it contributes nothing to steady yawing.

If augmentation signals deflect the ailerons as well, similar equations could be written in terms of ϕ, β, and the pilot-commanded deflections δr_c and δa_c.

Two simplified cases will be considered: β and δa signals to δr $\left(\frac{\partial \delta r}{\partial a_y} = 0\right)$, and a_y feedback to δr $\left(\frac{\partial \delta r}{\partial \beta} = \frac{\partial \delta r}{\partial \delta a} = 0\right)$.

(a.) Sideslip and Aileron Feedback to Rudder

$$\frac{d\delta r_c}{d\beta} = -\frac{C_{n_\beta}}{C_{n_{\delta r}}}\left[\frac{1-\frac{C_{n_{\delta a}}}{C_{\ell_{\delta a}}}\frac{C_{\ell_\beta}}{C_{n_\beta}} - \frac{\partial \delta r}{\partial \delta a}\left(\frac{C_{n_{\delta r}}}{C_{\ell_{\delta a}}}\frac{C_{\ell_\beta}}{C_{n_\beta}} - \frac{C_{\ell_{\delta r}}}{C_{\ell_{\delta a}}}\right)}{1-\frac{C_{n_{\delta a}}}{C_{\ell_{\delta a}}}\frac{C_{\ell_{\delta r}}}{C_{n_{\delta r}}}}\right] - \frac{\partial \delta r}{\partial \beta}$$

$$\frac{d\delta r_c}{d\delta a} = \frac{C_{\ell_{\delta a}}}{C_{n_{\delta r}}}\frac{C_{n_\beta}}{}\left[\frac{1-\frac{C_{n_{\delta a}}}{C_{\ell_{\delta a}}}\frac{C_{\ell_\beta}}{C_{n_\beta}} + \frac{\partial \delta r}{\partial \beta}\frac{C_{n_{\delta r}}}{C_{n_\beta}}\left(1-\frac{C_{n_{\delta a}}}{C_{\ell_{\delta a}}}\frac{C_{\ell_{\delta r}}}{C_{n_{\delta r}}}\right)}{C_{\ell_\beta}-\frac{C_{\ell_{\delta r}}}{C_{n_{\delta r}}}C_{n_\beta}}\right] - \frac{\partial \delta r}{\partial \delta a}$$

Total derivatives not involving δr such as $d\delta a/d\beta, d\phi/d\beta, d\phi/d\delta a$ are not affected by any feedback through the rudder. That this statement holds in general follows from the rules governing linear operations on determinants. Likewise, feedback through the ailerons affects only those total derivatives that involve δa.

It is seen that for an aft rudder, negative $\partial \delta r/\partial \beta$ is stabilizing. Adverse yaw (negative $C_{n_{\delta a}}$ and C_{ℓ_β}) reduces apparent directional stability, $d\delta r_c/d\beta$, while "favorable"yaw increases it. These effects can be offset by

$$\frac{\partial \delta r}{\partial \delta a} = -\frac{C_{n_{\delta a}}}{C_{n_{\delta r}}} \Big/ \left(1-\frac{C_{\ell_{\delta r}}}{C_{n_{\delta r}}}\frac{C_{n_\beta}}{C_{\ell_\beta}}\right)$$

but the necessary gain may vary with flight condition."

(b.) Lateral Acceleration Feedback to Rudder ($a_y \rightarrow \delta r$)

When

$$\left|\frac{C_{n_{\delta a}}}{C_{\ell_{\delta a}}}\frac{C_{\ell_{\delta r}}}{C_{n_{\delta r}}}\right| \ll 1 \quad \text{and} \quad \left|\frac{C_{y_{\delta a}}}{C_{\ell_{\delta a}}}\right| \ll \left|\frac{C_{n_{\delta a}}}{C_{\ell_{\delta a}}}\frac{C_{y_\beta}}{C_{n_\beta}}\right|$$

there results

$$\frac{d\delta r_c}{d\beta} \doteq -\frac{C_{n_\beta}}{C_{n_{\delta r}}}\left\{1-\frac{C_{n_{\delta a}}}{C_{\ell_{\delta a}}}\frac{C_{\ell_\beta}}{C_{n_\beta}} + \frac{\partial \delta r}{\partial a_y}\frac{qq^*S}{W}C_{n_{\delta r}}\left[\frac{C_{y_\beta}}{C_{n_\beta}} - \frac{C_{y_{\delta r}}}{C_{n_{\delta r}}}\left(1-\frac{C_{n_{\delta a}}}{C_{\ell_{\delta a}}}\frac{C_{\ell_\beta}}{C_{n_\beta}}\right)\right]\right\}$$

Further approximation yields

$$\frac{d\delta r_c}{d\beta} \doteq -\frac{C_{n_\beta}}{C_{n_{\delta r}}}\left[1 - \frac{\partial \delta r}{\partial a_y}\frac{g}{C_{L_1}}\left(C_{y_{\delta r}} - \frac{C_{y_\beta}}{C_{n_\beta}} C_{n_{\delta r}}\right)\right]$$

As before, of course, total derivatives not involving δr remain unchanged. Normally

$$\left|\frac{C_{y_\beta}}{C_{n_\beta}} C_{n_{\delta r}}\right| >> \left|C_{y_{\delta r}}\right| ,$$

so the major effect of a_y augmentation is given by the gross approximation

$$\frac{d\delta r_c}{d\beta} \doteq -\frac{C_{n_\beta}}{C_{n_{\delta r}}} + \frac{\partial \delta r}{\partial a_y}\frac{g}{C_{L_1}} C_{y_\beta}$$

Thus for an aft rudder, negative $\partial \delta r / \partial a_y$ gives an apparently stiffer vehicle; that is, more rudder pedal for a given sideslip angle. Comparing the result to the effect of $\beta \rightarrow \delta r$ feedback, as a gross approximation there is an equivalence

$$\frac{\partial \delta r}{\partial a_y}\frac{g}{C_{L_1}}\left(-C_{y_\beta}\right) \doteq \frac{\partial \delta r}{\partial \beta}$$

The effect of $\partial \delta r / \partial a_y$ tends to vary inversely with C_L in level flight: at a typical gain on a supersonic fighter, $d\delta r_c / d\beta$ might be increased by about 10 percent at low speed and by an order of magnitude at maximum dynamic pressure.

(c.) Nonlinear Aerodynamics

If the aerodynamic data are nonlinear to such an extent that linearization at large angles is not permissible, a graphical procedure may be followed:

Solve the first two sideslip equilibrium equations below graphically for rudder and aileron deflections. Solve the third equation for bank angle.

$$C_n(\delta a) + C_n(\delta r, \beta) = 0$$

$$C_\ell(\delta a) + C_\ell(\delta r, \beta) = 0$$

$$C_y(\delta a) + C_y(\delta r, \beta) + C_{L_1} \sin\phi = 0$$

Step 1: Plot rolling-moment coefficient C_ℓ against yawing-moment coefficient C_n with sideslip angle and rudder deflection as parameters as shown in Figure 6a. Only a small range of data about $C_n = 0$ is required.

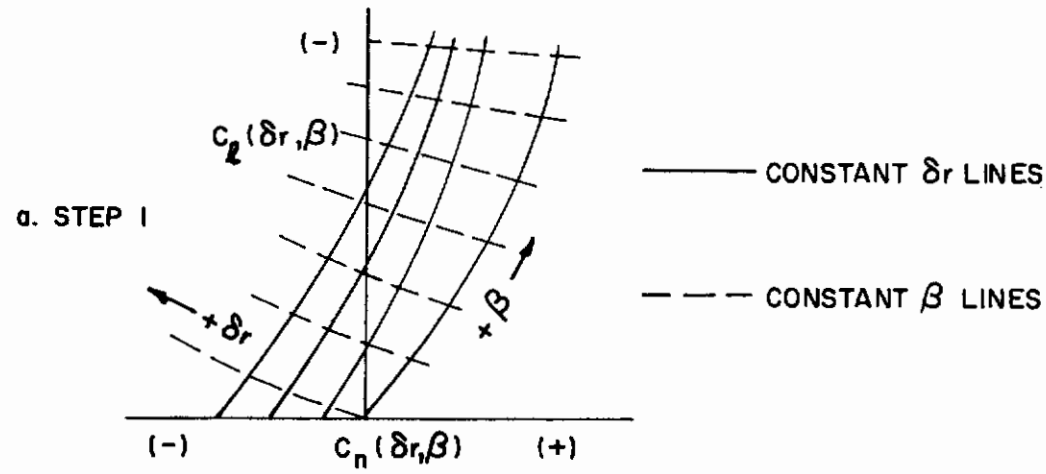

Figure 6. Determination of δr and δa in Sideslips

Step 2: Plot the negative of the rolling and yawing-moment increments due to aileron deflection as function of sideslip angle as shown in Figure 6b. These increments are given by the functional equations

$$-C_\ell(\delta a) = -\left[C_\ell(\delta a,\beta) - C_\ell(\beta)\right]$$

$$-C_n(\delta a) = -\left[C_n(\delta a,\beta) - C_n(\beta)\right]$$

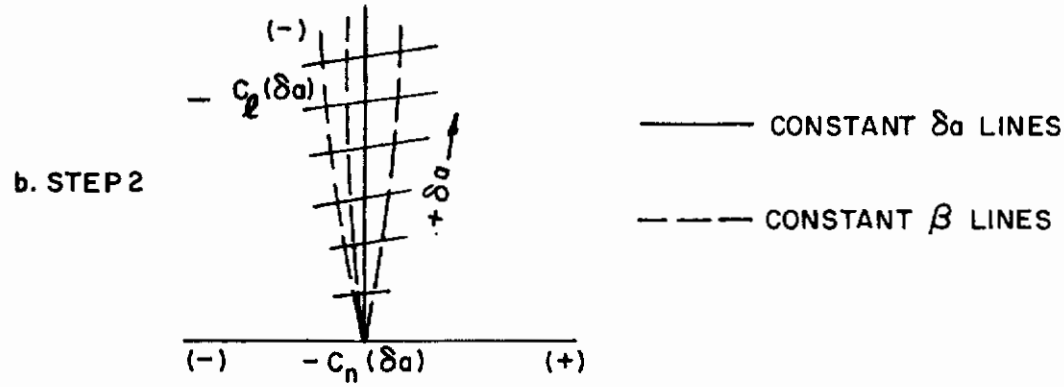

Figure 6. (Continued)

Step 3: Superimpose the data of Figures 6a and 6b.

Step 4: The rudder and aileron angles required to maintain a given sideslip angle are determined by the intersection of the curves for the given sideslip angle from Figures 6a and 6b respectively.

Step 5: Bank angle is then found from the third equation of the original set by using the solutions for δr and δa from Step 4.

Thus

$$\phi = \sin^{-1}\left[\frac{-C_y(\delta a) - C_y(\delta r, \beta)}{C_{L_1}}\right]$$

Usually there is negligible pitching-moment change with steady sideslip. If that is not the case and if, further, any of the directional derivatives are functions of longitudinal control position (for example, short-coupled aircraft or combined lateral and longitudinal control surfaces), the magnitude of the interaction can be found by iterating the separate longitudinal and lateral-directional trim solutions.

2. Controls Free

Current military and civil flying-quality specifications require static controls-free lateral-directional stability in steady sideslips. Rudder pedal forces are allowed to lighten at sideslip angles greater than 15 degrees but are not permitted to reduce to zero or to reverse.

The controls-free stability is determined by the total derivatives

$$\frac{dF_r}{d\beta} = \left(\frac{\partial F_r}{\partial \delta r}\right)\frac{d\delta r}{d\beta} + \left(\frac{\partial F_r}{\partial \phi}\right)\frac{d\phi}{d\beta} + \frac{\partial F_r}{\partial \beta}$$

$$\frac{dF_a}{d\beta} = \left(\frac{\partial F_a}{\partial \delta a}\right)\frac{d\delta a}{d\beta} + \frac{\partial F_a}{\partial \beta}$$

References 24 and 25 also require stability in rudder-free and aileron-free sideslips or skids. Generally, rudder and aileron force stability as given here assure meeting those requirements also. Details can be found with the equations of Section IV, eliminating rate and acceleration terms.

(a.) Reversible Control System

The control-system terminology in this report is used widely but not universally. Especially for lateral control, different sign conventions and definitions of δa are sometimes used. Care must be taken that all equations are consistent in sense and magnitude. For linear hinge moments,

$$F_r = \frac{G_r}{B_r}\left[q^* S_r \bar{c}_r \left(C_{h_{r_o}} + C_{h_{r_\beta}}\beta + C_{h_{r_{\delta r}}}\delta r + C_{h_{r_{\delta t_r}}}\delta t_r\right) + W_r \bar{r}_r \phi\right] + (\Delta F_r)_{feel}$$

$$F_a = \frac{1}{2}\frac{G_a}{B_a} q^* S_a \bar{c}_a \left(C_{h_{a_\beta}}\beta + C_{h_{a_{\delta a}}}\delta a + C_{h_{a_{\delta t_a}}}\delta t_a\right) + (\Delta F_a)_{feel}$$

where $\bar{r}_r$ is the distance normal to the rudder hinge line from the hinge line forward to the rudder center of gravity. The derivative $C_{h_{a\beta}}$ is normally negligible. On the ailerons, if $G_{a_R} = G_{a_L}$ as assumed here (See Appendix III) the effect of mass unbalance is evident only in the control-system rigging; the hinge-moment increments of the two sides cancel. For the effect of control tabs, see Appendix II. A

similar expression can be written for spoilers; when only one spoiler is deflected at a time, the factor 1/2 disappears [The factor (1/2) (G_a) comes from the definition $G_a = d(\delta a_R + \delta a_L)/d\Delta'_s$].

As in the longitudinal case, $(\Delta F_r)_{feel}$ and $(\Delta F_a)_{feel}$ include friction, preload, etc. forces. Artificial stabilization can be handled as in the preceding subsection.

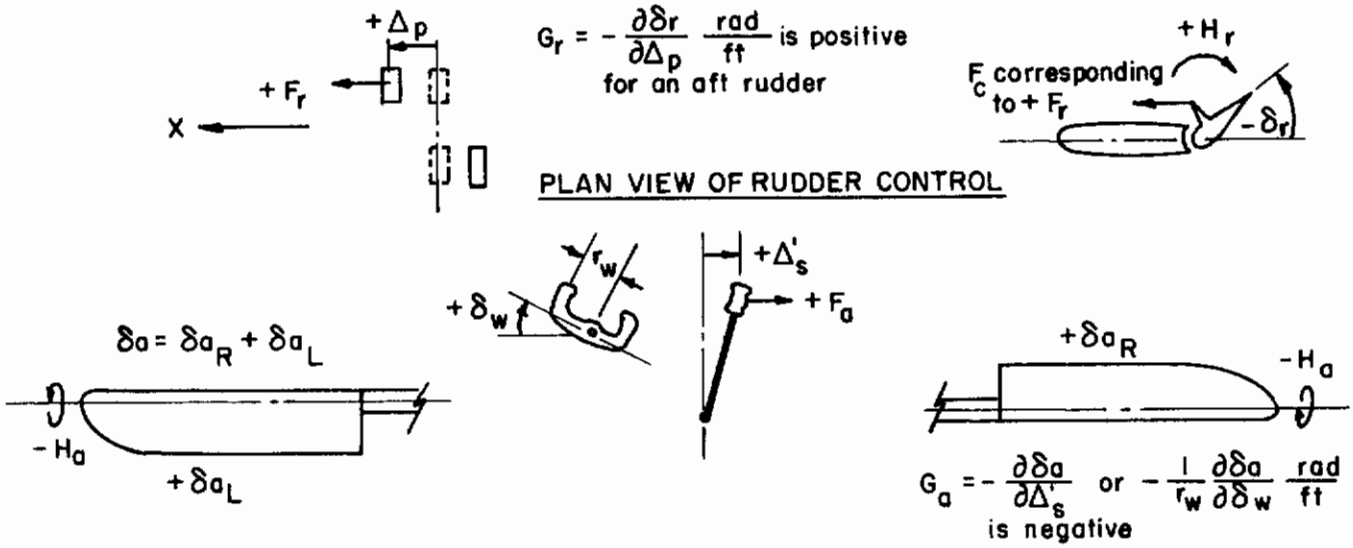

Figure 7. Lateral-Directional Control Terminology

To account for nonlinear aerodynamic hinge-moment characteristics such as rudder lock, the control forces should be found for various sideslip angles from the functional equations

$$F_r = \frac{G_r}{B_r} C_{h_r}(\delta r, \beta, \delta t_r)\, q^* S_r \bar{c}_r + (\Delta F_r)_{feel}$$

$$F_a = \frac{1}{2} \frac{G_a}{B_a} C_{h_a}(\delta a, \beta, \delta t_a)\, q^* S_a \bar{c}_a + (\Delta F_a)_{feel}$$

and plotted versus β .

B. ROLLING PERFORMANCE

A primary lateral-control consideration is the rolling performance available for a given lateral control force or deflection. Although rolling performance is often specified as the wing-tip helix angle pb/2V in radians or as a roll rate, p, in degrees per second, some rolling-performance requirements are specified in terms of a bank-angle change during the first second following control deflection or as a wing-tip velocity in feet per second. The roll-mode time constant, which many investigators have found to be an important rolling-performance parameter in itself,

is discussed later, in Section IVB2. Since one of the most important functions of rolling is to initiate course changes, roll performance should be determined about stability axes.

Calculated time histories of aileron rolls are very useful, since the required information is made available directly. A linearized lateral three-degree-of-freedom analysis is generally sufficient unless the configuration is subject to appreciable nonlinear inertia-coupling effects. Although hand computation is possible, digital or analog computers are recommended for this analysis. In view of the bank-angle-change requirements, ramp control inputs representing actual control-surface rates should be used. Step control inputs may be used if the bank-angle change during the first second is not of interest, or to get insight or an approximate answer for time-to-bank. When roll rate is of interest, the steady-state value corresponding to constant control deflection is the value to be concerned with. If no apparent steady rate exists, the roll rate at the first point of minimum rolling acceleration may normally be quoted. In some cases the peak roll rate may not occur prior to rolling 360 degrees. In this event, it may be desirable to restrict consideration to the roll rate that can be achieved in rolls that are completed at 360 degrees.

The conventional three-degree-of-freedom, stability-axes equations (Section IVB2), modified by (a) eliminating the spiral mode[8] and (b) omitting the $g\phi$ term (which is wrong for large ϕ and generally small anyway), give the transfer function

$$\frac{\phi(s)}{\delta a(s)} = \frac{b_2 s^2 + b_1 s + b_0}{s(a_3 s^3 + a_2 s^2 + a_1 s + a_0)}$$

For conventional lateral-directional modes the response to a step input, $\delta a(s) = \delta a/s$, is given by

$$\phi(s) = \frac{L'_{\delta a}\,\delta a \left[s^2 + (2\zeta\omega_n)_\phi s + (\omega_n^2)_\phi \right]}{s^2 \left(s + \frac{1}{T_R} \right) \left[s^2 + (2\zeta\omega_n)_d s + (\omega_n^2)_d \right]}$$

The factors are detailed in Section IVB2, and

$$L'_{\delta a} = \frac{L_{\delta a} + \frac{I_{xz}}{I_x} N_{\delta a}}{1 - \frac{I_{xz}^2}{I_x I_z}} = \frac{q^* Sb \left(C_{\ell \delta a} + \frac{I_{xz}}{I_z} C_{n \delta a} \right)}{I_x \left(1 - \frac{I_{xz}^2}{I_x I_z} \right)}$$

[8] The assumption is that a steady roll rate is reached before the spiral motion has progressed very far (e^{-t/T_s} is still close to 1). Otherwise no steady rolling motion exists.

The time response to a step input has the form

$$p(t) = B_1 + C_1 e^{-t/T_R} + D_1 e^{-(\zeta\omega_n)_d t} \sin(\omega_{n_d}\sqrt{1-\zeta_d^2}\,t + \psi_1)$$

$$\phi(t) = A_2 + B_2 t + C_2 e^{-t/T_R} + D_2 e^{-(\zeta\omega_n)_d t} \sin(\omega_{n_d}\sqrt{1-\zeta_d^2}\,t + \psi_2)$$

The amount of Dutch roll in an aileron roll can be shown[9] to depend inversely on the damping ratio ζ_d and stiffness ω_{n_d}, and directly on

$$1 - \left(\frac{\omega_{n_\phi}}{\omega_{n_d}}\right)^2 \doteq \frac{(C_{n_{\delta a}} + \frac{I_{xz}}{I_x} C_{\ell_{\delta a}})(C_{\ell_\beta} + \frac{I_{xz}}{I_z} C_{n_\beta})}{(C_{\ell_{\delta a}} + \frac{I_{xz}}{I_z} C_{n_{\delta a}})(C_{n_\beta} + \frac{I_{xz}}{I_x} C_{\ell_\beta})}$$

With stable (negative) C_{ℓ_β}, adverse yaw (negative aileron yawing-moment derivative) tends to reduce the steady roll rate; it can even cause a roll reversal, which is not acceptable. For low Dutch-roll damping, according to Reference 26, $(\omega_{n_\phi}/\omega_{n_d})^2$ must exceed 0.5 to avoid reversal. Favorable yaw tends to create a closed-loop control problem for the pilot (Reference 26).

1. Steady Roll Rate

The steady-state roll rate, p_∞, is given by the limit value theorem (Reference 17, for example). For a step aileron deflection,

$$\frac{p_\infty}{\delta a} = \left(\frac{\omega_{n_\phi}}{\omega_{n_d}}\right)^2 T_R L'_{\delta a} = \frac{b_o}{a_o}$$

In terms of stability derivatives, neglecting $C_{n_{\dot\beta}}$, $C_{\ell_{\dot\beta}}$, C_{y_r}, C_{y_p}, and g,

$$\frac{p_\infty}{\delta a} \doteq -\frac{2V}{b}\frac{C'_{\ell_{\delta a}}}{C'_{\ell_p}}\left[\frac{1 + \frac{C_{y_\beta} C'_{n_r}}{4\mu_2 C'_{n_\beta}} - \frac{C'_{n_{\delta a}}}{C'_{\ell_{\delta a}}}\left(\frac{C'_{\ell_\beta}}{C'_{n_\beta}} + \frac{C_{y_\beta} C'_{\ell_r}}{4\mu_2 C'_{n_\beta}}\right) + \frac{C_{y_{\delta a}}}{4\mu_2 C'_{\ell_{\delta a}}}\left(C'_{\ell_r} - \frac{C'_{\ell_\beta} C'_{n_r}}{C'_{n_\beta}}\right)}{1 + \frac{C_{y_\beta} C'_{n_r}}{4\mu_2 C'_{n_\beta}} - \frac{C'_{n_p}}{C'_{\ell_p}}\left(\frac{C'_{\ell_\beta}}{C'_{n_\beta}} + \frac{C_{y_\beta} C'_{\ell_r}}{4\mu_2 C'_{n_\beta}}\right)}\right]$$

where

$$C'_{\ell_i} = \frac{C_{\ell_i} + \frac{I_{xz}}{I_z} C_{n_i}}{1 - \frac{I_{xz}^2}{I_x I_z}}$$

[9] See Section IVD and Reference 26.

and

$$C_{n_i}' = \frac{C_{n_i} + \frac{I_{xz}}{I_x} C_{\ell_i}}{1 - \frac{I_{xz}^2}{I_x I_z}}$$

$$i = \beta, p(b/2V_0), r(b/2V_0), \delta a .$$

Various further simplifications are possible. When $|C_{y_{\delta a}}| << |4\mu_2 C_{\ell_{\delta a}}'|$ the simplification is obvious. When $|C_{y_{\delta a}}| << |4\mu_2 C_{\ell_{\delta a}}'|$, $|C_{\ell_r}'| << |4\mu_2 C_{\ell_\beta}'/C_{y_\beta}|$, and $|C_{n_r}'| << |4\mu_2 C_{n_\beta}'/C_{y_\beta}|$,

$$\frac{p_\infty}{\delta a} \doteq -\frac{2V}{b}\frac{C_{\ell_{\delta a}}'}{C_{\ell_p}'}\left[\frac{1 - \frac{C_{n_{\delta a}}'}{C_{\ell_{\delta a}}'}\frac{C_{\ell_\beta}'}{C_{n_\beta}'}}{1 - \frac{C_{n_p}'}{C_{\ell_p}'}\frac{C_{\ell_\beta}'}{C_{n_\beta}'}}\right]$$

Further neglecting N_p',

$$\frac{p_\infty}{\delta a} \doteq -\frac{2V}{b}\frac{C_{\ell_{\delta a}}'}{C_{\ell_p}'}\left[1 - \frac{C_{n_{\delta a}}'}{C_{\ell_{\delta a}}'}\frac{C_{\ell_\beta}'}{C_{n_\beta}'}\right]$$

When product of inertia effects are ignorable, the primed notation can be dropped in any of these expressions. The relation reduces in its simplest form to the one-degree-of-freedom roll result

$$\left(\frac{pb}{2V}\right)_\infty \doteq -\frac{C_{\ell_{\delta a}}}{C_{\ell_p}}\,\delta a$$

Note that all angular dimensions are in radian measure.

By using effective values of the derivatives as in Section IIIA1, account can be taken of stability augmentation, aileron-rudder interconnection, etc. For control system synthesis, however, the techniques of References 8 and 9 are recommended. Augmentation displacement limiting can be important.

2. Time to Bank

This is a much more complicated problem than the simple version considered here. Flight control system dynamics and control rate limiting, as well as aircraft yawing

and sideslipping, affect the result. However, it is instructive to consider the single-degree-of-freedom roll response to a step aileron deflection. The result will be more optimistic, of course, than one based on the above control-system factors. The single-degree-of-freedom response is

$$\Delta\phi(t) = \frac{L_{\delta a}\,\delta a}{\left(\frac{1}{T_R}\right)^2}\left[e^{-t/T_R} + \frac{t}{T_R} - 1\right],$$

where

$$\frac{1}{T_R} \doteq -\frac{q^* S b}{I_x}\,\frac{b}{2V}\,C_{\ell_p}$$

and

$$L_{\delta a} = \frac{q^* S b}{I_x}\,C_{\ell_{\delta a}}$$

A more refined approximation for $1/T_R$ is given in Section IVB2. To approximate the effect of control rate limiting, use an effective time increment:

$$t_{eff} = t + \frac{1}{2}\,\frac{\delta a_{max}}{\dot{\delta a}_{max}}$$

Figure 8 interprets this analysis for several forms of requirements. The time to 95 percent p_∞ is $3T_R$.

A requirement is sometimes stated in terms of banking to and stopping at a given angle in a certain time. The analysis that follows is subject to all the faults of the time-to-bank analysis above, and also to a pilot's difficulty in trying to perform such a maneuver. (He could not do it both rapidly and accurately.) Intuitively, the best command for minimum time is the double pulse sketched.

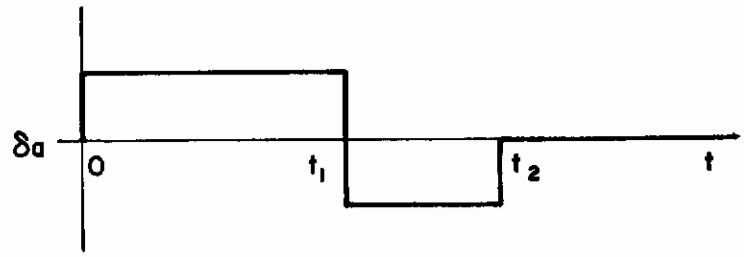

As a result of a linear analysis using a method from Reference 17,

$$t_1 = \frac{1}{2}\left(\frac{\phi_c}{p_\infty} + t_2\right)$$

where ϕ_c is the commanded bank angle. An explicit expression for ϕ_c in terms of t_2 is

$$\phi_c = p_\infty \left[t_2 + 2T_R \ln \left(\frac{1 + e^{-t_2/T_R}}{2} \right) \right]$$

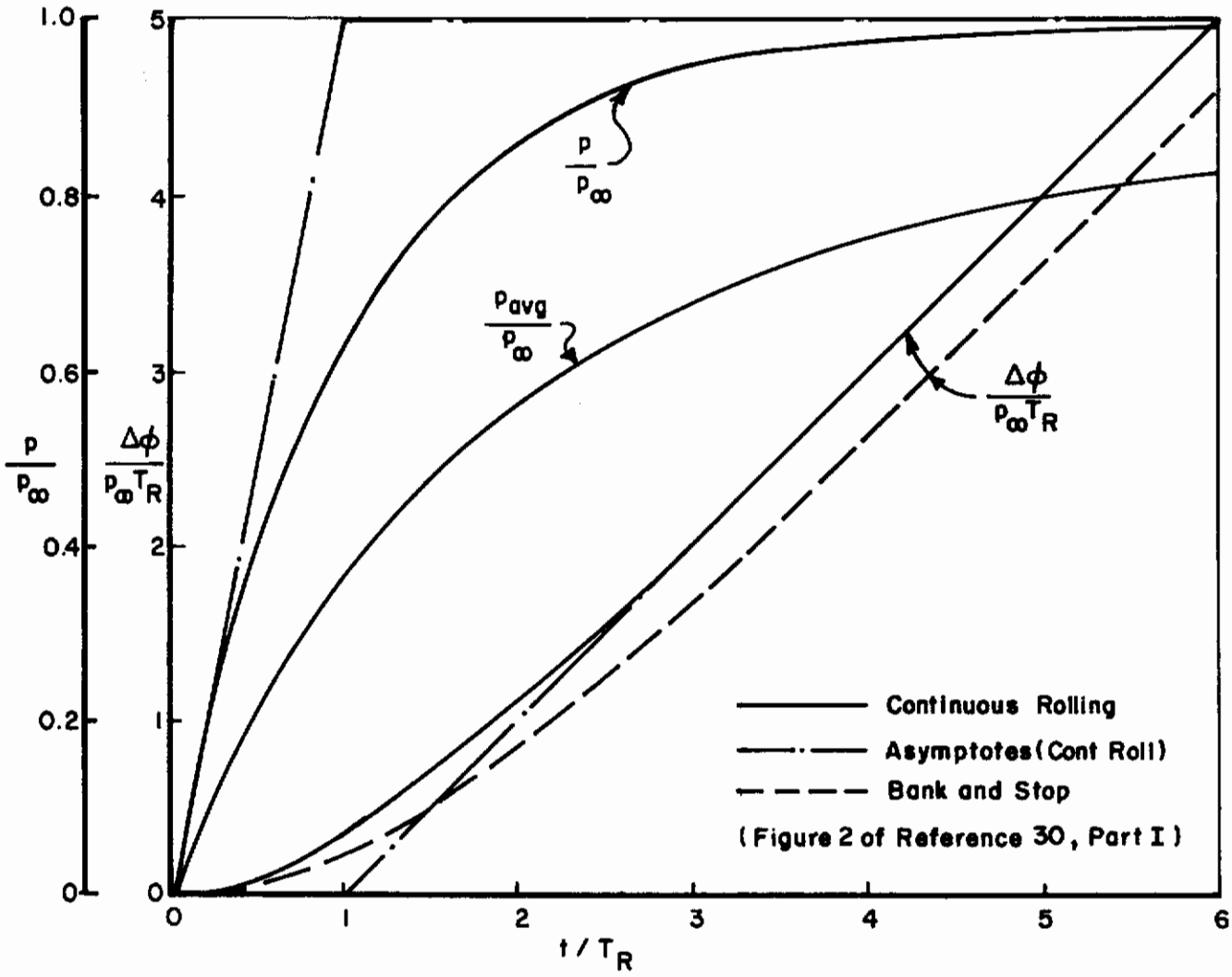

Figure 8. Idealized Roll Response to Step Aileron

3. Aileron Forces

For a reversible lateral control system, in a steady roll if $\delta a_L = \delta a_R$

$$F_a \doteq \frac{1}{2} \frac{G_a}{B_a} q^* S_a \bar{c}_a \left[C_{h_{a_{\delta a}}} \delta a + C_{h_{a_p}} \frac{pb}{2V} \right] + (\Delta F_a)_{feel} + \Delta F_a$$

The nonlinear equivalent and the extension to spoilers, etc. are readily apparent (Appendix III and Section IIIA2). For a conventional irreversible system with force proportional to control deflection:

$$F_a = \frac{dF_a}{d\delta a}\,\delta a + \Delta F_a$$

In each case ΔF_a includes friction, preload, etc. This equation represents a linear feel spring with constant stick-to-surface gearing. Nonlinear feel springs and varying stick-to-surface gearing should be treated appropriately.

Although control-surface hinge moments are of little interest in determining cockpit control forces with an irreversible system, they still determine the available control-surface deflections. Thus hinge moments and control-system power or pilot-force limitations must be considered in estimating maximum rolling performance.

C. CROSSWIND TAKEOFF AND LANDING

Reference 15 requires maintaining a straight course in stated crosswind conditions, with or without braking. These requirements must be met with a pedal force not exceeding 180 pounds. Although drag parachutes or other special considerations may cause difficulty, crosswind directional control usually is not a problem at high forward speeds. There effective sideslip angle is small, and the resulting moments and forces can be overcome by conventional aerodynamic controls. Since lifting forces may be high, the landing-gear ground reactions may be low; thus it may be necessary to depress the upwind wing as in a steady sideslip to achieve balanced lateral forces.

When lateral control is lost at lower speeds and it is no longer possible to hold the wings level, the resulting lateral component of lift may cause a large unbalance of lateral forces. Although it may be possible to maintain heading, the aircraft skids downwind. Application of upwind brake to counteract the skidding may or may not be successful. A full analysis, as will be seen, gets rather involved. For this reason the general case is only indicated. Simplified equations are developed, and a further-simplified solution given.

Note that in the following methods all angles are assumed to be expressed in radians and all derivatives, per radian. Ground effect should, of course, be considered.

The desired condition, shown in Figure 9, is that vehicle velocity parallel the runway centerline. Small bank angles (not shown) are possible. Each of the main gear, then, slips at the angle ψ, giving a y force opposing the crosswind (comparable to wing lift variation with α), as well as a drag force in line with the x axis. Nose-gear forces are "drag" at an angle δ_N (Figure 9) to the x axis and a "side" force proportional to $(\delta_N + \psi)$ at an angle δ_N to the y axis. All these forces, of course, are proportional to the respective ground reactions. Interest is in conditions where the wheels are not skidding, though braking is considered.

Aerodynamic forces and moments are proportional to q* based on the relative wind, β, δa, and δr. For a given forward speed and wind, the variable $\left[(\psi + \beta) - \psi\right]$ may be substituted for β.

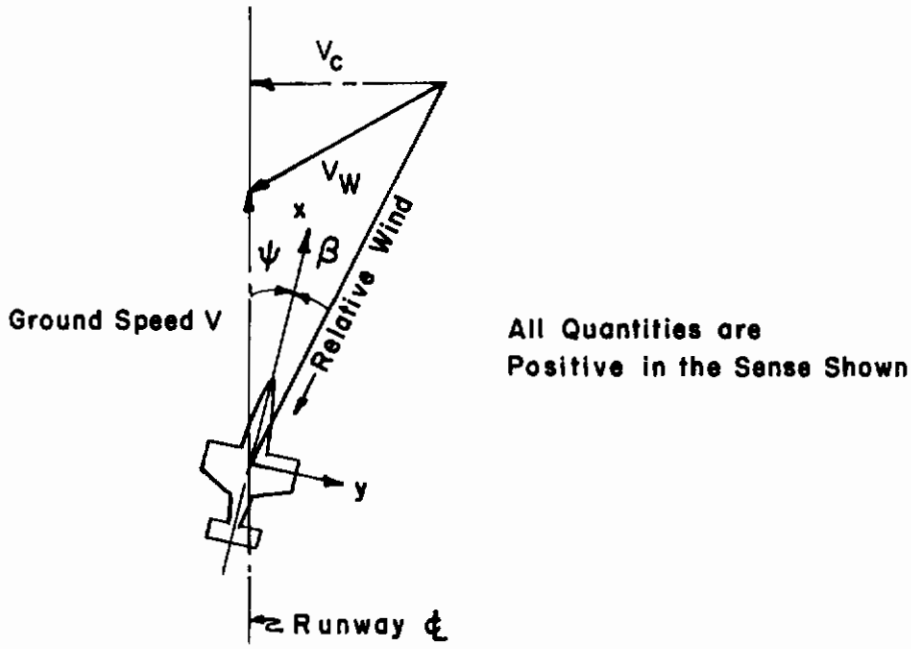

Figure 9. Crosswind Relationships on Runway

The tire forces (See Figures 9 and 10 for notation), allowing for differential braking, are:

$$X_R = -\left(\mu_{x_R} - \frac{\partial (X/R)_M}{\partial \psi}\,\psi\right) R_R$$

$$Y_R = \frac{\partial (Y/R)_M}{\partial \psi}\,\psi\, R_R$$

$$X_L = -\left(\mu_{x_L} - \frac{\partial (X/R)_M}{\partial \psi}\,\psi\right) R_L$$

$$Y_L = \frac{\partial (Y/R)_M}{\partial \psi}\,\psi\, R_L$$

$$X_N = -\left[\mu_{x_N} - \frac{\partial (X/R)_N}{\partial \psi}\,(\psi + \delta_N)\right] R_N \cos\delta_N - \frac{\partial (Y/R)_N}{\partial \psi}\,(\psi + \delta_N)\, R_N \sin\delta_N$$

$$Y_N = \frac{\partial (Y/R)_N}{\partial \psi}\,(\psi + \delta_N)\, R_N \cos\delta_N - \left[\mu_{x_N} - \frac{\partial (X/R)_N}{\partial \psi}\,(\psi + \delta_N)\right] R_N \sin\delta_N$$

When the nose wheel is off the ground, the method of Section IID gives $R_M = R_R + R_L$ directly when three of α , δe , q*, and T are specified. The discussion below gives R_R and R_L in terms of R_M and ϕ . Adding R_n terms to the basic equations of Section IID, both R_M and R_N can be found:

$$\begin{bmatrix} 1 & 1 & q^*S\left(C_{L_\alpha}+\frac{T}{q^*S}\right) \\ \mu_M(h_{cg}+r) & \mu_N(h_{cg}+r)-\ell_G & -q^*S\bar{c}\left(C_{m_\alpha}+\frac{\ell_{cg}}{\bar{c}}C_{L_\alpha}\right) \\ -\frac{1}{K_M} & \frac{1}{K_N} & \ell_G \end{bmatrix} \begin{Bmatrix} R_M \\ R_N \\ \alpha \end{Bmatrix} = \begin{Bmatrix} W-Ti_T+q^*S(C_{L_\alpha}\alpha_o-C_{L_\delta}\delta) \\ q^*S\bar{c}\left[C_{m_o}-C_{m_\alpha}\alpha_o+(C_{m_\delta}+\frac{-\ell_{cg}}{\bar{c}}C_{L_\delta})\delta\right]+(h_{cg}-h_T)T-\ell_{cg}W \\ \ell_G\alpha_{FE} \end{Bmatrix}$$

References 27 through 29 indicate characteristics of the tire derivatives.

The expressions above are complicated; the derivatives $\frac{\partial(X/R)}{\partial\beta}$ and $\frac{\partial(Y/R)}{\partial\beta}$ are not well known and vary with tire pressure, runway condition, etc. To continue the analysis we therefore assume that ψ is very much smaller than β ; that is, that the angle between the runway and the relative wind is approximately β . This appears a reasonable assumption for calculating controllability in high crosswinds. Further, in the analysis below, the gear x forces due to ψ are not stated explicitly and the gear y forces are stated in the form $\mu_y R$. Thus the lateral coefficient of friction μ_y is an implicit function of ψ (and, for the nose gear, δ_N). This form is handy for cases involving maximum gear drag and side forces. Conservative estimates of limits are:

$$0 \text{ (on ice or planing on wet runway)} \leq \mu_x \leq \begin{cases} 0.015 \text{ (rolling)} \\ 0.25 \text{ (static; braking)} \end{cases}$$

$$0 \leq |\mu_y| \leq 0.25 \text{ (static)}$$

Gear structural side-load limits may be more restrictive.

To consider a crosswind landing gear, in Figure 10 the gear can be aligned with the direction of motion. Without braking, its y force will be small ($-\mu_x R_M \sin \delta_M$ with δ_M positive in the same sense as δ_N in Figure 10), possibly negligible.

In design it is usual to consider 90-degree crosswinds. Then, neglecting ψ as discussed above,

$$\beta = \tan^{-1}(V_c/V) \doteq V_c/V$$

$$q^* = \frac{1}{2}\rho(V/\cos\beta)^2 \doteq \frac{1}{2}\rho V^2 \qquad (V \text{ in ft/sec})$$

This approximation for q* is useful when β is not specified but is to be found. However, it underestimates q* and thus the aerodynamic forces and moments at large β . If desired, the solution can be iterated to get a better result.

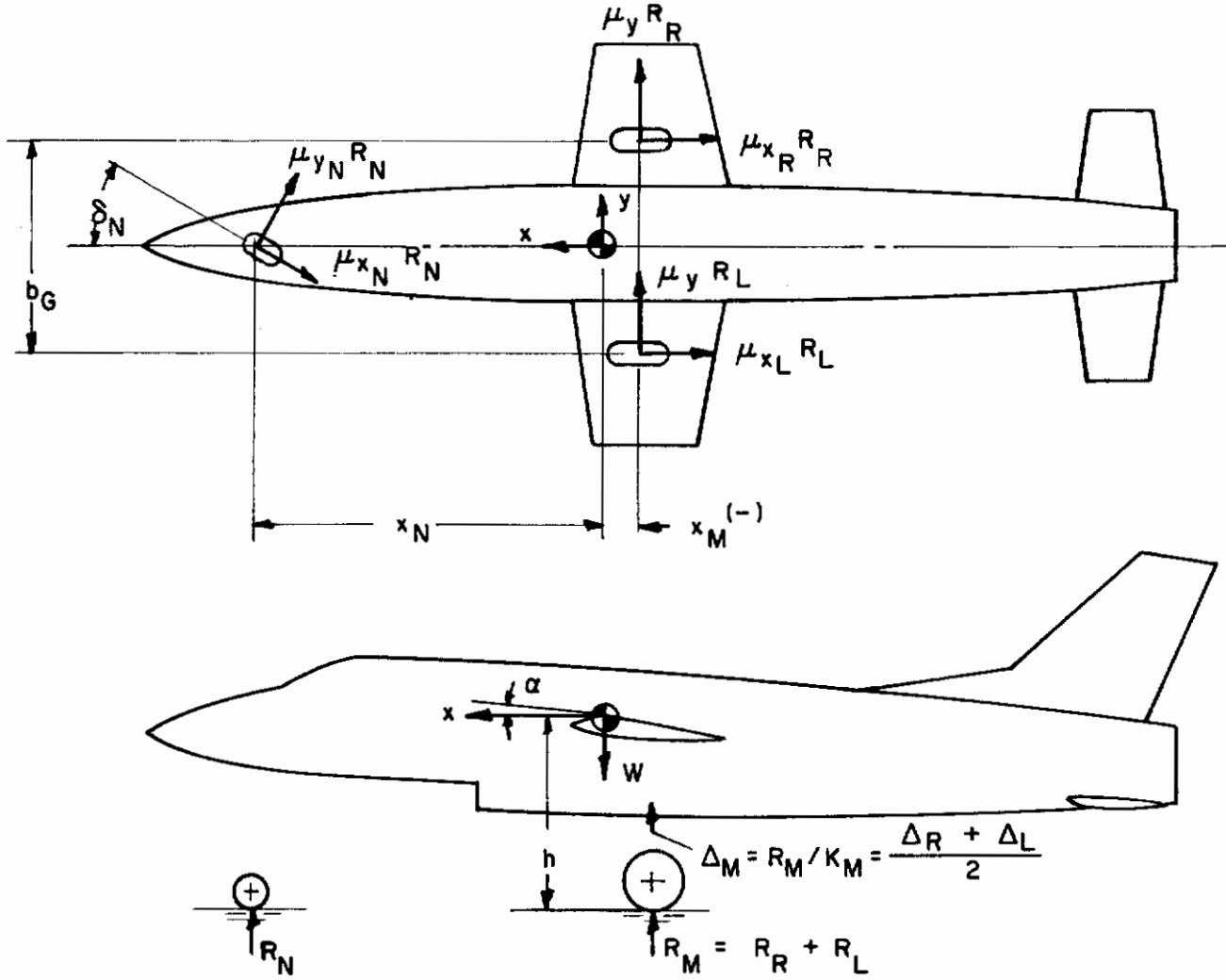

Figure 10. Lateral-Directional Ground Reactions

R_N and R_M are found separately, knowing T, α , q*, and δe. Then

$$R_R = \frac{1}{2}\left(R_M + \frac{b_G}{K_M}\phi \right) = \frac{K_M}{2}\Delta_R$$

$$R_L = \frac{1}{2}\left(R_M - \frac{b_G}{K_M}\phi \right) = \frac{K_M}{2}\Delta_L$$

With these substitutions the linear lateral-directional trim equations become

$$W\phi + q^*S\left[C_{y_{\delta a}}\delta a + C_{y_{\delta r}}\delta r + C_{y_\beta}\beta \right] + \mu_{y_M} R_M + \left(\mu_{y_N}\cos\delta_N - \mu_{x_N}\sin\delta_N \right) R_N = 0$$

$$\frac{b_G^2 K_M}{8}\left(\mu_{x_R} + \mu_{x_L} \right)\phi + q^*Sb\left[C_{n_{\delta a}}\delta a + C_{n_{\delta r}}\delta r + C_{n_\beta}\beta \right]$$

$$+ \left[\mu_{y_M} x_M + \frac{b_G}{4}\left(\mu_{x_R} - \mu_{x_L} \right) \right] R_M + \left(\mu_{y_N}\cos\delta_N - \mu_{x_N}\sin\delta_N \right) x_N R_N = 0$$

$$-\frac{b_G^2 K_M}{4}\phi + q^*Sb\left[C_{\ell_{\delta a}}\delta a + C_{\ell_{\delta r}}\delta r + C_{\ell_\beta}\beta \right] - \mu_{y_M} h R_M - \left(\mu_{y_N}\cos\delta_N - \mu_{x_N}\sin\delta_N \right) h R_N = 0$$

where the variable coefficients of friction μ define the drag and side loads on the gear. For the nose gear, μ_{x_N} and μ_{y_N} include loads due to δ_N; see the gear-force discussion preceding. For the main gear, the maximum linear lateral force is reached when either wheel starts skidding; with wings level the maximum lateral force is $\mu_y R_M$. The equations apply equally well for a tail-wheel configuration; then x_N is negative, x_M positive. The equations hold as long as bank angle, gear side loads, and control deflections are within limits; the ground path is straight; R_L, R_R, and R_N are all non-negative; and the aerodynamics remain linear. The derivatives should include ground effect where applicable. Extension to the nonlinear case is apparent.

The three equations in many unknowns (ϕ, δa, δr, β, δ_N, μ_{x_R}, or μ_{x_L}, etc; at a given airspeed, q* is known) can be solved for equilibrium in terms of one unknown when others are specified. For example, stated braking action and nose-gear steering angle allow solution for ϕ, δa, and δr in terms of $\beta \doteq V_c/V$,

As a useful simplified example, consider the case of:

(1) Wings held level

(2) No braking ($\mu_{x_R} = \mu_{x_L} = \mu_{x_N} = \mu_x$; $\mu_{y_M} = \mu_{y_N} = \mu_y$)

(3) $\delta_N = 0$

(4) Negligible $C_{y_{\delta a}}$ and $C_{n_{\delta a}}$

The first three of these assumptions permit a unique solution for δr, δa, and μ_y as functions of β. The simpler of the forms given below apply when the nose gear is off the ground, or approximately when the nose gear trails.

$$\mu_y = -\frac{q^* S C_{y_\beta}}{R}\left[\frac{1-\frac{C_{y_{\delta r}}}{C_{n_{\delta r}}}\frac{C_{n_\beta}}{C_{y_\beta}}}{1-\left(\frac{x_M}{b}\frac{R_M}{R}+\frac{x_N}{b}\frac{R_N}{R}\right)\frac{C_{y_{\delta r}}}{C_{n_{\delta r}}}}\right]\beta$$

$$\doteq -\frac{q^* S C_{y_\beta}}{R_M}\left[\frac{1-\frac{C_{y_{\delta r}}}{C_{n_{\delta r}}}\frac{C_{n_\beta}}{C_{y_\beta}}}{1-\frac{x_M}{b}\frac{C_{y_{\delta r}}}{C_{n_{\delta r}}}}\right]\beta \qquad \text{when } \mu_{y_N} R_N \doteq 0$$

$$\delta r = -\frac{C_{n_\beta}}{C_{n_{\delta r}}}\left[\frac{1-\left(\frac{x_M}{b}\frac{R_M}{R}+\frac{x_N}{b}\frac{R_N}{R}\right)\frac{C_{y_\beta}}{C_{n_\beta}}}{1-\frac{x_M}{b}\frac{R_M}{R}+\frac{x_N}{b}\frac{R_N}{R}\frac{C_{y_{\delta r}}}{C_{n_{\delta r}}}}\right]\beta$$

$$\doteq -\frac{C_{n_\beta}}{C_{n_{\delta r}}}\left[\frac{1-\frac{x_M}{b}\frac{C_{y_\beta}}{C_{n_\beta}}}{1-\frac{x_M}{b}\frac{C_{y_{\delta r}}}{C_{n_{\delta r}}}}\right]\beta \qquad \text{when } \mu_{y_N} R_N \doteq 0$$

$$\delta_a = -\frac{C_{\ell_\beta} - \frac{C_{\ell_{\delta_r}}}{C_{n_{\delta_r}}} C_{n_\beta} + \frac{h}{b}\left(C_{y_\beta} - \frac{C_{y_{\delta_r}}}{C_{n_{\delta_r}}} C_{n_\beta}\right) + \left(\frac{x_M}{b}\frac{R_M}{R} + \frac{x_N}{b}\frac{R_N}{R}\right)\left(\frac{C_{\ell_{\delta_r}}}{C_{n_{\delta_r}}} C_{y_\beta} - \frac{C_{y_{\delta_r}}}{C_{n_{\delta_r}}} C_{\ell_\beta}\right)}{C_{\ell_{\delta_a}}\left[1 - \left(\frac{x_M}{b}\frac{R_M}{R} + \frac{x_N}{b}\frac{R_N}{R}\right)\frac{C_{y_{\delta_r}}}{C_{n_{\delta_r}}}\right]}$$

$$\doteq -\frac{C_{\ell_\beta} - \frac{C_{\ell_{\delta_r}}}{C_{n_{\delta_r}}} C_{n_\beta} + \frac{h}{b}\left(C_{y_\beta} - \frac{C_{y_{\delta_r}}}{C_{n_{\delta_r}}} C_{n_\beta}\right) + \frac{x_M}{b}\left(\frac{C_{\ell_{\delta_r}}}{C_{n_{\delta_r}}} C_{y_\beta} - \frac{C_{y_{\delta_r}}}{C_{n_{\delta_r}}} C_{\ell_\beta}\right)}{C_{\ell_{\delta_a}}\left(1 - \frac{x_M}{b}\frac{C_{y_{\delta_r}}}{C_{n_{\delta_r}}}\right)}$$

when

$$\mu_{y_N} R_N \doteq 0$$

where $R = R_M + R_N$. For a 90-degree crosswind,

$$\beta = \tan^{-1}(V_c/V)$$

$$q^* = \frac{1}{2}\rho(V^2 + V_c^2)$$

In this simple case the gear side loads and the control deflections to maintain a straight ground path can be calculated easily for a given combination of V and V_c. When the wings can no longer be kept level with maximum aileron deflection, or where the vehicle is banked into the crosswind, the more complicated equations involving ϕ must be used for any analysis.

Control forces can be estimated by the method of Section IIIA2.

D. CONTROL WITH ASYMMETRIC THRUST

Military requirements (Reference 15) are placed on controllability with ailerons only and with both rudder and ailerons. At and above the minimum control speed it must be possible to maintain steady, straight flight with asymmetric power using only ailerons to bank and sideslip; and also to control the transient motion upon engine failure to achieve and maintain straight flight with a bank angle of less than 5 degrees. Civil aeronautics regulations (References 24 and 25) require a "reasonable" excess of directional control to remain in straight, wings-level flight; and the ability to execute 15 degrees or 20-degree banked turns in either direction. At high speed the tail load associated with the dynamic sideslip excursion and rudder deflection (manual plus automatic) can be critical.

Compliance with the dynamic requirements should be shown by time histories calculated with the equations of Section IV. The static conditions in straight flight, found by a modification of the equations in Section IIIA, are given below (Ordinarily the effect of aerodynamic damping in a 20-degree banked turn will be minor). With ΔT negative for an engine failure, $C_{L_1} = W/q^*S$, radian angular measure, and both rudder and aileron control,

$$\beta \doteq \frac{-\left[C_{L_1}\phi + C_y(\Delta T)\right]\left(1 - \frac{C_{n_{\delta a}}}{C_{\ell_{\delta a}}}\frac{C_{\ell_{\delta r}}}{C_{n_{\delta r}}}\right) + \frac{C_{y_{\delta r}}}{C_{n_{\delta r}}}\left[C_n(\Delta T)\left(1 - \frac{C_{y_{\delta a}}}{C_{\ell_{\delta a}}}\frac{C_{\ell_{\delta r}}}{C_{y_{\delta r}}}\right) - C_\ell(\Delta T)\left(\frac{C_{n_{\delta a}}}{C_{\ell_{\delta a}}} - \frac{C_{y_{\delta a}}}{C_{\ell_{\delta a}}}\frac{C_{n_{\delta r}}}{C_{y_{\delta r}}}\right)\right]}{C_{y_\beta}\left(1 - \frac{C_{n_{\delta a}}}{C_{\ell_{\delta a}}}\frac{C_{\ell_{\delta r}}}{C_{n_{\delta r}}}\right) - C_{n_\beta}\frac{C_{y_{\delta r}}}{C_{n_{\delta r}}}\left(1 - \frac{C_{n_{\delta a}}}{C_{\ell_{\delta a}}}\frac{C_{\ell_\beta}}{C_{n_\beta}}\right) - \frac{C_{y_{\delta a}}}{C_{\ell_{\delta a}}}\left(C_{\ell_\beta} - \frac{C_{\ell_{\delta r}}}{C_{n_{\delta r}}}C_{n_\beta}\right)}$$

$$\doteq \frac{-C_{L_1}\phi + \frac{C_{y_{\delta r}}}{C_{n_{\delta r}}}\left[C_n(\Delta T) - \frac{C_{n_{\delta a}}}{C_{\ell_{\delta a}}}C_\ell(\Delta T)\right]}{C_{y_\beta} - \frac{C_{y_{\delta r}}}{C_{n_{\delta r}}}C_{n_\beta}\left(1 - \frac{C_{n_{\delta a}}}{C_{\ell_{\delta a}}}\frac{C_{\ell_\beta}}{C_{n_\beta}}\right)}$$

Slipstream effects can cause significant $C_\ell(\Delta T)$; while a canted engine thrust line or, on some configurations, aerodynamic interference can produce a $C_y(\Delta T)$. Values used for the derivatives should account for any alteration to stability or control effectiveness caused by the partial thrust loss. The approximation holds when

$$\frac{C_{n_{\delta a}}}{C_{\ell_{\delta a}}}\frac{C_{\ell_{\delta r}}}{C_{n_{\delta r}}} << 1$$

and $C_y(\Delta T) \doteq C_{y_{\delta a}} \doteq 0$. Thus, given ϕ we can find β, or conversely. Once β and ϕ are known, the control deflections can be found:

$$\delta r = \frac{-C_{n_\beta}\left(1 - \frac{C_{n_{\delta a}}}{C_{\ell_{\delta a}}}\frac{C_{\ell_\beta}}{C_{n_\beta}}\right)\beta - C_n(\Delta T) + \frac{C_{n_{\delta a}}}{C_{\ell_{\delta a}}}C_\ell(\Delta T)}{C_{n_{\delta r}}\left(1 - \frac{C_{n_{\delta a}}}{C_{\ell_{\delta a}}}\frac{C_{\ell_{\delta r}}}{C_{n_{\delta r}}}\right)}$$

$$\delta a = \frac{-\left(C_{\ell_\beta} - \frac{C_{\ell_{\delta r}}}{C_{n_{\delta r}}}C_{n_\beta}\right)\beta - C_\ell(\Delta T) + \frac{C_{\ell_{\delta r}}}{C_{n_{\delta r}}}C_n(\Delta T)}{C_{\ell_{\delta a}}\left(1 - \frac{C_{n_{\delta a}}}{C_{\ell_{\delta a}}}\frac{C_{\ell_{\delta r}}}{C_{n_{\delta r}}}\right)}$$

Alternatively, β corresponding to maximum δr can be found from the relation above. Simplifications when $C_{n_{\delta a}} = 0$, $C_\ell(\Delta T) = 0$, etc. are obvious. The control forces can be estimated from Section IIIA2.

Of course, δr and δa are the actual control-surface deflections. In straight flight rate feedback will have no effect, but any augmentation involving β, ϕ, a_y, $\delta a \rightarrow \delta r$, or $\delta r \rightarrow \delta a$ must be accounted for in finding the cockpit-control deflections. Equivalent derivatives can be found as in Section IIIA and substituted in the equations

above, as long as augmentation authority limits are not exceeded. Lateral-acceleration feedback gives effective C_{n_ϕ} and C_{ℓ_ϕ}, not accounted for above, but a solution can be found from the steady-state equations as in Section IIIA. With tab control it is necessary to check both tab and surface deflections (See Appendix II). Control forces can be found as in Section IIIA2.

A suggested general procedure to find the minimum control speed is to calculate the control deflections at three speeds and interpolate. Some cases, however, are so simple that an explicit formula can be written. Using the approximations indicated above, and further assuming that $C_n(\Delta T) = -y_T \Delta T$ and $C_\ell(\Delta T) = 0$, and that the derivatives are invariant with angle of attack, if rudder control is critical the minimum control speed is

$$V_{MC} = 17.2 \sqrt{\frac{-.0873(W/S)\left|\frac{y_T}{b}\frac{\Delta T}{S}\frac{C_{y_\beta}}{C_{n_\beta}\left(1-\frac{C_{n_{\delta a}}}{C_{\ell_{\delta a}}}\frac{C_{\ell_\beta}}{C_{n_\beta}}\right)}\right| - .0873(w/s)}{\left|\left(\frac{C_{y_\beta}C_{n_{\delta r}}}{C_{n_\beta}\left(1-\frac{C_{n_{\delta a}}C_{\ell_\beta}}{C_{\ell_{\delta a}}C_{n_\beta}}\right)}-C_{y_{\delta r}}\right)\delta r_{max}\right|}} \text{ kt EAS}$$

with ϕ = 5 degrees in the failed-engine-up sense. (For ϕ = 0, delete the W/S term in the numerator.) Then the corresponding β and δ a can be found from simplified versions of the δr and δa equations above.

1. Rudder Free

To calculate the steady-state conditions, take

$$C_{y_\beta}^* = C_{y_\beta} - \frac{C_{h_{r_\beta}}}{C_{h_{r_{\delta r}}}} C_{y_{\delta r}}$$

$$C_{n_\beta}^* = C_{n_\beta} - \frac{C_{h_{r_\beta}}}{C_{h_{r_{\delta r}}}} C_{n_{\delta r}}$$

$$C_{\ell_\beta}^* = C_{\ell_\beta} - \frac{C_{h_{r_\beta}}}{C_{h_{r_{\delta r}}}} C_{\ell_{\delta r}}$$

Then (with no stability augmentation)

$$\beta = - \frac{C_n(\Delta T)}{C_{n_\beta}^*} \left[\frac{1 - \frac{C_{n_{\delta a}}}{C_{\ell_{\delta a}}} \frac{C_\ell(\Delta T)}{C_n(\Delta T)}}{1 - \frac{C_{n_{\delta a}}}{C_{\ell_{\delta a}}} \frac{C_{\ell_\beta}^*}{C_{n_\beta}^*}} \right]$$

$$\delta a = \frac{\frac{C_{\ell_\beta}^*}{C_{n_\beta}^*} C_n(\Delta T) - C_\ell(\Delta T)}{C_{\ell_{\delta a}} \left(1 - \frac{C_{n_{\delta a}}}{C_{\ell_{\delta a}}} \frac{C_{\ell_\beta}^*}{C_{n_\beta}^*} \right)}$$

$$\sin \phi = \frac{1}{C_{L_1}} \left[- C_y(\Delta T) + \left(\frac{1 - \frac{C_{y_{\delta a}}}{C_{\ell_{\delta a}}} \frac{C_{\ell_\beta}^*}{C_{y_\beta}^*}}{1 - \frac{C_{n_{\delta a}}}{C_{\ell_{\delta a}}} \frac{C_{\ell_\beta}^*}{C_{n_\beta}^*}} \right) \frac{C_{y_\beta}^*}{C_{n_\beta}^*} C_n(\Delta T) + \left(\frac{C_{y_{\delta a}} - \frac{C_{y_\beta}^*}{C_{n_\beta}^*} C_{n_{\delta a}}}{1 - \frac{C_{n_{\delta a}}}{C_{\ell_{\delta a}}} \frac{C_{\ell_\beta}^*}{C_{n_\beta}^*}} \right) \frac{C_\ell(\Delta T)}{C_{\ell_{\delta a}}} \right]$$

These relations hold for rudder deflections within the linear hinge-moment range:

$$\delta r = - \frac{C_{h_{r_\beta}}}{C_{h_{r_{\delta r}}}} \beta$$

SECTION IV

DYNAMIC STABILITY AND CONTROL

A. GENERAL REMARKS

Approximate relations are presented here to desribe aircraft motion in conventional flight (at suborbital speeds where the vehicle is supported principally by aerodynamic lift rather than by thrust). The approximations being based on Reference 8, the same assumptions generally apply: linearity; constant coefficients; small perturbations from steady level flight; no steady wind; neglect of $X_{\dot{w}}$, X_q, $Z_{\dot{w}}$, Z_q, etc. All coefficients and derivatives are to be evaluated at the operating point. The body-fixed stability axes used here are aligned at the operating point with the projection of the vehicle velocity in the plane of symmetry. Therefore, in general, the motions do not correspond exactly to those measured by instrumentation aboard the airplane (See, for example, References 6 and 20). In the exceptional case where engine gyroscopic effects are strong enough to alter the motion, References 31 and 32 give a simple method for including them. For treatment of a large moving mass, as in tilt-wing VTOL transition, see Reference 18. For additional terms that arise in perturbations from steady curved flight, see References 6 and 32 and Appendix III.

In practice the linear equations have proved more useful than one might suspect. Still, there are times when nonlinearities cannot be ignored. The analytical complications are formidable: the very character of the motion can depend on amplitude, there are different concepts of stability, solutions cannot be superimposed, the transfer-function concept may not be valid, etc. Analysis techniques are still rather primitive; the interested reader can consult References 10 and 11. Systems of equations with slowly-varying coefficients can probably be handled adequately by "freezing" the coefficients; other available analysis methods are summarized in Reference 12.

The rolling pullout is often a critical maneuver for stability as well as flight loads. Nonlinear inertial coupling may be involved. If not, the combined longitudinal and lateral-directional linear equations can be used with proper consideration of initial conditions and any derivative variations with α and u.

Requirements can be given in several forms. Conversion relations are given in Table II and Figure 11, taken from Reference 4, for roots of the form $s = \sigma + j\omega$. Times are scale time; seconds, if the equations are written in terms of real time.

While present requirements specify only the characteristics of the free motion (for example, period and damping), research has shown that other response parameters are also important (See, for example, References 33 and 34). For that reason, and to aid in other aspects of analysis, a number of approximate aircraft transfer functions are tabulated for control and gust inputs. No control-system dynamics are included. Artificial stabilization is not considered explicitly, but may be included by using modified derivatives that include its linear effect or by applying servo analysis techniques. (See, for example, Section II, Appendix IV, or Reference 8 or 9.)

TABLE II

DYNAMIC STABILITY PARAMETERS

Frequency (cps)	$f = \frac{1}{2\pi}\omega$
Period	$T = \frac{1}{f} = \frac{2\pi}{\omega}$
Undamped natural frequency	$\omega_n = \omega/\sqrt{1-\zeta^2} = \sqrt{\omega^2+\sigma^2}$
Damping ratio	$\zeta = -\sigma/\omega_n$
Time to 1/10 (or 10x) amplitude (See Footnote 10)	$T_{1/10}$ (or T_{10}) $= -\frac{\ln 10}{\sigma} = \frac{\ln 10}{\zeta\omega_n}$
Cycles to 1/10 (or 10x) amplitude (See Footnote 10)	$C_{1/10}$ (or C_{10}) $= \frac{\sqrt{1-\zeta^2}}{2\pi\zeta}\ln 10$
Logarithmic decrement (of amplitude ratio per cycle)	$\delta = -\sigma T = \zeta\omega_n T = \frac{2\pi\zeta}{\sqrt{1-\zeta^2}}$

The approximations have been developed for perturbations from straight, level flight and assume small i_T. The stability derivatives must of course be evaluated at the correct center of gravity. Changes to derivatives caused by a shift in center of gravity can be determined, for example, from Reference 20.

The transfer functions have the general form, where o is the output, δ the input:

$$Y(s) = \frac{o(s)}{\delta(s)} = \frac{N(s)}{\Delta(s)}$$

Most characteristics of the free motion are determined by forming $\Delta(s) = 0$, the characteristic equation. Responses in terms of time, for particular inputs, can be found readily from tables of Laplace transforms such as the one in Reference 17.

1. Initial, Steady-State, Maximum Values

The steady-state response o(t) of a stable linear system to a step control input $\left[\delta(t) = \delta,\ \delta(s) = \delta/s\right]$ is given by the limit value theorem (Reference 17):

$$\lim_{t\to\infty} o(t) = \lim_{s\to 0}\left[s\cdot\frac{\delta}{s}Y(s)\right] = \delta\lim_{s\to 0}Y(s)$$

[10] Positive numbers indicated damped motion; negative numbers, divergence.

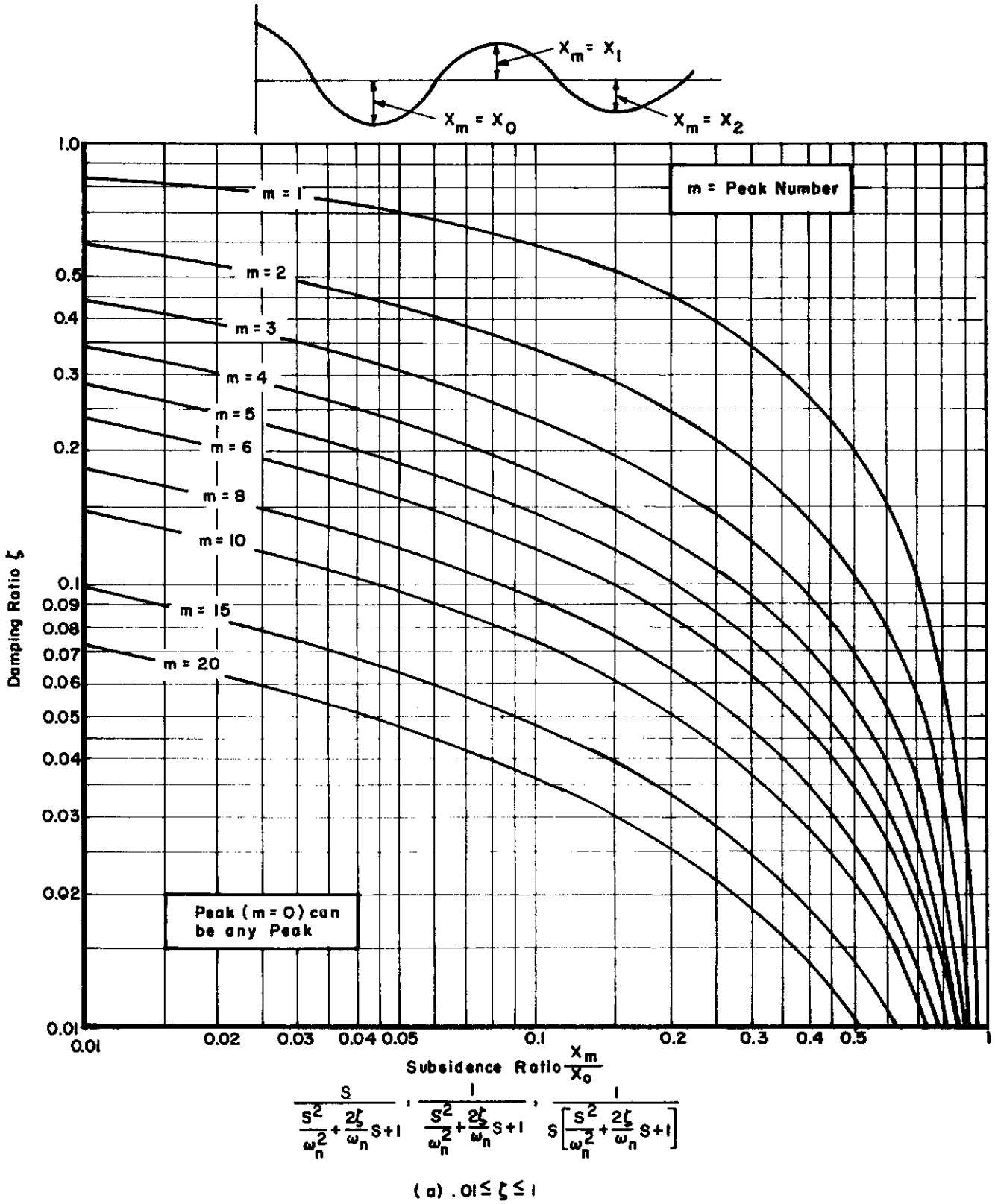

Figure 11. Damping Ratio of Oscillatory Transients as a Function of Subsidence Ratio for Second Order System

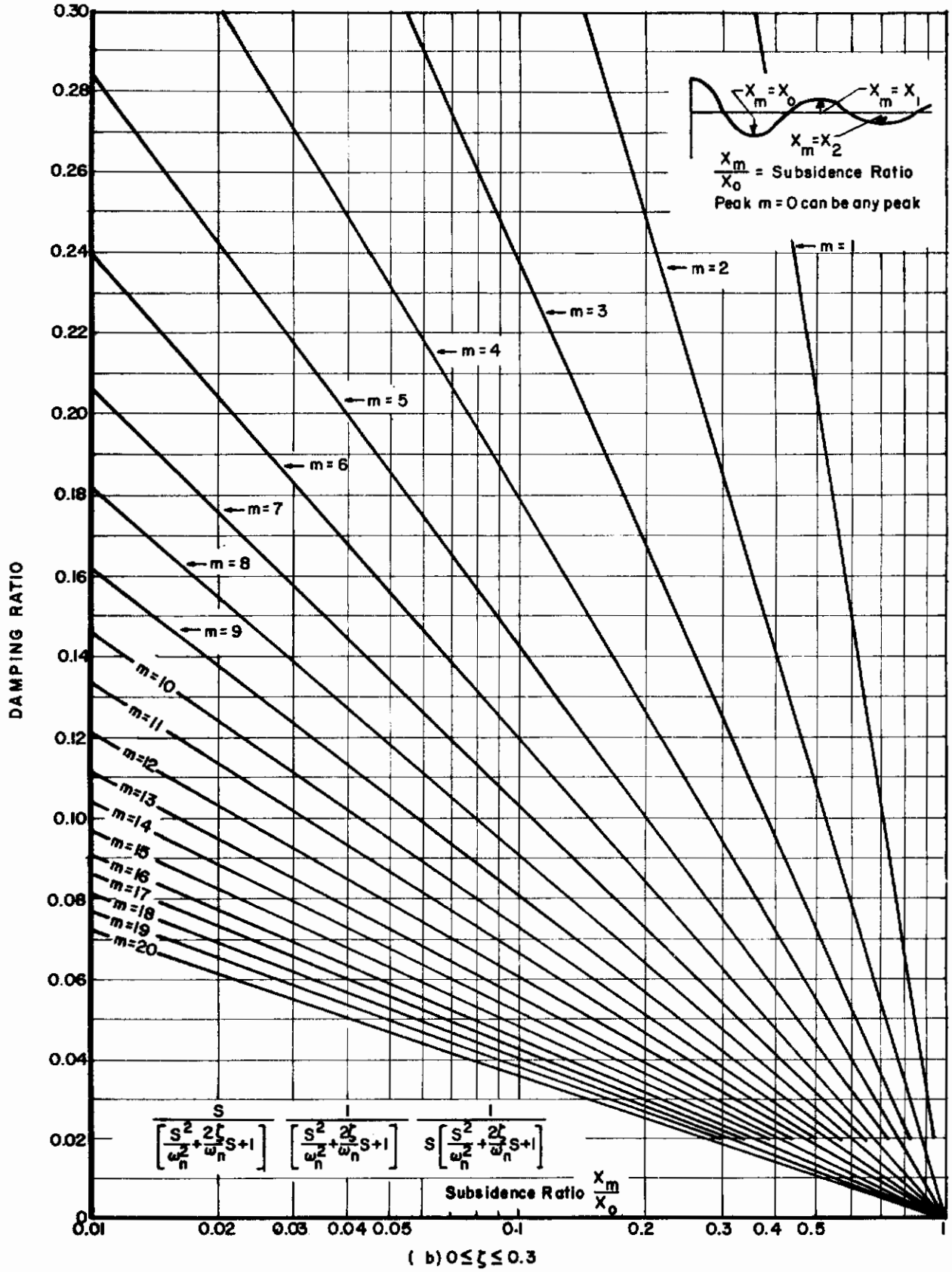

Figure 11. Damping Ratio of Oscillatory Transients as a Function of Subsidence Ratio for Second Order Systems

Of course, by definition, if one response (say $\dot{\theta}_\infty$) is finite, its integrals and derivatives will not be finite (θ_∞ would then be infinite; $\ddot{\theta}_\infty$, zero). Similarly, the initial response to a step input is

$$\lim_{t \to 0} o(t) = \delta \lim_{s \to \infty} Y(s)$$

giving, for example, the maximum value of $\ddot{\theta}$ for a control input. With a rate-limited control, $\dot{\delta}(s) = \dot{\delta}_{max}/s^2$ until maximum deflection is reached, and peak angular acceleration normally will occur at about $t_1 = \delta_{max}/\dot{\delta}_{max}$.

When the damping ratio ζ of a characteristic mode is small, maximum values (of $\dot{\theta}$, for example) can be somewhat higher than final values because of overshoot. One can often separate out that oscillatory mode, adjust its maximum response accordingly, and add approximate values of the same output quantity in other modes at the time of maximum response of the lightly damped mode, in search of a higher maximum response value.

B. STICK-FIXED DYNAMICS

The material in this section is largely a reduction of relations from Reference 8 to nondimensional notation.

1. Longitudinal Motion

Although exceptions occur, the longitudinal motion normally involves two oscillatory modes well separated in frequency. The discussion below is limited to well-separated short-period and phugoid modes, except that the "full" longitudinal equations presented under "Phugoid Mode" give the total motion in any case. When the two modes are not well separated, Reference 8 can supply a more general treatment. Some of such flight-test cases are analyzed in Reference 35.

(a.) Short-Period Mode

These transfer functions for the stick-fixed case hold fairly generally. The derivatives $\partial T/\partial \alpha$, $C_{L_{\dot{\alpha}}}$, and C_{L_q} are assumed to have negligible effect, and the short-period frequency should be at least several times as great as the phugoid frequency. The vertical gust velocity, w_g, is positive downward.

The approximate short-period linear equations of motion, in terms of acceleration derivatives ($\dot{\alpha}$ and $\dot{\theta}$ for perturbations $\Delta\alpha, \Delta\theta, \cdots$) are given below for initially trimmed, straight near-horizontal[11] flight:

$$\begin{bmatrix} s - Z_\alpha & -1 \\ -M_{\dot{\alpha}}s - M_\alpha & s - M_q \end{bmatrix} \begin{pmatrix} \Delta\alpha \\ s\Delta\theta \end{pmatrix} = \begin{pmatrix} Z_\delta \\ M_\delta \end{pmatrix} \delta - \begin{pmatrix} Z_\alpha \\ M_\alpha \end{pmatrix} \frac{w_g}{V_o}$$

where

$$Z_\alpha = \frac{1}{mV_o}\frac{\partial Z}{\partial \alpha} = -\frac{\rho V_o S}{2m}(C_{L_\alpha} + C_D) \qquad M_q = \frac{1}{I_y}\frac{\partial M}{\partial q} = \frac{\rho V_o S \bar{c}^2}{4I_y} C_{m_q}$$

$$M_\alpha = \frac{1}{I_y}\frac{\partial M}{\partial \alpha} = \frac{\rho V_o^2 S \bar{c}}{2I_y} C_{m_\alpha} \qquad Z_\delta = \frac{1}{mV_o}\frac{\partial Z}{\partial \delta} = -\frac{\rho V_o S}{2m} C_{L_\delta}$$

$$M_{\dot{\alpha}} = \frac{1}{I_y}\frac{\partial M}{\partial \dot{\alpha}} = \frac{\rho V_o S \bar{c}^2}{4I_y} C_{m_{\dot{\alpha}}} \qquad M_\delta = \frac{1}{I_y}\frac{\partial M}{\partial \delta} = \frac{\rho V_o^2 S \bar{c}}{2I_y} C_{m_\delta}$$

$$|Z_{\dot{\alpha}}| = \left|\frac{1}{mV_o}\frac{\partial Z}{\partial \dot{\alpha}}\right| = \left|-\frac{\rho S \bar{c}}{4m} C_{L_{\dot{\alpha}}}\right| << 1 \qquad |Z_q| = \left|\frac{1}{mV_o}\frac{\partial Z}{\partial q}\right| = \left|-\frac{\rho S \bar{c}}{4m} C_{L_q}\right| << 1$$

The quantity C_{L_1} is defined as W/q*S. (Reference 3 has a more rigorous treatment of gust response.)

Control dynamics can be represented by a third equation, the control law, or by multiplying δ by the control transfer function. Neither is done here. Solution of such linear equations is discussed somewhat more fully under "Phugoid Mode" following.

---

[11] When the operating-point flight path is not horizontal, a suggestion of the phugoid motion creeps in. The quantity in the upper right corner of the square matrix becomes $-\left(1 - \frac{g \sin\gamma_o}{V_o s}\right)$. For small γ_o (such that $\sin\gamma_o = \gamma_o$, $\cos\gamma_o = 1$), gravity effects on the short-period motion per se are normally negligible but begin to appear at extremely low speed. At large $|\gamma_o|$ density changes during the motion can make the coefficients time-varying, and also modify many of the transfer-function coefficients by quantities proportional to $(g \sin\gamma_o)/V_o$. In perturbations from steady turns, additional terms proportional to the steady angular rates appear in the equations; see Appendix III and Reference 32.

TABLE III

SHORT-PERIOD DYNAMICS, CONTROLS FIXED

Quantity	Form	Coefficients
Δ_{sp}	$s^2 + 2\zeta\omega_n s + \omega_n^2$	$2\zeta\omega_n = \frac{1}{2\tau}\left[C_{N_\alpha} - \frac{1}{2K_y^2}(C_{m_q} + C_{m_{\dot\alpha}})\right]$
	(N_m = maneuvering neutral point; $N_m - cg = -\left(\frac{C_{m_\alpha}}{C_{N_\alpha}} + \frac{1}{4\mu_1}C_{m_q}\right)\frac{\%\,\bar c}{100}$)	$\omega_n^2 = \frac{g}{C_{L_1}K_y^2\bar c}C_{N_\alpha}(N_m - cg)$
N_{θ_δ}	$\frac{K}{s}(s + \frac{1}{T})$	$K = \frac{g}{C_{L_1}K_y^2\bar c}(C_{m_\delta} - \frac{1}{4\mu_1}C_{m_{\dot\alpha}}C_{L_\delta}) \doteq \frac{g}{C_{L_1}K_y^2\bar c}C_{m_\delta}$
		$\frac{1}{T} \doteq \frac{1}{2\tau}\left(\frac{C_{N_\alpha}C_{m_\delta} - C_{m_\alpha}C_{L_\delta}}{C_{m_\delta} - \frac{1}{4\mu_1}C_{m_{\dot\alpha}}C_{L_\delta}}\right) \doteq \frac{1}{2\tau}C_{N_\alpha}$
$N_{\theta_{\alpha_g}}$	K	$K \doteq \frac{g}{C_{L_1}K_y^2\bar c}C_{N_\alpha}\left(\frac{C_{m_\alpha}}{C_{N_\alpha}} - \frac{1}{4\mu_1}C_{m_{\dot\alpha}}\right)$
N_{α_δ}	$K(s + \frac{1}{T})$	$K = -\frac{1}{2\tau}C_{L_\delta}$
		$\frac{1}{T} = -\frac{V_o}{K_y^2\bar c}\left(\frac{C_{m_\delta}}{C_{L_\delta}} + \frac{1}{4\mu_1}C_{m_q}\right) \doteq -\frac{V_o}{K_y^2\bar c}\frac{C_{m_\delta}}{C_{L_\delta}}$
	Approximation for $C_{L_\delta} = 0$: K'	$K' \doteq \frac{g}{C_{L_1}K_y^2\bar c}C_{m_\delta}$
$N_{\alpha_{\alpha_g}}$	$K(s + \frac{1}{T})$	$K = \frac{-1}{2\tau}C_{N_\alpha}$
		$\frac{1}{T} = -\frac{V_o}{K_y^2\bar c}\left(\frac{C_{m_\alpha}}{C_{N_\alpha}} + \frac{1}{4\mu_1}C_{m_q}\right) = \frac{2\tau(\omega_n^2)_{sp}}{C_{N_\alpha}}$
$N_{a_{z_\delta}}$	$K(s^2 + a_1 s + a_0)$	$K = -\frac{g}{C_{L_1}}C_{L_\delta}$
	[aft control: $\sim K(s + \frac{1}{T})(s - \frac{1}{T})$; fwd control: $K(s^2 + 2\zeta\omega_n s + \omega_n^2)$]	a_1 or $2\zeta\omega_n = -\frac{1}{4\tau K_y^2}(C_{m_q} + C_{m_{\dot\alpha}})$
		$a_o, \frac{-1}{T^2}$ or $\omega_n^2 = \frac{g}{C_{L_1}K_y^2\bar c}C_{N_\alpha}\left(\frac{C_{m_\delta}}{C_{L_\delta}} - \frac{C_{m_\alpha}}{C_{N_\alpha}}\right)$
	Approximation for $C_{L_\delta} = 0$: K'	$K' = -\left(\frac{g}{C_{L_1}}\right)^2\frac{1}{K_y^2\bar c}C_{N_\alpha}C_{m_\delta}$
$N_{a_{z_{\alpha_g}}}$	$Ks(s + \frac{1}{T})$	$K = \frac{-g}{C_{L_1}}C_{N_\alpha}$
		$\frac{1}{T} = \frac{-1}{4\tau K_y^2}(C_{m_q} + C_{m_{\dot\alpha}})$

To convert to other variables, for our rigid airframe

$$a'_z = \dot{w} - V_0 q - x\dot{q} = -g\Delta n'_z$$

at a distance x ahead of the center of gravity (An accelerometer measures the difference between inertial and gravitational acceleration: $a_z - g\cos\Theta\cos\Phi$, modified by structural deformation).

$$\gamma(t) = \gamma_0 - \left[\frac{w(t)}{V_0} - \Delta\theta(t)\right] = \gamma_0 - \frac{1}{V_0}\int_0^t a_z\,dt; \qquad \gamma(s) = \frac{1}{s}\left(\gamma_0 - \frac{a_z(s)}{V_0}\right)$$

$$q(t) = d\theta/dt; \qquad q(s) = s\theta(s) \quad \text{or} \quad \theta(s) = \frac{1}{s}\left[\theta_0 + q(s)\right]$$

$$w = V_0\Delta\alpha; \qquad w_g = -V_0\alpha_g$$

$$\dot{h}(t) = U\sin\theta - W\cos\theta = V_0\left[\sin\gamma_0 + (\cos\gamma_0)\Delta\gamma\right] \quad \text{or} \quad \dot{h} = V\sin\gamma$$

$$\Delta h(t) = V_0\left[(\sin\gamma_0)t + (\cos\gamma_0)\int_0^t \dot{\gamma}\,dt\right]; \quad \Delta h(s) = V_0\left[\frac{\sin\gamma_0}{s^2} + (\cos\gamma_0)\gamma(s)\right]$$

Note that all variables of interest are linear combinations of the variables in the equations of motion.

It is seen that the required positive maneuver margin ($N_m - cg > 0$; see Section IIC1) guarantees a stable short-period motion. This motion will generally be oscillatory, but for a very small maneuver margin it becomes aperiodic with time constants T_1 and T_2. This occurrence is signalled by $\zeta \geq 1$; with the decreased separation between short-period and phugoid modes then, these approximations are suspect.

(b.) Phugoid Mode

The classical long-period longitudinal (phugoid) motion occurs at constant thrust and constant angle of attack ($M_u = 0$). Except at low speed, density variation with altitude has a significant effect on the phugoid motion; at speeds above half the orbital speed, earth curvature also becomes important. Reference 1 derives corrections to the simplified two-degree-of-freedom (V, θ) equations. When stability-derivative, thrust, and moment variations with speed (Mach number, etc.) are negligible

$$\omega_{n_p} \doteq \sqrt{2}\,\frac{g}{V_0}\left[1 - \frac{V_0^2}{2g}(1 - F^2)\frac{\rho'}{\rho}\right]^{1/2} \quad \text{rad/sec}$$

where

$F^2 = V_0^2/gR < 1$

R = height above earth's center ($R > 21 \times 10^6$ ft)

$\rho' = d\rho/dh$, slugs/ft^4

Neglecting the density gradient and earth curvature makes the quantity in square brackets unity. The two results are compared in Figure 12. The simple classical solution holds at landing approach speeds and is a fair approximation at all subsonic speeds, but it is totally inadequate at supersonic and hypersonic speeds, even in the absence of compressibility effects.

Similarly, the damping of the "classical" phugoid is given by Reference 1 as

$$2(\zeta\omega_n)_p \doteq \frac{1}{\tau} C_D + 2\frac{C_D}{C_L}\left[\frac{-\left[(\rho'/\rho) + \frac{1}{R}\right]V_o + (2g/V_o)}{-(\rho'/\rho)R + (2/F^2) + \left[F^2/(1-F^2)\right]}\right]$$

with the same assumptions and constant (or zero) thrust. The last term gives a correction, inversely proportional to L/D, for density gradient and earth curvature effects. Note that C_L is here

$$C_L \doteq \frac{W}{q^* S}(1-F^2)$$

while

$$C_D = \frac{D}{q^* S}$$

is independent of thrust level. The correction is inconsequential except at hypersonic speeds.

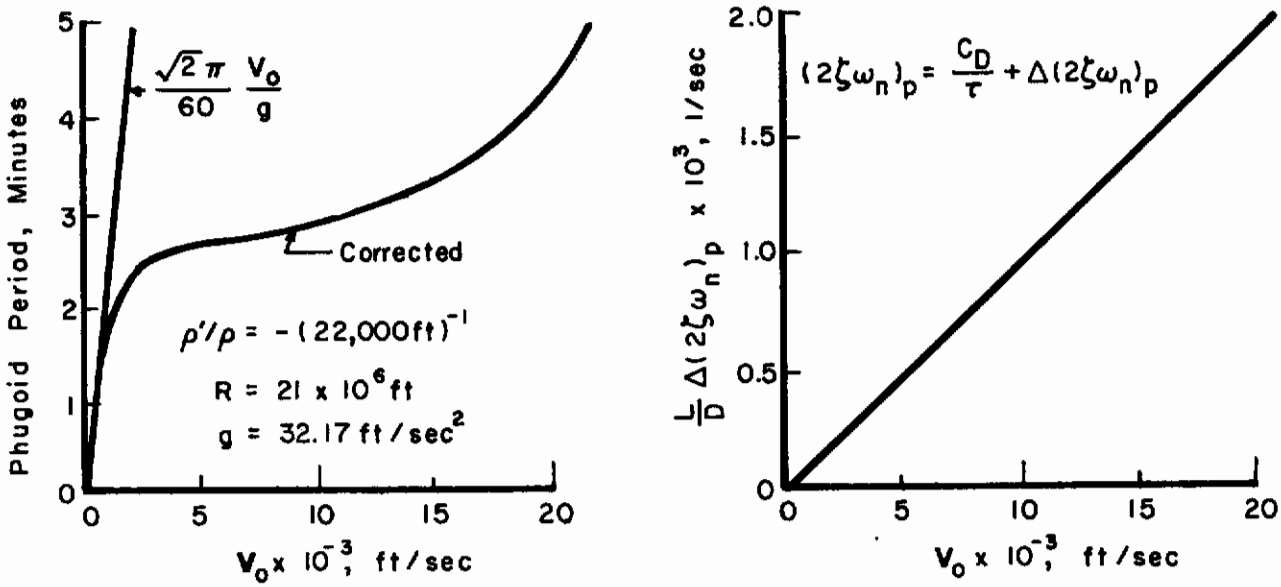

Figure 12. Phugoid Characteristics

The simplified theory gives phugoid frequency and damping adequately when stability derivatives and thrust are independent of speed and when $\omega_{n_p} << \omega_{n_{sp}}$. However, when that is not so or when transfer functions are desired, the pitching-moment equation should also be considered. Another limitation to any linear,

constant-coefficient equations is that, of course, $\dot{h}_o = V_o \gamma_o$ must be small so that the aerodynamic derivatives (that depend on ρ) can be considered non-time-varying during the course of the phugoid motion.

In the "full" development next presented, earth curvature is neglected (See Reference 1 or 36). The aerodynamic derivatives are defined to include thrust effects. For completeness we include certain derivatives that are usually negligible: $X_{\dot{\alpha}}$, X_q, $Z_{\dot{\alpha}}$, Z_q, $\partial T/\partial \alpha$, etc. The operating point is straight, steady flight with flight-path angle γ_o . The first three equations are given in terms of real-time "angular" acceleration (F/mV_o, M/I_y) derivatives with variables

$$(u/V_o),\ \Delta\alpha \triangleq (w/V_o),\ \Delta\theta,\ (\Delta h/\bar{c}),\ \Delta\delta.$$

The last equation is the kinematic relation among these variables.

$$\begin{bmatrix} s - X_u & -X_{\dot{\alpha}}s - X_\alpha & -X_q s + \frac{q}{V_o}\cos\gamma_o & -X_h \\ -Z_u & (1 - Z_{\dot{\alpha}})s - Z_\alpha & -(1+Z_q)s + \frac{q}{V_o}\sin\gamma_o & -Z_h \\ -M_u & -M_{\dot{\alpha}}s - M_\alpha & s^2 - M_q s & -M_h \\ -\frac{V_o}{\bar{c}}\sin\gamma_o & \frac{V_o}{\bar{c}}\cos\gamma_o & -\frac{V_o}{\bar{c}}\cos\gamma_o & s \end{bmatrix} \begin{Vmatrix} u/V_o \\ \Delta\alpha \\ \Delta\theta \\ \Delta h/\bar{c} \end{Vmatrix}$$

$$= \begin{Vmatrix} 0 \\ 0 \\ 0 \\ \frac{V_o}{\bar{c}}\frac{\sin\gamma_o}{s} \end{Vmatrix} + \begin{Vmatrix} X_\delta \\ Z_\delta \\ M_\delta \\ 0 \end{Vmatrix} \Delta\delta + \begin{Vmatrix} -X_u \\ -Z_u \\ -M_u \\ 0 \end{Vmatrix} u_g/V_o + \cdots$$

(Reference 3 has a more rigorous treatment of gust response.)

where, initially, $u = \Delta\alpha = \Delta\theta = \Delta h = 0$, u_g is positive in the direction of flight, and the derivatives are defined as follows:

$$X_u = \frac{1}{mV_o}\frac{\partial X}{\partial(u/V_o)} = -\frac{1}{\tau}\left(C_D + \frac{V_o}{2}\frac{\partial C_D}{\partial u}\right) + \frac{1}{m}\frac{\partial T}{\partial u}\cos\xi$$

$$X_\alpha = \frac{1}{mV_o}\frac{\partial X}{\partial \alpha} = -\frac{1}{2\tau}(C_{D_\alpha} - C_L) + \frac{1}{mV_o}\frac{\partial T}{\partial \alpha}\cos\xi$$

$$X_{\dot{\alpha}} = \frac{1}{mV_o}\frac{\partial X}{\partial \dot{\alpha}} \doteq 0$$

$$X_q = \frac{1}{mV_o}\frac{\partial X}{\partial q} \doteq 0$$

$$X_h = \frac{1}{mV_o}\frac{\partial X}{\partial(h/\bar{c})} = \frac{-\bar{c}}{2\tau}\left(\frac{C_D}{\rho}\frac{d\rho}{dh} + \frac{\partial C_D(M, q^*, R)}{\partial h}\right) + \frac{\bar{c}}{mV_o}\frac{\partial T}{\partial h}\cos\xi$$

$$X_\delta = \frac{1}{mV_o}\frac{\partial X}{\partial \delta} = \frac{-1}{2\tau}C_{D_\delta} \quad \text{or} \quad \frac{\cos\xi}{mV_o}\frac{\partial T}{\partial \delta}$$

$$Z_u = \frac{1}{mV_0}\frac{\partial Z}{\partial (u/V_0)} = \frac{-1}{\tau}\left(C_L + \frac{V_0}{2}\frac{\partial C_L}{\partial u}\right) - \frac{1}{m}\frac{\partial T}{\partial u}\sin\xi$$

$$Z_\alpha = \frac{1}{mV_0}\frac{\partial Z}{\partial \alpha} = \frac{-1}{2\tau}(C_{L_\alpha} + C_D) - \frac{1}{mV_0}\frac{\partial T}{\partial \alpha}\sin\xi$$

$$Z_{\dot\alpha} = \frac{1}{mV_0}\frac{\partial Z}{\partial \dot\alpha} = \frac{-1}{4\mu_1}C_{L_{\dot\alpha}}$$

$$Z_q = \frac{1}{mV_0}\frac{\partial Z}{\partial q} = \frac{-1}{4\mu_1}C_{L_q}$$

$$Z_h = \frac{1}{mV_0}\frac{\partial Z}{\partial (h/\bar c)} = \frac{-\bar c}{2\tau}\left(\frac{C_L}{\rho}\frac{d\rho}{dh} + \frac{\partial C_L(M,q^*,R)}{\partial h}\right) - \frac{\bar c}{mV_0}\frac{\partial T}{\partial h}\sin\xi$$

$$Z_\delta = \frac{1}{mV_0}\frac{\partial Z}{\partial \delta} = \frac{-1}{2\tau}C_{L_\delta} \quad \text{or} \quad \frac{-\sin\xi}{mV_0}\frac{\partial T}{\partial \delta}$$

$$M_u = \frac{1}{I_y}\frac{\partial M}{\partial (u/V_0)} = \frac{2g}{C_{L_1}K_y^2\bar c}\left(\frac{V_0}{2}\frac{\partial C_m}{\partial u}\right) - \frac{2z_T}{I_y}\left(T - \frac{V_0}{2}\frac{\partial T}{\partial u}\right)$$

$$M_\alpha = \frac{1}{I_y}\frac{\partial M}{\partial \alpha} = \frac{g}{C_{L_1}K_y^2\bar c}C_{m_\alpha}$$

$$M_{\dot\alpha} = \frac{1}{I_y}\frac{\partial M}{\partial \dot\alpha} = \frac{1}{4\tau K_y^2}C_{m_{\dot\alpha}}$$

$$M_q = \frac{1}{I_y}\frac{\partial M}{\partial q} = \frac{1}{4\tau K_y^2}C_{m_q}$$

$$M_h = \frac{1}{I_y}\frac{\partial M}{\partial (h/\bar c)} = \frac{g}{C_{L_1}K_y^2}\frac{\partial C_m(M,q^*,R)}{\partial h} - \frac{z_T\bar c}{I_y}\left(\frac{T}{\rho}\frac{d\rho}{dh} - \frac{\partial T}{\partial h}\right)$$

$$M_\delta = \frac{1}{I_y}\frac{\partial M}{\partial \delta} = \frac{g}{C_{L_1}K_y^2\bar c}C_{m_\delta} \quad \text{or} \quad \frac{z_T}{I_y}\frac{\partial T}{\partial \delta}$$

$$\xi = \alpha_{trim} + i_T$$

Thrust data are needed for the specific installed propulsion system, but it may be helpful to note general trends. Thrust of a fixed-pitch propeller varies about linearly with dynamic pressure: $T \doteq T_{static} - kq^*$. A constant-speed propeller tends to deliver constant power (TV), while a turbojet engine tends to give thrust invariant with speed. Thrust depends on mass flow, which (for unsupercharged engines) varies with altitude as the free-stream density, ρ. These direct thrust changes are in addition to the induced effects of thrust on derivatives such as C_{m_α} (See, for example, Reference 21). δ is a generic control deflection: it can represent elevator, engine, flaps, etc. Control dynamics can be incorporated by multiplying $\Delta\delta(s)$ by the control transfer function. For example, $\Delta\delta_T/(T_L s + 1)$ could represent thrust lag when δ_T is throttle deflection. Although X_{δ_e} and Z_{δ_e} are commonly neglected, this practice can occasionally lead to error. An example is the calculation of minimum approach speed of a modern fighter by the method of Reference 33.

A solution for u, $\Delta\alpha$, $\Delta\theta$, or Δh is obtained by superposition, adding solutions for each combination of the left-hand side with an element of the right-hand side. For example,

$$u(s) = V_0\left[\frac{N_{uO}(s)}{\Delta(s)} + \frac{N_{u\delta}(s)}{\Delta(s)}\delta(s) + \frac{N_{uu_g}(s)}{\Delta(s)}\frac{u_g(s)}{V_0} + \cdots\right]$$

where Δ is the characteristic determinant, N_{uo} is the determinant formed from the same matrix by substituting

$$\begin{pmatrix} 0 \\ 0 \\ 0 \\ \frac{V_o}{s}\sin\gamma_o \end{pmatrix}$$

for the first column, $N_{u\delta}$ is the determinant formed by substituting

$$\begin{pmatrix} X_\delta \\ Z_\delta \\ M_\delta \\ 0 \end{pmatrix}$$

for the first column, etc.

The transfer functions $Y_{ij}(s)$ are defined by the alternate statement

$$u(s) = V_o\left[Y_{uO}(s) + Y_{u\delta}(s)\Delta\delta(s) + Y_{uu_g}(s)\,\frac{u_g(s)}{V_o} + \cdots \right]$$

Analysis by hand is lengthy; machine solution is recommended. Note that the equations yield both phugoid and short-period characteristics, and an extra mode related to Δh as well. Normally the inverse time constant of this last mode is negligibly small, compared even to the phugoid frequency. The other modes are usually oscillatory, but may become aperiodic; for example, transonic "tuck."

In several instances, immediate simplification is possible. The classical analysis indicated regions where the density gradient effect is negligible. A quick check will give the speed above which it is not rational to consider nonzero initial flight-path angle in a constant-coefficient analysis. Requirements are usually stated in terms of level-flight trim. On the other hand, effects of small γ_o are not negligible at low speed and high C_L (as might be found high on the back side of the thrust-required curve) but, neglecting the density gradient, are generally negligible at any higher speed, lower C_L.

Solution of the equations above is recommended for accurate analysis, but it may be worthwhile to develop approximations for specific cases. A few simplified phugoid results are presented in Table IV as a guide. All apply only when $\gamma_o \doteq 0$, the phugoid and short-period frequencies are well separated, and any thrust derivatives are subsumed into the nondimensional aerodynamic derivatives (for example, following the definition above of X_u, substitute

$$\frac{\partial C_D}{\partial u} - \frac{\cos\xi}{q^* S}\,\frac{\partial T}{\partial u}$$

for $\partial C_D / \partial u$.)

TABLE IV
PHUGOID DYNAMICS, CONTROLS FIXED

Quantity	Form
Δ_p	$s^2 + 2\zeta\omega_n s + \omega_n^2$ or $(s + \frac{1}{T_1})(s + \frac{1}{T_2})$
	$(2\zeta\omega_n)_p$ or $(\frac{1}{T_1} + \frac{1}{T_2})_p \doteq \frac{1}{\tau}\left[C_D + \frac{V_o}{2}\frac{\partial C_D}{\partial u} + \frac{(C_{D_\alpha} + C_D \tan\xi)}{C_{N_\alpha}}\frac{\left(-\frac{Tz_T}{q^*S\bar{c}} + \frac{V_o}{2}\frac{\partial C_m}{\partial u}\right)}{(N_m - cg)}\right] -$
	$- \frac{\left(C_L + \frac{V_o}{2}\frac{\partial C_L}{\partial u}\right)}{2\mu_1 C_{N_\alpha}(N_m - cg)}\left[\frac{1}{2\tau}(C_L - C_{D_\alpha})C_{m_q} + \frac{g}{V_o}C_{m_{\dot\alpha}}\right] - (2\zeta\omega_n)_{sp}(\omega_n^2)_p / (\omega_n^2)_{sp} \doteq \frac{C_D}{\tau}$
	$(\omega_n^2)_p$ or $(\frac{1}{T_1} * \frac{1}{T_2})_p \doteq \frac{\rho S g}{m}\frac{1}{(N_m - cg)}\left[\frac{-Tz_T}{q^*S\bar{c}} + \frac{V_o}{2}\frac{\partial C_m}{\partial u} - \frac{C_{m_\alpha}}{C_{N_\alpha}}\left(C_L + \frac{V_o}{2}\frac{\partial C_L}{\partial u}\right)\right] \doteq 2\left(\frac{g}{V_o}\right)^2\left(\frac{-\frac{C_{m_\alpha}}{C_{N_\alpha}}}{N_m - cg}\right)$
	the latter approximation for negligible C_{m_u}, C_{L_u}, z_T, and small ξ.
$\frac{\Delta\theta s}{\delta e(s)}$	$\frac{K(s + \frac{1}{T_1})(s + \frac{1}{T_2})}{\Delta_p \Delta_{sp}}$ when $C_{L_\delta} \doteq C_{D_\delta} \doteq 0$ and $\frac{1}{T_2} >> \frac{1}{T_1}$
	$K = \frac{g}{C_{L_1} K_y^2 \bar{c}} C_{m_{\delta e}}$
	$\frac{1}{T_2} \doteq \frac{1}{2\tau}\left[C_{N_\alpha} + 2\left(C_D + \frac{V_o}{2}\frac{\partial C_D}{\partial u}\right)\right] \doteq \frac{1}{2\tau}C_{N_\alpha}$
	$\frac{1}{T_1} \doteq \frac{T_2}{2\tau^2}\left[\left(C_D + \frac{V_o}{2}\frac{\partial C_D}{\partial u}\right)C_{N_\alpha} + \left(C_L + \frac{V_o}{2}\frac{\partial C_L}{\partial u}\right)(C_L - C_{D_\alpha})\right]$
	Δ_{sp}: See Table III, Short-Period Dynamics.
$\frac{\Delta\gamma(s)}{\delta e(s)}$	$\frac{K(s + \frac{1}{T})}{\Delta_p \Delta_{sp}}$ when $C_{L_\delta} \doteq C_{D_\delta} \doteq 0$
	$K \doteq \frac{g}{2\tau C_{L_1} K_y^2 \bar{c}} C_{m_{\delta e}} C_{N_\alpha}$
	$\frac{1}{T} \doteq \frac{1}{\tau}\left[C_D + \frac{V_o}{2}\frac{\partial C_D}{\partial u} - \frac{\left(C_L + \frac{V_o}{2}\frac{\partial C_L}{\partial u}\right)}{C_{N_\alpha}}(C_{D_\alpha} + C_D \tan\xi)\right]$
$\frac{\Delta\gamma(s)}{\delta T(s)}$	$\frac{K(s^2 + 2\zeta\omega_n s + \omega_n^2)}{\Delta_p \Delta_{sp}}$ when $\frac{\partial Z}{\partial \delta T} \doteq \frac{\partial M}{\partial \delta T} \doteq 0$
	$K \doteq \frac{1}{\tau}\left(C_L + \frac{V_o}{2}\frac{\partial C_L}{\partial u}\right)\frac{1}{mV_o}\frac{\partial X}{\partial \delta T}$
	$2\zeta\omega_n \doteq -\frac{1}{4\tau K_y^2}(C_{m_q} + C_{m_{\dot\alpha}})$
	$\omega_n^2 \doteq -\frac{g}{C_{L_1} K_y^2 \bar{c}} C_{N_\alpha}\left[\frac{C_{m_\alpha}}{C_{N_\alpha}} + \frac{\left(\frac{Tz_T}{q^*S\bar{c}} - \frac{V_o}{2}\frac{\partial C_m}{\partial u}\right)}{C_L + \frac{V_o}{2}\frac{\partial C_L}{\partial u}}\right]$
$\frac{u(s)}{\delta T(s)}$	$\frac{K}{s\Delta_p}$ when $\frac{\partial Z}{\partial \delta T} \doteq \frac{\partial M}{\partial \delta T} \doteq 0$
	$K = \frac{1}{m}\frac{\partial X}{\partial \delta T}$

These approximations do not account for density-gradient effects, but may be useful in establishing trends even at high speed. Where derivative changes with speed (Mach number, etc.) are small, it may be valid to apply the corrections given above for the classical theory to phugoid period and damping. Similar corrections could be derived for transfer-function numerator coefficients.

When interested only in frequencies well below the short-period natural frequency, one can substitute

$$\omega_{n_{sp}}^2 \doteq \frac{g}{C_{L_1} K_y^2 \bar{c}} C_{N_\alpha} (N_m - cg)$$

for Δ_{sp} where the latter occurs and keep only the constant term in any numerator factor not of interest per se.

The preceding auxiliary relations for a_z, γ, q, and w hold here, but when considering small speed changes the altitude change is given by

$$\dot{h} = V \sin\gamma = U \sin\theta - W \cos\theta$$

$$\doteq V_0 \sin\gamma_0 + (V_0 \cos\gamma_0)\Delta\theta + (V_0 \sin\gamma_0)\frac{u}{V_0} - (V_0 \cos\gamma_0)\Delta\alpha$$

in the stability axis system.

2. Lateral-Directional Motion

Current requirements, where quantitative, relate Dutch-roll damping to the ratio of bank-angle and side-velocity amplitudes in the Dutch-roll mode, $|\phi| / |v_e|$ (See Figure 13) and bound the permissible spiral divergence.

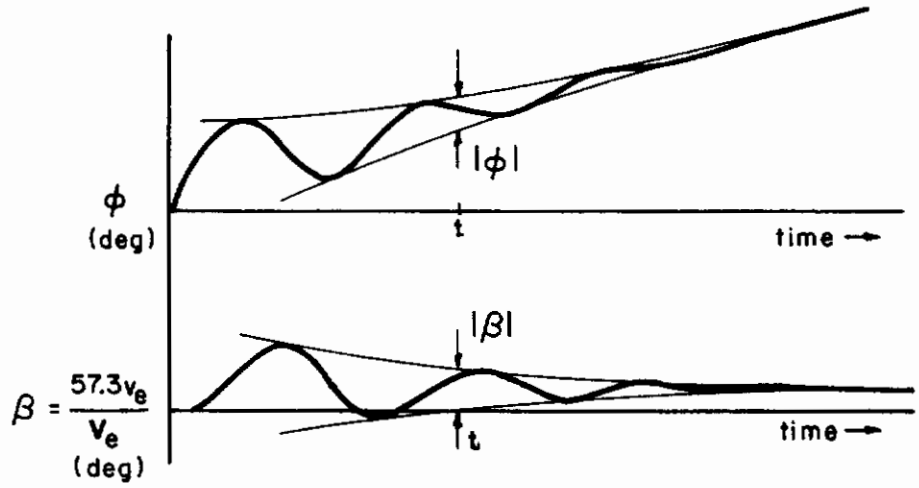

Figure 13. Definition of $|\phi| / |v_e|$

Quantitative specification of adequate lateral-directional dynamics is difficult; a number of interrelated parameters are involved (See, for example, (Reference 33).

Since the importance of a parameter depends upon the values of other factors, it is again appropriate to present more-or-less-general equations of motion and typical approximate transfer functions.

It is possible (for example, with large dihedral) for the usual roll and spiral modes to combine into another oscillatory mode, as shown in Reference 8. There is no essential difficulty in analyzing that case, just the conversion from

$$\left(s + \frac{1}{T_s}\right)\left(s + \frac{1}{T_R}\right) \quad \text{to} \quad \left[s^2 + (2\zeta\omega_n)_{SR}\, s + \omega_n{}^2_{SR}\right]$$

in the characteristic equation. However, the flying qualities of such a vehicle would generally be unacceptable. For that reason attention is restricted to distinct spiral and roll modes. Similarly, the approximate factors consider only oscillatory Dutch roll motion. However, the equations of motion below apply in any case. The equations represent lateral-directional motion uncoupled from longitudinal motion. They assume small perturbations of a stability-axes system at constant speed and unity normal load factor. Sections IIIB and IVF discuss large-amplitude rolling. Nonlinearities, including nonlinear inertial coupling, are neglected below as are engine gyroscopic effects. The effect of constant normal acceleration, ignored here, is to change those derivatives that vary with angle of attack, and to add often-negligible trim and perturbation terms proportional to the steady rates P_o, Q_o, and R_o (References 6 and 32) and Appendix III). At supersonic speeds, aerodynamic stiffness in yaw tends to decrease with increasing angle of attack, Mach number, and dynamic pressure.

The linear small-perturbation equations can be written in terms of real-time acceleration derivatives

$$L_i = \frac{1}{I_x}\frac{\partial L}{\partial i}, \quad N_i = \frac{1}{I_z}\frac{\partial N}{\partial i}, \quad Y_i = \frac{1}{mV_o}\frac{\partial Y}{\partial i}, \quad i = \beta, p, r, \delta a, \delta r, \cdots$$

modified to include the effects of I_{xz} in the derivatives:

$$L'_i = \frac{L_i + \frac{I_{xz}}{I_x} N_i}{1 - \frac{I_{xz}{}^2}{I_x I_z}}, \qquad N'_i = \frac{N_i + \frac{I_{xz}}{I_z} L_i}{1 - \frac{I_{xz}{}^2}{I_x I_z}}$$

With this nomenclature, for no air-mass motion (implying that $v = V \sin\beta \doteq V_o \beta$) and zero initial conditions on β, ϕ, ψ, and their time derivatives,

$$\begin{bmatrix} s - Y_\beta & -Y_p s - \frac{g}{V_o}\cos\gamma_o & (1 - Y_r)s - \frac{g}{V_o}\sin\gamma_o \\ -L'_{\dot\beta} s - L'_\beta & s^2 - L'_p s & -L'_r s \\ -N'_{\dot\beta} s - N'_\beta & -N'_p s & s^2 - N'_r s \end{bmatrix} \begin{pmatrix} \beta \\ \phi \\ \psi \end{pmatrix} = \begin{pmatrix} Y_\delta \\ L'_\delta \\ N'_\delta \end{pmatrix} \delta + \begin{pmatrix} Y_\beta \\ L'_\beta \\ N'_\beta \end{pmatrix} \beta_g + \cdots$$

where $\delta = \delta a$, δr or any specified combination (the equations being linear, the principle of superposition applies), β is v/V_o, and β_g is $-v_g/V_o$. (Reference 3 has a more rigorous treatment of gust response.)

A detailed analysis should start with at least these equations, but insight can often be gained more simply from the approximations below, based on Reference 8. These approximations neglect Y_p, Y_r, $N_{\dot{\beta}}$, $L_{\dot{\beta}}$, and γ_o. Additional assumptions for estimating the characteristic determinant Δ are:

$$\left| C_{y_\beta} C'_{n_r} - \frac{1}{2K_x^2} C'_{n_p} C'_{\ell_r} \right| \ll 4\mu_2 \left| C'_{n_\beta} \right|$$

$$\left| C_{y_\beta} C'_{\ell_r} \right| \ll 4\mu_2 \frac{K_x^2}{K_z^2} \left| C'_{\ell_\beta} \right|$$

when C'_{ℓ_β} is not negligible itself

$$\left| C'_{\ell_p} \left(C_{y_\beta} + \frac{1}{2K_z^2} C'_{n_r} \right) \right| \ll 4\mu_2 \frac{K_x^2}{K_z^2} \left| C'_{n_\beta} \right|$$

$$\left| \frac{C'_{\ell_\beta}}{C'_{n_\beta}} \left(C'_{n_p} - 2C_{L_1} K_z^2 \right) \right| \ll \left| C'_{\ell_p} \right|$$

and $\zeta_d < 0.2$. (Reference 8 indicates corrections when ζ_d is larger). The approximation for $(\omega_n^2)_\phi$ involves assumptions that:

$$\left| C_{y_\beta} C'_{n_r} \right| \ll 4\mu_2 \left| C'_{n_\beta} \right|, \qquad \left| C_{y_\beta} C'_{\ell_r} \right| \ll 4\mu_2 \left| C'_{\ell_\beta} \right| \text{ when } C'_{\ell_\beta} \text{ is not negligible itself}$$

$$\left| C_{y_\delta} \left(C'_{\ell_r} - \frac{C'_{\ell_\beta}}{C'_{n_\beta}} C_{n'_r} \right) \right| \ll 4\mu_2 \left| C'_{\ell_\delta} \right|$$

when C'_{ℓ_β} or C'_{ℓ_δ} is not negligible. Again defining $C_{L_1} = W/q*S$, the approximation for B_1 uses the assumption that

$$\left| C_{y_\delta} \left(C'_{\ell_p} C'_{n_r} - C'_{n_p} C'_{\ell_r} \right) \right| \ll 4\mu_2 \left| C'_{n_\delta} C'_{\ell_p} - C'_{\ell_\delta} \left(C'_{n_p} + 2C'_{L_1} K_z^2 \right) \right|$$

As used in this report, primed nondimensional derivatives are the counterparts of the primed acceleration derivatives; that is,

$$C'_{\ell_i} = \frac{C_{\ell_i} + \frac{I_{xz}}{I_z} C_{n_i}}{1 - \frac{I_{xz}^2}{I_x I_z}}, \qquad C'_{n_i} = \frac{C_{n_i} + \frac{I_{xz}}{I_x} C_{\ell_i}}{1 - \frac{I_{xz}^2}{I_x I_z}},$$

$$i = \beta, p(b/2V_o), r(b/2V_o), \delta a, \delta r, \cdots$$

Derivatives with respect to δ should be consistent with the input: δa, δr, or a specified combination. (One or two of C'_{n_δ}, C_{y_δ}, C'_{ℓ_δ} may be negligible.) For side-gust inputs, substitute β derivatives in place of δ derivatives.

TABLE V

LATERAL-DIRECTIONAL DYNAMICS, CONTROLS FIXED

$$\Delta(s) = \left(s + \frac{1}{T_s}\right)\left(s + \frac{1}{T_R}\right)\left[\, s^2 + (2\zeta\omega_n)_d\, s + \omega_{n_d}^2 \,\right]$$

$$\frac{1}{T_R} \doteq \frac{-1}{4\tau K_x^2}\left[C'_{\ell_p} - \frac{C'_{\ell_\beta}}{C'_{n_\beta}}\left(C'_{n_p} - 2K_z^2 C_{L_1}\right)\right]$$

$$\frac{1}{T_s} \doteq T_R \frac{g}{4V_0\tau K_x^2}\left(\frac{C'_{\ell_\beta}}{C'_{n_\beta}} C'_{n_r} - C'_{\ell_r}\right)$$

$$\omega_{n_d}^2 \doteq \frac{g}{C_{L_1} K_z^2 b} C'_{n_\beta}$$

$$(2\zeta\omega_n)_d \doteq \frac{-1}{2\tau}\left[C_{y_\beta} + \frac{1}{2K_z^2} C'_{n_r} - \frac{K_z^2}{K_x^2}\frac{C'_{\ell_\beta}}{C'_{n_\beta}}\left(C_{L_1} - \frac{1}{2K_z^2} C'_{n_p}\right)\right]$$

$$N_{\phi_\delta}(s) = K_{\phi_\delta}\left[\, s^2 + (2\zeta\omega_n)_\phi s + (\omega_n^2)_\phi \,\right] = K_{\phi_\delta} s^2 + K_{\phi_\delta}(2\zeta\omega_n)_\phi s + K_{\phi_\delta}(\omega_n^2)_\phi$$

$$K_{\phi_\delta} \doteq \frac{g}{C_{L_1} K_x^2 b} C'_{\ell_\delta}$$

$$(\omega_n^2)_\phi \doteq \frac{g}{C_{L_1} K_z^2 b} C'_{n_\beta}\left(1 - \frac{C'_{n_\delta}}{C'_{\ell_\delta}}\frac{C'_{\ell_\beta}}{C'_{n_\beta}}\right)$$

$$(2\zeta\omega_n)_\phi \doteq -\frac{1}{2\tau}\left[C_{y_\beta} + \frac{1}{2K_z^2}\left(C'_{n_r} - \frac{C'_{n_\delta}}{C'_{\ell_\delta}} C'_{\ell_r}\right) - \frac{C'_{y_\delta}}{C'_{\ell_\delta}} C'_{\ell_\beta}\right]$$

$$N_{\beta_\delta}(s) = B_3 s^3 + B_2 s^2 + B_1 s + B_0$$

$$B_3 \doteq \frac{1}{2\tau} C_{y_\delta}$$

$$B_2 \doteq -\frac{g}{C_{L_1} K_z^2 b}\left[C'_{n_\delta} + \frac{1}{4\mu_2} C_{y_\delta}\left(C'_{n_r} + \frac{K_z^2}{K_x^2} C'_{\ell_p}\right)\right] \doteq -\frac{g}{C_{L_1} K_z^2 b} C'_{n_\delta}$$

$$B_1 \doteq \frac{g}{4\tau C_{L_1} K_x^2 K_z^2 b}\left[C'_{n_\delta} C'_{\ell_p} - C'_{\ell_\delta}\left(C'_{n_p} - 2K_z^2 C_{L_1}\right)\right]$$

$$B_0 \doteq \frac{g}{8\tau^2 K_x^2 K_z^2 b}\left(C'_{n_\delta} C'_{\ell_r} - C'_{\ell_\delta} C'_{n_r}\right)$$

$$N_{r_\delta}(s) = R_3 s^3 + R_2 s^2 + R_1 s + R_0$$

$$R_3 \doteq \frac{g}{C_{L_1} K_z^2 b} C'_{n_\delta}$$

$$R_2 \doteq \frac{g}{4\tau C_{L_1} K_x^2 K_z^2 b}\left[C'_{\ell_\delta} C'_{n_p} - C'_{n_\delta}\left(C'_{\ell_p} + 2K_x^2 C_{y_\beta}\right) + 2K_x^2 C_{y_\delta} C'_{n_\beta}\right]$$

$$R_1 \doteq \frac{g}{8\tau^2 C_{L_1} K_x^2 K_z^2 b}\left[C_{y_\beta}\left(C'_{n_\delta} C'_{\ell_p} - C'_{\ell_\delta} C'_{n_p}\right) + C_{y_\delta}\left(C'_{\ell_\beta} C'_{n_p} - C'_{n_\beta} C'_{\ell_p}\right)\right]$$

$$R_0 \doteq \frac{g^2}{2\tau C_{L_1} K_x^2 K_z^2 b^2}\left(C'_{\ell_\delta} C'_{n_\beta} - C'_{n_\delta} C'_{\ell_\beta}\right)$$

$$a_y = V_0(\dot{\beta} + r)$$

A lateral accelerometer x feet ahead of the center of gravity of a rigid airframe will sense (See References 4, 6, and 8)

$$a''_y = V_0(\dot{\beta} + r) - g(\phi \cos\gamma_0 + \Delta\psi \sin\gamma_0) + x\dot{r}$$

A yaw-rate gyro mounted rigidly in the vehicle will in general be inclined to the z stability axis at an angle, say θ_r, that varies with angle of attack. Such a gyro will sense a rate

$$\omega = r \cos\theta_r + p \sin\theta_r .$$

Similarly, a roll-rate gyro will generally sense a component of yaw rate:

$$\omega = p \cos\theta_p - r \sin\theta_p$$

where θ_p is the inclination of the roll-gyro axis to the x stability axis. See Reference 4 for a more comprehensive discussion of instrument readings, and of axes transformations in general.

Stability augmentation involving simple feedbacks of β, p, and r with negligible lag can be accounted for by using equivalent derivatives (See Section IIIA1, for example) in the approximate factors above. In any case one can always solve the equations of motion simultaneously with the control laws or use the method of Reference 9 to find the characteristics of the augmented airframe. It may be more convenient to use axes aligned with the sensor axes, accounting explicitly for product of inertia and initial Z velocity (for example, Reference 8). The results will be valid for motions that do not call for control-surface deflections beyond the limits of augmentation authority or rate.

The ratio $(\omega_{n\phi}/\omega_{n_d})^2$, of interest for aileron control, is approximately

$$\left(\frac{\omega_{n\phi}}{\omega_{n_d}}\right)^2_{\delta a} \doteq 1 - \frac{C'_{n\delta a}}{C'_{\ell\delta a}} \frac{C'_{\ell\beta}}{C'_{n\beta}}$$

A general expression for the Dutch-roll roll-to-sideslip ratio, valid for any input, is

$$\frac{|\phi|}{|\beta|} \doteq \frac{V_e}{57.3} \frac{|\phi, \text{deg.}|}{|v_e|} = \frac{|N_{\phi\delta}(s_d)|}{|N_{\beta\delta}(s_d)|}; \qquad \frac{V_e}{V} = \frac{v_e}{v} = \sqrt{\frac{\rho}{\rho_{SL}}}$$

where

$$s_d \text{ is } -(\zeta\omega_n)_d + j\omega_{n_d}\sqrt{1-\zeta_d^2} \text{ or } -(\zeta\omega_n)_d - j\omega_{n_d}\sqrt{1-\zeta_d^2}.$$

When the input is a pure yawing moment, a fairly simple form results. Again neglecting Y_p, Y_r, $N_{\dot{\beta}}$, $L_{\dot{\beta}}$, and γ_o, in terms of the dimensional acceleration derivatives there results

$$\frac{|\phi|}{|\beta|} \doteq \left| \frac{-L'_r s_d + (L'_\beta + Y_\beta L'_r)}{s_d^2 - L'_p s_d - \frac{g}{V_o} L'_r} \right|$$

When $\left|\frac{g}{V} L'_r\right| << |s_d^2|$, upon substitution for s_d, the magnitude of the quantity becomes

$$\frac{|\phi|}{|\beta|} \doteq \left[\frac{(L'_\beta + Y_\beta L'_r)^2 + (2\zeta\omega_n)_d L'_r (L'_\beta + Y'_\beta L'_r) + (\omega_n^2)_d (L'_r)^2}{(\omega_n^2)_d \left[(L'_p)^2 + (2\zeta\omega_n)_d L'_p + (\omega_n^2)_d \right]} \right]^{1/2}$$

When this expression is simplified to the full degree of approximation used in deriving the transfer functions,

$$\frac{|\phi|}{|\beta|} \doteq \frac{K_z^2 C'_{\ell_\beta}}{K_x^2 C'_{n_\beta}} \left[\frac{1 - \frac{1}{4\mu_2}\left[C_{y_\beta} + \frac{1}{2K_z^2} C'_{n_r} - \frac{K_z^2}{K_x^2}\frac{C'_{\ell_\beta}}{C'_{n_\beta}}\left(C_{L_1} - \frac{1}{2K_z^2} C'_{n_p}\right)\right]\frac{C'_{\ell_r}}{C'_{\ell_\beta}} + \frac{1}{8\mu_2 K_z^2}\left(\frac{C'_{\ell_r}}{C'_{\ell_\beta}}\right)^2 C'_{n_\beta}}{1 - \frac{1}{4\mu_2}\frac{K_z^2}{K_x^2}\left[C_{y_\beta} + \frac{1}{2K_z^2} C'_{n_r} - \frac{K_z^2}{K_x^2}\frac{C'_{\ell_\beta}}{C'_{n_\beta}}\left(C_{L_1} - \frac{1}{2K_z^2} C'_{n_p}\right)\right]\frac{C'_{\ell_p}}{C'_{n_\beta}} + \frac{K_z^2}{8\mu_2 K_x^4}\frac{(C'_{\ell_p})^2}{C'_{n_\beta}}} \right]^{1/2}$$

Note that $|\phi|/|\beta|$ is not quite zero when $C'_{\ell_\beta} = 0$.

C. STICK-FREE DYNAMICS

Requirements are stated (for example, Reference 15) on dynamic stability with the cockpit controls free. Vehicle response to pilot-force inputs is also of interest, since pilot feel is usually related more to force than to deflection. From the material in this section can be found vehicle transfer functions for control-force and gust inputs, as well as general characteristics of the controls-free motion.

With an irreversible control system, the effect of freeing the pilot's control is generated only through the artificial feel system (including detent, friction, etc. effects). A bobweight can affect the vehicle response (See Appendix IV), but a simple spring feel system will merely tend to move the controls to their force-trim position or keep them fixed there.

In the presence of friction, the effect of freeing the controls is liable to be highly nonlinear at all amplitudes. A positive detent will reduce limit cycling, but at the expense of higher breakout force. A simple limit-cycle residual oscillation can be analyzed by several methods: phase-plane, describing-function, etc. (See, for example, References 10 or 11.) In view of the many places throughout the control and stability augmentation systems where nonlinearities conducive to residual oscillations can exist, it seems impractical to present detailed nonlinear analysis methods here. Reference 16 analyzes a simplified longitudinal residual oscillation caused by friction.

To gain a little insight on controls-free dynamics, however, we will consider only idealized cases with no nonlinearities. We will further assume that control-system dynamics (excluding feel) forward of the surface themselves are negligible (Appendix III). Aside from residual oscillations, actual controls-free dynamics will generally tend to fall between the controls-fixed and the idealized controls-free cases, the characteristics varying with amplitude.

Stick-free motion with a reversible control system involves all the force, moment, and hinge-moment equations developed in Appendix III, although decoupling the longitudinal and lateral-directional sets is still generally possible. Separation of the longitudinal motion into simpler short-period and phugoid equations is also often legitimate. Aeroelastic deformations can be important, but here we neglect them.

It is common practice to ignore the control-inertia-and-damping coupling terms in the vehicle force and moment equations, leaving such coupling only in the hinge-moment equations (Appendix III notes an exception). Often the control-surface natural frequencies will be far enough beyond the controls-fixed vehicle frequencies that surface damping and inertia can be ignored even in the hinge-moment equations. In that case equivalent stability derivatives can be formed to use in the controls-fixed equations, so that the hinge-moment equations are entirely eliminated.

1. Longitudinal Motion, Stick Free

Consider first an irreversible control system. A bobweight near the center of gravity, for example, will change the stick-free maneuvering neutral point, N'_m; the effect on short-period frequency is immediately apparent. As can be inferred from the discussion that follows, such a bobweight has no effect on total short-period damping, $(2\zeta\omega_n)_{sp}$.

A bobweight far removed from the center of gravity, however, adds a new term in the z-force equation proportional to pitching acceleration. This term changes the form of some transfer-function numerators (Appendix IV); the equations of motion are then a simplified form of those shown next for the reversible-control case. For linear control force, a bobweight contributes

$$\Delta\delta \doteq \frac{-G}{g\partial F_e/\partial\Delta_s}\left(\frac{\partial F_e}{\partial n}\right)_B \left[V(\dot{\alpha}-q) - x_B\dot{q}\right]$$

in near-level flight.

For a reversible control system in straight, level flight with a nonstatic-balanced bobweight, elevator mass unbalance, and a downspring, we have for force trim

$$F_e = 0 = \frac{G}{B}\left[q^* S_e \bar{c}_e C_h + H_D - W_e \bar{r}_e\right] + \left(\frac{\partial F_e}{\partial n}\right)_B$$

or

$$C_h = \frac{1}{q^* S_e \bar{c}_e}\left[W_e \bar{r}_e - H_D - \frac{B}{G}\left(\frac{\partial F_e}{\partial n}\right)_B\right]$$

where W_e is the weight of the elevator; $\bar{r}_e$ is the distance, normal to the hinge line, of the elevator center of gravity forward of the hinge line; and H_D is the downspring

hinge moment. From Appendix III the dynamic hinge-moment equation can be written in terms of angular acceleration derivatives (hinge moment ÷ I_e):

$$\ddot{\delta} + \left(\frac{1}{\cos\Lambda_e} + \frac{I_{\ell r_e}}{I_e}\right)\dot{q} - \frac{m_e \bar{r}_e V_o}{I_e}(\dot{\alpha} - q) = H_u \frac{u}{V_o} + H_\alpha \Delta\alpha + H_{\dot{\alpha}}\dot{\alpha} + H_q q$$

$$+ H_\delta \Delta\delta + H_{\dot{\delta}}\dot{\delta} + \frac{B}{qGI_e}\left(\frac{\partial F_e}{\partial n}\right)_B \left[x_B \dot{q} - V(\dot{\alpha} - q)\right] - \frac{B}{GI_e} F_e$$

where (C_h is given above):

$$H_u = \frac{\rho V_o^2 S_e \bar{c}_e}{I_e}\left(C_h + \frac{V_o}{2}\frac{\partial C_h}{\partial u}\right)$$

$$H_\alpha = \frac{q^* S_e \bar{c}_e}{I_e} C_{h_\alpha}$$

$$H_{\dot{\alpha}} = \frac{\rho V_o S_e \bar{c}_e \bar{c}}{4 I_e} C_{h_{\dot{\alpha}}} ; \quad C_{h_{\dot{\alpha}}} = \partial C_h / \partial\left(\frac{\dot{\alpha}\bar{c}}{2V_o}\right)$$

$$H_q = \frac{\rho V_o S_e \bar{c}_e \bar{c}}{4 I_e} C_{h_q} ; \quad C_{h_q} = \partial C_h / \partial\left(\frac{q\bar{c}}{2V_o}\right)$$

$$H_\delta = \frac{q^* S_e \bar{c}_e}{I_e} C_{h_\delta}$$

$$H_{\dot{\delta}} = \frac{\rho V_o S_e \bar{c}_e \bar{c}}{4 I_e} C_{h_{\dot{\delta}}} ; \quad C_{h_{\dot{\delta}}} = \partial C_h / \partial\left(\frac{\dot{\delta}\bar{c}}{2V_o}\right)$$

$$\frac{I_e}{\cos\Lambda_e} + I_{\ell r_e} = \int_e x\, r_e\, dm = \frac{I_e}{\cos\Lambda_e} + m\ell_e \bar{r}_e - \tan\Lambda_e \int_e |y|\, \bar{r}_e\, dm, \text{ slug ft}^2$$

I_e = elevator moment of inertia about its hinge line[12] slug ft^2

Λ_e = sweepback of elevator hinge line

---

[12] These should be considered effective values for the elevator control system. Reference 37 gives the effect of a control stick near the vehicle center of gravity for an unswept elevator hinge:

$$H = I_e(\dot{q} + \ddot{\delta}) - m_e \bar{r}_e\left[V_o(\dot{\alpha} - q) - \ell_e \dot{q}\right] + \frac{1}{G\ell_s}\left[I_s\left(\frac{1}{G\ell_s}\ddot{\delta} - \dot{q}\right) + H_s V_o(\dot{\alpha} - q)\right]$$

where I_e, m_e, and $\bar{r}_e$ are for the elevator alone, I_s is the control-stick moment of inertia about its pivot, and H_s is the mass moment of the control stick about its pivot: positive when it tends to move the stick forward.

ℓ_e = distance along the x reference axis from the center of gravity forward to intersection of x axis and elevator hinge line, ft

r_e = distance normal to elevator hinge line, positive forward of elevator hinge line, ft

$\bar{r}_e$ = r_e distance from elevator hinge line forward to elevator center of gravity, ft

x_B = x-reference-axis distance from the center of gravity forward to bobweight, ft

m_e = mass of elevator[12], slugs

This equation can be solved together with the others (Section IVB1).

The small $\ddot{\delta}$ coupling terms in the Z and M equations (See Appendix III) are normally neglected. Even so, elevator mass underbalance (or a large bobweight) and close aerodynamic balance (See, for example, Reference 21) can introduce a severe, detrimental coupling between short-period and elevator modes. Such coupling is to be avoided, but can be analyzed.

More commonly the coupling is weak, with the frequencies of the two modes well separated. It can then be assumed that (neglecting friction) the elevator follows the vehicle motion perfectly. Then the $\dot{\delta}$ and $\ddot{\delta}$ hinge-moment terms can be neglected. This is done in the following simplified analyses.

(a.) Short-Period Mode

The short-period equations then become, upon substitution for δ ,

$$\begin{bmatrix} (1 - Z'_{\dot{\alpha}})s - Z'_{\alpha} & -I_n \frac{Z_\delta}{H_\delta} s - (1 + Z'_q) \\ -M'_{\dot{\alpha}} s - M'_{\alpha} & (1 - \frac{M_\delta}{H_\delta} I_n)s - M'_q \end{bmatrix} \begin{pmatrix} \Delta\alpha \\ q \end{pmatrix} = \begin{pmatrix} Z_\delta \\ M_\delta \end{pmatrix} \frac{1}{H_\delta I_e} \frac{B}{G} F_e$$

where

$$Z'_i \triangleq Z_i - \frac{Z_\delta}{H_\delta} H_i^\dagger , \qquad i = \alpha, \dot{\alpha}, q$$

$$M'_i \triangleq M_i - \frac{M_\delta}{H_\delta} H_i^\dagger , \qquad i = \alpha, \dot{\alpha}, q$$

$$H_\alpha^\dagger \triangleq H_\alpha = \frac{q^* S_e \bar{c}_e}{I_e} C_{h_\alpha}$$

$$H_{\dot{\alpha}}^\dagger \triangleq H_{\dot{\alpha}} - \frac{V_o}{I_e}\left[\frac{B}{Gg}\left(\frac{\partial F_e}{\partial n}\right)_B - m_e \bar{r}_e\right] = \frac{q^* S_e \bar{c}_e}{I_e} \frac{\bar{c}}{2V_o}(C_{h_{\dot{\alpha}}} - h_n)$$

$$H_q^\dagger \triangleq H_q + \frac{V_o}{I_e}\left[\frac{B}{Gg}\left(\frac{\partial F_e}{\partial n}\right)_B - m_e \bar{r}_e\right] = \frac{q^* S_e \bar{c}_e}{I_e} \frac{\bar{c}}{2V_o}(C_{h_q} + h_n)$$

$$I_n \triangleq \frac{1}{\cos\Lambda_e} + \frac{I_{\ell} r_e}{I_e} - \frac{Bx_B}{GI_e g}\left(\frac{\partial F_e}{\partial n}\right)_B$$

$$h_n = \frac{4}{\rho S_e \bar{c}_e \bar{c}}\left[\frac{B}{Gg}\left(\frac{\partial F_e}{\partial n}\right)_B - m_e \bar{r}_e\right]$$

The characteristic equation has the form

$$K_\Delta \Delta(s) = K_\Delta\left[s^2 + 2\zeta\omega_n s + \omega_n^2\right] = 0$$

and the transfer functions are

$$\frac{K_N N(s)}{K_\Delta \Delta(s)}$$

When $I_n \doteq 0$ (this differs from the usual definition of mass balance, $\bar{r}_e = 0$) the equations become much simpler. Still neglecting effective C_{L_q} and $C_{L_{\dot\alpha}}$, the approximate elevator-force transfer functions can then be interpreted in terms of the (controls-fixed) elevator-deflection transfer functions previously given, with

δ replaced by $\frac{1}{q^* S_e \bar{c}_e C_{h_\delta}} \frac{B}{G}\left[F_e - (\Delta F_e)_{feel}\right]$

C_{N_α} replaced by $\left(C_{N_\alpha} - \frac{C_{L_\delta}}{C_{h_\delta}} C_{h_\alpha}\right)$

C_{m_α} replaced by $\left(C_{m_\alpha} - \frac{C_{m_\delta}}{C_{h_\delta}} C_{h_\alpha}\right)$

$C_{m_{\dot\alpha}}$ replaced by $\left[C_{m_{\dot\alpha}} - \frac{C_{m_\delta}}{C_{h_\delta}}(C_{h_\alpha} - h_n)\right]$

C_{m_q} replaced by $\left[C_{m_q} - \frac{C_{m_\delta}}{C_{h_\delta}}(C_{h_q} + h_n)\right]$

N_m replaced by N_m', the stick-free maneuver point.

Generally, the major effect of freeing the elevator is equivalent to changes in C_{m_α} and N_m. In this simple case a bobweight near the center of gravity does not change the stick-free $(2\zeta\omega_n)_{sp}$ but increases the stick-free $(\omega^2_{n_{sp}})$ for an aft control surface (See also Appendix IV). For forward control the bobweight effect is the same because G is then negative, but the mass-unbalance effects are reversed. The normal elevator floating tendency (negative C_{h_α} and C_{h_δ}), on the other hand, decreases stick-free C_{N_α} and gives positive increments of stick-free C_{m_q} and $C_{m_{\dot\alpha}}$ for any control-surface location.

Control-system friction can introduce a limit-cycle oscillation, controls free. This nonlinearity is discussed in Reference 16 for simplified vehicle dynamics.

(b.) Phugoid Mode

With control force trimmed in straight, level flight, substitute $\Delta\delta$ obtained from the hinge-moment equation. Then the three simplified longitudinal equations, neglecting density-gradient effects and control-surface dynamics, can be written

$$\begin{bmatrix} s - X'_u & -X'_{\dot\alpha}s - X'_\alpha & -\frac{X_\delta}{H_\delta}I_n s^2 - X'_q s + \frac{g}{V_o} \\ -Z'_u & (1-Z'_{\dot\alpha})s - Z'_\alpha & -\frac{Z_\delta}{H_\delta}I_n s^2 - (1+Z'_q)s \\ -M'_u & -M'_{\dot\alpha}s - M'_\alpha & (1-\frac{M_\delta}{H_\delta}I_n)s^2 - M'_q s \end{bmatrix} \begin{pmatrix} \frac{u}{V_o} \\ \Delta\alpha \\ \Delta\theta \end{pmatrix} = \begin{pmatrix} X_\delta \\ Z_\delta \\ M_\delta \end{pmatrix} \frac{1}{H_\delta I_e} \frac{B}{G} F_e$$

where $X'_i = X_i - \frac{X_\delta}{H_\delta}H_i^\dagger$ and the rest of the terms are as defined previously; $H_u^\dagger = H_u$.

In the absence of stability augmentation, it can be shown (Reference 3, for example) that freeing a mass-balanced elevator has negligible effect on the classical constant - α phugoid motion. For the usual oscillatory phugoid, well below the short-period frequency, $\dot\theta$, θ , and $\dot\alpha$ contributions are negligibly small.

The major effect (beyond that noted for the short-period motion) is the modification of the u derivatives, M_u in particular, through C_h. The bobweight, mass underbalance (negative $\bar r_e$), and downspring each contribute negative C_h, or smaller negative X_u and Z_u; and, for either forward or aft control surface (negative or positive G), the bobweight contributes a positive incremental M_u. A downspring would have to become an upspring for forward control, and mass underbalance ($\bar r < 0$) contributes positive M_u for an aft control, negative M_u for a forward control.

As can be seen from the stick-fixed phugoid approximate factors preceding, a bobweight increases $(\omega_n^2)_p$ through positive ΔM_u but the effect is reduced when C_{L_δ} is significant. The bobweight decreases $(2\zeta\omega_n)_p$ through smaller $-X_u$ and positive ΔM_u.

2. Lateral-Directional Motion, Stick Free

The result with both ailerons and rudder free is quite cumbersome, but the equivalent derivatives given below may be of some use in simpler problems where many of the modifying terms are lacking. For that purpose we neglect $\dot\delta$ and $\ddot\delta$ terms.

In the hinge-moment equations of Appendix III, taking

$$H_r = q^* S_r \bar c_r \left(C_{h_{r_\beta}}\beta + C_{h_{r_{\dot\beta}}}\frac{\dot\beta b}{2V_o} + C_{h_{r_r}}\frac{rb}{2V_o} + C_{h_{r_p}}\frac{pb}{2V_o} + C_{h_{r_{\delta r}}}\Delta\delta r\right)$$

$$H_a = q^* S_a \bar c_a \left(C_{h_{a_\beta}}\beta + C_{h_{a_{\dot\beta}}}\frac{\dot\beta b}{2V_o} + C_{h_{a_r}}\frac{rb}{2V_o} + C_{h_{a_p}}\frac{pb}{2V_o} + C_{h_{a_{\delta a}}}\Delta\delta a\right)$$

carefully match the reference dimensions to those of the data used. Some, if not most, of these derivatives will be negligible. Substituting into the hinge-moment equations

and the controls-fixed lateral-directional equations (with the product-of-inertia terms retained explicitly), we get for a straight-and-level-flight operating point

$$\left(C^{\dagger}-\frac{1}{4\mu_2}C^{\dagger}_{y_{\dot\beta}}\right)\dot\beta-\frac{1}{2\tau}C^{\dagger}_{y_\beta}\beta-Y_I\ddot\phi-\frac{1}{4\mu_2}C^{\dagger}_{y_p}\dot\phi-\frac{g^{\dagger}}{V_o}\phi-Y_m\dot r+\left(C^{\dagger}-\frac{1}{4\mu_2}C^{\dagger}_{y_r}\right)r$$

$$=\frac{2S}{mV_oS_a\bar c_a}\frac{C_{y_{\delta a}}}{C_{h_{a_{\delta a}}}}\frac{B_a}{G_a}\left[F_a-(\Delta F)_{a_{feel}}\right]+\frac{S}{mV_oS_r\bar c_r}\frac{C_{y_{\delta r}}}{C_{h_{r_{\delta r}}}}\frac{B_r}{G_r}\left[F_r-(\Delta F_r)_{feel}\right]$$

where

$$C^{\dagger}=1-\frac{m_rS\bar r_r}{mS_r\bar c_r}\frac{C_{y_{\delta r}}}{C_{h_{r_{\delta r}}}}$$

$$C^{\dagger}_{y_{\dot\beta}}=C_{y_{\dot\beta}}-\frac{C_{h_{a_{\dot\beta}}}}{C_{h_{a_{\delta a}}}}C_{y_{\delta a}}-\frac{C_{h_{r_{\dot\beta}}}}{C_{h_{r_{\delta r}}}}C_{y_{\delta r}}$$

$$C^{\dagger}_{y_\beta}=C_{y_\beta}\left(1-\frac{C_{h_{a_\beta}}}{C_{h_{a_{\delta a}}}}\frac{C_{y_{\delta a}}}{C_{y_\beta}}-\frac{C_{h_{r_\beta}}}{C_{h_{r_{\delta r}}}}\frac{C_{y_{\delta r}}}{C_{y_\beta}}\right)$$

$$Y_I=\frac{2I_{yr_a}S}{mV_oS_a\bar c_a}\frac{C_{y_{\delta a}}}{C_{h_{a_{\delta a}}}}-\frac{I_{zr_r}S}{mV_oS_r\bar c_r}\frac{C_{y_{\delta r}}}{C_{h_{r_{\delta r}}}}$$

$$C^{\dagger}_{y_p}=C_{y_p}-\frac{C_{h_{a_p}}}{C_{h_{a_{\delta a}}}}C_{y_{\delta a}}-\frac{C_{h_{r_p}}}{C_{h_{r_{\delta r}}}}C_{y_{\delta r}}$$

$$g^{\dagger}=g\left(1-\frac{m_rS\bar r_r}{mS_r\bar c_r}\frac{C_{y_{\delta r}}}{C_{h_{r_{\delta r}}}}\right)$$

$$Y_m=\frac{I_{xr_r}S}{mV_oS_r\bar c_r}\frac{C_{y_{\delta r}}}{C_{h_{r_{\delta r}}}}$$

$$C^{\dagger}_{y_r}=C_{y_r}-\frac{C_{h_{a_r}}}{C_{h_{a_{\delta a}}}}C_{y_{\delta a}}-\frac{C_{h_{r_r}}}{C_{h_{r_{\delta r}}}}C_{y_{\delta r}}$$

(For I_{yr_a}, I_{zr_r}, I_{xr_r}, see Appendix III.)

and

$$-\frac{1}{4\tau K_x^2}C^{\dagger}_{\ell_{\dot\beta}}\dot\beta-\frac{g}{C_{L_1}K_x^2b}C^{\dagger}_{\ell_\beta}\beta+L_I\ddot\phi-\frac{1}{4\tau K_x^2}C^{\dagger}_{\ell_p}\dot\phi+L_m\phi-\frac{I^{\dagger}_{xz}}{I_x}\dot r-\frac{1}{4\tau K_x^2}C^{\dagger}_{\ell_r}r$$

$$=\frac{2Sb}{I_xS_a\bar c_a}\frac{C_{\ell_{\delta a}}}{C_{h_{a_{\delta a}}}}\frac{B_a}{G_a}\left[F_a-(\Delta F_a)_{feel}\right]+\frac{Sb}{I_xS_r\bar c_r}\frac{C_{\ell_{\delta r}}}{C_{h_{r_{\delta r}}}}\frac{B_r}{G_r}\left[F_r-(\Delta F_r)_{feel}\right]$$

where

$$C^{\dagger}_{\ell_{\dot\beta}} = \frac{4m_r\bar r_r}{\rho S_r \bar c_r b}\frac{C_{\ell_{\delta r}}}{C_{h_{r_{\delta r}}}} + C_{\ell_{\dot\beta}} - \frac{C_{h_{a_{\dot\beta}}}}{C_{h_{a_{\delta a}}}} C_{\ell_{\delta a}} - \frac{C_{h_{r_{\dot\beta}}}}{C_{h_{r_{\delta r}}}} C_{\ell_{\delta r}}$$

$$C^{\dagger}_{\ell_\beta} = C_{\ell_\beta} - \frac{C_{h_{a_\beta}}}{C_{h_{a_{\delta a}}}} C_{\ell_{\delta a}} - \frac{C_{h_{r_\beta}}}{C_{h_{r_{\delta r}}}} C_{\ell_{\delta r}}$$

$$L_I = 1 - \frac{2I_{yr_a} Sb}{I_x S_a \bar c_a}\frac{C_{\ell_{\delta a}}}{C_{h_{a_{\delta a}}}} + \frac{I_{zr_r} Sb}{I_x S_r \bar c_r}\frac{C_{\ell_{\delta r}}}{C_{h_{r_{\delta r}}}}$$

$$C^{\dagger}_{\ell_p} = C_{\ell_p}\left(1 - \frac{C_{h_{a_p}}}{C_{h_{a_{\delta a}}}}\frac{C_{\ell_{\delta a}}}{C_{\ell_p}} - \frac{C_{h_{r_p}}}{C_{h_{r_{\delta r}}}}\frac{C_{\ell_{\delta r}}}{C_{\ell_p}}\right)$$

$$L_m = \frac{gm_r\bar r_r Sb}{I_x S_r \bar c_r}\frac{C_{\ell_{\delta r}}}{C_{h_{r_{\delta r}}}}$$

$$\frac{I^{\dagger}_{xz}}{I_x} = \frac{I_{xz}}{I_x} + \frac{I_{xr_r} Sb}{I_x S_r \bar c_r}\frac{C_{\ell_{\delta r}}}{C_{h_{r_{\delta r}}}}$$

$$C^{\dagger}_{\ell_r} = C_{\ell_r} - \frac{C_{h_{a_r}}}{C_{h_{a_{\delta a}}}} C_{\ell_{\delta a}} - \frac{C_{h_{r_r}}}{C_{h_{r_{\delta r}}}} C_{\ell_{\delta r}} + \frac{4m_r\bar r_r}{\rho S_r \bar c_r b}\frac{C_{\ell_{\delta r}}}{C_{h_{r_{\delta r}}}}$$

and

$$-\frac{1}{4\tau K_z^2} C^{\dagger}_{n_{\dot\beta}}\dot\beta - \frac{g}{C_{L_1} K_z^2 b} C^{\dagger}_{n_\beta}\beta - \frac{I^{*}_{xz}}{I_z}\ddot\phi - \frac{1}{4\tau K_z^2} C^{\dagger}_{n_p}\dot\phi + N^{\dagger}_m\phi + N_I\dot r - \frac{1}{4\tau K_z^2} C^{\dagger}_{n_r} r$$

$$= \frac{2Sb}{I_z S_a \bar c_a}\frac{C_{n_{\delta a}}}{C_{h_{a_{\delta a}}}}\frac{B_a}{G_a}\left[F_a - (\Delta F_a)_{feel}\right] + \frac{Sb}{I_z S_r \bar c_r}\frac{C_{n_{\delta r}}}{C_{h_{r_{\delta r}}}}\frac{B_r}{G_r}\left[F_r - (\Delta F_r)_{feel}\right]$$

where

$$C^{\dagger}_{n_{\dot\beta}} = \frac{4m_r\bar r_r}{\rho S_r \bar c_r b}\frac{C_{n_{\delta r}}}{C_{h_{r_{\delta r}}}} + C_{n_{\dot\beta}} - \frac{C_{h_{a_{\dot\beta}}}}{C_{h_{a_{\delta a}}}} C_{n_{\delta a}} - \frac{C_{h_{r_{\dot\beta}}}}{C_{h_{r_{\delta r}}}} C_{n_{\delta r}}$$

$$C^{\dagger}_{n_\beta} = C_{n_\beta}\left(1 - \frac{C_{h_{a_\beta}}}{C_{h_{a_{\delta a}}}}\frac{C_{n_{\delta a}}}{C_{n_\beta}} - \frac{C_{h_{r_\beta}}}{C_{h_{r_{\delta r}}}}\frac{C_{n_{\delta r}}}{C_{n_\beta}}\right)$$

$$\frac{I^{*}_{xz}}{I_z} = \frac{I_{xz}}{I_z} + \frac{2I_{yr_a} Sb}{I_z S_a \bar c_a}\frac{C_{n_{\delta a}}}{C_{h_{a_{\delta a}}}} - \frac{I_{zr_r} Sb}{I_z S_r \bar c_r}\frac{C_{n_{\delta r}}}{C_{h_{r_{\delta r}}}}$$

$$C_{n_p}^{\dagger} = C_{n_p} - \frac{Ch_{a_p}}{Ch_{a_{\delta a}}} C_{n_{\delta a}} - \frac{Ch_{r_p}}{Ch_{r_{\delta r}}} C_{n_{\delta r}}$$

$$N_m^{\dagger} = \frac{gm_r \bar{r}_r Sb}{I_z S_r \bar{c}_r} \frac{C_{n_{\delta r}}}{Ch_{r_{\delta r}}}$$

$$N_I = 1 - \frac{I_{xr_r} Sb}{I_z S_r \bar{c}_r} \frac{C_{n_{\delta r}}}{Ch_{r_{\delta r}}}$$

$$C_{n_r}^{\dagger} = C_{n_r}\left(1 - \frac{Ch_{a_r}}{Ch_{a_{\delta a}}} \frac{C_{n_{\delta a}}}{C_{n_r}} - \frac{Ch_{r_r}}{Ch_{r_{\delta r}}} \frac{C_{n_{\delta r}}}{C_{n_r}}\right) + \frac{4m_r \bar{r}_r}{\rho S_r \bar{c}_r b} \frac{C_{n_{\delta r}}}{Ch_{r_{\delta r}}}$$

It will be noted that:

(1) Rudder mass unbalance adds terms proportional to bank angle in the rolling and yawing moment equations and alters the ϕ term in the side-force equation.

(2) Freeing the ailerons adds a rolling acceleration term to the side-force equation. Free ailerons also modify the coefficients of $\ddot{\phi}$ in the rolling and yawing moment equations; one effect is to modify I_{xz} only in the yawing-moment equation. This last effect limits the accuracy obtained by substituting modified derivatives into the controls-fixed transfer function approximations. Also, modification of the equations to eliminate I_{xz} is not as convenient when ailerons are free.

(3) Terms heretofore neglected (Y_p, Y_r, $N_{\dot{\beta}}$,...) can at times become significant when modified for the effects of free controls.

In practice, control-system nonlinearities can cause a limit-cycle oscillation when the controls are free.

D. RUDDER USE IN ROLLING MANEUVERS

In entering a turn, perfect coordination can require fancy footwork. Analysis of large-amplitude transient rolling is complicated by the nonlinear (sinusoidal) variation of the gravitational side force with bank angle, and possibly by nonlinear inertial coupling as well. Within the limitations of linear analysis, characteristics with aileron control only should be examined. If sideslip angles developed during aileron rolls are marginal or excessive, servo analysis techniques to get modal response coefficients (See Reference 31) can be used to determine acceptable gains of a proportional aileron-rudder interconnect and other stability augmentation or pilot action. Obviously, increasing Dutch-roll stiffness or damping should help. Alternatively, the interconnect gain can be found that will introduce no Dutch roll or no sideslip bias.

The sideslip transfer function for control deflection is, from Sections IVB2 and IIIB,

$$\frac{\beta(s)}{\delta(s)} = \frac{Y_\delta s^3 + B_2 s^2 + B_1 s + B_0}{\left(s + \frac{1}{T_s}\right)\left(s + \frac{1}{T_R}\right)\left[s^2 + 2(\zeta\omega_n)_d s + (\omega_{n_d}^2)^2\right]} \doteq \frac{B_2 s^2 + B_1 s + B_0}{s\left(s + \frac{1}{T_R}\right)\left[s^2 + (2\zeta\omega_n)_d s + \omega_{n_d}^2\right]}$$

In the approximation, according to the limit value theorem (References 17), prolonged aileron application leads to continuously increasing sideslip unless $B_0 = g/V \cdot (N'_\delta L'_r - L'_\delta N'_r) = 0$. Thus, step aileron deflection will eventually result in a constant sideslip only at high speed or when $(N'_\delta/L'_\delta) = (N'_r/L'_r)$. The linear β time response, then, is a combined logarithmic and oscillatory approach to a sideslip angle that is either constant or steadily increasing with time as long as lateral control is held in.

Reference 28, for example, shows that Dutch roll in rolls is approximately zero when $\omega_{n_\phi}/\omega_{n_d} = 1$, where

$$\omega_{n_\phi}^2 = N'_\beta + Y_\beta N'_r - \frac{N'_\delta}{L'_\delta}(L'_\beta + Y_\beta L'_r) + \frac{Y_\delta}{L'_\delta}(N'_\beta L'_r - L'_\beta N'_r)$$

$$\omega_{n_d}^2 \doteq N'_\beta + Y_\beta N'_r$$

$$L'_\delta = L'_{\delta_a} + \frac{\partial\delta_r}{\partial\delta_a} L'_{\delta_r}$$

$$N'_\delta = N'_{\delta_a} + \frac{\partial\delta_r}{\partial\delta_a} N'_{\delta_r}$$

$$Y_\delta = Y_{\delta_a} + \frac{\partial\delta_r}{\partial\delta_a} Y_{\delta_r}$$

It was assumed in developing the lateral-directional dynamics that $|Y_\beta L'_r| \ll |L'_\beta|$. Then it can be shown that the interconnect gain must be

$$\frac{\partial\delta_r}{\partial\delta_a} = \frac{-N'_{\delta_a} L'_\beta + Y_{\delta_a}(L'_r N'_\beta - N'_r L'_\beta)}{N'_{\delta_r} L'_\beta - Y_{\delta_r}(L'_r N'_\beta - N'_r L'_\beta)}$$

Paralleling the assumptions already stated, assume that

$$| Y_{\delta_r} (L'_r N'_\beta - N'_r L'_\beta) | \ll | N'_{\delta_r} L'_\beta |$$

(Note that when $L'_\beta \doteq 0$, $\frac{\partial \delta_r}{\partial \delta_a} = - \frac{Y_{\delta_a}}{Y_{\delta_r}}$). In most cases Y_{δ_a} is negligible; even when it is not, one would normally expect $| Y_{\delta_a} |$ not to be much greater than $| Y_{\delta_r} |$. Then with fairly wide generality the gain

$$\frac{\partial \delta_r}{\partial \delta_a} \doteq - \frac{N'_{\delta_a}}{N'_{\delta_r}} = - \frac{C_{n_{\delta_a}} + \frac{I_{xz}}{I_x} C_{\ell_{\delta_a}}}{C_{n_{\delta_r}} + \frac{I_{xz}}{I_x} C_{\ell_{\delta_r}}}$$

will keep the Dutch roll from appearing in rolls. This gain is similar, but not identical, to the steady-sideslip gain of Section IIIA1. It can vary widely with angle of attack, since the product of inertia and possibly the derivatives, too, are functions of α.

Where a step lateral control deflection produces steady sideslip,

$$\frac{\beta_\infty}{\delta} \doteq \frac{T_R}{\omega_{n_d}^2} \left[- L'_\delta (N'_p - \frac{g}{V}) + N'_\delta L'_p + Y_\delta (L'_p N'_r - N'_p L'_r) \right]$$

which gives the interconnect gain for zero steady sideslip:

$$\frac{\partial \delta_r}{\partial \delta_a} = - \frac{-L'_{\delta_a} (N'_p - \frac{g}{V}) + N'_{\delta_a} L'_p + Y_{\delta_a} (L'_p N'_r - N'_p L'_r)}{-L'_{\delta_r} (N'_p - \frac{g}{V}) + N'_{\delta_r} L'_p + Y_{\delta_r} (L'_p N'_r - N'_p L'_r)}$$

This corresponds to our previous result to the extent that, in a particular case, Y_{δ_a}, Y_{δ_r}, and $(N'_p - g/V)$ are negligible (As in Section IIIB, the g/V term is incorrect at large bank angles). That is, it may prove quite feasible to reduce both oscillatory and bias sideslip in roll entries by proportional rudder. Again, the interconnect ratio can vary greatly with α and M. Lead-lag networks can shape the response.

In a steady, level, coordinated turn, the side force is zero:

$$\beta = \frac{-1}{C_{y_\beta}} (C_{y_{\delta_a}} \delta_a + C_{y_{\delta_r}} \delta_r + C_{y_r} \frac{rb}{2V}) \doteq 0$$

$$r = \frac{g}{V} \sin \phi$$

$$C_{\ell'_{\delta_a}} \delta_a + C_{\ell'_{\delta_r}} \delta_r + C_{\ell'_r} \frac{rb}{2V} \doteq 0$$

$$C_{n'_{\delta_a}} \delta_a + C_{n'_{\delta_r}} \delta_r + C_{n'_r} \frac{rb}{2V} \doteq 0$$

yielding the control deflections for coordination:

$$\delta_a \doteq \frac{-gb \sin\phi}{2V^2 C_{\ell'_{\delta a}}} \frac{C_{\ell'_r} - \frac{C_{\ell'_{\delta r}}}{C_{n'_{\delta r}}} C_{n'_r}}{1 - \frac{C_{n'_{\delta a}}}{C_{\ell'_{\delta a}}} \frac{C_{\ell'_{\delta r}}}{C_{n'_{\delta r}}}}$$

$$\delta_r \doteq \frac{-gb \sin\phi}{2V^2 C_{n'_{\delta r}}} \frac{C_{n'_r} - \frac{C_{n'_{\delta a}}}{C_{\ell'_{\delta a}}} C_{\ell'_r}}{1 - \frac{C_{n'_{\delta a}}}{C_{\ell'_{\delta a}}} \frac{C_{\ell'_{\delta r}}}{C_{n'_{\delta r}}}}$$

where $\phi = \cos^{-1}(1/n)$. See References 3 and 21 for further discussion.

Phasing of the yaw and sideslip in rolling maneuvers can be investigated by using the transfer functions of Section IVB and their inverse Laplace transforms. The initial side acceleration for a step input is zero (neglecting Y_δ). The initial yawing acceleration is

$$\dot{r}_o = N'_\delta = \frac{q^* Sb\left(C_{n_\delta} + \frac{I_{xz}}{I_x} C_{\ell_\delta}\right)}{I_z\left(1 - \frac{I_{xz}^2}{I_x I_z}\right)}$$

E. PILOT-INDUCED OSCILLATIONS

Based on NACA research, Reference 15 requires that the force in sudden pullups be not less than that in steady pullups to the same load factor. The requirement is an attempt to prevent pilot-induced oscillations (PIO) but, as noted in the reference cited, many other attributes of a flight control system can make a vehicle PIO-prone. High short-period damping and control-system damping and inertia help satisfy the requirement. Reference 38 notes that in a reversible control system small C_{h_δ} and small positive C_{h_α}, or a bobweight, gives lower forces in abrupt maneuvers; although large negative C_{h_α} and C_{h_δ} can give initially high force followed by a reversal in abrupt maneuvers. These reversible-system extremes have generally been avoided for other reasons as well (See Section IVC).

More generally, PIO tendency is related intimately to control system nonlinearities and to the form of control adopted by the pilot. Causes are still somewhat controversial and cures are laborious, but Reference 39 and articles and comments in Reference 40 by Richardson and A'Harrah, Levi and Nelson, Ashkenas, and A'Harrah summarize the present state of knowledge and give additional references. Among the factors to be considered are vehicle response characteristics, control-system inertia and damping, friction and backlash in various places, cable stretch, actuator dynamics (including nonlinearities such as rate limiting), stability augmentation dynamics, pilot arm inertia, pilot time delay and neuromuscular lag, form of pilot control (normal acceleration, rate of climb, pitch attitude), variable gearing and force gradients, etc.

As noted for example in Reference 26, linear coupling of pilot and vehicle can produce a PIO; in that case a lateral-directional oscillation attributable to favorable aileron yaw. A bobweight not far forward of the center of gravity causes loss of anticipation, while pitch rate or pitch acceleration feedback can improve it. Reference 41 describes these longitudinal effects in a specific configuration.

F. INERTIAL COUPLING

Linearization of the equations of motion and separation of longitudinal from lateral-directional motion require neglect of inertial terms involving products and squares of the time-varying components of linear and angular acceleration (Appendix III gives a complete statement of the vector acceleration on a particle with respect to a moving reference frame). Trends in both aircraft and missile design have sometimes led to violent motions caused by these usually-neglected phenomena, involving large excursions, high structural loads, or both. Observed motions have been duplicated analytically by incorporating these gyroscopic terms, and by representations of the gravity force that hold at large angles. Reference 42 gives a number of analyses in more detail than can be presented here. The motion has essentially five degrees of freedom, with only forward speed reasonably constant.

While a full analysis, including control motions and significant aerodynamic nonlinearities as well, is absolutely necessary with vehicles suspected of being prone to inertial coupling, insight can be gained by a simpler analysis. The method presented here is a modification of supplementary notes by Schmidt, Bergrun, and Merrick of the (then) NACA Ames Aeronautical Laboratory. Assume, for a start, that $\dot{u} = \beta_0 = P_0 = Q_0 = R_0 = \Theta_0 = \Phi_0 = \Psi_0 = 0$,[13] and let α_0 be the initial inclination of the principal x axis. The principal axes ($I_{xz} = 0$) used here are slightly more convenient,

[13] As the requirement of Reference 15 states, other entry conditions must also be considered. Here, because of the necessarily limited scope of the approximations presented, such consideration has not been given. See References 32 and 42 and Appendix III for appropriate modifications to consider motion from turns, pushovers, and pullups.

provided that the derivatives are available in that system. The equations of motion can be written in two notations:

$$\begin{cases} \dot{\beta} + r - p(\alpha_o + \alpha) \doteq \frac{g}{V}\sin\phi + \frac{1}{2\tau}\left(C_{y_\beta}\beta + C_{y_r}\frac{rb}{2V} + C_{y_p}\frac{pb}{2V} + C_{y_{\delta a}}\delta a + C_{y_{\delta r}}\delta r\right) \\ \dot{\beta} + r - p(\alpha_o + \alpha) \triangleq \frac{g}{V}\sin\phi + Y_\beta\beta + Y_r r + Y_p p + Y_{\delta a}\delta a + Y_{\delta r}\delta r \end{cases}$$

$$\begin{cases} \dot{\alpha} - q + p\beta \doteq \frac{g}{V}(\cos\phi - 1) - \frac{1}{2\tau}\left(C_{N_\alpha}\alpha + C_{L_{\dot{\alpha}}}\frac{\dot{\alpha}\bar{c}}{2V_o} + C_{L_q}\frac{q\bar{c}}{2V_o} + C_{L_{\delta e}}\Delta\delta e\right) \\ \dot{\alpha} - q + p\beta \triangleq \frac{g}{V}(\cos\phi - 1) + Z_\alpha\alpha + Z_{\dot{\alpha}}\dot{\alpha} + Z_q q + Z_{\delta e}\Delta\delta e \end{cases}$$

$$\begin{cases} \dot{q} - \frac{I_z - I_x}{I_y}pr + \frac{I_e\omega_e}{I_y}r \doteq \frac{q^*S\bar{c}}{I_y}\left(C_{m_\alpha}\alpha + C_{m_{\dot{\alpha}}}\frac{\dot{\alpha}\bar{c}}{2V} + C_{m_q}\frac{q\bar{c}}{2V} + C_{m_{\delta e}}\delta e + C_{m_{\delta a}}\delta a\right) \\ \dot{q} - I_1 pr + I_M r \triangleq M_\alpha\alpha + M_{\dot{\alpha}}\dot{\alpha} + M_q q + M_{\delta e}\delta e + M_{\delta a}\delta a \end{cases}$$

$$\begin{cases} \dot{r} + \frac{I_y - I_x}{I_z}pq - \frac{I_e\omega_e}{I_z}q \doteq \frac{q^*Sb}{I_z}\left(C_{n_\beta}\beta + C_{n_{\dot{\beta}}}\frac{\dot{\beta}b}{2V} + C_{n_r}\frac{rb}{2V} + C_{n_p}\frac{pb}{2V} + C_{n_{\delta a}}\delta a + C_{n_{\delta r}}\delta r\right) \\ \dot{r} + I_3 pq - I_N q \triangleq N_\beta\beta + N_{\dot{\beta}}\dot{\beta} + N_r r + N_p p + N_{\delta a}\delta a + N_{\delta r}\delta r \end{cases}$$

$$\begin{cases} \dot{p} + \frac{I_z - I_y}{I_x}qr \doteq \frac{q^*Sb}{I_x}\left(C_{\ell_\beta}\beta + C_{\ell_{\dot{\beta}}}\frac{\dot{\beta}b}{2V} + C_{\ell_r}\frac{rb}{2V} + C_{\ell_p}\frac{pb}{2V} + C_{\ell_{\delta a}}\delta a + C_{\ell_{\delta r}}\delta r\right) \\ \dot{p} + I_5 qr \triangleq L_\beta\beta + L_{\dot{\beta}}\dot{\beta} + L_r r + L_p p + L_{\delta a}\delta a + L_{\delta r}\delta r \end{cases}$$

where α, β, θ, ϕ, p, q, r, and the δ's are perturbations (with p, ϕ, and δ possibly large) from operating-point (trim) conditions. For accuracy, significant nonlinearities such as $Cn(\beta, \alpha)$ or $Cm(\beta)$ should be incorporated. One way to express the gravity vector in full is with direction cosines (Reference 41). Machine solution is indicated in any case. It is important to analyze recoveries as well as the rolls themselves, and a range of elevator and rudder inputs.

The formidable equations above can be linearized by assuming a steady roll rate p_∞ that is large compared to the other motion components. Then $\dot{\phi} = 0$, $\phi = p_\infty t$, and the degrees of freedom are reduced from five to four; the assumption is similar to that in the two-degree-of-freedom (ψ, β) Dutch-roll approximation; it holds when $|\phi/\beta|_d$ is small, or when the Dutch roll motion is not significant. This approximation, then, should yield the steady-state response fairly accurately. The forced motion with constant control-deflection input will now involve steady angles of attack and sideslip, upon which is superimposed a sinusoidally varying gravity effect. (At the high speed normally required to get a high roll rate, the gravity effect should be minor.) The characteristic equation differs, of course, from the product of the approximate short-period and Dutch roll characteristic equations because of the inertial coupling terms retained. Typically, as roll rate, p_∞, is increased the short-period or Dutch-roll natural frequency decreases until a divergence occurs in angle of attack or sideslip.

At this stage of analysis the expressions for the steady-state conditions are still fairly messy, so further simplification is indicated. Engine angular momentum normally causes a small difference between left and right rolls. Neglecting that, $\dot{p}$, $Z_{\dot{\alpha}}$, Z_q, Y_r, and the gravity effect, the constant term in the fourth-degree characteristic equation is

$$a_o \doteq (\omega_{n_{sp}}^2 - I_1 p_\infty^2)(\omega_{n_d}^2 - I_3 p_\infty^2) + (I_1 Y_\beta + M_q)(I_3 Z_\alpha + N_r) p_\infty^2$$

using the uncoupled short-period and two-degree-of-freedom Dutch-roll approximations:

$$\omega_{n_{sp}}^2 \doteq -(M_\alpha - Z_\alpha M_q)$$
$$\omega_{n_d}^2 \doteq N_\beta + Y_\beta N_r$$

The divergence boundary is defined by $a_o = 0$. Negative a_o indicates divergence. Calculating the change in a_o with available roll control (p_∞) is a fairly simple, yet fairly accurate, way to estimate the degree of roll coupling tendency. The method is useful in defining level-flight conditions for which a more detailed analysis is needed. Extension to other initial conditions is possible by using appropriate values for derivatives, etc., but then the accuracy cannot be attested.

The steady-state incremental angles of attack and sideslip are $\alpha_\infty = b_o/a_o$, $\beta_\infty = c_o/a_o$ where, neglecting Y_p and Y_r as well,

$$b_o \doteq \frac{-\underline{a_o I_1 I_3 p_\infty^4} - Y I_1 I_3 p_\infty^3 - \underline{\left[a_o(M_q N_r - I_1 Y_\beta) + N_p(M_q + I_1 Y_\beta) + I_3(M + Z I_1 Y_\beta)\right] p_\infty^2}}{-\left[N(M_q + I_1 Y_\beta) + Y(M_q N_r - I_1 N_\beta)\right] p_\infty - (Z M_q - M)\omega_{n_d}^2}$$

$$c_o \doteq \frac{\underline{I_1\left[N_p - I_3(a_o Z_\alpha - Z)\right] p_\infty^3} + I_1(N - Y I_3 Z_\alpha) p_\infty^2 + \underline{\left[-(a_o N_r + N_p)\omega_{n_{sp}}^2\right.}}{\left. - M(I_3 Z_\alpha + N_r) + Z(I_3 M_\alpha + M_q N_r)\right] p_\infty - (N + Y N_r)\omega_{n_{sp}}^2}$$

The underlined terms contribute even when the control input is a pure rolling moment. The remaining terms represent:

$$Y = \frac{1}{2\tau}(C_{y_{\delta a}} \delta a + C_{y_{\delta r}} \delta r)$$
$$Z = -\frac{1}{2\tau} C_{L_{\delta e}} \delta e$$
$$M = \frac{q^* S \bar{c}}{I_y}(C_{m_{\delta e}} \delta e + C_{m_{\delta a}} \delta a)$$
$$N = \frac{q^* S b}{I_z}(C_{n_{\delta a}} \delta a + C_{n_{\delta r}} \delta r)$$

Where lateral-directional characteristics vary with α, calculation of α_∞ allows iteration to refine the a_o calculation.

Directly from the force equations come the steady-state solutions

$$q_\infty \doteq p_\infty \beta_\infty - Z_\alpha \alpha_\infty - Z$$

$$r_\infty \doteq \frac{p_\infty (\alpha_o + \alpha_\infty + Y_p) + Y_\beta \beta_\infty + Y}{1 - Y_r} \doteq p_\infty (\alpha_o + \alpha_\infty) + Y_\beta \beta_\infty + Y$$

The rolling-moment equation then gives a check on the applied moments assumed:

$$\delta a \doteq -\frac{1}{L_{\delta a}} \left[L_{\delta r} \delta r + L_r r_\infty + L_\beta \beta_\infty + L_p p_\infty \right]$$

For a stable steady-state solution to exist, the necessary conditions are (1) $a_o > 0$, and (2) increased δa must produce increased p_∞ ; that is, $dp_\infty / d\delta a > 0$.

It can be seen that the steady-state excursions and the inertial-coupling contribution to effective aileron deflection tend to remain small until p_∞ approaches a critical value (giving $a_o \to 0$). Typical steady-state responses illustrating inertial coupling are shown in Figure 14, taken from Reference 43, in terms of principal axes.

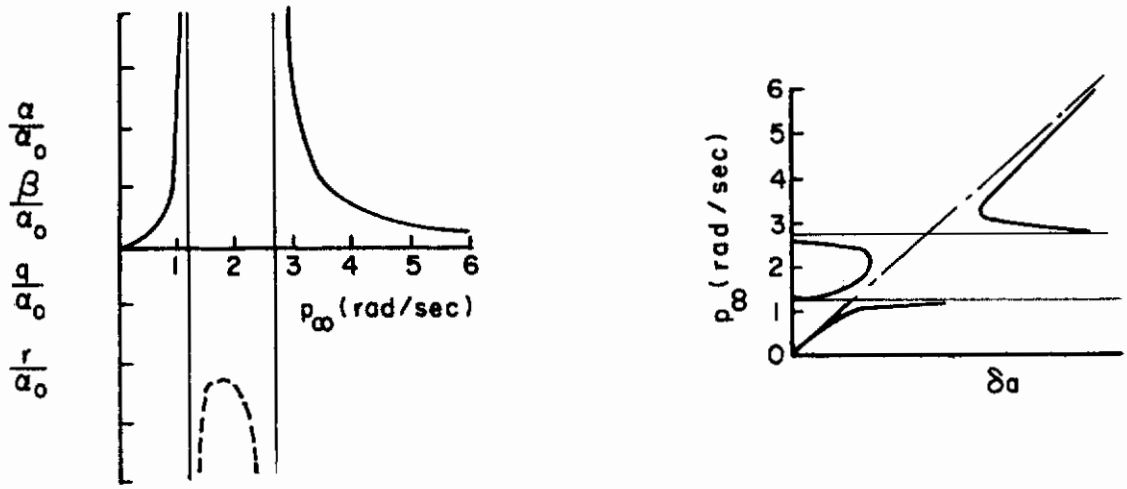

Figure 14. Inertial Coupling Trends with p_∞ and δa

Inertial coupling may increase adverse yaw in rolling pullups and favorable yaw in rolling pushovers. A possible result is a large, rapid change in "steady-state" roll rate. Engine gyroscopic effects also vary with pitch rate. Stability augmentation possibilities include feedback of nonlinear quantities such as $p\alpha$, pq, or pr, in addition to the feedbacks and control coupling used to augment the linear response. As the equations of motion imply, accelerometer measurements include nonlinear-coupling components. Linear acceleration at a point other than center of gravity is complicated even more.

G. SPINNING AND SPIN RECOVERY

Spin recovery must be demonstrated by flight test only for relatively small aircraft. For example, Specification MIL-S-25015 (USAF). Military experience indicates, however, that for flying safety the spin and spin-recovery characteristics of <u>any</u> piloted flight vehicle should be determined before the first flight.

Spin characteristics can be determined analytically through six-degree-of-freedom dynamic analyses with large high-speed digital or electronic analog computers (Reference 44), but determination of the aerodynamic data needed for the analysis requires both static and dynamic wind-tunnel tests to extreme angles of attack. The computer analysis may nevertheless be quite worthwhile for unusual configurations or those which show evidence of critical spin or recovery characteristics, and for analysis of incipient spins, other post-stall gyrations, or flight-test results.

Spin-tunnel tests provide usually accurate estimations of characteristics of fully developed spins and recoveries (Reference 45). Incipient spins often are not critical if steady-state spin and spin-recovery characteristics are satisfactory and not unusual. The two spin tunnels in the United States are on a standby basis-one at the Air Force Flight Dynamics Laboratory, Wright-Patterson AFB, Ohio, the other at the NASA Langley Research Center, Langley AFB, Virginia. Problems may also be investigated by drop or catapult tests of dynamically similar, radio-controlled models.

Occasionally, flight tests show completely different spin and recovery characteristics from those found in the spin tunnel. The discrepancy may result from failure to simulate the spin entry, or perhaps from inadequate simulation of Mach number or Reynolds number when Froude number is matched.

In preliminary design, the spin and spin-recovery characteristics can be estimated to a fair degree of accuracy by comparison with similar configurations of known characteristics.

Spin entry is sometimes difficult, but Murphy's Law applies generally; if there is a way, someone will find it. For that reason, launched-model tests and flight demonstrations at times will have to encompass all conceivable entry techniques. These include the normal rudder kick at the stall and falling out of maneuvers such as turns, loops, and zooms.

1. Developed Spin

Spins can be steady or oscillatory, depending on vehicle characteristics. Some aircraft have exhibited two distinct modes of spin, one steep and the other flat. References 45 and 46 together give a good qualitative and analytical picture of the steady spin. See also Reference 20. The use of rotation-balance wind-tunnel data in dynamic spin analyses is discussed in Reference 46; apparently the spin axis was through the model's center of gravity.

Spinning is associated with stalled flight, which differentiates it from the inertial coupling in roll of Section IVF. To avoid an infinity of spin investigations, standard control positions are generally specified: full pro-spin rudder, full nose-up (away from the ground) elevator. In a steady spin the flight path is a vertical helix, with centrifugal force balanced by the horizontal component of the resultant aerodynamic force. Generally $|C_y| << \sqrt{C_x^2 + C_z^2}$, so the airplane nose points down and roughly inward, through or toward the spin axis. Commonly the wings are nearly level in a steady spin, so the pitch angle Θ is approximately $-\frac{\pi}{2} + \alpha$ and the generally small sideslip angle is approximately $\sin^{-1}(-\Omega R/V) + \Delta\beta$ where R is the radius of the spin helix and Ω the spin rate. The balance of vertical forces gives

$$V^2 \doteq \frac{2W}{\rho S C_D} \doteq \frac{-2(W/S)}{\rho(C_x \cos\alpha + C_z \sin\alpha)}$$

Combining this result with the balance of horizontal forces, we have

$$R \doteq -\frac{g}{\Omega^2}\left(\frac{C_x \sin\alpha - C_z \cos\alpha}{C_x \cos\alpha + C_z \sin\alpha}\right) \doteq \frac{g}{\Omega^2 \tan\alpha}$$

the last approximation holding when, as usual, $|C_z| >> |C_x|$.

The body-axis rates p, q, r in a steady spin can be found from the Euler-angle rates $\dot{\Psi} = \Omega, \dot{\Theta} = \dot{\Phi} = 0$. Then the principal-axes nonlinear moment equations of Section IVF can be shown to reduce in the steady state to

$$\frac{1}{2}\rho V^2 S b C_\ell = \frac{1}{2}(I_z - I_y)\Omega^2 \cos^2\Theta \sin 2\Phi \doteq \frac{1}{2}(I_z - I_y)\Omega^2 \sin^2\alpha \sin 2\Phi$$

$$\frac{1}{2}\rho V^2 S \bar{c} C_m = \frac{1}{2}(I_z - I_x)\Omega^2 \sin 2\Theta \cos\Phi \doteq -\frac{1}{2}(I_z - I_x)\Omega^2 \sin 2\alpha \cos\Phi$$

$$\frac{1}{2}\rho V^2 S b C_n = -\frac{1}{2}(I_y - I_x)\Omega^2 \sin 2\Theta \sin\Phi \doteq \frac{1}{2}(I_y - I_x)\Omega^2 \sin 2\alpha \sin\Phi$$

A steady spin requires a balance of aerodynamic and inertial moments and stable variation of aerodynamic-plus-inertial moments with spin rate. One can consider an oscillatory spin to consist of oscillations about a steady spin; then the moments are never all nulled at once, but may average out in time. With I_z generally greater than I_x, the spin rate is determined by the magnitude of the nose-down aerodynamic pitching moment:

$$\Omega^2 \doteq \frac{-\rho V^2 S \bar{c} C_m}{(I_z - I_x)\sin 2\alpha}$$

Airplane-nose-down elevator thus tends to increase the spin rate, up elevator to decrease it. The aerodynamic yawing moments vary with α as well as with β, δr, r, etc. A potential spin (with wings approximately level) exists at the α for which $C_n \doteq 0$ (in the simplest case, where $C_{n_r}\frac{rb}{2V} \doteq -C_{n_{\delta r}}\delta r$). The rolling-moment equation is usually satisfied easily by finding the appropriate sideslip angle; this does not upset the yawing-moment balance very much because C_{n_β} is usually small at the spin angle of attack.

Aside from a few generalities, the only value of a steady-spin analysis when the actual spin is oscillatory is to furnish a starting point for further analysis.

2. Recovery

The most natural spin recovery procedure is anti-spin rudder. The yawing moment gives the proper $\dot{r}$ to bring r to zero, terminating the spin. Except where $I_y \doteq I_x$, the yawing-moment equation indicates that the gyroscopic yawing moment can also be used for recovery:

$$\dot{r} \doteq \frac{N}{I_z} - \frac{1}{2}\frac{(I_y - I_x)}{I_z}\sin 2\alpha \sin\Phi.$$

When I_x is much smaller than I_y or I_z, the most effective recovery technique thus may be to bank into the spin (right aileron in a right erect spin[14]). Ailerons normally remain effective, but spoilers generally do not because they are blanketed at high angle of attack. Some configurations, then, inherently require an auxiliary spin-recovery device. In any case, emergency-recovery parachutes or rockets are required for military spin demonstrations.

3. Aerodynamic Factors

At the normal low sideslip angle in a spin the rudder remains unstalled, but its effectiveness is reduced by blanketing at high angle of attack, at least in erect spins. The tail-damping power factor (TDPF) assesses the remaining rudder control:

$$TDPF = \frac{F\ell^2}{S(b/2)^2} \times \frac{(R_1\ell_1 + R_2\ell_2)}{S(b/2)}$$

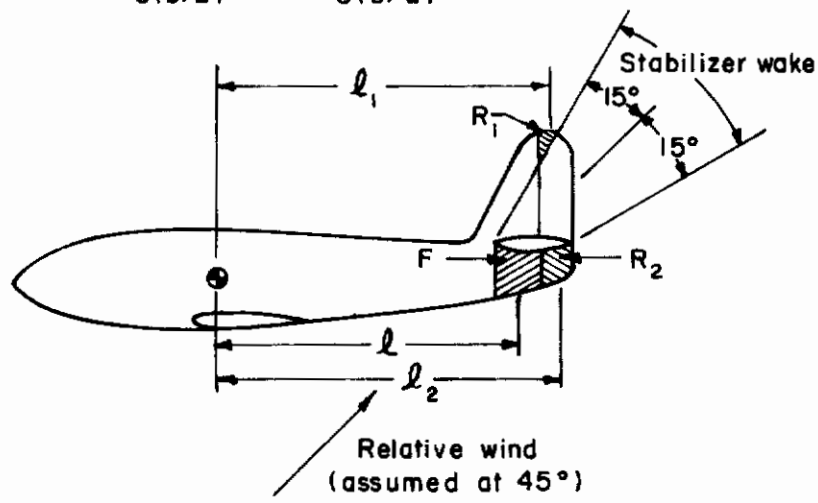

Figure 15. Tail Damping Power Factor

A rough measure of the fuselage contribution to aerodynamic yawing moment can be got from the side-area moment factor (SAMF).

[14] In an inverted spin, pilot orientation must be considered. A right spin as viewed by an upright observer is a left spin to the pilot who is inverted. To depress (toward the ground) the retreating wing then requires, from the pilot's viewpoint, "right" control deflection in the inverted "left" spin.

$$SAMF = \frac{A_2 \ell_2}{A_1 \ell_1}$$

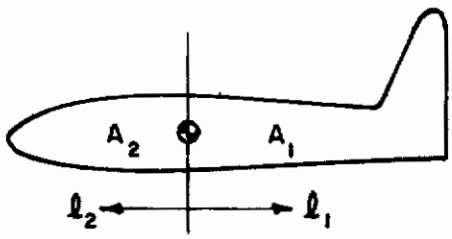

ℓ_1, ℓ_2 measured from center of gravity to centroid of A_1 and A_2 respectively.

Figure 16. Side Area Moment Factor

These parameters can be used to get a rough idea of spin and recovery characteristics in terms of the inertia yawing moment parameter, $\frac{I_x - I_y}{mb^2}$

Figures 17 and 18 summarize NASA spin-research data on the steadiness or oscillatory nature of spins and on recovery procedures. Although these charts may be used for preliminary estimation, it is recommended that a similar configuration of known characteristics be "carried along" for comparative purposes.

References 44 to 49 contain a number of analyses and test results that may be useful in solving design problems.

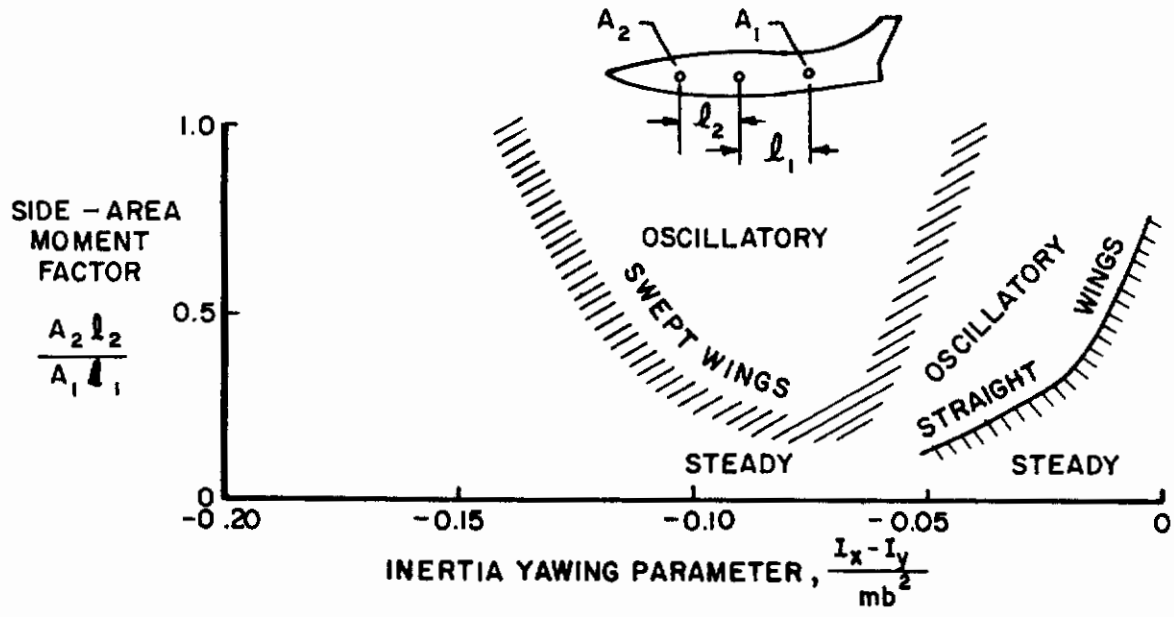

Figure 17. Influence of Mass and Side-Area Distribution on Nature of Spin

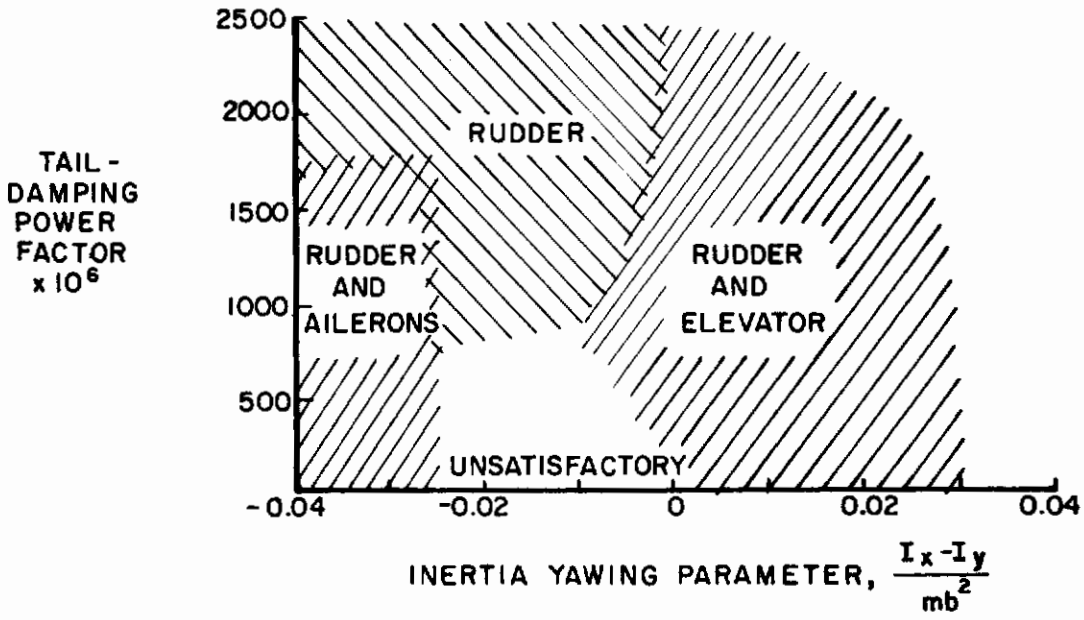

Figure 18. Control Required for Satisfactory Spin Recovery

A spin energy factor E_s can be defined (Reference 46):

$$E_s = \frac{\frac{1}{2} I_v \Omega^2}{\frac{1}{2} \rho V_R^2 Sb} \doteq \frac{-I_v C_m}{(I_z - I_x) \sin 2\alpha}$$

where I_v is the moment of inertia about a vertical axis. Generally, the higher the value of E_s, the more difficult is the recovery.

Model-testing techniques to simulate full-scale boundary-layer transition are discussed in Reference 45. Use of rotary-balance and oscillatory-balance data is described in Reference 46, which also treats the rough estimation of spin rate, vertical speed, and angle of attack from wind-tunnel data.

Nose strakes, canards, and changed fuselage nose cross sections on occasion have improved spin and recovery characteristics. As noted earlier, spoilers are often ineffective roll controls during a spin. Differential horizontal-tail deflection has been suggested in that case. Engine thrust (if available at high α), leading-edge slats, and other factors tried as a last resort have saved a few airplanes.

SECTION V

SPECIAL TOPICS TREATED LIGHTLY

A. STALLING AND PITCH-UP

Analysis of the stall is still an aerodynamic art, generally beyond the scope of this report. As an introduction see References 50 and 51, which describe the effects of wing geometry on straight and swept wings, respectively. Reference 52 shows the effect of vertical location of the horizontal tail. The effects of power and flaps must be considered. Controllability, including pilot force, is also an important factor. Icing, or even deicer boots, can influence stall characteristics.

1. Stall Warning

Wind-tunnel tests at high Reynolds number may indicate the angle of attack for buffet onset. Tuft studies can give clues to areas where local separation might be triggered to cause wing buffet before the stall, or wake surveys could aid in horizontal-tail placement. Beyond that, the designer is on his own. Getting adequate margin and intensity of warning for all required combinations of power, flap setting, gear position, etc. is quite tricky. See, for example, Reference 53.

When artificial devices are resorted to, it still may not be simple to find a good sensor location for all configurations, or even a sufficiently rugged, reliable unit. Military and civil aeronautics specifications differ on acceptability of warning form (aircraft or control shaking, aural, visual, etc.) and on speed margins between warning and stall, but all specifications agree on the need for stall warning. Obviously, the poorer the stall characteristics, the greater is the need for warning.

2. Roll-Off

There is no good way to analyze the severity of rolling tendency at the stall, except by comparison to vehicles of known characteristics. Reference 54 shows a relation between full-scale rolling moments measured in a wind tunnel and pilot rating, but viscous effects and model inaccuracies can mask results of less-ambitious wind-tunnel tests. The best recourse is to design carefully for a stall that starts inboard and lateral control that remains effective.

3. Pitch-Up

Configuration variables such as wing planform and horizontal-tail vertical location can lead to an unstable pitching-moment break associated with development of the stall. This phenomenon sometimes occurs at angles of attack well below the full stall. Control-stick gearing nonlinearity and rapid speed reduction through the range of transonic aerodynamic-center shift can also contribute to pitch-up not necessarily related to the stall. Emphasis here is on the first-mentioned characteristic, illustrated in the sketch.

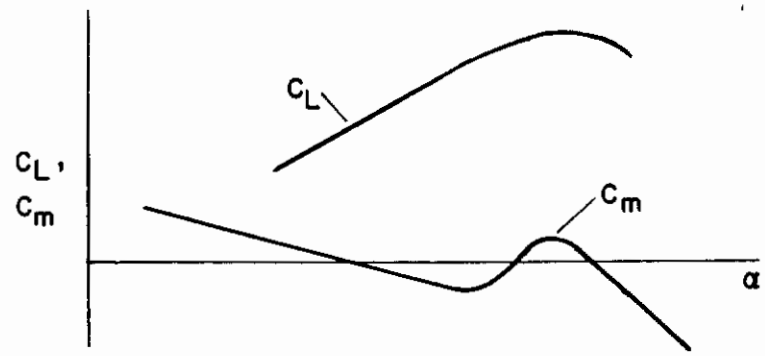

At any altitude, pitch-up makes pilot control difficult. At low altitude, high speed, there is danger of structural failure during pitch-up or recovery. At other flight conditions, angles of attack may be reached where lateral-directional stability and control become unacceptable or the airplane is prone to enter a spin. Even if pitch-up is followed at higher angles of attack by a stable moment break, there then exists a second stable trim angle of attack. Since control effectiveness is often reduced in and beyond the pitch-up range, recovery can become impossible from such a flat descent.

Thus safety considerations limit the tolerable amount of pitch-up. The acceptability of lesser degrees of pitch-up is a matter of pilot opinion related to the mission and use of the vehicle. Reference 55 gives pilot ratings of six aircraft that exhibit pitch-up, while References 56 and 57 describe analytical comparisons of other airplanes to these six. Starting at a constant initial rate of normal acceleration to the pilot's threshold of perception, estimated at $\ddot{\theta}$ = .15 deg/sec, an 0.4-second lag is assumed before the pilot begins to move his control forward at a constant rate. The analysis uses two-degree-of-freedom equations of motion with pertinent nonlinear forms of $C_m(\alpha,\delta)$, accounting for aeroelasticity where necessary. Simplified nonlinear equations that account for speed changes, also, are given in Reference 58.

Pitch-up often is most severe at high subsonic speed. Important overshoot parameters to evaluate are angle of attack, normal acceleration, and flight loads during pitch-up and recovery. The severity of pitch-up is influenced by entry rate, degree and extent of nonlinear pitching moment, and recovery-control rate. Control-effectiveness parameters suggested in Reference 56 for comparison are:

$$\text{angle of attack} - \frac{\partial M/\partial \delta_{stick}}{I_y \ddot{\theta}_{max}}$$

$$\text{load factor} - \frac{W}{\partial Z/\partial \alpha} \frac{\partial M/\partial \delta_{stick}}{I_y \ddot{\theta}_{max}}$$

where $\partial Z/\partial \alpha$ is an average value in the unstable pitching-moment range. Increasing control effectiveness helps decrease the overshoot up to a point, but may increase tail loads even more.

These preliminary design methods should be supplemented, if a problem exists, by pilot evaluations in simulators and finally by thorough flight evaluation.

Fixes, in order of preference, have included one or more of aerodynamic changes, stability augmentation, and automatic recovery (stick pushers). Anything much short of eliminating the instability will generally limit the useful flight envelope to some extent and fall short of completely eliminating the hazard.

B. DIVE RECOVERY

The flight envelopes required by Reference 15 are bounded at high speed, low altitude, by the need to recover from a dive to level flight without ground contact. Also, civil aeronautics requirements specify that no unsafe flight conditions result during specified upsets or recoveries.

Summing forces along and normal to the flight path, in a vertical-plane maneuver

$$\dot{V} = g\left(\frac{T\cos\xi - D}{W} - \sin\gamma\right)$$

$$\dot{\gamma} = \frac{g}{V}(n - \cos\gamma)$$

Also,

$$\dot{h} = V\sin\gamma$$

In a pullout, minimum altitude is reached when γ becomes zero. Combining the equations above,

$$dh = \frac{V^2}{g}\,\frac{\sin\gamma}{(n-\cos\gamma)}\,d\gamma$$

$$dV = \frac{V}{(n-\cos\gamma)}\left(\frac{T\cos\xi - D}{W} - \sin\gamma\right)d\gamma$$

Now we need, in general, other equations that specify stick and throttle action, $\rho(h)$, $T(h, V, \delta_{throttle})$, n and (from Sections IIA and IIC) C_D and α. Step-by-step integration from $\gamma = \gamma_0$ to $\gamma = 0$ can then yield the altitude loss.

For a constant-n, constant-V pullout, however, only the dh equation is needed and it can be integrated explicitly:

$$|\Delta h| = \frac{V^2}{g}\,\ln\left(\frac{n - \cos\gamma_0}{n - 1}\right)$$

where γ_0 is the initial dive angle.

An incremental altitude loss should be added to account for normal-acceleration lag in response to recovery control. At constant γ,

$$dh = V\sin\gamma\,dt$$

For a nominal two-second response time (see sketch below),

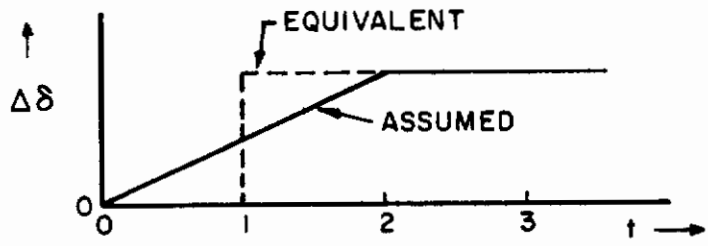

a $\Delta h = (V \sin \gamma_0)$ (1) should be added. Then for constant load factor and speed,

$$|\Delta h| = \frac{V^2}{g} \ln \left(\frac{n - \cos \gamma_0}{n - 1} \right) + V |\sin \gamma_0|$$

In pullout charts for pilot's handbooks, a 25-percent safety margin may be added.

C. FUEL SLOSH

Thorough analysis of the dynamic effect of sloshing liquids involves the combined equations of elastic and rigid vehicle motion. Such treatment is beyond the scope of this report. Further, such analysis for stability and control normally is needed only on vehicles that have large tanks (relative to vehicle size), are very flexible, or both. Commonly the liquid is represented by spring-mass-damper combinations. See Reference 59 for an example, Reference 6 for some data, or Reference 60 for a bibliography. In aircraft, large fuel motions are usually limited by baffles. Smaller motions, for example in a tip tank, can change effective stability derivatives by modifying elastic modes.

Some configurations are liable to significant center-of-gravity shifts because of longitudinal acceleration. In at least one case, the resulting trim change and instability have been embarrasing during, for example, a balked landing. The shift in center of gravity can be calculated easily for the worst case.

D. FLIGHT CONTROL SYSTEM DESIGN

Design of primary, trim, augmentation, and automatic control systems is a field in itself, beyond the scope of this report. Reference 61 is a representative flight control system specification. Normally, somewhat idealized characteristics are assumed in preliminary design. The important factors at that stage are the acceptability of the concept; necessarily rough estimates of maximum hinge moments, friction, required surface rates, reliability, etc; and functional assessment of normal and emergency operation. Successively fuller treatments follow, up to a complete implementation of the actual flight control system in an "iron bird," with vehicle dynamics supplied by an analog computer, before flight. This procedure has been found necessary for "debugging" the design of powered flight controls, and extremely valuable in aiding the flight test program.

The discussion here is general, far from exhaustive, hardly indicative of the depth of the subject. The practical problems of synthesis are themselves thorny. The material presented may serve as a brief overview, with mention of a few current developments and problems.

1. Normal Operation

Authority limits are generally set by performance considerations. The primary control and trim systems must in a broad sense allow full utilization of the flight envelope. Stability augmentation authority is usually a compromise between large-amplitude stabilization and hard-over failure considerations. Interrelations among the flight control subsystems can be important. For example, consider a control surface actuated by both the primary-control and stabilization systems. To augment stick-fixed stability requires that augmentation not move the cockpit controls; therefore, the primary and augmentation signals must be in series. Then, when primary control authority is set by a stop at the surface, full primary control deflection allows no further deflection in that direction for stability augmentation. Such interactions can influence control-surface deflection limits. Other interrelations involve failure considerations discussed farther on.

Primary and augmentation-system maximum rates depend on vehicle dynamics. The control rates should minimize additional lags in vehicle response to cockpit-control inputs of large amplitude, such as in landing flare or full-aileron rolls. A distracting interaction analogous to the one discussed above can arise when primary control rate command "bottoms" the actuator valve. Then series augmentation signals may cause unwanted control-stick movement.

Slow aileron and rudder trim rates are acceptable, but selection of longitudinal trim rate is touchy: the final choice is best made in a piloted flight simulator. Control forces, the time they are held, their frequency of occurrence, and their variation over the flight envelope must be balanced against failure-transient considerations.

Other nonlinearities, elasticity, etc. can have important effects on the acceptability of a flight control system. See, for example, Sections IVC and IVE. Vehicle aeroelasticity can assume prime importance in gust-alleviation control systems.

2. Failure Considerations

Specifications govern both transients upon failure and system performance after failure. Resulting trim changes are specified in terms of allowable pilot force or equivalent normal acceleration, roll rate, etc. These quantities, as well as stability, maneuverability, and trimmability after failure, can be estimated by the methods of this report. Control authority, rate, or integrity can be affected by a flight-control, hydraulic, electrical, or secondary power system failure. Failures can be of several types, including hard-over, soft, and oscillatory. Other subsystems such as fuel transfer or engine inlet control have important flight-control ramifications in some designs.

Pilot force can be assisted by adding a proportional supplementary hydraulic force. This boost has the safety advantage of retaining a direct mechanical connection between stick and surface, but at higher boost ratios the extremely high pilot force after boost failure renders that advantage meaningless. A fully powered primary control system with artificial feel then becomes easier to mechanize; it can be made redundant to the degree necessary for safety. Some aircraft with completely dual systems have been lost, ejection or bailout having been relied upon for ultimate crew survival. Modern techniques show promise of sufficient reliability even for commercial operation with triply redundant, self-monitoring, fail-operational, second-failure-soft, powered flight control systems. Electrical signal paths can improve

response, incorporation of artificial stabilization is simple, and a mechanical path can be retained for backup. Ingenuity has also increased the flight spectrum over which boost or powered systems are unnecessary, through artful aerodynamic balance, tabs, etc.

Primary and trim systems in series can result in inability to maneuver, to maintain 1-g flight, or even to recover, descend, and make an emergency landing following a trim failure if trim authority is too large a portion of primary-control authority. Runaway trim is a prime consideration in setting maximum trim rates.

A major design goal has been to have a flyable vehicle without augmentation, so minimum flyable levels of unaugmented dynamics have generally been maintained. There has commonly been little need to augment static stability electronically, although reliable mechanical devices (springs, bobweights, etc.) have been used extensively. Normally, sufficient authority has resulted without exceeding structural limits if a hard-over failure should occur. There is clear indication, however, that these practices cannot always be followed for some advanced missions. In those cases it is necessary to design (and prove) commensurate levels of authority, reliability, and safety in the augmentation system as well. References 9 and 14 indicate how the problem can be attacked, considering all reasonably and remotely probable combinations of failures.

A pilot, after perceiving an augmentation failure, can adapt his control characteristics rapidly to the new situation. Danger exists, though, that he will not immediately detect an unexpected soft failure. In some cases his consequent failure to adapt can result in a rapidly divergent pilot-vehicle response, even though both the vehicle alone and the closed-loop system after adaptation may still be stable. In failure analyses, the techniques of Reference 33 can be used to establish probable pilot characteristics in normal flight. That pilot model can then be used to determine closed-loop stability before adaptation to an augmentation failure. In simulator evaluations the pilot can be given occasional random failures to cope with, spaced out to minimize his alertness.

APPENDIX I

AN ILLUSTRATION OF AEROELASTIC EFFECTS

The analysis of aeroelasticity is a field in itself (for example, Reference 62). The intent of this appendix is only to give an uninitiated reader a little insight and to indicate the kinds of changes that aeroelasticity causes.

Two kinds of aeroelastic loads distort the structure and thus modify the aerodynamic coefficients and derivatives: air loads and inertia loads. To illustrate the mechanism, consider the effect of wing torsion on

$$C_L = C_{L_\alpha}(\alpha - \alpha_o) + C_{L_q}\frac{q\bar{c}}{2V} + C_{L_{\dot{\alpha}}}\frac{\dot{\alpha}\bar{c}}{2V}$$

The static aeroelastic effect is to change the local angle-of-attack distribution over the wing. In many cases this amounts to changing the section angle-of-attack distribution along the wing span. The local angle of attack can be envisioned to comprise contributions from the rigid vehicle, from airloads, and from inertia loads in linear superposition:

$$\alpha_s = \alpha_s^R + \Delta\alpha_s^A + \Delta\alpha_s^I \qquad \text{(See Footnote 15)}$$

With the kinematic relation

$$\frac{g}{V}(n - \cos\gamma) = \dot{\gamma} = q - \dot{\alpha}$$

we have

$$\Delta\alpha_s^I = n\frac{\partial\alpha_s^I}{\partial n} = \left[\frac{V}{g}(q - \dot{\alpha}) + \cos(\theta - \alpha)\right]\frac{\partial\alpha_s^I}{\partial n}$$

so that

$$C_L = \frac{1}{S}\int_{-b/2}^{b/2} c_{\ell_\alpha} c(\alpha_s - \alpha_{s_o})\,dy + C_{L_q}^R\frac{q\bar{c}}{2V} + C_{L_{\dot{\alpha}}}^R\frac{\dot{\alpha}\bar{c}}{2V}$$

$$= \frac{1}{S}\int_{-b/2}^{b/2} c_{\ell_\alpha} c\left\{\alpha - \alpha_{s_o}^R + \Delta\alpha_s^A(\alpha = 0) + \frac{\partial\alpha_s^A}{\partial\alpha}\alpha + \left[\frac{2V^2}{g\bar{c}}\left(\frac{q\bar{c}}{2V} - \frac{\dot{\alpha}\bar{c}}{2V}\right) + \cos(\theta - \alpha)\right]\frac{\partial\alpha_s^I}{\partial n}\right\}dy$$

$$+ C_{L_q}^R\frac{q\bar{c}}{2V} + C_{L_{\dot{\alpha}}}^R\frac{\dot{\alpha}\bar{c}}{2V}$$

---

[15] $(\ )_s$ refers to section characteristic; $(\ )^R$ and $(\ )^E$ to rigid or elastic value; $(\ )^A$, $(\ )^I$ to airload or inertia load contribution. The section lift-coefficient slope is c_{ℓ_α}, and the local wing chord is c.

It is apparent that the static aeroelastic effects on lift can be represented by:

(1) Change in α_o:

$$\alpha_o^E = \alpha_o^R + \Delta\alpha_o^A + \Delta\alpha_o^I$$

or

$$\alpha_o^E = -\frac{C_L^E(\alpha=0)}{C_{L_\alpha}^E} = \frac{-1}{C_{L_\alpha}^E S}\int_{-b/2}^{b/2} c_{\ell_\alpha} c \left[-\alpha_{s_o}^R + \Delta\alpha_s^A(\alpha=0) + \frac{\partial\alpha_s^A}{\partial\alpha}\alpha + \frac{\partial\alpha_s^I}{\partial n}\cos\gamma\right] dy$$

Airload, redistribution at zero overall lift coefficient and deflection under the vehicle's own weight cause this change. Thrust from an engine below the wing for example would similarly cause a change in α_o. ($\partial\alpha_s^A/\partial\alpha$ and similar terms are to be found by separate analysis.)

(2) Change in C_{L_α}:

$$C_{L_\alpha}^E = \left(\frac{C_{L_\alpha}^E}{C_{L_\alpha}^R}\right) C_{L_\alpha}^R$$

where

$$\left(\frac{C_{L_\alpha}^E}{C_{L_\alpha}^R}\right) = \frac{1}{C_{L_\alpha}^R}\left(C_{L_\alpha}^R + \frac{1}{S}\int_{-b/2}^{b/2} c_{\ell_\alpha} c \frac{\partial\alpha_s^A}{\partial\alpha} dy\right)$$

for small γ.

(3) Change in C_{L_q}:

$$C_{L_q}^E = \left(\frac{C_{L_q}^E}{C_{L_q}^R}\right) C_{L_q}^R$$

where

$$\left(\frac{C_{L_q}^E}{C_{L_q}^R}\right) \doteq 1 + \frac{2V^2}{q\,S\bar{c}\,C_{L_q}^R}\int_{-b/2}^{b/2} c_{\ell_\alpha} c \frac{\partial\alpha_s^I}{\partial n} dy$$

(4) Change in $C_{L_{\dot\alpha}}$:

$$C_{L_{\dot\alpha}}^E = \left(\frac{C_{L_{\dot\alpha}}^E}{C_{L_{\dot\alpha}}^R}\right) C_{L_{\dot\alpha}}^R$$

where

$$\left(\frac{C_{L_{\dot\alpha}}^E}{C_{L_{\dot\alpha}}^R}\right) \doteq 1 - \frac{2V^2}{q\,S\bar{c}\,C_{L_{\dot\alpha}}^R}\int_{-b/2}^{b/2} c_{\ell_\alpha} c \frac{\partial\alpha_s^I}{\partial n} dy$$

[Note that the integrals in the first, third, and fourth effects are identical, and that $(C_{L_q} + C_{L_{\dot\alpha}})$ is not affected by deformations under inertial loading.]

(5) Change in C_{L_u}, since the aeroelastic effect on C_{L_α}, through $\partial\alpha_s^A/\partial\alpha$, varies as $1/2\rho V^2$. Cross-plot C_L^E versus V at constant α and zero pitch rate to get the correct C_{L_u}.

(6) Change in wing downwash, which will affect a tail.

Moments, as well as forces, naturally are affected by aeroelastic distortions.

There also arise derivatives due to pitching acceleration, $\dot{q}$ or $\ddot{\theta}$. In a dynamic maneuver a tail on a flexible aft fuselage, for example, will lag behind because of its inertia. This lag gives rise to $C_{m_{\dot{q}}}$ and possibly $C_{L_{\dot{q}}}$ (though at least the latter would likely be negligible), and similar lateral-directional derivatives due to $\dot{p}$ and $\dot{r}$. See Reference 63 for a short exposition on $C_{m_{\dot{q}}}$. An aeroelastic analysis commonly includes also unsteady-flow effects as a function of the reduced frequency, $\omega \bar{c} / 2V$. At and below rigid-body frequencies, unsteady flow usually can be neglected. Other possible problems include static and dynamic coupling of structural deflections with the flight control system.

The intent has been to show the effects that can occur. Naturally, the insignificance or imprecision of some derivatives may obviate their aeroelastic correction. Another approach, using normal modes of aeroelastic vibration, is commonly used (Reference 3 has a short introduction). If structural and rigid-body frequencies are fairly close together (say, well within one order of magnitude), the aeroelastic and rigid-body effects can couple in a more complicated way. Then aeroelastic "corrections" are useless and a more-involved dynamic analysis must be undertaken (Reference 64). In calculating aeroelastically-modified stability derivatives, it is important to consider the effects of all structural modes. Reference 64 gives a way to include the residual stiffness effects of higher-frequency structural modes. Then if rigid and elastic modes are not closely coupled, and if aeroelasticity introduces no significant new derivatives, the methods of this report can be used directly with the modified derivatives.

APPENDIX II

CONTROL TABS

Especially at subsonic speeds, tabs are useful in adjusting stick (pedal) force levels. (Trans- and supersonic applications are limited because of transonic hinge-moment variations, loss of effectiveness of the more common inset tabs at the higher Mach numbers, and the general use of fully powered control systems anyway on such vehicles.) Control tabs can obviate the need for high boost ratios or fully powered controls, even on quite large aircraft.

As will soon be seen, there is an inexhaustible variety of tab mechanizations. Some incorporate springs (sometimes preloaded) to keep forces high at low speed while lightening them at high speed; some increase the stick-force gradient with speed. A representative sample will be discussed, so that the reader can readily analyze his own system if it is not covered here. See References 22, 23, and 65 for more discussion and references. Tab flutter can be a problem, but it is not discussed here.

Two approaches are fruitful in linear analysis: expanding the matrix representation of the static (or dynamic) equations of motion to include the tab degrees of freedom and expressions for the linkages, or modifying the derivatives in the relations presented earlier. Both approaches will be illustrated. Hinge moments can be quite nonlinear at moderate-to-large deflections, as in rudder lock; and linkages, springs, preload, etc. can contribute other nonlinearities. A tab may have to operate in a region where separated flow is present or impending, as on an aileron at the stall. The simple methods of nonlinear analysis given in this report may be of use in a rigorous analysis. The basic action of the control system, however, can normally be analyzed with fair accuracy over most of the flight envelope by linear methods.

Pound-foot-radian measure is used throughout these examples. As a result, care must be taken with quantities that are often given in other units: angular deflections, linear dimensions, spring constants, etc.

GEARED TAB

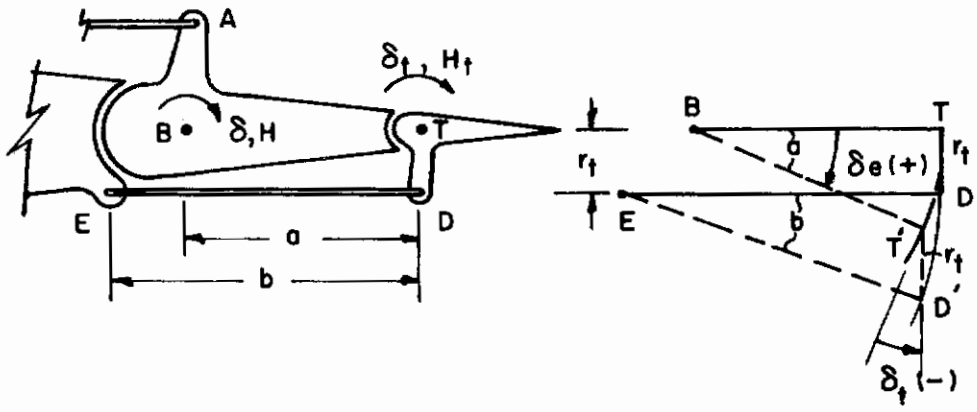

Figure 19. Geared Tab

The ratio δ_t / δ can be found by the simple graphical process shown. In this arrangement the control-surface hinge moment is reduced more, proportionately, than is its control moment. The effect is to modify the derivatives C_{h_δ} and C_{m_δ} (here considering C_m a generalized moment coefficient: pitch, yaw, etc.):

$$C_m(\delta, \delta_t) = C_{m_\delta}\delta + C_{m_{\delta_t}}\delta_t = \left(C_{m_\delta} + \frac{d\delta_t}{d\delta} C_{m_{\delta_t}}\right)\delta$$

$$C_h(\delta, \delta_t) = C_{h_\delta}\delta + C_{h_{\delta_t}}\delta_t = \left(C_{h_\delta} + \frac{d\delta_t}{d\delta} C_{h_{\delta_t}}\right)\delta$$

The force in the tab link is, of course,

$$F_b \doteq - \frac{q^* S_t \bar{c}_t}{r_t}\left[C_{h_{t_o}} + C_{h_{t_\alpha}}(\alpha - \alpha_o) + \cdots + \left(C_{h_{t_\delta}} + \frac{d\delta}{d\delta_t} C_{h_{t_{\delta_t}}}\right)\delta\right] .$$

The minus sign indicates a compression force for positive tab hinge-moment H_t.

LINKED TAB

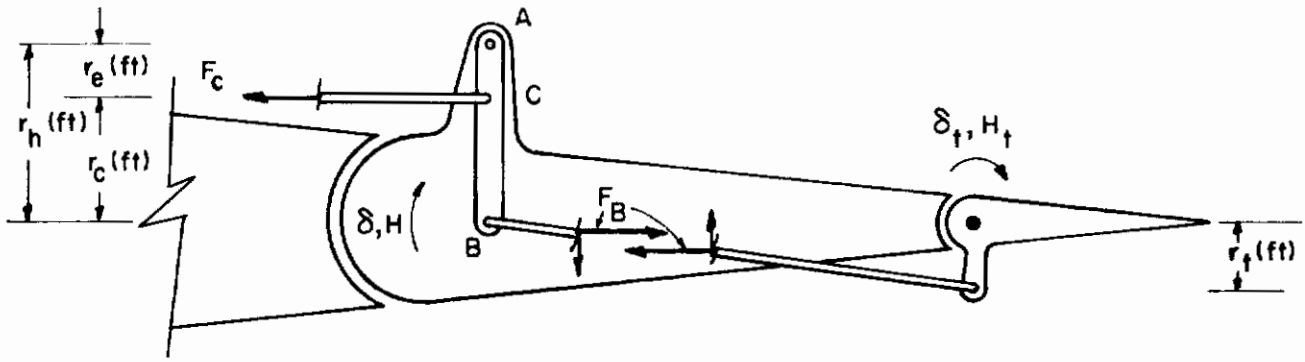

Figure 20. Linked Tab

F_c is applied at point C to an arm pivoted at A, the top of the control-surface horn. The lower end of the arm, B, nominally on the control-surface hinge line extended, is free to rotate about the upper pin at A, while the control surface rotates about a fixed hinge line. This generalized arrangement of Reference 65 can depict the essence of most any control tab arrangement with the addition of any necessary spring or gear link. The relation between F_e and F_c can be seen in Figure 21 similar to Figure 4:

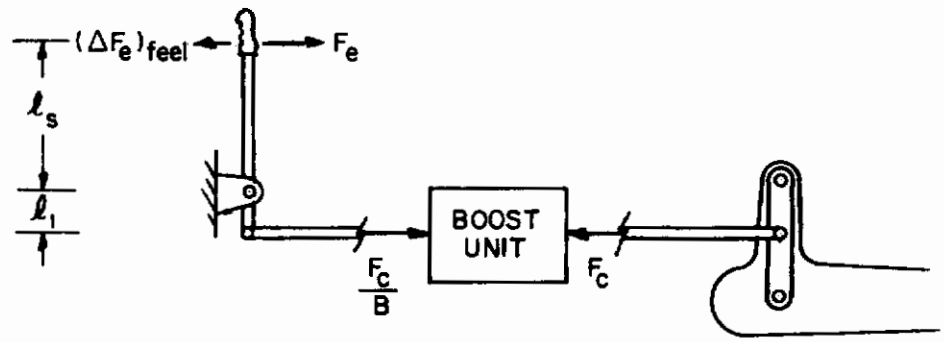

Figure 21. Pilot Force Related to F_c

Now summing moments on the arm about point B,

$$F_C = H / r_C \quad \text{lb}$$

Force balance on the arm then gives

$$F_B = F_C - \frac{H}{r_h} = \frac{r_e}{r_h r_C} H \quad \text{lb}$$

giving the tab hinge moment:

$$H_t = - r_t F_B = - \frac{r_e r_t}{r_h r_C} H \quad \text{lb - ft}$$

For this arrangement forward of the control surface,

$$B \left[F_e - (\Delta F_e)_{feel} \right] = \frac{\ell_1}{\ell_s} F_C = \frac{\ell_1}{\ell_s r_C} H \quad \text{lb}$$

Defining $G = -(\partial \delta / \partial \Delta_s)_{\delta_t}$ rad/ft $= \frac{\ell_1}{\ell_s r_C}$ (See Figure 4; the subscript δt here denotes the tab held immovable), we have in general

$$F_e - (\Delta F_e)_{feel} = \frac{G}{B} H \quad \text{lb}$$

The control-surface and tab hinge-moment equations become, upon substitution of the above relations,

$$F_e = \frac{G}{B} q^* S_e \bar{c}_e \left[C_{h_o} + C_{h_\alpha} (\alpha - \alpha_o) + \cdots + C_{h_\delta} \delta + C_{h_{\delta_t}} \delta t \right] + (\Delta F_e)_{feel}$$

$$(C_{h_o} + K_1 C_{h_{t_o}}) + (C_{h_\alpha} + K_1 C_{h_{t_\alpha}})(\alpha - \alpha_o) + \cdots + (C_{h_\delta} + K_1 C_{h_{t_\delta}}) \delta + (C_{h_{\delta_t}} + K_1 C_{h_{t_{\delta_t}}}) \delta t = 0$$

where

$$K_1 = \frac{r_h r_C}{r_e r_t} \frac{S_t \bar{c}_t}{S_e \bar{c}_e}$$

Eliminating δt from these two equations,

$$F_e = \frac{\frac{G}{B} q^* S_e \bar{c}_e}{1 + \frac{1}{K_1} \frac{C_{h_{\delta_t}}}{C_{h_{t_{\delta_t}}}}} \left[(C_{h_o} - \frac{C_{h_{\delta_t}}}{C_{h_{t_{\delta_t}}}} C_{h_{t_o}}) + (C_{h_\alpha} - \frac{C_{h_{\delta_t}}}{C_{h_{t_{\delta_t}}}} C_{h_{t_\alpha}})(\alpha - \alpha) + \cdots \right.$$

$$\left. + (C_{h_\delta} - \frac{C_{h_{\delta_t}}}{C_{h_{t_{\delta_t}}}} C_{h_{t_\delta}}) \delta \right] + (\Delta F_e)_{feel} \quad \text{lb}$$

From the definition of K_1 it is apparent that $K_1 = 0$ corresponds to a "flying tab" (see below), while $K_1 = \infty$ corresponds to pure surface control with a floating tab.

With a flying tab, F_c is applied at point B so that only the tab is controlled directly; control-surface hinge moment is balanced by tab deflection. The stick-force equation then degenerates; but analysis like that above gives an alternate expression for the generalized linked-tab arrangement shown:

$$F_e = \frac{G_t}{B} H_t + (\Delta F_e)_{feel} \qquad lb$$

where

$$G_t = -\left(\frac{\partial \delta t}{\partial \Delta_s}\right)_{\delta} = -\frac{\ell_r}{\ell_s}\frac{r_h}{r_e r_t} \qquad rad/ft$$

Then, eliminating δt as before, one can derive a single general expression for $F_e(\alpha, \cdots, \delta)$ in terms of G_t. This is done further on.

To calculate longitudinal trim conditions, for example, the elevator force equation can be solved together with the pitching moment, lift, etc. equations. Digital computer solution is quick, or the methods of this report can be used.

FLYING TAB

As discussed above, this is a special case of the linked tab where the pilot controls only the tab directly. In turn, the tab deflects the control surface by its aerodynamic moment about the control-surface hinge. Control-surface aerodynamic hinge moments are set equal to zero, and with F_e applied at point B we have directly

$$F_e - (\Delta F_e)_{feel} = \frac{G_t}{B} q^* S_t \bar{c}_t \left[C_{h_{t_o}} + \cdots + C_{h_{t_\delta}} \delta + C_{h_{t_{\delta t}}} \delta t \right]$$

where $G_t = -(\partial \delta t / \partial \Delta_s)_{\delta}$, rad/ft. (Watch dimensions throughout.) Combining this with the control-surface hinge-moment equation to eliminate δt,

$$F_e - (\Delta F_e)_{feel} = \frac{G_t}{B} q^* S_t \bar{c}_t \left[\left(C_{h_{t_o}} - \frac{C_{h_{t_{\delta t}}}}{C_{h_{\delta t}}} C_{h_o}\right) + \left(C_{h_{t_\alpha}} - \frac{C_{h_{t_{\delta t}}}}{C_{h_{\delta t}}} C_{h_\alpha}\right)(\alpha - \alpha_o) + \cdots \right.$$
$$\left. + \left(C_{h_{t_\delta}} - \frac{C_{h_{t_{\delta t}}}}{C_{h_{\delta t}}} C_{h_\delta}\right)\delta \right]$$

This is the same expression that would have been derived for the flying tab from the general expression given for the linked tab. It is used, of course, in the same way.

LINKED SPRING TAB

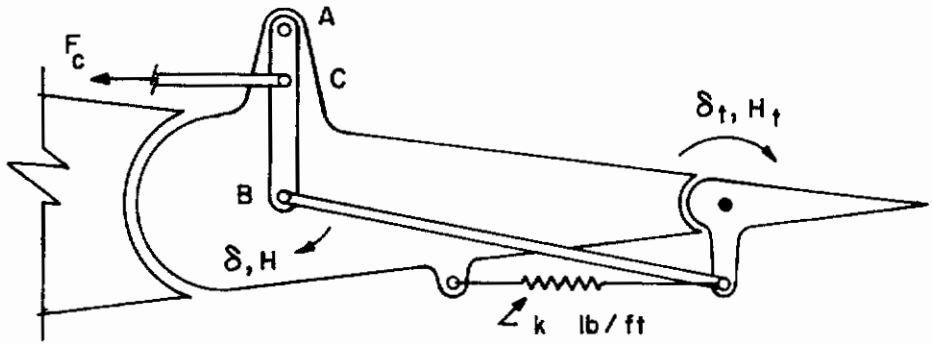

Figure 22. Linked Spring Tab

In the same manner as for the plain linked tab we have:

$$F_e = \frac{G}{B} H + (\Delta F_e)_{feel}$$

$$F_c r_c = H$$

$$F_B = \frac{r_e}{r_h r_c} H$$

$$H_t = -\frac{r_e r_t}{r_h r_c} H + k r_t^2 \delta t$$

The equations are the same as for the linked tab except:

(1) The coefficient of δt in the hinge-moment equation becomes

$$(C_{h_{\delta t}} + K_1 C_{h_{t_{\delta t}}} - \frac{K_2}{q^*})$$

where

$$K_2 = \frac{r_h r_c}{r_e r_t} \frac{r_t^2}{S_e \bar{c}_e} k$$

(2) The control-force equation with δt eliminated becomes:

$$F_e = -\frac{G}{B} \frac{q^* S_e \bar{c}_e C_{h_{\delta t}} K_1}{C_{h_{\delta t}} + K_1 C_{h_{t_{\delta t}}} - \frac{K_2}{q^*}} \left[(C_{h_{t_0}} - K_3 C_{h_0}) + (C_{h_{t_\alpha}} - K_3 C_{h_\alpha}) + \cdots + (C_{h_{t_\delta}} - K_3 C_{h_\delta}) \right] + (\Delta F_e)_{feel}$$

where

$$K_3 = \frac{1}{C_{h_{\delta t}}} (C_{h_{t_{\delta t}}} - \frac{k r_t^2}{q^* S_t \bar{c}_t})$$

SPRINGY TAB

With F_c applied at point A the arrangement can become a "springy tab," useful to improve the longitudinal stick-force gradient with speed. Then $K_1 = \infty$. In this application the spring is rather heavily loaded to move the tab trailing-edge up, so that the spring force varies only slightly with tab deflection (See Reference 21). The effect is to add only a constant tab hinge moment:

$$\Delta C_{h_t} = - \frac{(\text{spring force})\, r_t}{q^* S_t \bar{c}_t}$$

The 1-g-flight equations might be written about the trim point:

$$\begin{bmatrix} C_{h_{t\alpha}} & C_{h_{t\delta}} & C_{h_{t\delta_t}} & 0 \\ C_{h_\alpha} & C_{h_\delta} & C_{h_{\delta_t}} & -\frac{B}{G}\frac{1}{q^* S_e \bar{c}_e} \\ C_{m_\alpha} & C_{m_\delta} & C_{m_{\delta_t}} & 0 \\ C_{N_\alpha} & C_{L_\delta} & C_{L_{\delta_t}} & 0 \end{bmatrix} \begin{pmatrix} \Delta\alpha \\ \Delta\delta \\ \Delta\delta_t \\ \Delta F_e \end{pmatrix} = \begin{pmatrix} -\Delta C_{h_t} \\ 0 \\ 0 \\ 0 \end{pmatrix}$$

The principal effect is found by neglecting $C_{L_{\delta_t}}$ and $C_{m_{\delta_t}}$. Then only the first two equations are pertinent ($\Delta\alpha = \Delta\delta = 0$) and

$$\Delta F_e = \frac{G}{B}\frac{S_e \bar{c}_e}{S_t \bar{c}_t}\frac{C_{h_{\delta_t}}}{C_{h_{t\delta_t}}}(\text{spring force})\, r_t$$

which, neglecting compressibility effects, is independent of speed. At any speed, the springy tab requires about the same incremental pull force to balance it. Reference 21 shows that such a pull force increased speed stability, dF_e/dV. Also, the springy tab acts like the downspring of Section IVC1.

SPRING TAB

A common spring-tab mechanization is shown below. The arm is pivoted on the control-surface hinge line but is free to rotate with respect to the control surface. The angle between the arm and the normal to the control-surface chord line is δ_{arm}.

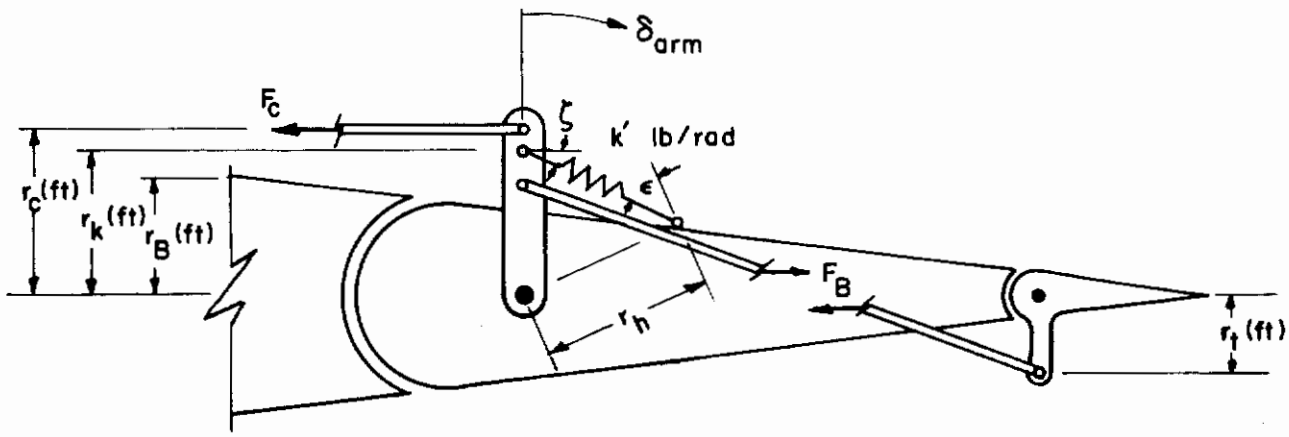

Figure 23. Spring Tab

In expanded form the longitudinal trim equations might be written:

$$\begin{bmatrix} C_{L_\alpha}+\frac{T}{q^*S} & C_{L_\delta} & C_{L_{\delta t}} & 0 & 0 & 0 & 0 \\ C_{m_\alpha} & C_{m_\delta} & C_{m_{\delta t}} & 0 & 0 & 0 & 0 \\ C_{h_\alpha} & C_{h_\delta} & C_{h_{\delta t}} & \frac{r_h k' \cos\epsilon}{q^* S_e \bar{c}_e} & 0 & 0 & 0 \\ C_{h_{t_\alpha}} & C_{h_{t_\delta}} & C_{h_{t_{\delta t}}} & 0 & \frac{r_t}{q^* S_t \bar{c}_t} & 0 & 0 \\ 0 & 0 & 0 & -r_k k' \cos\zeta & r_B & -r_c & 0 \\ 0 & 0 & r_t & r_B & 0 & 0 & 0 \\ 0 & 0 & 0 & 0 & 0 & -\frac{G}{B} r_c & 1 \end{bmatrix} \begin{pmatrix} \alpha \\ \delta \\ \delta_t \\ \delta_{arm} \\ F_B \\ F_c \\ F_e \end{pmatrix} = \begin{pmatrix} \frac{W - Ti_T}{q^* S} \\ -C_{m_o} - \frac{Tz_T}{q^* S \bar{c}} \\ -C_{h_o} \\ -C_{h_{t_o}} \\ 0 \\ 0 \\ (\Delta F_e)_{feel} \end{pmatrix}$$

where $G = -(\partial\delta/\partial\Delta_s)_{\delta t}$ as before. Upon eliminating δ_{arm}, F_B, and F_c there results

$$\begin{bmatrix} C_{L_\alpha}+\frac{T}{q^*S} & C_{L_\delta} & C_{L_{\delta t}} & 0 \\ C_{m_\alpha} & C_{m_\delta} & C_{m_{\delta t}} & 0 \\ C_{h_\alpha} & C_{h_\delta} & C_{h_{\delta t}} - \frac{r_h r_t}{r_B S_e \bar{c}_e} \frac{k'}{q^*} \cos\epsilon & 0 \\ C_{h_{t_\alpha}} & C_{h_{t_\delta}} & C_{h_{t_{\delta t}}} - \frac{r_t^2 r_k}{r_B^2 S_t \bar{c}_t} \frac{k'}{q^*} \cos\zeta & \frac{B r_t}{G r_B q^* S_t \bar{c}_t} \end{bmatrix} \begin{pmatrix} \alpha - \alpha_o \\ \delta \\ \delta_t \\ F_e \end{pmatrix} = \begin{pmatrix} \frac{W - Ti_T}{q^* S} \\ -C_{m_o} - \frac{Tz_T}{q^* S \bar{c}} \\ -C_{h_o} \\ \begin{bmatrix} -C_{h_{t_o}} \\ + \frac{B r_t (\Delta F_e)_{feel}}{G r_B q^* S_t \bar{c}_t} \end{bmatrix} \end{pmatrix}$$

The effect of the spring is to modify $C_{h_{\delta t}}$ and $C_{h_{t_{\delta t}}}$ as an inverse function of q*. The last two equations can be combined to give

$$F_e = \frac{-G r_B}{B r_t} q^* S_t \bar{c}_t \left[(C_{h_{t_o}} - R C_{h_o}) + (C_{h_{t_\alpha}} - R C_{h_\alpha})\alpha + \cdots + (C_{h_{t_\delta}} - R C_{h_\delta})\delta \right] - (\Delta F_e)_{feel}$$

where

$$R = \frac{C_{h_{t_{\delta t}}} - \left(\frac{r_t^2 r_k \cos\zeta}{r_B^2 S_t \bar{c}_t}\right)\left(\frac{k'}{q^*}\right)}{C_{h_{\delta t}} - \left(\frac{r_t r_h \cos\epsilon}{r_B S_e \bar{c}_e}\right)\left(\frac{k'}{q^*}\right)}$$

This form of spring tab, it is seen, acts as a geared tab with gear ratio a function of speed. There is also a marked similarity to the effect of a linked spring tab.

TAB-ON-TAB

Reference 23 gives the following example of using tabs to correct for an aerodynamic nonlinearity. The C-133A rudder incorporated a simple overhang balance which tended to overbalance at larger sideslip angles. As a result large, structurally unsafe sideslip angles could be developed with allowable pedal forces: with its single linked tab system, tab deflection was approximately proportional to rudder hinge moment. This problem can be solved by incorporating on the basic tab a subtab which is linked to both the rudder and the basic tab in equal ratio. The subtab increases the basic-tab hinge moment due to rudder deflection and decreases the basic-tab hinge moment due to basic-tab deflection. At zero sideslip, then, the two effects cancel and no subtab deflection occurs, giving normal rudder control for asymmetric thrust. At large sideslip angles the rudder is overbalanced, so the basic-tab deflection is small. As a result, the subtab is moved much more by the rudder than by the basic tab. The pedal force F_p, proportional to basic-tab hinge moment, is thereby increased as shown in Figure 24.

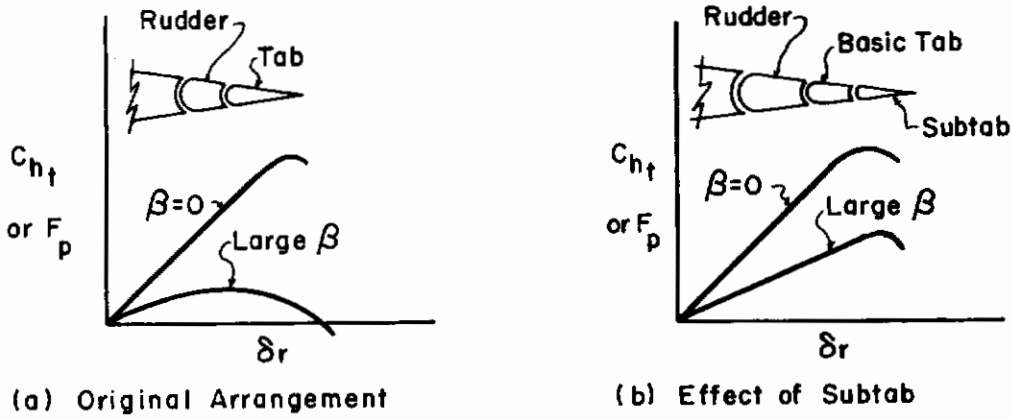

Figure 24. Tab-on-Tab

APPENDIX III

CONTROLS-FREE EQUATIONS OF MOTION

This development is limited to the linear case, with no friction, breakout force, etc. Only the control surfaces are treated in detail; the effects of the rest of the flight control system are only indicated briefly. Stability axes are used.

The acceleration a of a particle dm at a distance r from an origin moving with linear velocity $\vec{V}$ and angular velocity $\vec{\omega}$ with respect to inertial space can be stated:

$$\vec{a} = \dot{\vec{V}} + \vec{\omega} \times \vec{V} + \ddot{\vec{r}} + 2\vec{\omega} \times \dot{\vec{r}} + \dot{\vec{\omega}} \times \vec{r} + \vec{\omega} \times (\vec{\omega} \times \vec{r})$$

where the dots denote time differentiation in the moving-origin coordinate system. The linear acceleration of dm can be derived from this vector expression or written intuitively from Figure 1. Take

$$\vec{V} = (U_o + u)\vec{i} + (V_o + v)\vec{j} + (W_o + w)\vec{k}$$

$$\omega = (P_o + p)\vec{i} + (Q_o + q)\vec{j} + (R_o + r)\vec{k}$$

$$\vec{r} = x\vec{i} + y\vec{j} + z\vec{k}$$

$P_o = Q_o = R_o = V_o = W_o = \dot{\delta}_o = 0$; and small dihedral, etc. For small perturbations of a rigid vehicle with conventional control surfaces, the acceleration components of a particle are then

$$a_x = \dot{u} + z\dot{q} - y\dot{r}$$

$$a_y = \dot{v} + U_o r + x\dot{r} - z\dot{p} + r_r \ddot{\delta}r$$

$$a_z = \dot{w} - U_o q - x\dot{q} + y\dot{p} - r_e \ddot{\delta}e - r_a \ddot{\delta}a_L + r_a \ddot{\delta}a_R$$

where the control-surface deflections are positive in the sense shown in Figure 1 and the r_i are measured normal to the hinge lines, positive forward.

Applying Newton's Second Law (for constant mass, $\vec{dF} = \vec{a}dm$) and integrating over the vehicle or the individual control surfaces, as appropriate, when the origin is the center of gravity there results:

$$X\ (\text{aero} + \text{gravity} + \text{thrust}) = m\dot{u}$$

$$Y\ (\text{aero} + \text{gravity} + \text{thrust}) = m(\dot{v} + U_o r) + m_r \bar{r}_r \ddot{\delta}r$$

$$Z\ (\text{aero} + \text{gravity} + \text{thrust}) = m(\dot{w} - U_o q) - m_e \bar{r}_e \ddot{\delta}_e + \frac{1}{2} m_a \bar{r}_a (\ddot{\delta}a_R - \ddot{\delta}a_L)$$

where m_r, m_e, and m_a are effective masses of the rudder, elevator, and aileron control systems respectively; and the $m_i \bar{r}_i$ are positive for control-surface mass overbalance.

The applied moment is $\vec{r} \times d\vec{F} = \vec{r} \times \vec{a}\, dm$. When the xz plane is a plane of symmetry, $\int xy\,dm = \int yz\,dm = \int_e yr_e\,dm = 0$; then, upon substituting appropriate moments and products of inertia, we have

$$L(\text{aero + thrust}) = \left[\int \vec{r} \times \vec{a}\, dm\right]_x = \int (ya_z - za_y)\, dm$$
$$= I_x\dot{p} - I_{xz}\dot{r} + I_{yr_a}(\ddot{\delta}a_R + \ddot{\delta}a_L) - I_{zr_r}\ddot{\delta}r$$

$$M(\text{aero + thrust}) = \left[\int \vec{r} \times \vec{a}\, dm\right]_y = \int (za_x - xa_z)\, dm$$
$$= I_y\dot{q} + I_{xr_e}\ddot{\delta}e - I_{xr_a}(\ddot{\delta}a_R - \ddot{\delta}a_L)$$

$$N(\text{aero + thrust}) = \left[\int \vec{r} \times \vec{a}\, dm\right]_z = \int (xa_y - ya_x)\, dm$$
$$= I_z\dot{r} - I_{xz}\dot{p} + I_{xr_r}\ddot{\delta}r$$

$$H_e(\text{aero + static unbalance + feel}) - \frac{B_e}{G_e}F_e = -\int_e r_e a_z\, dm$$
$$= -m_e\bar{r}_e(\dot{w} - U_0 q) + I_{xr_e}\dot{q} + I_e\ddot{\delta}e$$

$$H_r(\text{aero + static unbalance + feel}) - \frac{B_r}{G_r}F_r = \int_r r_r a_y\, dm$$
$$= m_r\bar{r}_r(\dot{v} + U_0 r) + I_{xr_r}\dot{r} - I_{zr_r}\dot{p} + I_r\ddot{\delta}r$$

$$H_{a_R}(\text{aero + static unbalance + feel}) - \frac{B_a}{G_{a_R}}F_{a_R} = \int_{a_R} r_a a_z\, dm$$
$$= \frac{1}{2}m_a\bar{r}_a(\dot{w} - U_0 q) + I_{yr_a}\dot{p} + \frac{1}{2}I_a\ddot{\delta}a_R - I_{xr_a}\dot{q}$$

$$H_{a_L}(\text{aero + static unbalance + feel}) - \frac{B_a}{G_{a_L}}F_{a_L} = -\int_{a_L} r_a a_z\, dm$$
$$= -\frac{1}{2}m_a\bar{r}_a(\dot{w} - U_0 q) + I_{yr_a}\dot{p} + \frac{1}{2}I_a\ddot{\delta}a_L + I_{xr_a}\dot{q}$$

where

$$I_{xr_e} = \int_e xr_e\, dm$$

$$I_{xr_r} = \int_r xr_r\, dm$$

$$I_{zr_r} = \int_r zr_r\, dm$$

$$I_{xr_a} = \int_{a_R} xr_a\, dm$$

$$I_{yr_a} = \int_{a_R} yr_a\, dm$$

For conventional ailerons the two equations indicated must be combined in terms of $F_a = F_{a_R} + F_{a_L}$. To counteract adverse yaw or nonlinear hinge moments the trailing-edge-up aileron is often designed to deflect more than the down aileron. It can be seen that this practice introduces nonlinearity and aileron hinge moments proportional to normal and pitching accelerations.

We will assume that, for these reasons, at least for small deflections, $G_{a_L} = G_{a_R} = 1/2\ G_a$ and $\delta a_R = \delta a_L = 1/2\ \delta a$. Extension to spoilers or elevons is obvious.

For a symmetrical elevator surface with hinge line swept back at an angle Λ_e, interpret Figure 25 for an elevator. Then

$$I_{xr_e} = \int_e xr_e\, dm = \int_e \left(\ell_e - |y| \tan\Lambda_e + \frac{r_e}{\cos\Lambda_e}\right) r_e\, dm$$

$$= \frac{I_e}{\cos\Lambda_e} + m_e \ell_e \bar{r}_e - \tan\Lambda_e \int |y|\, r_e\, dm$$

$$\triangleq \frac{I_e}{\cos\Lambda_e} + I_{\ell r_e}$$

where ℓ_e is the x-distance (positive forward) in the plane of symmetry from the center of gravity to the elevator hinge line extended. (Note that in this formulation y is the distance to the elemental mass itself.) At normal angles of attack, the zero-α value can be used.

For a similar (but not symmetrical) rudder,

$$I_{xr_r} = \int_r xr_r\, dm = \int_r \left(\ell_r + h_r \tan\Lambda_r + \frac{r_r}{\cos\Lambda_r}\right) r_r\, dm$$

$$= m_r \ell_r \bar{r}_r + \frac{I_r}{\cos\Lambda_r} + \tan\Lambda_r \int_r h_r r_r\, dm$$

$$\triangleq \frac{I_r}{\cos\Lambda_r} + I_{\ell r_r}$$

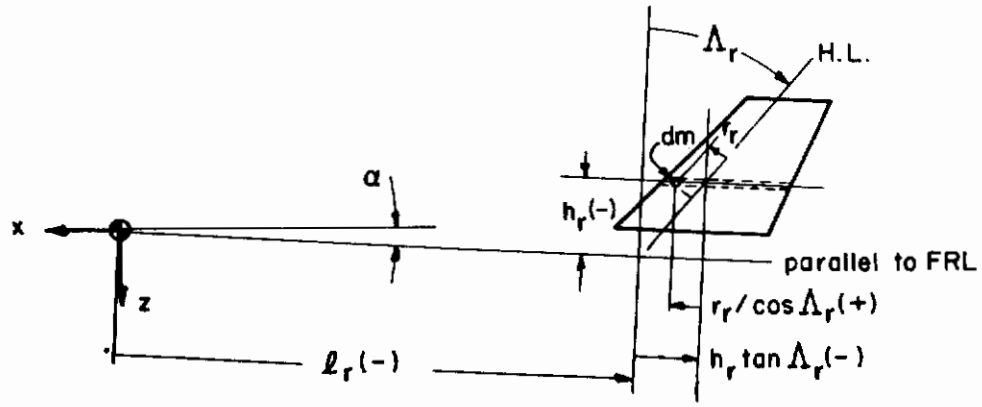

Figure 25. I_{xr_r} Calculation

$$I_{zr_r} = \int_r zr_r\,dm = \int_r (h_r - x\alpha)\,r_r\,dm$$

$$= m_r \int_r hr_r\,dm - \alpha\left(\frac{I_r}{\cos\Lambda_r}\right) + I_{\ell r_r}$$

$$\triangleq I_{hr_r} - \alpha\left(\frac{I_r}{\cos\Lambda_r} + I_{\ell r_r}\right)$$

Similarly, for the ailerons

$$I_{xr_a} = \int_{a_R} xr_a\,dm = \int_{a_R} (\ell_a - y\tan\Lambda_a + \frac{r_a}{\cos\Lambda_a})\,r_a\,dm$$

$$= \frac{I_a}{2\cos\Lambda_a} + \frac{1}{2} m_a \ell_a \bar{r}_a - \tan\Lambda_a \int_{a_R} yr_a\,dm$$

$$\triangleq \frac{1}{2}\left(\frac{I_a}{\cos\Lambda_a} + I_{\ell r_a}\right)$$

where ℓ_a is the distance (positive forward) from the center of gravity to the plan-view intersection of the x axis and the aileron hinge line extended.

Perhaps a word is in order to explain the relation of the Euler angles Ψ, Θ, and Φ to the body-axis rates P, Q, and R. Customary aeronautical practice results in about the simplest form, but known derivations can be misleading on the point considered here. Starting from orthogonal inertial reference axes X, Y, and Z, aligned with the gravity vector and an arbitrary heading, the vehicle is rotated in turn through a heading angle Ψ_o, a pitch angle Θ_o, and a bank angle Φ_o to the operating-point attitude (orthogonal axes x_o, y_o, and z_o). Perturbations ψ, θ, and ϕ are taken from this x_o, y_o, and z_o axis system in the same order as before, so that in general the angles ψ and Ψ_o are not coplanar; neither are θ and Θ_o or ϕ and Φ_o. In the equations of motion the initial, or operating-point, rates $\dot{\psi}_o$, $\dot{\theta}_o$, and $\dot{\phi}_o$ are taken about the operating-point axes z_o, y_o, x_o respectively, so $\dot{\psi}_o = R_o$, $\dot{\theta}_o = Q_o$, and $\dot{\phi}_o = P_o$. For small perturbations, then, with the customary division

$$P = P_o + p \qquad \dot{\phi}_{total} \doteq \dot{\phi}_o + \dot{\phi}$$

$$Q = Q_o + q \qquad \dot{\theta}_{total} \doteq \dot{\theta}_o + \dot{\theta}$$

$$R = R_o + r \qquad \dot{\psi}_{total} \doteq \dot{\psi}_o + \dot{\psi}$$

and the readily-derived (Reference 4, for example) small-perturbation relations

$$P \doteq \dot{\phi}_{total} - \dot{\psi}_{total}\,\theta$$

$$Q \doteq \dot{\theta}_{total} + \dot{\psi}_{total}\,\phi$$

$$R \doteq \dot{\psi}_{total} - \dot{\theta}_{total}\,\phi$$

there result

$$P_o = \dot{\phi}_o \qquad p \doteq \dot{\phi} - R_o\theta$$
$$Q_o = \dot{\theta}_o \qquad q \doteq \dot{\theta} + R_o\phi$$
$$R_o = \dot{\psi}_o \qquad r \doteq \dot{\psi} - Q_o\phi$$

When $R_o \doteq 0$, $q \doteq \dot{\theta}$ and $p \doteq \dot{\phi}$. When $Q_o = 0$, $r = \dot{\psi}$. Both of these assumptions have already been made in developing the present equations of motion, so conversion from p, q, and r to $\dot{\phi}$, $\dot{\theta}$, and $\dot{\psi}$ is simple in our case. For a good derivation of the gravity components, see Reference 4.

Substituting these expressions and the gravity terms into the equations with all our assumptions, when $\Psi_o = \Phi_o = 0$ and $\Theta_o = \gamma_o$ the aerodynamic-plus-thrust forces and moments are, in the linear range of vehicle and control-surface motion,

$$X - mg(\sin\gamma_o + \theta\cos\gamma_o) = m\dot{u}$$

$$Y + mg(\psi\sin\gamma_o + \phi\cos\gamma_o) = mV_o(\dot{\beta} + \dot{\psi}) + m_r\bar{r}_r\ddot{\delta}r$$

$$Z + mg(\cos\gamma_o - \theta\sin\gamma_o) = mV_o(\dot{\alpha} - \dot{\theta}) - m_e\bar{r}_e\ddot{\delta}e$$

$$L = I_x\ddot{\phi} - I_{xz}\ddot{\psi} + I_{yr_a}\ddot{\delta}a - \left[I_{hr_r} - \alpha\left(\frac{I_r}{\cos\Lambda_r} + I_{\ell r_r}\right)\right]\ddot{\delta}r$$

$$M = I_y\ddot{\theta} + \left(\frac{I_e}{\cos\Lambda_e} + I_{\ell r_e}\right)\ddot{\delta}e$$

$$N = I_z\ddot{\psi} - I_{xz}\ddot{\phi} + \left(\frac{I_r}{\cos\Lambda_r} + I_{\ell r_r}\right)\ddot{\delta}r$$

$$H_e - \frac{B_e}{G_e}\left[F_e - (\Delta F_e)_{feel}\right] = I_e\ddot{\delta}e - m_e\bar{r}_eV_o\left[(\dot{\alpha} - \dot{\theta}) + \frac{g}{V_o}\cos\gamma_o\theta\sin\gamma_o\right] + \left(\frac{I_e}{\cos\Lambda_e} + I_{\ell r_e}\right)\ddot{\theta}$$

$$H_r - \frac{B_r}{G_r}\left[F_r - (\Delta F_r)_{feel}\right] = I_r\ddot{\delta}r + \left(\frac{I_r}{\cos\Lambda_r} + I_{\ell r_r}\right)\ddot{\psi} + m_r\bar{r}_rV_o\left[\dot{\beta} + \dot{\psi} - \frac{g}{V_o}(\phi\cos\gamma_o + \psi\sin\gamma_o)\right]$$
$$- \left[I_{hr_r} - \alpha\left(\frac{I_r}{\cos\Lambda_r} + I_{\ell r_r}\right)\right]\ddot{\phi}$$

$$\frac{1}{2}H_a - \frac{B_a}{G_a}\left[F_a - (\Delta F_a)_{feel}\right] = \frac{1}{4}I_a\ddot{\delta}a + I_{yr_a}\ddot{\phi}$$

All control-surface inertia coefficients are taken with respect to the hinge lines. The control-system inertia, etc. "forward" of the hinge can be considered to produce external forces and moments, or the inertial-acceleration coefficients can be modified to become effective values for the entire system. For example, Reference 66 considers the effect on aileron hinge moment of a wheel-type cockpit control that is influenced by rolling acceleration.

These linear equations are normally further reduced before use. The two sets (X,Z,M,H_e) and (Y,L,N,H_r,H_a) are independent, provided that the yet-unspecified aerodynamic terms introduce no coupling. The control-surface coupling terms in the force and moment equations are generally small, though massive control surfaces can produce a "tail-wags-dog" effect through these terms. Often control-surface inertia and damping can be neglected. The explicit I_{xz} terms can be suppressed by manipulating the L and M equations (Sections IIIB1, IVB2, and IVD), or by choosing principal reference axes (Sections IVF and IVG).

APPENDIX IV

EFFECT OF BOBWEIGHT ON ROOT LOCUS

As an introduction to one servo-analysis technique, consider a bobweight at an arbitrary location. Assume a rigid vehicle with feel also proportional to control deflection. Denote the load-factor response at the pilot's location by n_p, at the bobweight location by n_B. (These correspond to the a_z' of Section IV; for simplicity, here we do not use Δ to denote the change in a quantity.) The block diagram below shows several of the vehicle responses schematically. Of course other response

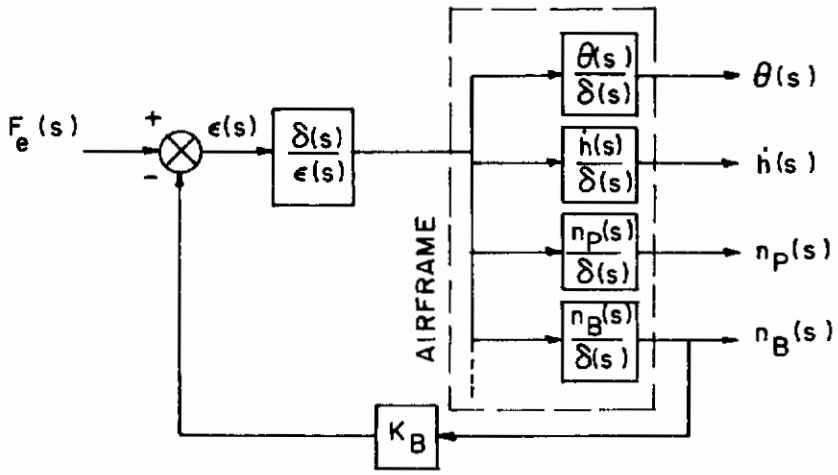

Figure 26. Block Diagram with Bobweight

quantities such as angle of attack are also present. Rather than form equivalent derivatives for each bobweight gain, we will express the vehicle transfer function in terms of bobweight gain K_B. By sacrificing realism for simplicity, we will neglect nonlinearities such as friction.

n_B Control

This simplest case is representative of pilot control of normal acceleration when a bobweight is on the control stick. To find the closed-loop transfer function:

$$n_B = \left(\frac{n_B}{\delta}\right)\left(\frac{\delta}{\epsilon}\right)\left(F_e - K_B n_B\right) \triangleq \left(\frac{n_B}{F_e}\right)_{OL}\left(F_e - K_B n_B\right)$$

where the subscript OL denotes an open-loop ($K_B \equiv 0$) characteristic $\left[\Delta_{OL} = (\Delta_{\text{airframe}})(\Delta_{\text{control system}})\right]$. Then the closed-loop transfer function is

$$\frac{n_B}{F_e} = \frac{\left(\frac{n_B}{F_e}\right)_{OL}}{1 + K_B\left(\frac{n_B}{F_e}\right)_{OL}} = \frac{\left(N_{n_{B_{F_e}}}\right)_{OL}}{\Delta_{OL} + K_B\left(N_{n_{B_{F_e}}}\right)_{\alpha}} = \frac{N_{n_{B_\epsilon}}}{\Delta_{OL} + K_B N_{n_{B_\epsilon}}}$$

since

$$\left(\frac{n_B}{F_e}\right)_{OL} = \left(N_{n_{B_{F_e}}}\right)_{OL} \Big/ \Delta_{OL}$$

When $K_B = 0$, the closed-loop transfer function reverts to its open-loop counterpart, as indeed it must. At any gain the numerator is composed entirely of open-loop factors (presumed known), so the problem is reduced to calculating and factoring a new denominator (which is generally a polynomial of the same order as for the open-loop denominator) for each value of K_B. It will be seen below that these remarks hold equally well for all response quantities.

n_p Control

Here again the pilot is controlling the normal load factor that he feels (or sees on a panel-mounted accelerometer), but the bobweight is not necessarily nearby. Proceeding as before, we find

$$n_P = \left(\frac{n_P}{\delta}\right)\left(\frac{\delta}{\epsilon}\right)\left(F_e - K_B n_B\right) = \left(\frac{n_P}{F_e}\right)_{OL}\left[F_e - K_B\left(\frac{n_B}{\delta}\right)\left(\frac{\delta}{n_P}\right) n_P\right]$$

giving the closed-loop transfer function in terms of open-loop quantities:

$$\frac{n_P}{F_e} = \frac{\left(\frac{n_P}{F_e}\right)_{OL}}{1 + K_B\left(\frac{n_B}{\delta}\right)\left(\frac{\delta}{n_P}\right)\left(\frac{n_P}{F_e}\right)_{OL}} = \frac{N_{\delta_\epsilon} N_{n_{P_\delta}}}{\Delta_{OL} + K_B N_{\delta_\epsilon} N_{n_{B_\delta}}}$$

This expression reduces to the one for n_B control when $n_P = n_B$.

$\dot{h}$ Control

Rate of climb is another commonly-controlled quantity. In the same way as before, we find

$$\frac{\dot{h}}{F_e} = \frac{\left(\frac{\dot{h}}{F_e}\right)_{OL}}{1 + K_B\left(\frac{n_B}{\delta}\right)\left(\frac{\delta}{\dot{h}}\right)\left(\frac{\dot{h}}{F_e}\right)_{OL}} = \frac{N_{\delta_\epsilon} N_{\dot{h}_\delta}}{\Delta_{OL} + K_B N_{\delta_\epsilon} N_{n_{B_\delta}}}$$

θ Control

Similarly, the pitch-attitude transfer function becomes

$$\frac{\theta}{F_e} = \frac{\left(\frac{\theta}{F_e}\right)_{OL}}{1 + K_B\left(\frac{n_B}{\delta}\right)\left(\frac{\delta}{\theta}\right)\left(\frac{\theta}{F_e}\right)_{OL}} = \frac{N_{\delta_\epsilon} N_{\theta_\delta}}{\Delta_{OL} + K_B N_{\delta_\epsilon} N_{n_{B_\delta}}}$$

Gust Response

For a vertical gust, a block diagram can be drawn:

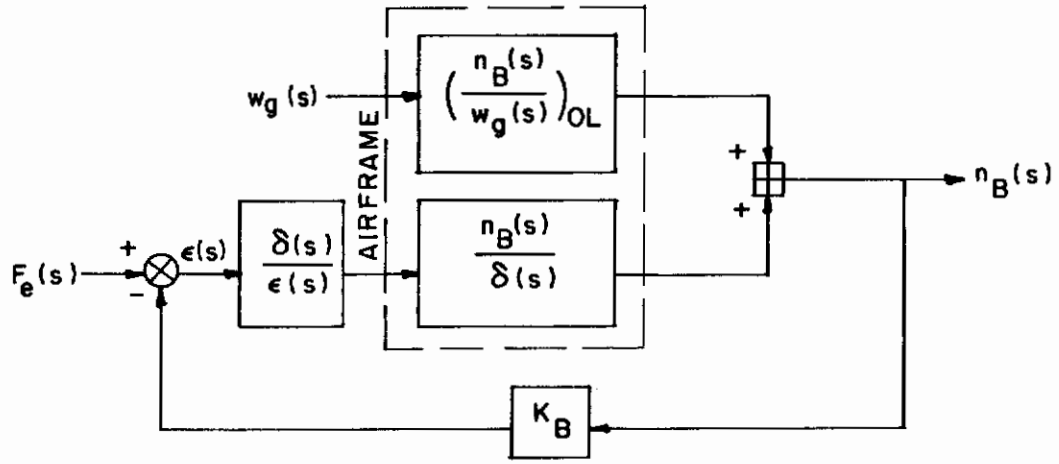

Figure 27. Gust Response with Bobweight

The controls-free ($F_e \equiv 0$) response is found by setting

$$n_B = \left(\frac{n_B}{w_g}\right)_{OL} w_g - \left(\frac{n_B}{\delta}\right)\left(\frac{\delta}{\epsilon}\right) K_B n_B$$

giving the closed-loop transfer function

$$\frac{n_B}{w_g} = \frac{\left(\frac{n_B}{w_g}\right)_{OL}}{1 + K_B\left(\frac{n_B}{\delta}\right)\left(\frac{\delta}{\epsilon}\right)} = \frac{\Delta_{\delta_\epsilon}\left(N_{n_{B_{w_g}}}\right)_{OL}}{\Delta_{OL} + K_B N_{\delta_e} N_{n_{B_\delta}}}$$

By substituting u_g for w_g, the horizontal-gust transfer function can be found.

Observe that all these transfer functions have the same denominator, and thus the same characteristic equation.

Root Locus

A handy way to visualize the effect of feedback gain is the root locus, a complex-plane plot of the denominator roots as they vary with gain. A root locus can be plotted readily by hand (using a "spirule" or similar device), but the plots in Figures 29 and 30 were done with the aid of a computer.

Some of the motion quantities commonly specified (Section IVA) are easily discernible in a complex-plane plot such as a root locus. Figure 28 illustrates these quantities for a real root and a complex pair. Poles (denominator roots) in

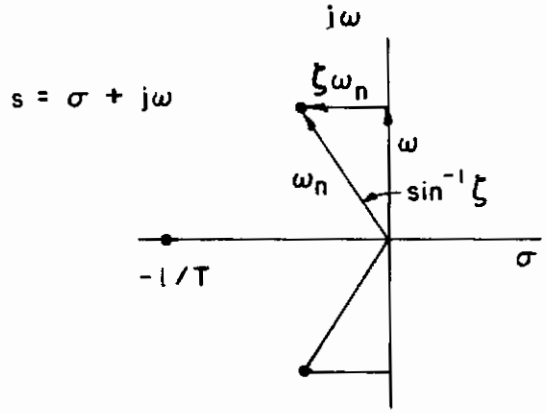

Figure 28. Properties of Roots

the left half-plane, where σ is negative, are stable. Poles on the $j\omega$ axis have neutral stability, while right-half-plane poles represent instability.

As a numerical example, consider an airplane in level flight at 0.7 Mach number at 35,000 feet, with the transfer functions shown below. Dynamics of the irreversible control system are neglected, equivalent to assuming that control-system natural frequencies are much greater than those of the vehicle. Then

$$\delta(s)/\epsilon(s) = K_{\delta_\epsilon} = -.0114 \text{ rad/lb}$$

Initial level flight is assumed. The aircraft is described by

$$\Delta_{OL}(s) = \left[s^2 + 2(.031)(.0668)s + (.0668)^2\right]\left[s^2 + 2(.312)(1.00)s + 1.00\right]$$

$$\frac{\theta(s)}{\delta(s)} = \frac{-4.46}{\Delta(s)}(s + .0143)(s + .289)$$

$$\frac{u(s)}{\delta(s)} = \frac{-1.23}{\Delta(s)}(s + .641)(s - 54.5)$$

$$\frac{\alpha(s)}{\delta(s)} = \frac{0.0706}{\Delta(s)}\left[s^2 + 2(.0412)(.0674)s + (.0674)^2\right](s + 63.4)$$

$$\frac{\dot{h}(s)}{\delta(s)} = \frac{48.1}{\Delta(s)}(s - .00140)(s - 4.27)(s + 4.41)$$

$$\frac{n_z(s)}{\delta(s)} = \frac{s\dot{h}(s)}{g\,\delta(s)} \text{ at the center of gravity}$$

$$\frac{n'_z(s)}{\delta(s)} = \frac{-1.79}{\Delta(s)}s\left[s^2 + 2(.0369)(3.97)s + (3.97)^2\right](s - .00140)$$

at the cockpit, 2.62 $\bar{c}$ ahead of the center of gravity. In the steady state, the unaugmented stick-force gradient is 3 lb/g.

A bobweight modifies the control-force transfer-function denominator (with K_B lb/g from the bobweight) to

$$\Delta(s) = \Delta_{OL}(s) + K_B(-.0114)(1.495)s(s-.00140)(s-4.27)(s+4.41)$$

with the bobweight located at the center of gravity, or to

$$\Delta(s) = \Delta_{OL}(s) + K_B(-.0114)s(-1.79)\left[s^2 + 2(.0369)(3.97)s + (3.97)^2\right](s-.0014)$$

with the bobweight on the control stick. In each case the gain is indexed along the root loci of Figure 29. Since this is a linear-analysis technique, it does not show the effects of any nonlinearities such as friction.[16]

---

[16] The interested reader can insert the zeros of the various transfer functions into Figure 29 to get an idea of the change in magnitude the bobweight causes in time histories of each output quantity. When there are no repeated poles, we have from Reference 17

$$G(s) = \frac{K\prod_{i=1}^{m}(s+z_i)}{\prod_{j=1}^{n}(s+p_j)} = K\sum_{k=1}^{n}\frac{C_k}{(s+p_k)}$$

$$g(t) = K\sum_{k=1}^{n} C_k e^{-p_k t}$$

where

$$|C_k| = \frac{\prod_{i=1}^{n}|Z_i - p_k|}{\prod_{\substack{j=1 \\ (j\neq k)}}^{n}|p_j - p_k|}$$

$$\text{sign of } C_k = \begin{cases} +, \text{even number of real roots to right of } p_k \\ -, \text{odd number of real roots to right of } p_k \end{cases}$$

C_k, the modal response coefficients, thus can be calculated from factors scaled from the root-locus plot. Thus one can trace the varying amounts of each mode in the response of any output quantity as the feedback gain varies. Analytical determination of the sensitivity of modal response coefficients is treated in Reference 13.

Note the similarity of the two cases. In our example the phugoid loci (shown magnified ten times) are identical. For gains of interest, the augmented short-period roots, too, behave similarly. The bobweight effect is about as predicted in Section VIC1: increased short-period frequency, $\omega_{n_{sp}}$, with little change in damping coefficient $(\zeta\omega_n)_{sp}$. The phugoid frequency is reduced. The gross difference in short-period behavior at larger gains has no practical consequence, since such high gains would not be used here in any case.

Without the bobweight, short-period damping is marginal. At either location, a bobweight of given gain decreases the damping ratio about the same amount:

K_B	$\sin^{-1}\zeta_{sp}$ (scaled)	ζ_{sp}
0	18.5 deg.	.32
1 lb/g	16.8	.29
2	14.4	.25
4	12.2	.21
8	10.0	.17

The value $\zeta_{sp} = .32$ corresponds marginally to damping to 1/10 amplitude in one cycle, the requirement of Reference 15. If a bobweight is needed to get an acceptable steady-state force gradient, further augmentation such as pitch damping might be employed to regain the damping-ratio loss. With an irreversible control system, augmentation signals in series with pilot inputs will not be noticed at the stick. Then, according to the approximate factors of Section IVB1, there will be only a small effect on steady-state dF_e/dn. (A moderate increase in pitch damping magnitude, $|C_{m_q}|$, slightly increases $\omega_{n_{sp}}$, thus decreasing the steady-state gain a little; the force gradient can be recalculated easily.)

Consider our example with a 2-lb/g bobweight on the control stick. The pitch-rate transfer function, as we have seen, is a combination of the denominator evaluated at $K_B = 2$ and the open-loop numerator, as follows:

$$\left(\frac{\dot\theta(s)}{\delta(s)}\right)_{OL} = \frac{-4.46s(s+.0143)(s+.289)}{\left[s^2+2(.025)(.0519)s+(.0519)^2\right]\left[s^2+2(.25)(1.18)s+(1.18)^2\right]}$$

A pitch damper modifies this transfer function to

$$\frac{\dot\theta(s)}{\delta(s)} = \frac{\left(\frac{\dot\theta(s)}{\delta(s)}\right)_{OL}}{1+K_{\dot\theta}\left(\frac{\dot\theta(s)}{\delta(s)}\right)_{OL}} = \frac{N_{\dot\theta_\delta}}{\Delta_{OL}+K_{\dot\theta}N_{\dot\theta_\delta}}$$

Naturally, there is much more to consider in mechanization, but the gross effect of a perfect linear pitch damper is shown in Figure 30. The device deserves its name.

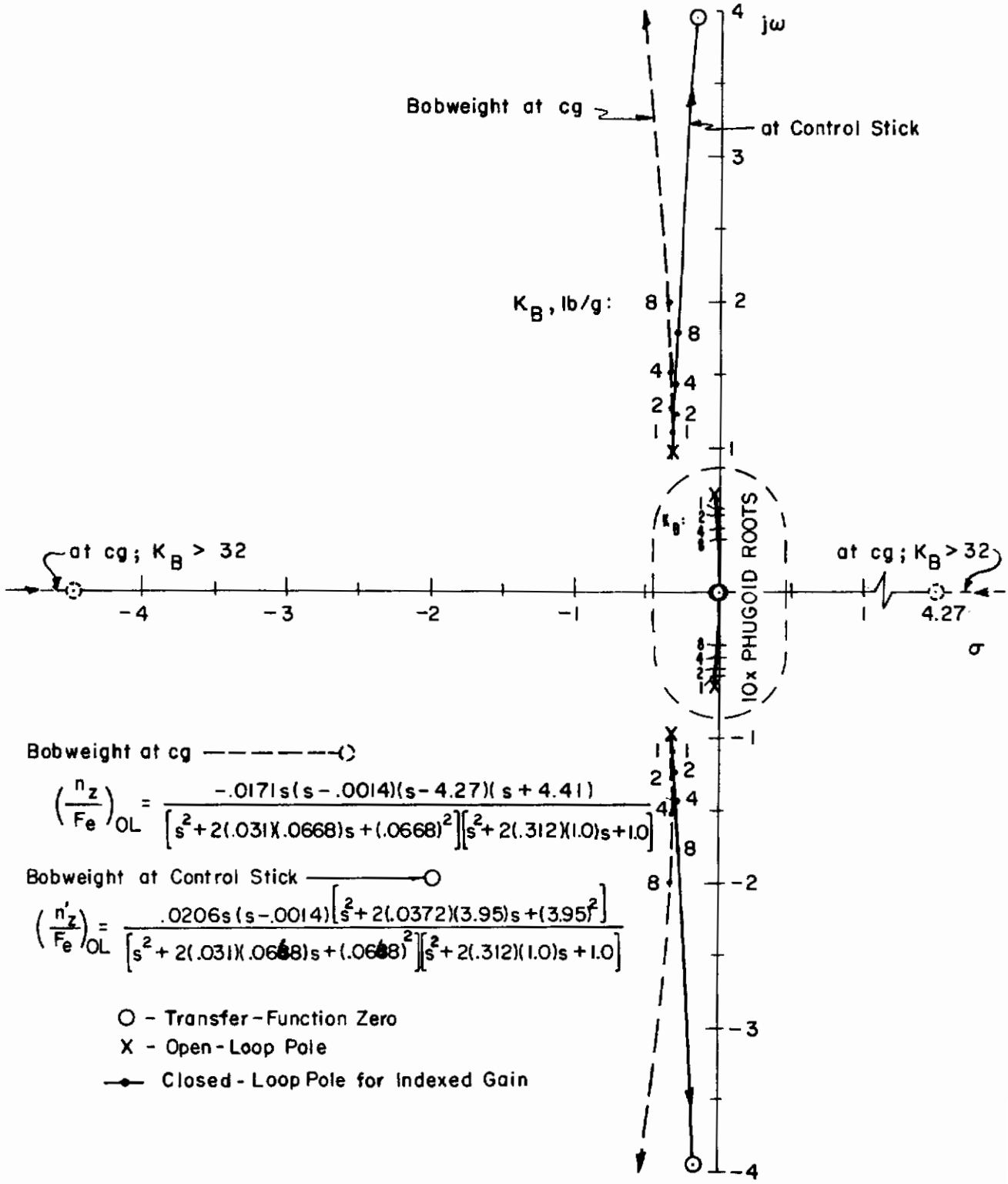

Figure 29. Root Loci for Bobweight

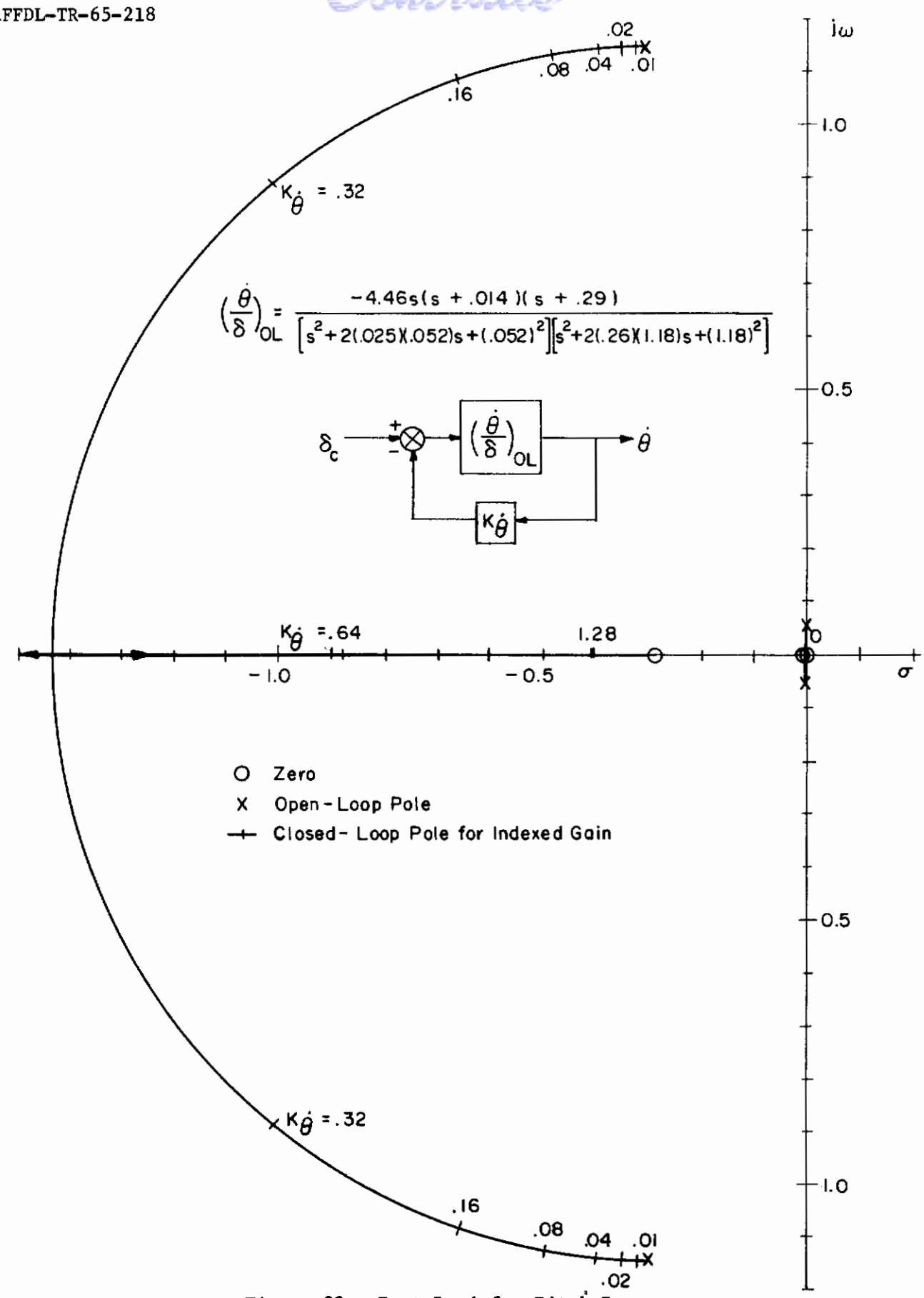

Figure 30. Root Loci for Pitch Damper

REFERENCES

1. Laitone, E. V., and Chou, Y. S., "Phugoid Oscillations at Hypersonic Speeds", AIAA Journal, Vol. 2, No. 4, April 1965

2. Stapleford, R. L., Wolkovitch, J., et al., An Analytical Study of V/STOL Handling Qualities in Hover and Transition, AFFDL TR 65-73, May 1965, Air Force Flight Dynamics Laboratory, Wright-Patterson AFB, Ohio

3. Etkin, B, Dynamics of Flight, 1959, Wiley

4. Dynamics of the Airframe, BuAer Report AE-61-4, Vol. II, February 1953

5. USAF Stability and Control DATCOM, ed: D. Hoak, J. Carlson; FDCC, Air Force Flight Dynamics Laboratory, Wright-Patterson AFB, Ohio, rev. July 1963

6. Thelander, J. A., Aircraft Motion Analysis, FDL-TDR-64-70, March 1965, Air Force Flight Dynamics Laboratory, Wright-Patterson AFB, Ohio

7. McRuer, D. T., and Ashkenas, I, Operating Points, Particle Dynamics, and Coordinate Systems for Aerospace Vehicle Stability and Control, ASD-TDR-61-668, March 1961, Aeronautical Systems Division, Wright-Patterson AFB, Ohio

8. Ashkenas, I. L., and McRuer, D. T., Approximate Airframe Transfer Functions and Application to Single Sensor Control Systems, WADC-TR-58-82, June 1958, Wright Air Development Center, Wright-Patterson AFB, Ohio

9. McRuer, D., Ashkenas, I., and Pass, H, Analysis of Multiloop Vehicular Control Systems, ASD-TDR-62-1014, March 1964, Aeronautical Systems Division, Wright-Patterson AFB, Ohio

10. Truxal, J. G., Automatic Feedback Control System Synthesis, McGraw-Hill, 1955

11. Ergin, E. I., et al., Technique for Analysis of Nonlinear Attitude Control Systems for Space Vehicles, Vol. II, Techniques for Analysis and Synthesis of Nonlinear Control Systems, ASD-TDR-62-208, June 1962, Aeronautical Systems Division, Wright-Patterson AFB, Ohio

12. Graham, D., Brunelle, E. J., Jr., et al., Engineering Analysis Methods for Linear Time Varying Systems, ASD-TDR-62-362, Aeronautical Systems Division, Wright-Patterson AFB, Ohio

13. McRuer, D. T., and Stapleford, R. L., Sensitivity and Modal Response for Single-Loop and Multiloop Systems, ASD-TDR-62-812, Aeronautical Systems Division, Wright-Patterson AFB, Ohio

14. Cole, G., et al, Final Report: Study of Pilot-Controller Integration for Emergency Conditions, RTD-TDR-63-4092, January 1964, Research and Technology Division, Wright-Patterson AFB, Ohio

15. Flying Qualities of Piloted Airplanes, Specification MIL-F-8785 (ASG), Amendment 4, April 1959

REFERENCES (Continued)

16. Seckel, E., Stability and Control of Aircraft and Helicopters, Academic Press, 1964

17. Gardner, M. F., and Barnes, J. L. Transients in Linear Systems, Vol. I, Lumped-Constant Systems, Wiley, 1942

18. Solarski, A., (U) Survey and Study of VTOL-STOL Stability and Control Characteristics, WADC-TR-59-357, August 1959, Wright Air Development Center, Wright-Patterson AFB, Ohio (CONFIDENTIAL Report)

19. Koven., W., and Wasicko, R. J., Flying Qualities Requirements for United States Navy and Air Force Aircraft, AGARD Report 336, April 1961

20. Duncan, W. J., The Principles of the Control and Stability of Aircraft, Cambridge Univ. Press, 1952

21. Perkins, C. D., and Hage, R. E., Airplane Performance, Stability and Control, Wiley, 1949

22. Ashkenas, I. L. (U) Summary and Review of Aeromechanical Devices and Possible Applications, WADC-TN-58-159, Wright Air Development Center, Wright-Patterson AFB, Ohio (CONFIDENTIAL Report)

23. Musil, J., and Meyer, R. A., (U) An Investigation of Control Devices and Methods for Achieving Reduction in Hinge Moment Parameters, WADC-TR-58-216, July 1958, Wright Air Development Center, Wright-Patterson AFB, Ohio (CONFIDENTIAL Report)

24. Airworthiness Standards: Transport Category Airplanes, Federal Aviation Regulations Part 25, Federal Aviation Agency, Washington 25, D. C. (Revised periodically)

25. Airworthiness Standards: Normal, Utility, and Acrobatic Category Airplanes, Federal Aviation Regulations Part 23, Federal Aviation Agency, Washington 25, D. C. (Revised periodically)

26. Ashkenas, I., and McRuer, D., The Determination of Lateral Handling Quality Requirements for Airframe - Human Pilot System Studies, WADC-TR-59-135, June 1959, Wright Air Development Center, Wright-Patterson AFB, Ohio

27. Fonda, A., "Tyre Tests and Interpretation of Experimental Data," Research in Automobile Stability and Control and in Tyre Performance, Automobile Division, The Institution of Mechanical Engineers, London, c. 1956 (Reprinted for Cornell Aeronautical Laboratory)

28. Smiley, R. F., and Horn, W. B., Mechanical Properties of Pneumatic Tires with Special Reference to Modern Aircraft Tires, NASA-TR-R-64, 1960

29. Harrin, E. N., Low Tire Friction and Cornering Forces on a Wet Surface, NACA TN 4406, September 1958

REFERENCES (Continued)

30. Ashkenas, I. L., A Study of Conventional Airplane Handling Qualities Requirements; Part I, Roll Handling Qualties; Part II, Lateral-Directional Oscillatory Handling Qualities, AFFDL-TR-65-138, October 1965, Air Force Flight Dynamics Laboratory, Wright-Patterson AFB, Ohio

31. Paiewonsky, B. H., The Effects of Engine Angular Momentum on an Airplane's Longitudinal and Lateral-Directional Dynamic Stability, WADC-TR-56-225, June 1956, Wright Air Development Center, Wright-Patterson AFB, Ohio

32. McRuer, D. T., and Wolkovitch, J., Linearized Dynamics of Rotating Aerospace Vehicles with Internal Angular Momenta, ASD-TN-61-63, July 1961, Aeronautical Systems Division, Wright-Patterson AFB, Ohio

33. Ashkenas, I. L., and McRuer, D. T., "A Theory of Handling Qualities Derived from Pilot-Vehicle System Considerations," Aerospace Engineering, Vol. 21 No. 2, IAS, February 1962

34. Chalk, C. R., Fixed Base Simulator Investigation of the Effect of L_q and True Speed on Pilot Opinion of Longitudinal Flying Qualities, ASD-TDR-63-339, November 1963, Aeronautical Systems Division, Wright-Patterson AFB, Ohio

35. Goldberg, J. H., Effects of Spring and Inertia Devices on the Longitudinal Stability of Aircraft, WADC-TR-53-350, July 1953, Wright Air Development Center, Wright-Patterson AFB, Ohio

36. Etkin, B., "Longitudinal Dynamics of a Lifting Vehicle in Orbital Flight", Journal of the Aerospace Sciences, Vol. 28, October 1961

37. Greenberg, H., and Sternfield, L., Theoretical Investigation of Longitudinal Stability of Airplanes with Free Controls Including Effect of Friction in the Control System, NACA Report 791, 1944

38. Jones, R. T., and Greenberg, H., Effect of Hinge-Moment Parameters on Elevator Stick Forces in Rapid Maneuvers, NACA Report 798, 1944

39. Ashkenas, I. L., et al., Pilot-Induced Oscillations: Their Cause and Analysis, Norair Report NOR-64-143 (Systems Technology Inc, Report STI TR 239-2, 20 June 1964)

40. Journal of Aircraft, Vol. 1 No. 4, AIAA, July-August 1964

41. Crane, H. L., and Sommer, R. W., Effects of Control-Free Configuration on Airplane Longitudinal Control Response, NASA TN D-912, October 1961

42. (U) Wright Air Development Center Conference on Inertia Coupling of Aircraft - A Compilation of the Papers Presented 29 February and 1 March 1956; DDC No. AD 98655 (SECRET report)

43. Gates, O. B., and Minka, K., "Note on a Criterion for Severity of Roll-Induced Stability", Journal Aerospace Sciences, Vol. 26, No. 5, May 1959

REFERENCES (Continued)

44. Wykes, J. H. Casteel, G. R., and Collins, R. A., An Analytical Study of the Dynamics of Spinning Aircraft; Part I, Flight Test Data Analyses and Spin Calculations; Part II, Wind Tunnel Tests; Part III, Calculated and Flight Test Spin Characteristics of an F-100F With Strakes; WADC-TR-58-381 (Parts I & II, December 1958; Part III, February 1960), Wright Air Development Center, Wright-Patterson AFB, Ohio

45. Neihouse, A. I., Klinar, W. J., and Scher, S. H., Status of Spin Research for Recent Airplane Designs, NASA TR R-57, 1960 (Supersedes NACA RM L57F12)

46. Anglin, E. L., and Scher, S. H., Analytical Study of Aircraft-Developed Spins and Determination of Moments Required for Satisfactory Spin Recovery, NASA TN D-2181, February 1964

47. (U) Wright Air Development Center Spin Symposium - A Compilation of the Papers Presented; 27 & 28 February 1957 (CONFIDENTIAL report)

48. Scher, S. H., Post-Stall Gyrations and Their Study on a Digital Computer, AGARD Report 359, April 1961

49. Klinar, W. J., & Grantham, W. D., Investigation of the Stability of Very Flat Spins and Analysis of Effects of Applying Various Moments Utilizing the 3 Moment Equations of Motion, NASA Memo 5-25-59L, June 1959

50. Soulé, H. A., and Anderson, R. F., Design Charts Relating to the Stalling of Tapered Wings, NACA TR 703, 1940

51. Harper, C. W., and Maki, R. L., A Review of the Stall Characteristics of Swept Wings, NASA TN D-2373, July 1964

52. Spreeman, K. P., Design Guide for Pitch-Up Evaluation and Investigation at High Subsonic Speeds of Possible Limitations Due to Wing-Aspect-Ratio Variations, NASA TM X-26, August 1959

53. (U) The Study and Flight Test of Several Methods for Improving Airplane Stall Warning, Cornell Aeronautical Laboratory, Inc., September 1955 (Prepared under U.S. Navy BuAer Contract NOa(s)53-753-C) (CONFIDENTIAL Report)

54. Anderson, S. B., Correlation of Flight and Wind Tunnel Measurements of Roll-Off in Low-Speed Stalls on a 35-Degree Swept-Wing Aircraft, September 1953

55. Sadoff, M., Stewart, J. D., and Cooper, G. F., Analytical Study of the Comparative Pitch-Up Behavior of Several Airplanes and Correlation with Pilot Opinion, NACA RM A57D04, 12 June 1957

56. Sadoff, M., and Stewart, J. D., An Analytical Evaluation of the Effects of an Aerodynamic Modification and of Stability Augmenters on the Pitch-Up Behavior and Probable Pilot Opinion of Two Current Fighter Airplanes, NACA RM A57K07, 21 April 1958

REFERENCES (Continued)

57. Sadoff, M., Pitch-Up Problem--A Criterion and Method of Evaluation, NASA Memo 3-7-59A, February 1959

58. Campbell, G. S., and Weil, J., The Interpretation of Nonlinear Pitching Moments in Relation to the Pitch-Up Problem, NASA TN D-193, December 1959

59. Lukens, D. R., Schmitt, A. F., et al., Approximate Transfer Functions for Flexible-Booster-and-Autopilot Analysis, WADD-TR-61-93, April 1961, Wright Air Development Division, Wright-Patterson AFB, Ohio

60. Bryce, B. A., The Literature of Fuel Slosh Characteristics: An Annotated Bibliography; Autonetics, a Division of North American Aviation, Inc. Report EM-1162-127, 16 July 1962

61. Flight Control Systems - Design, Installation, and Test of Piloted Aircraft, General Specifications For; Specification MIL-F-9490C (USAF), 13 March 1964

62. Bisplinghoff, R. L., Ashley, H., and Halfman, R. L., Aeroelasticity, Addison-Wesley, Cambridge, Mass., 1955

63. Paraghamian, B., and Lohmann, R. L., Methods for Predicting Aeroelastic Effects on Subsonic Static Longitudinal Stability of Aircraft, WADC-TR-54-265, 1954, Wright Air Development Center, Wright-Patterson AFB, Ohio

64. Schwendler, R. G., and MacNeal, R. H., Optimum Structural Representation in Aeroelastic Analyses, ASD-TR-61-680, 1961, Aeronautical Systems Division, Wright-Patterson AFB, Ohio

65. Dunn, O., Aerodynamically Boosted Surface Controls and Their Application to the DC-6 Transport, IAS Preprint (Second International Conference, IAS- RAeS, New York) May 1959

66. Jones, R. T., and Cohen, D., An Analysis of the Stability of An Airplane with Free Controls, NACA Report 709, 1941

UNCLASSIFIED
Security Classification

DOCUMENT CONTROL DATA - R&D
(Security classification of title, body of abstract and indexing annotation must be entered when the overall report is classified)

1. ORIGINATING ACTIVITY *(Corporate author)*
Air Force Flight Dynamics Laboratory (AFFDL)

2a. REPORT SECURITY CLASSIFICATION
Unclassified

2b. GROUP

3. REPORT TITLE
ESTIMATION OF FLYING QUALITIES OF PILOTED AIRPLANES

4. DESCRIPTIVE NOTES *(Type of report and inclusive dates)*
Final Report; 1960-1965

5. AUTHOR(S) *(Last name, first name, initial)*
Woodcock, Robert J. (AFFDL)
Drake, Douglas E. (Douglas Aircraft Co.)

6. REPORT DATE	7a. TOTAL NO. OF PAGES	7b. NO. OF REFS
March 1966	136	66

8a. CONTRACT OR GRANT NO.	9a. ORIGINATOR'S REPORT NUMBER(S)
AF 33(616)-6460	
b. PROJECT NO. 8219	AFFDL-TR-65-218
c.	9b. OTHER REPORT NO(S) *(Any other numbers that may be assigned this report)*
d.	

10. AVAILABILITY/LIMITATION NOTICES
Distribution of this document is unlimited. Copies are available from DDC and CFSTI.

11. SUPPLEMENTARY NOTES	12. SPONSORING MILITARY ACTIVITY
	Research and Technology Division Air Force Systems Command Wright-Patterson AFB, Ohio 45433

13. ABSTRACT

Methods, ranging from rigorous and complicated to simple and approximate, are presented for estimating flying qualities in accordance with such specifications as MIL-F-8785 (ASG). Aerodynamic and inertial data are assumed to be known. Intended mainly for design use, the report gives enough detail to indicate derivations and conditions for validity. Topics include the static and dynamic, controls-fixed and controls-free aspects of aircraft stability, control, and trim. Although emphasis is on linear analysis, methods are given or indicated for such nonlinear problems as drag, pitch-up, inertial coupling, and spinning. Appendixes give an introduction to aeroelastic effects, ways to analyze control tabs, a derivation of the controls-free equations of motion, and an introduction to root locus analysis.

DD FORM 1 JAN 64 1473

UNCLASSIFIED
Security Classification

14. KEY WORDS	LINK A		LINK B		LINK C	
	ROLE	WT	ROLE	WT	ROLE	WT
Stability and Control **Controllability** **Trim** **Flying Qualities** **Handling Qualities** **Aircraft Design Analysis** **Dynamic Stability** **Static Stability** **Control Tabs**						

INSTRUCTIONS

1. ORIGINATING ACTIVITY: Enter the name and address of the contractor, subcontractor, grantee, Department of Defense activity or other organization *(corporate author)* issuing the report.

2a. REPORT SECURITY CLASSIFICATION: Enter the overall security classification of the report. Indicate whether "Restricted Data" is included. Marking is to be in accordance with appropriate security regulations.

2b. GROUP: Automatic downgrading is specified in DoD Directive 5200.10 and Armed Forces Industrial Manual. Enter the group number. Also, when applicable, show that optional markings have been used for Group 3 and Group 4 as authorized.

3. REPORT TITLE: Enter the complete report title in all capital letters. Titles in all cases should be unclassified. If a meaningful title cannot be selected without classification, show title classification in all capitals in parenthesis immediately following the title.

4. DESCRIPTIVE NOTES: If appropriate, enter the type of report, e.g., interim, progress, summary, annual, or final. Give the inclusive dates when a specific reporting period is covered.

5. AUTHOR(S): Enter the name(s) of author(s) as shown on or in the report. Enter last name, first name, middle initial. If military, show rank and branch of service. The name of the principal author is an absolute minimum requirement.

6. REPORT DATE: Enter the date of the report as day, month, year, or month, year. If more than one date appears on the report, use date of publication.

7a. TOTAL NUMBER OF PAGES: The total page count should follow normal pagination procedures, i.e., enter the number of pages containing information.

7b. NUMBER OF REFERENCES: Enter the total number of references cited in the report.

8a. CONTRACT OR GRANT NUMBER: If appropriate, enter the applicable number of the contract or grant under which the report was written.

8b, 8c, & 8d. PROJECT NUMBER: Enter the appropriate military department identification, such as project number, subproject number, system numbers, task number, etc.

9a. ORIGINATOR'S REPORT NUMBER(S): Enter the official report number by which the document will be identified and controlled by the originating activity. This number must be unique to this report.

9b. OTHER REPORT NUMBER(S): If the report has been assigned any other report numbers *(either by the originator or by the sponsor)*, also enter this number(s).

10. AVAILABILITY/LIMITATION NOTICES: Enter any limitations on further dissemination of the report, other than those imposed by security classification, using standard statements such as:

(1) "Qualified requesters may obtain copies of this report from DDC."

(2) "Foreign announcement and dissemination of this report by DDC is not authorized."

(3) "U. S. Government agencies may obtain copies of this report directly from DDC. Other qualified DDC users shall request through _____."

(4) "U. S. military agencies may obtain copies of this report directly from DDC. Other qualified users shall request through _____."

(5) "All distribution of this report is controlled. Qualified DDC users shall request through _____."

If the report has been furnished to the Office of Technical Services, Department of Commerce, for sale to the public, indicate this fact and enter the price, if known.

11. SUPPLEMENTARY NOTES: Use for additional explanatory notes.

12. SPONSORING MILITARY ACTIVITY: Enter the name of the departmental project office or laboratory sponsoring *(paying for)* the research and development. Include address.

13. ABSTRACT: Enter an abstract giving a brief and factual summary of the document indicative of the report, even though it may also appear elsewhere in the body of the technical report. If additional space is required, a continuation sheet shall be attached.

It is highly desirable that the abstract of classified reports be unclassified. Each paragraph of the abstract shall end with an indication of the military security classification of the information in the paragraph, represented as *(TS), (S), (C), or (U)*.

There is no limitation on the length of the abstract. However, the suggested length is from 150 to 225 words.

14. KEY WORDS: Key words are technically meaningful terms or short phrases that characterize a report and may be used as index entries for cataloging the report. Key words must be selected so that no security classification is required. Identifiers, such as equipment model designation, trade name, military project code name, geographic location, may be used as key words but will be followed by an indication of technical context. The assignment of links, rules, and weights is optional.